Experimental and Molecular Mechanics Studies of the Conformations of Compounds Containing Oxygen and Sulfur

by

Glen D. Rockwell

Submitted in partial fulfilment of the requirements
for the degree of Doctor of Philosophy

at

Dalhousie University
Halifax, Nova Scotia
August 1997

DALHOUSIE UNIVERSITY

FACULTY OF GRADUATE STUDIES

The undersigned hereby certify that they have read and recommend to the Faculty of Graduate Studies for acceptance a thesis entitled "Experimental and Molecular Mechanics Studies of the Conformations of Compounds Containing Oxygen and Sulfur"

by Glen Donald Rockwell

in partial fulfillment of the requirements for the degree of Doctor of Philosophy.

Dated: August 22, 1997

External Examiner

Research Supervisor

Examining Committee

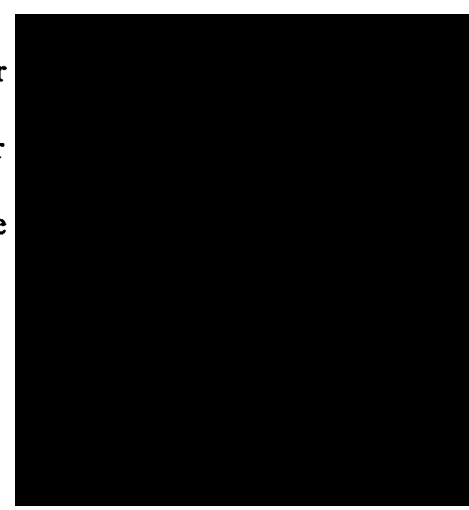

DALHOUSIE UNIVERSITY

DATE: Sept. 5/97

AUTHOR: Glen D. Rockwell

TITLE: "Experimental and Molecular Mechanics Studies of the Conformations of Compounds Containing Oxygen and Sulfur"

DEPARTMENT OR SCHOOL: Chemistry

DEGREE: Ph. D. CONVOCATION: October YEAR: 1997

Permission is herewith granted to Dalhousie University to circulate and to have copies for non-commercial purposes, at its discretion, the above title upon the request of individuals or institutions.

[redacted]

Signature of Author

To my parents

Table of Contents

List of Figures

List of Tables

Abstract

The positions of the equilibria between the diaxial and diequatorial conformers of ^{13}C-labelled *trans*-1,2-dimethoxycyclohexane (**2**) and *trans*-2-methoxycyclohexanol (**9**) were measured accurately using ^{13}C NMR at 193 K in a variety of solvents ranging in polarity from pentane to methanol. The population of the diequatorial conformer was observed to increase as solvent polarity increased. Improved parameters for the OCCO torsional term in the MM3(94) force field have been developed that fit experimental observations for a variety of ethers much better than the original values. The ^1H NMR spectrum of 1,2-dimethoxypropane (**5**) in cyclohexane-d_{12} was analysed and the composition of its conformational mixture was determined. The previous gas phase results for this compound have been shown to be inaccurate and have been reinterpreted.

Methyl 2,3,4,6-tetra-*O*-[$^2H_3$]methyl-α-D-glucopyranoside (**16a**), its 4-^{13}C-labelled analog, and methyl 2,3,4-tri-*O*-[$^2H_3$]methyl-α-D-glucopyranoside (**18**) were synthesized. The C5-C6 rotameric compositions for these compounds were determined in a range of solvents from the $^3J_{H5,H6R}$ and $^3J_{H5,H6S}$ values obtained from their 500 and 600 MHz ^1H NMR spectra. Unambiguous assignments of the H6R and H6S signals were made from the 4-^{13}C-labelled compound. The results showed that solvent had no significant effect on rotameric population unless OH-6 was available to form intramolecular hydrogen bonds.

Conformational analyses of tri-, tetra-, and pentathiacycloalkanes ranging in ring size from nine to sixteen membered were performed. The torsional terms in MM3(94) for CSCC, SCCC, and SCCS terms were improved and used in stochastic searches. For 1,4,7-trithiacyclononane (**23**), experimental results showed that the C_3 conformer (present in the solid phase) was not the dominant conformer in solution. Instead, a mixture of conformers was present. By contrast, 1,5,9-trithiacyclododecane (**25**) was found to adopt the same conformation in solution and in the solid phase. The calculations predict that at least two other macrocyclic thioethers would be good complex formers. The calculations successfully predicted the conformational stability of the D_4 conformer of 1,4,7,10-tetrathiacyclododecane (**26**). Thermal analyses of six macrocyclic thioethers were also performed using differential scanning calorimetry.

List of Abbreviations and Symbols Used

a,ax	axial
a	*anti*
Å	angstrom = 10^{-10} meters
Ac	acetyl
bp	boiling point
bs	broad singlet
Bu	butyl
°C	degrees Celsius
calc	calculated
CD	circular dichroism
cm^{-1}	wavenumber
conf	conformer
COSY	homonuclear correlation spectroscopy
CP/MAS	cross-polarization/magic angle spinning
CPU	central processing unit
CRD	carbohydrate recognition domain
d	doublet
D	debye, measure of dipole moment
ddd	doublet of doublets of doublets
DMSO	dimethyl sulfoxide
DNA	deoxyribonucleic acid

DMF	*N,N*-dimethylformamide
DSC	differential scanning calorimetry
e, eq	equatorial
E	energy
ED	electron diffraction
EI	electron ionization
E_T	solvatochromic solvent parameter
eV	electron volt = 96.487 kJ/mol
exp	experimental
f	fraction of a particular state
freq	frequency
FTIR	Fourier transform infrared
g	gram
g	*gauche* clockwise
g'	*gauche* counter-clockwise
G	Gibb's free energy
H	enthalpy
H_{conf}	conformational enthalpy
H_{melt}	enthalpy of melting
H_{trans}	enthalpy of a phase transition
HETCOR	heteronuclear correlation spectroscopy
HnR	*Pro-R* proton at the nth position

HnS	*Pro-S* proton at the nth position
Hz	hertz
Imag	imaginary
J	joule (unit of energy), coupling constant (NMR)
K	kelvin
kcal	kilocalorie
kJ	kilojoule
kPa	kilopascal
L	ligand, litre
lit	literature value
m	medium (infrared), multiplet (NMR)
M	molarity
$(M\text{-}OCH_3)^+$	ion formed from loss of an OCH_3 group
Me	methyl
MeOH	methanol
mg	milligram
MHz	megahertz
min	minute
mL	millilitre
mM	millimolarity
mol	mole
mp	melting point

MS	mass spectroscopy
NMR	nuclear magnetic resonance
NOE	nuclear Overhauser effect
PC	personal computer
ppm	parts per million
R	*R* stereochemistry
R^2	correlation coefficient
Ref	reference
RNA	ribonucleic acid
s	second (time), strong (infrared), singlet (NMR)
S	*S* stereochemistry
S	entropy
sh	shoulder
S_{melt}	entropy of melting
S_{trans}	entropy of a phase transition
std	standard
t	*trans* geometry
T	temperature
T_{melt}	temperature at which a compound begins to melt
T_{trans}	temperature at the beginning of a phase change
T_1	spin-lattice relaxation time
TBDMS	*tert*-butyl-dimethylsilyl

THF	tetrahydrofuran
TLC	thin-layer chromatography
TMS	tetramethylsilane
tot	total
vs	very strong
vw	very weak
w	weak
°	degrees
α_{KT}	Kamlet-Taft solvent hydrogen bond donor parameter
β_{KT}	Kamlet-Taft solvent hydrogen bond acceptor parameter
δ	chemical shift
ϵ	dielectric constant
ϵ_K	Kirkwood function
μ	dipole moment
ν	frequency
π^*	solvatochromic solvent parameter
τ	correlation time

Acknowledgments

I would like to thank my supervisor Dr. T. Bruce Grindley for all of his generous support, patience, advice and encouragement throughout all of the phases of this research. I would also like to thank him for modifying the MM3(94) program when needed and for the use of his office computer for running the stochastic searches of the crown thioethers. Financially, I would like to thank NSERC for funding the research and for providing scholarships. I would also like to thank the Walter C. Sumner Foundation for a scholarship.

I would like to thank Dr. D. L. Hooper and Dr. M. D. Lumsden and the ARMRC for their assistance in running many of the spectra. I would especially like to thank Dr. Lumsden for running *all* of the 400 MHz spectra presented here including all of the CP/MAS spectra.

I am grateful to Dr. N. L. Allinger for a copy of the microcomputer version of MM3(94) used in this research. I wish to thank Dr. J. S. Grossert for providing a program for calculation of NMR coupling constants using the Haasnoot-Altona equation.

I would like to thank Dr. J. Walter at IMB in Halifax for running the 500 MHz spectrum of compound **5** and Dr. I. Burton, also at IMB, for running the 500 MHz spectra of compound **18**. The 600 MHz spectra of **16a** were run at NRC in Ottawa and I wish to thank Dr. J. R. Brisson for this generous service. Dr. Grindley should be thanked for providing funding to allow me to personally deliver the samples to Ottawa.

Thanks also goes out to those who donated samples of materials including Dr A.S. Serianni for compound **17**, Dr. R. D. Adams for compound **25** and Dr. R. D. Guy for compound **28**. The DSC experiments were initiated after discussion with Dr. M. A. White and I would like to thank her for discussions on the topic and for the use of her equipment to prepare samples. The DSC experiments were performed by I. A. Keough at the DREA. I would like to thank him for his time and the DND for allowing the experiments to be run.

I would like to thank the faculty, staff, and graduate students at the Chemistry Department for assistance and friendship. I would like to thank Dr. J. Kim for running the EI-MS experiments. I especially want thank the other members of the Grindley group, past and present, especially H. Namazi, H. Qin, X. Kong, M. Kamau, M. Safatli, and Dr. C. K. Lee, for their friendship.

Chapter 1
Introduction to Conformational Analysis

This thesis deals with the improvement of the parameterization of torsional terms in the MM3(94) force field containing oxygen and sulfur, and application of these improvements to a number of conformational problems. In order to develop these improved parameters it was necessary to make accurate conformational measurements. This introduction to the thesis contains an outline of the terminology and methods of both experimental and computational conformational analysis. This chapter will be followed by chapters on the development and applications of new parameters for oxygen, including experimental measurements, an experimental study of the rotation about the C5-C6 bond in D-aldohexopyranosides, and development of new sulfur parameters and their use in the conformational analysis of a series of crown thioethers.

1.1 Structure and Conformation

1.1.1 Definitions

The structure of a compound is the most important piece of information that a chemist needs to know about a compound of interest. Structure can be broken down into three categories: constitution, configuration and conformation.[1,2] Constitution refers to the types and number of atoms within a molecule. It also defines the manner in which these atoms are

bonded together.[1] The constitution of a compound can be determined by physical, chemical and spectroscopic methods. Without complete knowledge of constitution, determining configuration and conformation is impossible.

Configuration refers to the three-dimensional arrangement of atoms around rigid centers in molecules that have the same constitution.[1] The simplest case is the asymmetric carbon atom.[2] Enantiomers and diastereomers are examples of configurational isomers that arise when the arrangement(s) of atoms around one or more asymmetric carbons are reversed. Another example of configurational isomerism is the *cis*- and *trans*-isomerism of substituted alkenes. Here, the rigid center about which the three-dimensional structure varies is the carbon-carbon double bond.

Conformation is also a property of the three-dimensional aspect of structure. It is a property that arises from the flexibility and motion of various arrangements of chemical bonds. Conformational isomers can be defined as molecules having identical constitutions and configurations but having different torsional angles about single bonds within the molecule.[1,2]

Conformation is different from configuration in that configuration is considered to be a fixed property of the molecule that does not change with time unless bonds are broken and reformed within the molecule. Conformational changes alter the three-dimensional arrangement of the atoms in the molecule without breaking bonds. Unlike constitution and configuration, most molecules cannot be said to have a single conformation.[2] Except under extreme circumstances, the constituent parts of a molecule are constantly in motion and thus the molecule is constantly undergoing conformational changes.

Some conformational arrangements are more energetically favourable than others, and are thus more populated. Conformations that are energy minima on the multidimensional potential energy surface of the molecule are termed conformers.[3] All other arrangements are called conformations. The most stable of the conformers is called the global minimum and this conformer has the highest population in a conformational mixture. Other minima are referred to as local minima. Another feature found on a potential energy surface is a saddlepoint. Saddlepoints are not conformers; instead they are the maxima on the lowest energy pathways between two conformers, like the highest point on a pass leading from one valley to another.[3]

For example, for *n*-butane[4], there are an infinite number of conformations about the C-C-C-C torsional bond, but there are only three energy minima (conformers) and three saddlepoints. In *n*-butane, these six special conformations are described according to the C-C-C-C torsional angle. The three conformers are at angles of 180°, 60°, and -60°. The saddlepoints are at torsional angles of 0°, 120°, and -120° (see Figure 1.1). The 180° conformer is termed the *anti* conformer. This conformer is the most stable of the conformers due to the lack of strong steric repulsions within the molecule. Two of the conformers (60°, -60°) are enantiomers and are energetically degenerate as are two of the saddlepoints (120°, -120°). The 60° and -60° conformers are called *gauche* conformers. The sign of the angle is usually distinguished by calling the counterclockwise (negative) angle *gauche'*. The three saddlepoint conformations are all termed *eclipsed*.[2]

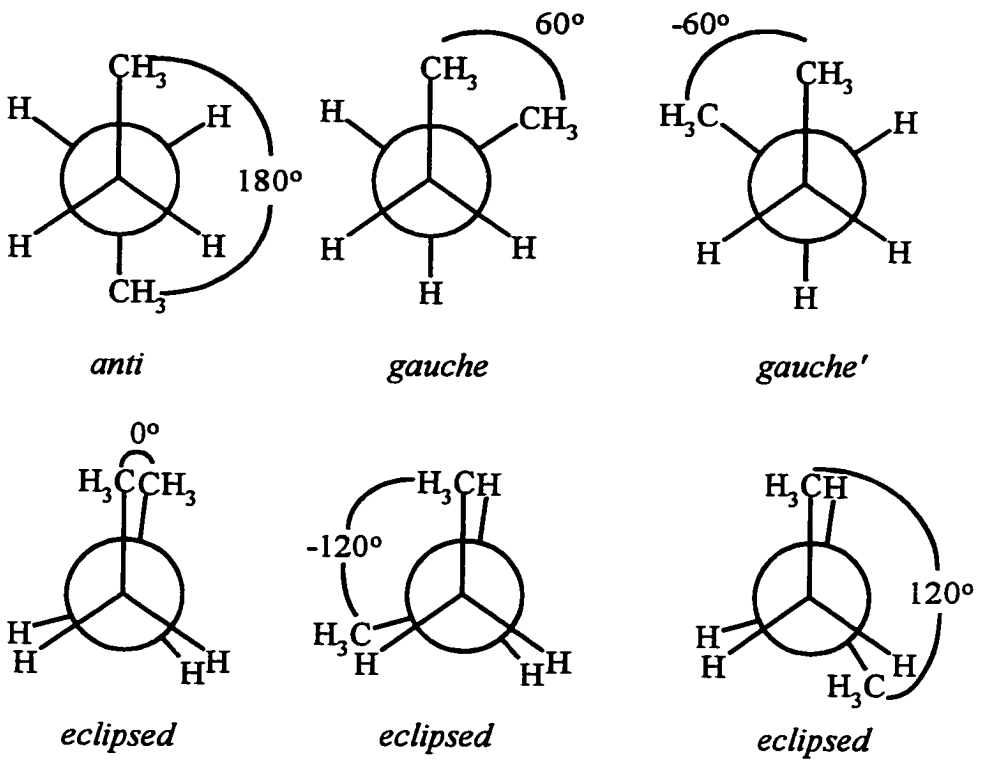

Figure 1.1 Conformers and saddlepoints of *n*-butane.

To fully characterize the three-dimensional structure of a molecule, it is necessary to completely examine the potential energy surface and determine all the possible conformers and, if possible, the conformations at saddlepoints between conformers. Experimentally, determining the geometry of saddlepoints is not possible due to their extremely short lifetimes. The best one can hope for is a complete analysis of the conformers present. For small or conformationally restricted molecules this can be done relatively easily using various techniques (see below). For most other molecules, due to experimental constraints, a complete examination of all the conformers is not possible. At best, the structures of only a few of the most stable conformers can be determined.

1.1.2 The Importance of Conformation

The conformation of a molecule plays a very important role in determining its biological, physical and chemical properties.[2] The importance of conformation in chemistry is illustrated by the Curtin-Hammett Principle and related concepts.[5] Physical properties that are affected by conformation include spectroscopic properties (which are the basis of many conformational analyses) and dipole moments. For example, the dipole moment of 1,2-difluoroethane reflects the fact that the *gauche* conformation is favoured rather than the non-polar *anti* conformation.[6,7] Conformation plays an especially important role in life itself. Many ways in which cells communicate with each other and react are based on molecular recognition where one molecule "fits" into another molecule called the receptor, thus triggering various biological responses. This "fit" is controlled by the three-dimensional conformation of the molecule and the conformation of the receptor.[8,9]

1.2 Experimental Methods of Conformational Analysis

Depending on the phase of the molecule under examination, different techniques are used to determine the populations and structures of conformers of a compound. Experimentally determining the precise geometry of a single conformation of a conformationally mobile molecule is possible in cases where a solid is being examined or at very low temperatures where the motion of the molecule has been slowed sufficiently to prevent the individual conformers from interconverting rapidly, or by using techniques like microwave spectroscopy, where the timescale for conformational interconversion is very short.

1.2.1 Solid Phase Methods

In the solid phase, molecular motion is usually restricted. This allows the chemist to determine the position of the atoms of a molecule and thus the conformation. When one is dealing with a crystalline solid, the most commonly used method of conformational analysis is X-ray diffraction.[10-12] X-rays are diffracted by electrons, so the positions of heavy atoms with many inner electrons can be determined easily. One disadvantage to this technique is the lack of accuracy in determining the positions of hydrogen atoms,[10] especially in large molecules, which can play a large role in the determination of conformation. Also, this technique requires that the compound exist as a regular crystal at the operating temperature of the diffractometer.

Neutron diffraction is a complementary technique to X-ray diffraction.[13] Here the diffraction of neutrons rather than X-rays is examined. The positions of hydrogen atoms are determined relatively precisely with neutron diffraction because neutrons are diffracted by nuclei. Its major weaknesses are the requirements for relatively large crystals and the availability of an atomic reactor as a source of neutrons. The use of solid phase conformational analysis suffers from the fact that in many cases the geometry of the molecule in the solution phase is required. Solid phase conformations and solution phase conformations can be strikingly different (see Section 4.1.1). Thus, the results obtained from X-ray and neutron diffraction are not necessarily applicable to the gas and solution phases.

1.2.2 Gas Phase

For molecules in the vapor phase, electron diffraction (ED)[14,15] and microwave spectroscopy[16] are favoured. Very accurate bond lengths can be determined from electron

diffraction, but one is limited by the necessity for the molecules to be in the gas phase and the difficulty of solving the structure as the molecule increases in size.[15] This limits one to molecules that are relatively small and volatile. Microwave spectroscopy yields dipole moments and moments of inertia that can then be used to determine conformation.[16] Microwave spectra contain numerous sharp lines that are difficult to assign even when only one conformer is present so that complex conformational mixtures represent difficult challenges.

Because both techniques are used in the gas phase, the data that result are a product of the sum of all of the conformations present in the vapor. Usually the spectra obtained reflect not one conformer but a mixture of conformers. To obtain accurate data from electron diffraction where the spectra observed are broad, it is necessary to combine the results with some form of molecular modeling (i.e., molecular mechanics or *ab initio* calculations) in order to derive possible conformational mixtures that best fit the experimental data.[17]

1.2.3 Solution Phase

The most versatile way to determine conformation in the solution phase is NMR spectroscopy.[18,19] There are a variety of two-dimensional experiments[20] that, in combination with NOE experiments[21] allow one to determine which atoms are close to each other in space. Combined with molecular modeling this can be a powerful tool for elucidating the conformation of a compound.[22]

Coupling constants between hydrogens and between hydrogens and carbons are also useful tools for conformational analysis. The Karplus equation[23] and its modifications (see

Equation 1) are key to using vicinal coupling constants to determine conformation. The torsional angle is given by θ and *A*, *B* and *C* are empirical parameters. This equation relates the magnitude of a three bond coupling constant to the torsional angle of the protons involved in the coupling (see Figure 1.2). By employing a correctly parameterized Karplus equation and simple algebra it is possible to determine the relative populations of various conformers in solution from the magnitude of the averaged coupling constants.[2,18]

$$^{3}J_{HH} = A\cos^{2}\theta - B\cos\theta + C \qquad (1)$$

As in the vapor phase, one does not usually obtain data which are the result of a single conformer. There is almost always a mixture of conformers present and the relevant NMR parameters, be they coupling constants or chemical shifts are a weighted average of the various conformers present in the solution. In any situation where accurate conformational analysis of large molecules is performed with NMR spectroscopy, molecular modeling is a useful tool to aid in the analysis of the spectra.

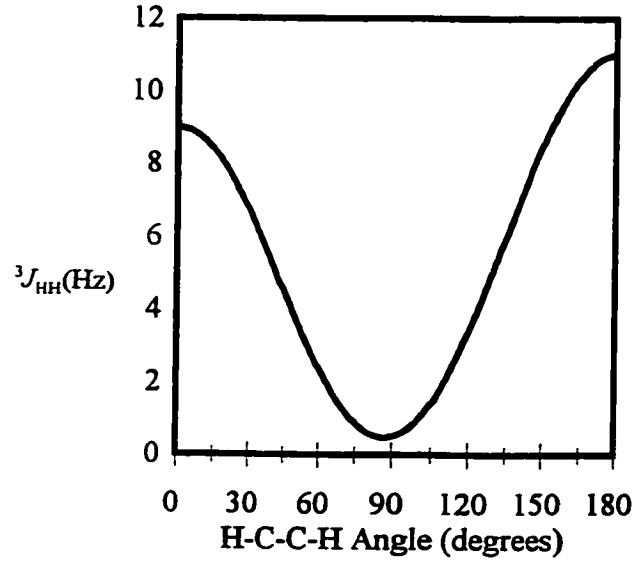

Figure 1.2 Plot of the Karplus relation (Equation 1) where A=9.5, B=1, C=0.5

1.3 Molecular Modeling as a Tool for Conformational Analysis

Molecular modeling is the use of physical or computer simulated models of molecules in order to study their structural properties. As shown above, molecular modeling is an important tool for assisting in the experimental evaluation of conformations. It can also be used for other purposes, for example to explore the properties of molecules that cannot currently be examined experimentally, such as CO_4.[24] Modeling can be used to examine potential energy surfaces in detail.[25] Models can be used to examine the pathways by which conformers interconvert.[26] With modeling it is possible to examine the structures of saddlepoints and conformers that have populations that are too small to be detected by experimental means but may be very important chemically.[27-29]

For the synthetic chemist, modeling can be used explain why a reaction did or did not work as predicted. Using the results of modeling, the chemist could then alter the conditions so that the reaction could be more efficient.[30] Molecular modeling is used as a means by which molecules that have not yet been synthesized can be evaluated as possible drugs through an examination of the conformers that a compound will form and whether or not they will bind to a receptor site in a biological system.[31] Solubility in aqueous or lipid-like environments, which will often influence a drug's usefulness, can also be examined using appropriate models. There is a variety of methods for molecular modeling and each one has its advantages and disadvantages.

1.3.1 Methods of Molecular Modeling

Before the advent of the computer, molecular modeling was done with handheld models that were prepared from a knowledge of bond lengths and bond angles. The double-

helical structure of DNA was theorized through a combination of X-ray diffraction data and models of this sort.[32] The major disadvantage of this method for modeling is the requirement for carefully machined models and a lack of flexibility, in that small amounts of bending or twisting within the molecule were not possible due to the rigidity of the models. The use of computers has greatly changed the face of molecular modeling.

There are three main types of computational molecular modeling: *ab initio*, semiempirical, and molecular mechanics. The first two are quantum mechanical techniques while the last is a "classical" technique. Each method has various advantages and disadvantages. The first two methods will be described only briefly while molecular mechanics will be discussed in more detail.

1.3.1.1 *Ab initio* methods

Ab initio calculation is a method for molecular modeling that does not rely on any experimental input. Instead, the method involves the calculation of molecular properties from theoretical equations, specifically the Schrodinger equation. The method first involves making the Born-Oppenheimer approximation. The Born-Oppenheimer approximation allows the motion of the nuclei and the motion of the electrons to be evaluated separately. The geometry of the molecule can then be optimized, if desired, and the Schrodinger equation for all the electrons is solved to determine the molecular properties.[33] The complexity of the Schrodinger equation is such that it cannot be solved exactly for molecules containing more than 1 electron. As a result, various approximations are made involving interelectron interactions and the size, shape, and properties of the atomic orbitals involved.

The chief advantage of this method is the number of properties, besides simple geometry, that can be determined by the calculation. Many electronic properties can be derived from *ab initio* calculations. These include resonance energies, bond energies, electron densities and ionization potentials. Another advantage of the method is that the experimental numbers used are well defined constants such as the speed of light and the charge on an electron. Empirical parameterization is not required. As a result it is possible to use *ab initio* calculations to model structures that have no experimental counterparts. This advantage makes it possible to model reaction transition states where bonds are only fractionally in existence such as in the transition state of an S_N2 reaction.[34]

The main disadvantage of *ab initio* calculations is the amount of computational time required for large and medium sized molecules. The amount of time can increase as N^4 or higher where N is the number of basis set orbitals.[33,35] The more precise the calculation, the more computational time is required. Improved software and computers are the main solution to these problems and as computer technology advances so does the efficiency of *ab initio* calculations. Another disadvantage is the fact that calculations are performed on small systems of molecules. This can result in large differences in properties between the calculated result and the bulk phase experimental results. Various methods have been used to allow for solvation and other effects of non-gas phase molecules.[36]

1.3.1.2 Semiempirical Methods

Semiempirical methods of modeling were developed as an answer to the high computational cost of *ab initio* calculations. In 1965, Pople[37,38] and coworkers developed the CNDO (Complete Neglect of Differential Overlap) method of modeling. They simplified *ab*

initio calculations by making various approximations regarding two-electron interactions and by neglecting the effects of the core electrons. Empirical parameters are used to make up for the accuracy lost in simplifying the calculations. Since that time, a large number of semiempirical methods has been developed.[39,40] If the programs are well parameterized, then it is possible to obtain answers as accurate as those from low-level *ab initio* calculations with a more efficient use of time. This is the major advantage of semiempirical calculations; they allow one to perform calculations on molecules too large for normal quantum calculations. They can also be used to calculate data for unstable systems like reaction transition states, which are not achievable with molecular mechanics, in less time than *ab initio* methods.

Semiempirical calculations combine the advantages of molecular mechanics and *ab initio* calculations. At the same time, however, semiempirical calculations also combine the disadvantages of the two methods. They are more time consuming than molecular mechanics calculations. Semiempirical calculations increase in time and computer requirements as N^2 to N^3 where N is the number of valence electron orbitals.[40] They also have the problems associated with parameterization which will be explained in more detail in the section on molecular mechanics.

1.3.1.3 Molecular Mechanics

Molecular mechanics is the term used to describe the methods of computational chemistry that use empirically derived equations to describe the energy and geometry of a molecule. The method is fully empirical in that all of the equations are classical approximations of intramolecular motion and the parameters used are derived from experiments or *ab initio* calculations.[3] Just as in the two quantum mechanical methods,

molecular mechanics uses the Born-Oppenheimer approximation that allows one to treat nuclei and electrons separately.[3] In molecular mechanics, electrons are treated implicitly except in a few cases. The electronic effects are included in the empirical parameters used in the calculation.

Using a linear array of energy equations, derived from classical physics, the energy of a trial structure is calculated relative to a hypothetical molecule that has "ideal" bond angles, bond lengths and non-bonded interactions. The set of equations and the parameters used is called the force field. The energy above the ideal energy is called steric energy.[2] To find the minimum energy and geometry, the program alters the coordinates of the molecule and then reevaluates the steric energy by various mathematical methods until a minimum in the potential energy surface is reached. This process is called energy minimization.

Molecular mechanics calculations will produce a variety of information depending on the complexity of the program used. The geometry of the molecule is obtained, including bond lengths, bond angles, and interatomic distances as are the relative energies of different conformations. The steric energy and heat of formation of the conformer can also be determined depending on the program used. Depending on what type of energy minimization is used, molecular mechanics can also calculate vibrational spectra. Using the vibrational data and statistical mechanics, entropy and free energy can be determined.

1.3.1.3a Methods of Minimization

The method of minimization used determines how much time is required to do a calculation and the accuracy of the result. The minimization method is the algorithm by which the program finds the geometry of a stationary state. The first general method was that of

Wiberg.[41] His technique involved following the path of "steepest descent" of the first derivative of energy versus the atomic coordinates. The advantage of the method is that at geometries far from the minimum, the convergence is very fast. At places on the potential energy surface where the derivative is small, such as close to a minimum or in a shallow valley, convergence becomes much slower.

A more advanced technique is Newton-Raphson minimization that uses second derivatives of energy to determine the stationary states.[3] Newton-Raphson techniques require matrix inversion during calculation and these evaluations take longer than methods of steepest descent. The Newton-Raphson technique is not very efficient for geometries far from the minimum. It is however, much more accurate and works very efficiently at sites close to minima or in valleys. The matrices used in full Newton-Raphson minimization can be used to produce vibrational spectra of the molecule.

In order to overcome the long calculation time at points far from a minimum, the Newton-Raphson technique can be simplified by a block-diagonalization method.[3] This reduces the sizes of matrices that are inverted. The ideal method for minimization uses the block diagonal method or the steepest descent method for calculation far from the minimum and switches to full Newton-Raphson when the minimum is approached.

The full Newton-Raphson algorithm makes it possible to observe saddlepoints and if one is searching for transitions between conformations, this is a useful feature.[3] In these cases, determining the vibrational spectrum of the conformation to confirm that it is a local maximum is prudent. A saddlepoint has one imaginary vibrational frequency. One important point to note is that the minimization techniques only optimize the geometry in the local area

of the potential energy surface. Thus, one does not necessarily obtain the global minimum after minimization. Most of the time, the resulting conformer is a local minimum. Only by selecting the proper starting geometry, or by using a conformational searching technique, is it possible to discover the global minimum.

1.3.1.3b Force Fields

The set of equations used to describe the potential energy of a given arrangement of atoms is called a force field. The term refers to the fact that the molecule is placed into field of potential energy described by the equations and the minimum is the geometry where the forces on the molecule are at equilibrium.[2] A simple molecular mechanics program requires a combination of classical energy terms as shown:

$$E_{total} = E_{stretch} + E_{bend} + E_{torsion} + E_{nonbonded} \qquad (2)$$

The above terms are common to all force fields; usually other terms are included such as solvation terms, electrostatic terms, and cross terms.

The bond stretching term above is usually represented as a Hooke's law relation and, as a result, they only simulate the bottom of energy wells with accuracy.[2,3] To overcome this, higher order terms may be added.[42] Bond angle bending also follows a Hooke's law relation.[2,3] The torsional term is often a three-fold cosine term[2] but other more complex relations can be used.[42] The non-bonded term incorporates a variety of terms and each may require a different equation, depending on the type of interaction such as 1,3 or 1,4 van der Waals interactions or hydrogen bonding. The van der Waals forces are approximated with 6-12 or 6-10 Lennard-Jones functions or Buckingham functions.[3] These equations are

simplifications and/or approximations of the energy functions in a molecule, but they can be made more accurate in two ways: add cross terms and put higher order terms in the primary equations. Cross terms are energy terms that relate two types of motion such as bond stretching and bond angle bending. This can lead to higher accuracy with very little increase in calculation times (most calculation time is used in determining van der Waals interactions and electrostatics).

Each of the energy terms in Equation 2 are equations that contain variables for the physical quantity being modified and empirical parameters that are dependent on the species being calculated. The parameters are perhaps the most important factor in determining the accuracy of molecular mechanics calculations. The sources of the values used in the parameterization invariably come from two sources: experimental data and *ab initio* calculations.

There are two major methods for parameterization.[43] One method involves the use of a large database of data, using regression analysis to fit parameters. The other method is to take a few, simple, well-understood molecules with well-determined characteristics (geometry, relative stability, and heat of formation) and use these as the basis for the parameterization using a trial and error procedure. Often, a combination of the two methods is used.

1.3.1.3c Advantages of Molecular Mechanics

The advantages of molecular mechanics calculations arise from their simplicity.[44] This simplicity manifests itself in three major areas. The first is in the area of speed. For all molecules, molecular mechanics calculations are much faster than *ab initio* calculations. If

a chemist is interested in the structure of a particular molecule to explain the result of a reaction or a spectroscopic result, molecular mechanics is much faster and more convenient than *ab initio* methods.

Molecular mechanics calculations are inexpensive compared to quantum mechanical methods of calculation. The programs are available at relatively low cost and they can be run on common laboratory PC's. Powerful computers can increase the efficiency of molecular mechanics calculations but they are not required to obtain reasonable calculation times. In molecular mechanics, the time required for a calculation increases roughly as N^2 where N is the number of atoms in the molecule. The third advantage arising from the simplicity of the method is the fact that the concepts behind the technique are simple (i.e., using "classical" relations). This makes the results easier to understand and interpret.

Molecular mechanics calculations are quite accurate when properly parameterized. Because they are based on experimental results, they will give answers that are close to the experimental. It should be emphasized that of the three types of computational methods mentioned above, none can be said to be better than the others except on a case by case basis. Each method has its advantages and disadvantages and the required method should be determined by the experimenter. The methods are in fact complementary, for example the results of *ab initio* calculations can be used to parameterize molecular mechanics force fields. Molecular mechanics results can be used to provide initial coordinates for *ab initio* calculations thus reducing the time required for geometry optimization.

1.3.1.3d Disadvantages of Molecular Mechanics

Some disadvantages of molecular mechanics stem from the empirical parameterization. The results of all molecular mechanics calculations are dependent on the quality of the parameterization. If poor or incorrect parameters are used then the results will reflect this. To overcome this one must make sure that the force field used has been correctly parameterized to solve the problem at hand.

Molecular mechanics does not result in information of an electronic nature. Thus, ionization energies cannot be determined and species that include resonance or transition states must be calculated by the introduction of SCF (self-consistent field) calculations.

The oversimplification of electronic interactions used in molecular mechanics can result in certain features not being correctly modeled unless terms are added to the force field. A good example of this is the stereoelectronic effect called the anomeric effect. In order for a molecular mechanics force field to calculate the correct bond lengths in an anomeric system, a special term has to be added.

The disadvantages of molecular mechanics mean that the user must be careful not to overinterpret the results. The user must carefully evaluate the problem and make sure that the force field used will give reasonable data.[44]

1.3.2 MM3 Force Field

There are many force fields available. A number of the force fields are used primarily to study biological molecules such as peptides, proteins, oligosaccharides and nucleic acids. Programs of this sort include AMBER[45] and CHARMm.[46]

There are force fields that are less specialized than those mentioned above. These force fields attempt to be as general as possible and are not necessarily limited to organic or bioorganic systems. The most popular of these programs are the MM family of force fields developed by Allinger and co-workers over a three-decade period.[3,42,47,48]

The history of the development of the MM force field and a detailed discussion of the equations and principles involved have been well documented.[3,42,47,48] The most recent, publically available, version of the program is MM3(96). Several comparisons of the various force fields have been done and the MM programs are usually considered among the most accurate.[49-51]

1.3.2.1 MM3(94)

MM3(94) is termed a class II force field and was state of the art when the work in the following chapters was performed.[52] The term class II is used, because the equations used are not the basic energy functions used in earlier force fields. The MM3 force field contains higher order functions and cross terms that refine the calculation and produce more accurate energies. Recently, results from the MM4 force field have been published.[53-57] MM4 contains additional cross-terms and is termed a class III force field.[53]

The details of the MM3(94) force field are well documented in the literature.[42,47,48] The force field is continually evolving. The program can be easily modified and the creators encourage experiment with the parameterization especially for species that are not well parameterized. This allows for a great deal of flexibility. MM3 and its predecessors have been used by a large number of researchers in a wide range of chemical areas to help solve structural problems.

All of the work presented later in this thesis that involves molecular mechanics was done with the MM3(94) force field. The major focus of the work is on the reparameterization of torsional energy terms for some oxygen and sulfur containing moieties. The general term for torsional energy in the force field is given as in Equation 3, where V_n (kcal/mole) is an empirical parameter (torsional constant) and ω is the dihedral angle (see Equation 3).

$$E_{torsional} = \frac{V_1}{2}(1 + \cos\omega) + \frac{V_2}{2}(1 - \cos 2\omega) + \frac{V_3}{2}(1 + \cos 3\omega) \qquad (3)$$

Each of the three terms above can be visualized as having a physical meaning.[43] Positive values of V_1 stabilize *anti* conformations. This reflects phenomena, such as residual dipole-dipole interactions and van der Waals interactions not taken into account by their respective terms. The V_2 term usually arises in bonding situations involving p orbitals. The V_2 term will stabilize eclipsed conformations such as those in alkenes and can be described as resulting from π overlap. The V_3 term is related to residual steric repulsions as for V_1 above and antibonding interactions. When V_3 is positive, staggered conformations will be stabilized. The differences in the three parts of the equation are well illustrated by graphs of each individual part of the equation (see Figure 1.3).

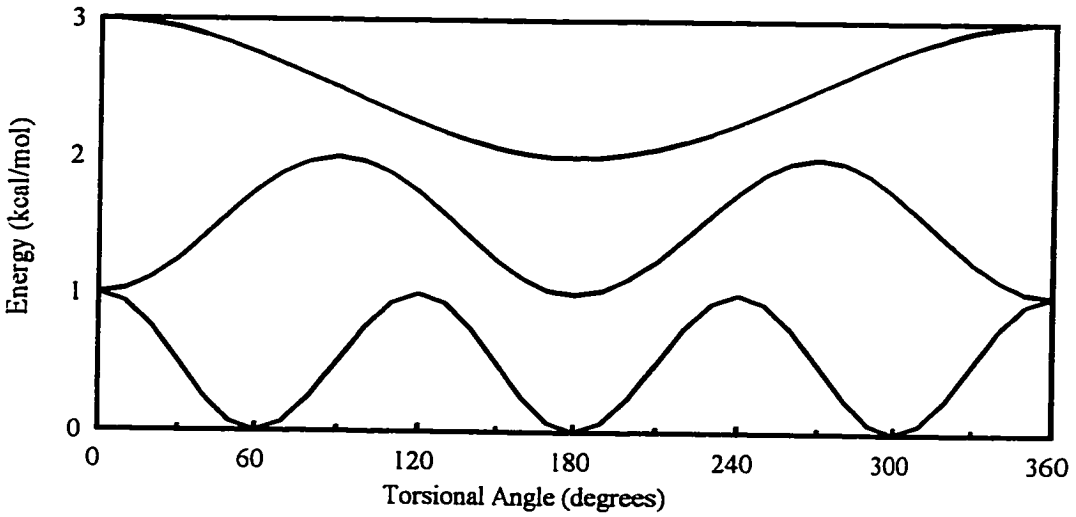

Figure 1.3 Plots of Equation 3 where (top) V_1 = 1 kcal/mol, $V_2 = V_3 = 0$ kcal/mol; (middle) V_2 = 1 kcal/mol, $V_1 = V_3 = 0$ kcal/mol; V_3 = 1 kcal/mol, $V_1 = V_2 = 0$ kcal/mol. The top and middle plots are offset by 2 and 1 kcal/mol respectively.

1.4 Summary

Conformation is a very important feature of molecular structure. Knowledge of conformation allows one to understand and predict many properties of molecules. In the conformational analysis of molecules, molecular mechanics is a very important tool. The goal of this thesis is to demonstrate methods of improving molecular mechanics calculations and to use these calculations to solve problems of a chemical and conformational nature. To this end MM3(94) will be used in conjunction with experimental techniques and stochastic search routines to perform conformational analyses and to solve problems of a conformational nature.

Chapter 2
Conformational Analysis of 1,2-Cyclohexanediol Derivatives and MM3 Parameter Improvement

2.1 Introduction

Biological recognition of cells is often mediated by the cell-surface oligosaccharides in glycoproteins or glycolipids.[9] The conformation adopted by the carbohydrate segment is a critical factor in this recognition. A determination of conformation often requires an examination of the possible conformers so they can be compared to the experimental data. Therefore, it is highly desirable to accurately model the conformations adopted by carbohydrates in order to enable the development of mimics for medicinal purposes and to understand the forces that affect carbohydrate conformation.[8,58]

As mentioned in Chapter 1, the computer program MM3 is one of many molecular modelling programs using empirically parameterized force fields. MM3[42,47] has been considered the state-of-the art for modelling organic molecules in the gas phase.[45] The MM3 force field is very well parameterized for many types of atoms in a variety of bonding arrangements and it has been used successfully in the examination of the conformations of carbohydrates.[59-61] It also contains a well parameterized function to simulate the anomeric effect which is very important in modelling carbohydrates. The use of the MM3 force field in calculating oligosaccharide conformations has been reviewed by Woods.[62] It is pointed out that MM3 is an excellent method for determining geometries and heats of formation for single molecules.

One of the most important terms in the force field for determining oligosaccharide geometries is the O-C-C-O torsional term. A hexopyranose unit in an oligosaccharide contains 5 O-C-C-O torsions. The major factor affecting O-C-C-O torsions is the *gauche* effect.[63-65] This effect is the extra stabilization of the *gauche* conformer of an ethane fragment bearing two electronegative atoms due to the interaction between the atoms. The effect is strongest in 1,2-difluoroethane.[6,7] Successful torsional parameters for the O-C-C-O unit will take into account the *gauche* effect. In addition to the *gauche* effect, intramolecular hydrogen bonding (when possible) can stabilize *gauche* conformations. Thus, for an accurate parameterization, the stabilizing effects of hydrogen bonding must be examined in addition to the *gauche* effect.

Molecular mechanics force-fields evaluate the energy of a conformation as the sum of a number of classical terms (see Section 1.3.1.3b);[3] those for non-bonded energy, bond compression and stretching, electrostatic effects, bond-angle bending, stretch-bend and bend-bend cross terms, and torsional effects are included in the MM3 force field. Most of the parameters required for each of the terms in this calculation have been well-tested for MM3 and cannot be changed without major implications for the rest of the force-field. In fact, the O-C-C-O torsional term is the one term that can be used to improve the agreement for carbohydrates without influencing the performance of the force-field for other types of molecules.

Allinger *et al.* first detailed the MM3 force-field for alcohols and ethers, including ethylene glycol derivatives in 1990[66] and a recent reevaluation of the part of the force-field for

compounds containing the O-C-C-O unit is incorporated in MM3(94).[67] They have also reexamined and improved the hydrogen bonding term in the force field.[67]

Grindley *et al.* used MM3(89) and MM3(92) to study the chair-boat conformational equilibria of derivatives of 1,6-anhydro-β-D-glucopyranose and found the agreement obtained very unsatisfactory.[68] The O-C-C-O torsion was reparameterized with some success but the experimental data available for the reparameterization were limited. Much of the parameter development for O-C-C-O containing molecules for MM3 was based on *ab initio* results for 1,2-dimethoxyethane (**1**), a molecule for which the experimental evidence about the populated conformations varied widely with the phase on which the measurement was made and on the technique that was used.[69,70] *trans*-1,2-Dimethoxycyclohexane (**2**) was also used as a model compound for parameterization but the experimental evidence showed what appeared to be a curious solvent dependence.[71]

In order to reparameterize the O-C-C-O system in MM3(94), structurally simple model compounds are required. The acquisition of accurate experimental data for molecules in which the relative populations of conformers can be measured unambiguously is also desirable. In addition, similarity to carbohydrate structures is important for the aim of modelling carbohydrates.

The simplest model of the O-C-C-O torsion is compound **1**. Although the experimental data for this compound are ambiguous (see below), it is still the best model. The ideal model for meeting both the first and second criteria above is *trans*-1,2-dimethoxycyclohexane (**2**). Conformational results from the literature (both experimental and theoretical) are presented below.

2.1.1 Experimental and Theoretical Results for Model Compounds

2.1.1.1 1,2-Dimethoxyethane (1)

2.1.1.1a Experimental Results

Fuchs *et al.* provide an excellent review of the literature to 1994.[69] A note on the three letter nomenclature of the conformers is in order at this point (see Figure 2.1 and 2.2). For the torsional unit RO-C-C-OR' the first and last letters refer to the R-O-C-C and R'-O-C-C torsional angles respectively. The central letter refers to the O-C-C-O torsional angle. The *g'* symbol indicates a *gauche* conformer in the counter-clockwise direction.

In the solid phase, compound **1** is found in the *aga* conformer exclusively.[72] An infrared study of **1** in an argon matrix revealed that the *aaa*, *aga*, and *agg'* were present and that the *aaa* was most stable.[73] The stability of the *agg'* was explained as the result of a 1,5-CH···O interaction. In the liquid phase various examinations have been performed by infrared[72,74] and NMR[75-77] spectroscopy and measurement of dipole moment.[78] The results indicate that the conformers with O-C-C-O *gauche* are most stable by 1.7-6.3 kJ/mol, but the conformational mixture is quite complex. More recent work by Dutkiewicz[78] using measurements of dielectric constants found the *g* conformer to be more stable by 0.4 kJ/mol.

Gas phase results for **1** are quite variable. Electron diffraction data[79] give a best fit for a mixture primarily composed of *agg'* > *aga* > *aaa*. Gas-phase NMR spectroscopy[80,81] showed the *gauche* conformer to be more stable by 1.7 kJ/mol. Infrared spectroscopy of gas phase **1** found *aaa* to be most stable followed by *agg'* (the energy difference between the two conformers was 1.3 kJ/mol).[82]

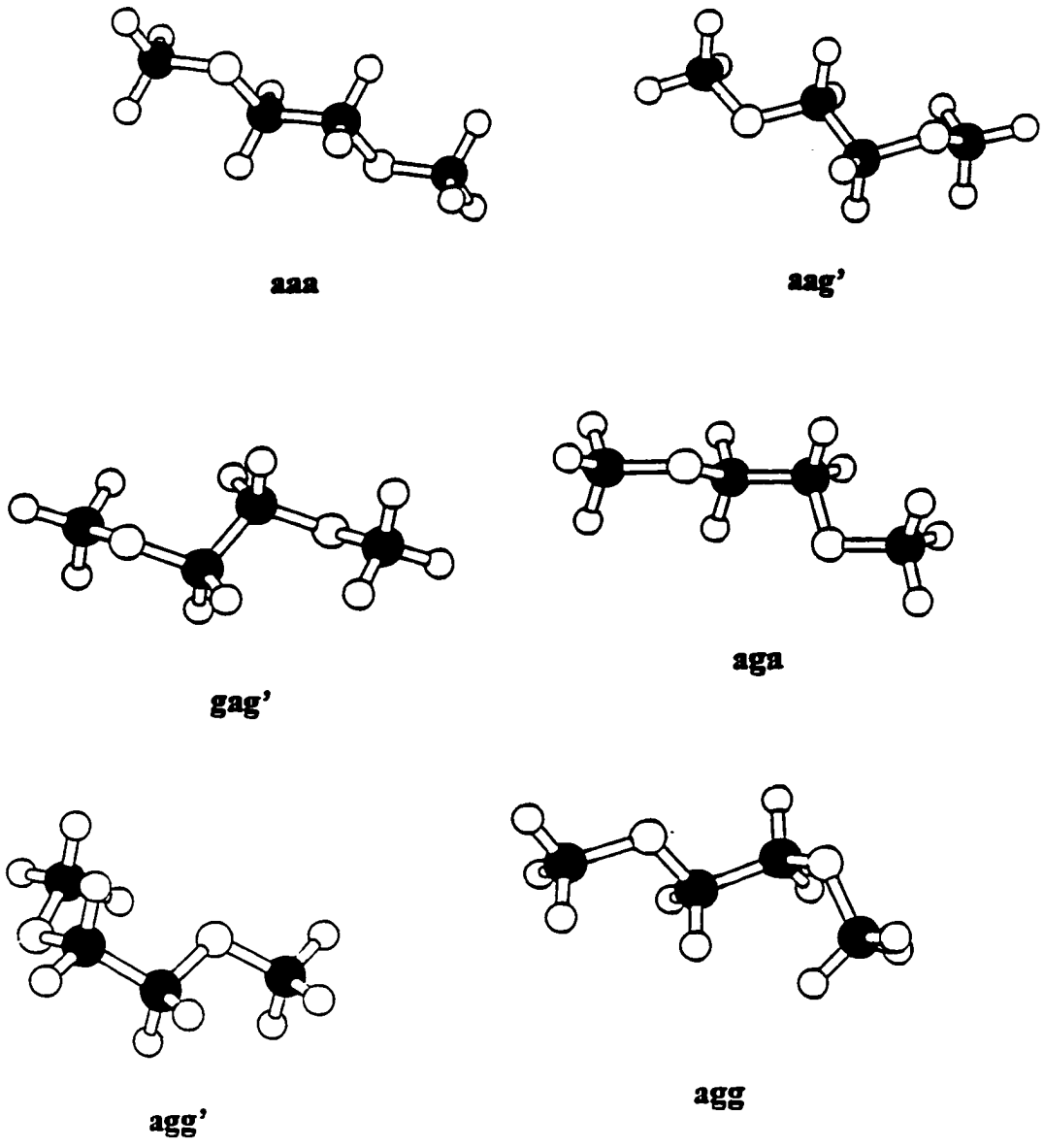

Figure 2.1. ATOMS diagrams of the most populated rotamers of 1,2-dimethoxyethane (**1**).

2.1.1.1b Theoretical Results

Ab initio calculations have been performed on **1** using a wide range of basis sets ranging from 3-21G to 6-311+G(3df).[69] Table 2.1 contains the results of the more recent (and higher level) calculations. In general, basis set effects were important and the key to obtaining good convergence was through the use of polarization and diffuse functions and the use of correlation energies.[69]

Table 2.1 *Ab initio* Results for 1,2-Dimethoxyethane (**1**)

Method	Energy (kJ/mol)			Reference
	aaa	*aga*	*agg'*	
MP2/6-31G*//3-21G*	0.0	2.3	0.6	83
MP3/6-311+G*//HF/6-311+G*	0.0	2.1	2.2	84
MP2/6-311++G**//6-31G*	0.0	0.88	--	85
MP2/6-311+G(3df)//HF/6-311+G(3df)	0.0	0.80	--	69
MP2/D95+(2df,p)//SCF/D95+(2df,p)	0.00	0.42	0.96	86

Molecular dynamics simulations of **1** in both the gas and liquid phases indicate that the gas phase shows a slight preference for the *aaa* conformer, but in the liquid phase or in solution, the *gauche* conformers are favoured.[87,88]

2.1.1.2 *trans*-1,2-Dimethoxycyclohexane (2)

There was a dearth of experimental data for *trans*-1,2-dimethoxycyclohexane and there have been no theoretical calculations. The equilibrium constants at 193 K had been obtained from integration of ^{13}C NMR spectra in CS_2 and dichloromethane-d_2.[71,89] These results showed that the O-C-C-O *gauche* conformer was favoured by 1.2 kJ/mol in CS_2 and

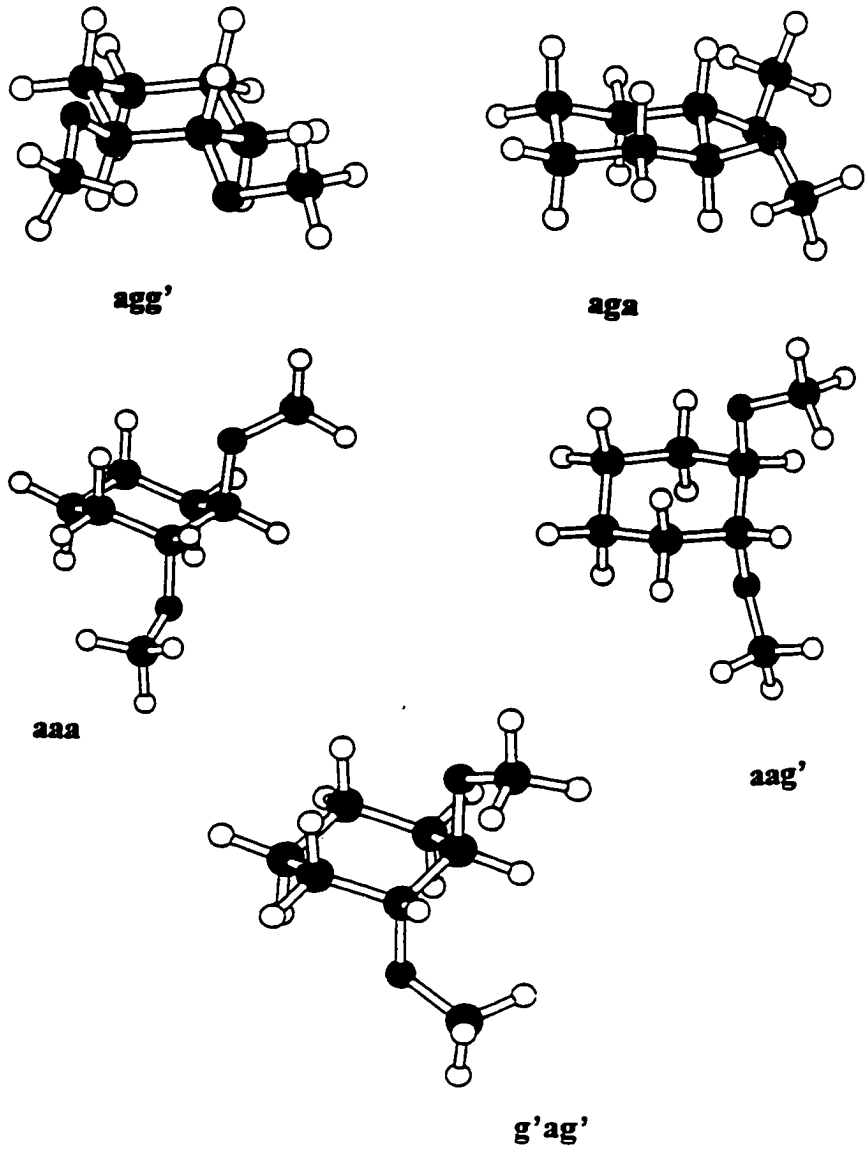

Figure 2.2 ATOMS diagrams of the most populated rotamers of *trans*-1,2-dimethoxy-cyclohexane (**2**).

4.4 kJ/mol in CD_2Cl_2. These results were intriguing in that they seemed to indicate that the equilibrium was highly solvent dependent.

2.1.2 Summary

Accurate parameterization of the O-C-C-O torsional term is a prerequisite for MM3(94) to model carbohydrates. Previous parameterizations have proven to be unsatisfactory in modelling both simple and complex O-C-C-O containing compounds. The goal of this research is to determine the equilibrium properties of *trans*-1,2-dimethoxycyclohexane and use this data in conjunction with previous data for compound **1** to reparameterize the O-C-C-O term in the MM3(94) force field. The results of this parameterization will be tested and applied to various test cases.

2.2 Results and Discussion

2.2.1 Conformational Equilibrium of *trans*-1,2-Dimethoxycyclohexane

2.2.1.1 Experimental Determination of Conformational Stability

trans-1,2-Di[^{13}C]methoxycyclohexane was prepared by reacting the dianion of *trans*-1,2-cyclohexanediol with [^{13}C]methyl iodide. In order to ensure that accurate intensities were obtained from ^{13}C NMR peak areas and to obtain information about molecular aggregation, carbon relaxation times were measured on non-degassed samples in acetone-d_6 and in pentane using the inversion recovery sequence. These are listed in Table 2.2.

Table 2.2 ^{13}C NMR Chemical Shifts and Relaxation Times for *trans*-1,2-Dimethoxycyclohexane (**2**)

Carbons	Diequatorial conformer (**2e**)				Diaxial conformer (**2a**)		
	δ^b (ppm)	$T_1{}^a$ (s)	$T_1{}^b$ (s)	$T_1{}^c$ (s)	δ^b (ppm)	$T_1{}^b$ (s)	$T_1{}^c$ (s)
C1, C2	83.6	13.3		2.7	75.8		2.9
C3, C6	30.1	6.2		1.1	23.9		*d*
C4, C5	24.2	6.2		0.90	19.9		0.71
OMe	56.9	13.5	0.90	3.3	55.7	1.19	3.3

[a] For a 0.5 M solution in acetone-d_6 at 293 K. [b] For a 0.5 M solution in acetone-d_6 at 193 K. [c] For a 0.5 M solution in pentane at 193 K. [d] Could not be measured because of signal overlap.

If motion of a molecule is isotropic and the dominant mechanism for spin-lattice relaxation is dipole-dipole then the T_1's of a ^{13}C nucleus should be indirectly proportional to the number of hydrogens attached to the carbon (e.g. $T_1(CH_2) = \frac{1}{2}T_1(CH)$).[90] After removal of multiplicity effects, relaxation times for all of the cyclohexane carbons in a particular

solvent at a particular temperature fit this pattern (see Table 2.2). This is consistent either with isotropic motion or with motion about an axis joining the mid-points of the C1-C2 and C4-C5 bonds. The latter motion might be observed if aggregates were formed through alignment of either C-O bond moments or molecular dipoles in associated molecules and the motion of the aggregate was restricted along all axes other than the axis mentioned above (see Figure 2.3). Motion of the aggregate along other axes would result in different correlation times (τ_c) and thus different T_1's for the cyclohexane carbons. Therefore the motion of the molecule is either isotropic or restricted within an aggregate.

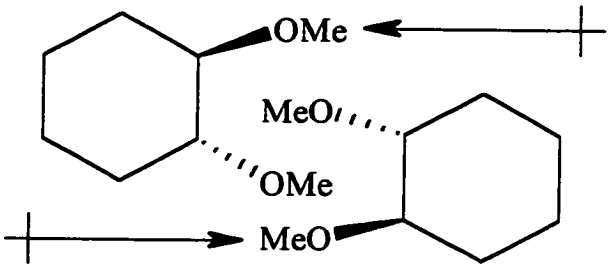

Figure 2.3 Structure of possible aggregate of **2** and the position of the molecular dipoles. The cyclohexane rings are in the diequatorial conformation.

If association did occur, it would be most important in the least polar solvents at low temperature. It would also be much more important for the diequatorial than the diaxial conformer because of the much larger molecular dipole in the former conformer and because steric effects would disfavour association in the latter. However, the T_1 values are nearly identical for the same carbons of the two conformers in pentane at 193 K. This evidence indicates that molecules of **2** are not strongly aggregated in solution and motion of these conformers of **2** is close to isotropic.

2.2.1.2 Conformational Equilibria of 2

The position of the equilibrium depicted in Figure 2.4 between the diequatorial and diaxial conformations was measured at 193 K by deconvolution of the ^{13}C NMR signals of the methoxy carbons of **2** recorded using an inverse gated decoupling sequence. With this decoupling technique, NOEs are not obtained and peak areas are directly proportional to the amount of compound present. The integrations can be used to provide equilibrium constants and these are related to energy by Equation 4. Results are reported in Table 2.3.

$$\Delta G^{o} = -RT\ln K \qquad (4)$$

The position of this equilibrium had been measured previously[71] in carbon disulfide and in dichloromethane-d_2 and the current results are in excellent agreement with the previous measurements, which are also given in Table 2.3.

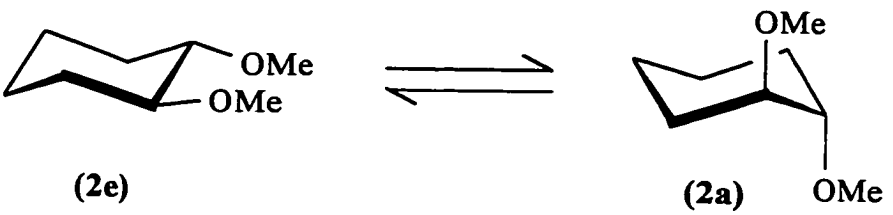

(2e) **(2a)**

Figure 2.4 The equilibrium between the diequatorial (e) and diaxial (a) conformations of *trans*-1,2-dimethoxycyclohexane (**2**).

To provide further evidence against aggregation effects, the effect of the concentration of **2** on the equilibrium was evaluated at different concentrations in pentane at 193 K. Percentages of the diequatorial conformer found by deconvolution of the methoxy carbons were: 57.1, 57.3, 55.4, and 56.2 % in 0.250, 0.125, 0.0625, and 0.031 M solutions,

respectively. The results show that the equilibrium was not influenced by concentration and confirmed that aggregation effects could be neglected.

Table 2.3 Conformational Equilibria for *trans*-1,2-Dimethoxycyclohexane (**2**)

Solvent	ϵ		% Dieq[a] (**2e**)	ΔG° (kJ/mol)[b]	ΔG° lit[a,c] (kJ/mol)
	298 K	193 K[d]			
Pentane	1.8	2.0	57.2 (±1.0)	0.46 (±0.08)	---
Toluene-d_8	2.4	2.7	72.0 (±1.0)	1.51 (±0.08)	---
CS_2	2.6	2.9	65.6 (±1.0)	1.05 (±0.08)	1.17
THF-d_8	7.6	10.1[e]	67.2 (±1.0)	1.13 (±0.08)	----
CD_2Cl_2	8.9	15.0	95.0 (±1.0)	4.70 (±0.3)	4.44
Acetone-d_6	20.7	32.5	80.0 (±1.0)	2.22 (±0.08)	----
Methanol-d_4	32.7	54	90.2 (±1.0)	3.60 (±0.2)	----

[a] For 0.5 M solutions at 193 K. [b] For the equilibrium (**2e**) ⇌ (**2a**). [c] Ref. 71 [d] Calculated from data in ref. 91. [e] Temperature dependence adjusted using slope for dimethyl ether.

2.2.1.3 Solvent Effects

The equilibrium favoured the diequatorial conformer **2e** in all solvents with percentages ranging from 57 to 95 % with more polar solvents favouring this more polar conformer to a greater extent. Solvent effects on conformational equilibria have been studied extensively[92-94] and have been related to the dipole and quadrupole moments of the conformers. Polar solvents help stabilize the molecular dipole of the equatorial form by reducing the potency of the electrostatic repulsions. Evaluation of dipole and quadrupole moments for **2** is difficult because the various methoxy rotamers (see below) each have different dipole and quadrupole moments and their individual populations are unknown. Plots

of the ΔG^{o} values against various measures of solvent polarity, including $(\epsilon-1)/(2\epsilon+1)$, only gave correlations with r values > 0.9 against E_T[93] (r = 0.96) and ϵ (r = 0.95), using either the room temperature or 193 K ϵ values, and only if the value for dichloromethane was omitted.

It is well-known that aromatic solvents often appear to be more polar than predicted by their ϵ values in plots of this type.[93,95] For the plot of ΔG^{o} values against ϵ (193 K values), the correlation coefficient improved from 0.95 to 0.987 when the value for toluene was omitted. The equation for this plot was $\Delta G^{o} = 0.0524\epsilon + 0.617$. Also, chlorinated solvents often deviate from plots of conformational energies against ϵ but the extent of deviation is larger here than previously noted.[93,94]

2.2.2 Parameter Development

Parameter development was based on conformational stabilities of compounds **1** and **2**. Because the experimental results for **1** are ambiguous, it was decided to use the energy difference between the *aaa* and *aga* conformations from high level *ab initio* calculations for parameter development. High-level *ab initio* calculations (see Table 2.1) give values of 0.4 to 0.8 kJ/mol for the equilibrium *aaa* ⇌ *aga*. When vibrational and temperature corrections were included to give ΔG values they ranged from 0.4-1.2 kJ/mol.[84,85] The lack of electron correlation during geometry optimization for all of these calculations may mean that the actual energy difference between these two conformers has not been duplicated by calculation yet. The energy used as the goal for parameterization was a compromise value of 0.6 kJ/mol.

The difference in stability between the diequatorial and diaxial conformers of **2** in pentane at 193 K (0.50 kJ/mol) listed in Table 2.3 was the other energy used for parameter

development. The pentane value was used because it would be the experimental value closest to the gas phase value. Rotamers of **2** are shown in Figure 2.2.

New torsional parameters for the O-C-C-O moiety were produced by systematic adjustment of each of the parameters (V_1, V_2,and V_3 in Equation 3 see Section 1.3.2.1) until satisfactory energy differences were obtained between the *aaa* and *aga* conformers of 1,2-dimethoxyethane and the diequatorial and diaxial conformers of *trans*-1,2-dimethoxycyclohexane. Further fine tuning of the parameters was performed by adjusting the V_3 term until a reasonable value (60.8°) of the heavy atom torsional angles in 1,4-dioxane was obtained. The standard parameters give 59.9°[67] and the electron diffraction value is 57.9°.[96,97]

The new V_2 and V_3 are fairly similar to the old values (-2.50 and 1.25 versus -2.00 and 1.90, respectively). The major change in the parameters is the large increase in the size of the V_1 term from 0.50 originally to 3.00 which is necessary to make the diequatorial conformation of **2** less stable relative to the diaxial conformation. Large V_3 terms improve the geometry but they decrease the *gauche* preference of **1**. It is possible to obtain excellent agreement with the experimental energy differences for both **1** and **2** by making the V_3 term negative but the geometries obtained for these molecules become extremely poor. The source of the *gauche* preference for **1** lies in the V_2 term. In the original MM3(94) parameters, the large V_3 parameter determines the geometry while the lack of a substantial V_1 term allows for duplication of the *gauche* preference. Introduction of a much larger V_1 term counteracts much of the *gauche* effect obtained through the V_2 term for **2**.

During the parameterization, it was noticed that when the parameters stabilized the *aga* conformation of **1** sufficiently, then the diequatorial conformer of **2** was overstabilized.

This observation must arise from small deficiencies in either the hydrocarbon or the ether part of the MM3(94) force-field but the precise source of the problem cannot be determined easily. The parameters obtained are a compromise in that they reproduce the *gauche* preference of **1** as much as possible without overstabilizing the diequatorial conformation of **2**.

The parameters obtained here are similar to those proposed in 1993 by Tsuzuki[84] for MM2 where a V_1 term with a value of 3.964 was parameterized using high level *ab initio* results on 1,2-dimethoxyethane including minima and saddlepoints for rotation. Tsuzuki obtained a rotational barrier of 39.77 kJ/mol for dimethoxyethane at the MP3/6-311+G//HF/6-311+G* level; the calculated value using the new parameters was in excellent agreement at 40.3 kJ/mol. The value obtained using the standard MM3(94) parameters was considerably lower, 32.5 kJ/mol.

Fuchs and coworkers also developed new parameters for MM3(92) in which the V_2 term is increased to -1.5 and a conformationally dependent bond-shortening of the central bond in the O-C-C-O unit is introduced.[69] Here, MM3(94) was altered to allow treatment of some carbon atoms differently than the rest and a new carbon type was defined to allow introduction of different parameters for desired carbon atoms only. The modified program gave results identical to those of the unmodified program when the parameters were identical. However, the suggested[69] alteration of the torsional parameters did not give improved results for *trans*-1,2-dimethoxycyclohexane. During parameter development, alterations of the equilibrium default C-C bond lengths in a conformationally dependent manner as detailed above were also evaluated. The results were mixed; 0.2 kJ/mol worse for **1** and 0.4 kJ/mol better for **2**. Thus, this approach with its added complexity was not pursued further.

2.2.2.1 1,2-Dimethoxyethane (1)

The energies obtained for the various rotamers of **1** and **2** are summarized in Tables 2.4 and 2.5. The free energies shown in these tables were calculated using the unmodified (other than the new parameters for the O-C-C-O torsional term) MM3(94) program using the default dielectric constant of 1.5. The result for the *agg'* conformer of **1** points out the need for a properly parameterized force field to perform molecular mechanics calculations. The MM3(94) force field does not have a term to describe the C-H···O attraction. Thus the ΔH^{o} for the *agg'* rotamer is calculated too high. The ΔG^{o} for the *agg'* conformer of **2** appears to simulate the stability induced by the C-H···O interaction but this too is probably an underestimation of the strength of the interaction.

MM3(94) calculates entropies for molecules using statistical mechanics from the vibrational spectra calculated by the MM3 program.[47] The entropies for each of the rotamers in Tables 2.4 and 2.5 were corrected for symmetry, optical isomerism, and internal rotation in cases where the MM3 program does not give the correct answers.[84] The internal rotation correction was calculated using tables produced by Pitzer and Gwinn.[98] This procedure gave a value of 14.93 J/mol/K for the rotation of a methoxy group at 298 K. The enthalpies of formation and corrected entropies were determined relative to the lowest energy Me-O-C-C rotamer of a given O-C-C-O conformation. These values were then used to determine ΔG^{o} values for the Me-O-C-C rotameric equilibria and hence equilibrium constants and rotamer mole fractions. The mole fractions could then be used to calculate the entropy of mixing due to the different rotamers for a given O-C-C-O conformation using Equation 5 where n is the number of rotamers considered and x_i is the mole fraction of rotamer i.

$$S_{mix} = -R\sum_{i}^{n} x_i \ln x_i \qquad (5)$$

After the most populated rotamers of each O-C-C-O conformation and their entropy of mixing were determined, their enthalpies and entropies were then used to obtain the free energy difference between the *anti* and *gauche* conformers.

Table 2.4 Relative Energies of 1,2-Dimethoxyethane (**1**) Conformers

Rotamer (multiplicity)[b]	ΔH° (kJ/mol)	ΔS° (J/mol/K)	ΔG° (298 K) (kJ/mol)	ΔE(lit)[a] (kJ/mol)
aaa (1)	0.00	0.00	0.00	0.00
aag (4)	7.36	19.4	1.59	5.98
aga (2)	4.14	5.23	2.59	0.58
agg' (4)	9.03	15.9	4.31	0.96
agg (4)	12.3	18.9	6.74	6.32
gag' (2)	14.6	16.6	9.71	12.9
gag (2)	14.4	9.20	11.6	13.1
ggg' (4)	16.9	17.1	11.8	7.78
ggg (2)	20.1	3.46	19.1	6.86
g'gg' (2)	*c*	*c*	*c*	10.1

[a] From D95+(2df,p) level *ab initio* calculations; see ref. 86. [b] Multiplicity refers to the number of equivalent rotamers. [c] This conformation was not a minimum using the modified MM3(94) force-field.

Table 2.5 Relative Energies of *trans*-1,2-Dimethoxycyclohexane (**2**) Conformers

Rotamer (Multiplicity)[a]	ΔH° (kJ/mol)	ΔS° (J/mol/ K)	ΔG° (193 K) (kJ/mol)
agg' (4)	1.30	7.36	-0.13
aga (2)	0.00	0.00	0.00
aag' (4)	3.68	9.04	1.92
aaa (2)	2.85	-2.31	3.30
g'ag' (2)	4.18	-2.79	4.73
agg (4)	13.0	9.46	11.1
g'gg (4)	15.0	7.53	13.6
ggg (2)	24.2	-6.36	25.4
aag (4)	33.9	7.36	32.5
gag' (4)	34.4	7.20	33.0
gag (2)	54.4	-14.6	57.3
g'gg' (2)	*b*	*b*	*b*

[a] Multiplicity refers to the number of equivalent rotamers. [b] This conformation was not a minimum using the MM3(94) force field.

2.2.2.2 Solvent Effects

MM3 treats solvent effects by altering the bulk dielectric constant. In the equation in which the electrostatic energy is calculated, the summation of the energies arising from the interactions of the bond moments is divided by the dielectric constant. Thus, most of the changes occur as the dielectric constant changes from 1.5 to 10. The preference for the diequatorial conformer of **2** was calculated to increase with increasing solvent polarity as observed but the changes did not match the observations well; at a dielectric constant of 2.9

(CS_2, 193 K), ΔG° was 3.3 kJ/mol (1.0 kJ/mol observed), at 10.1 (THF, 193 K), ΔG° was 3.6 kJ/mol (1.1 kJ/mol observed) , and at 54.0 (methanol, 193 K), ΔG° was 3.7 kJ/mol (3.5 kJ/mol observed).

2.2.3 Applications of the New Parameters to Ethers

Some applications of the new parameters (3.00, -2.50, and 1.25 for V_1, V_2, and V_3, respectively) are found in Tables 6-11. Unless otherwise noted, the energies in the tables are for the equilibria in which *gauche* O-C-C-O conformations are converted to *anti* conformations at 298 K. The new parameters give considerably improved agreement with experiment when compared with results obtained using the standard values present in MM3(94) (see Table 2.6).

2.2.3.1 2-Isopropyl-5-methoxy-1,3-dioxane

Equilibria between the *cis*- and *trans*- diastereomers of 2-isopropyl-5-methoxy-1,3-dioxane (**3**) (see Figure 2.5 and Table 2.6) have been studied in numerous solvents by Eliel, Abraham, and coworkers.[92,95,99] The experimental values for ΔG° for this equilibrium going from axial to equatorial (or *g,g* to *a,a*) in nonpolar solvents like *n*-hexane, cyclohexane, or CCl_4 are large and negative (-4.4, -4.3, and -3.8 kJ/mol, respectively) as was calculated here using the modified parameters. The standard MM3(94) parameters overstabilize the *gauche* conformation and as a result give a small positive energy difference. Abraham and coworkers[92] developed a solvation model that evaluated the interaction between calculated conformer dipole and quadrupole moments and the solvent and hence obtained the gas phase energy difference for the equilibrium. The results from the modified parameters fit the gas phase value (-5.2 kJ/mol)[92] slightly better than the solution value.

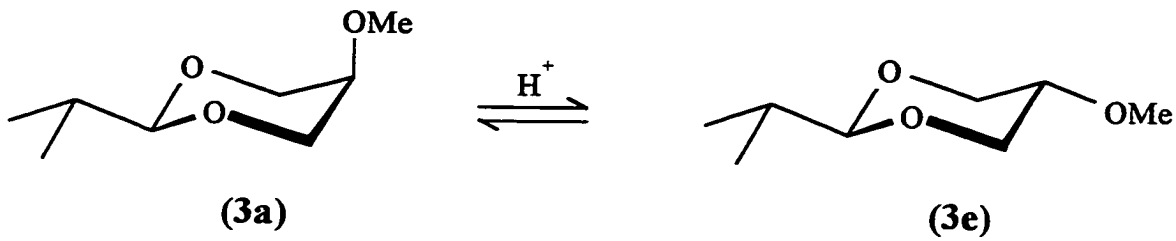

(3a) (3e)

Figure 2.5 Equilibrium of 2-isopropyl-5-methoxy-1,3-dioxane (**3**) diastereomers

2.2.3.2 1,2-Dimethoxy-2-methylpropane (4)

The results are of similar quality for the conformational equilibrium of 1,2-dimethoxy-2-methylpropane (**4**) (see Figure 2.6 and Table 2.7). The experimental values were determined by ^{13}C NMR spectroscopy in cyclohexane.[100] The standard MM3(94) parameters overcompensate for the *gauche* effect resulting in the excessive favouring of the *gauche* conformation. The new parameters favour the *anti* conformation slightly for **4**, in good agreement with the experimental result.

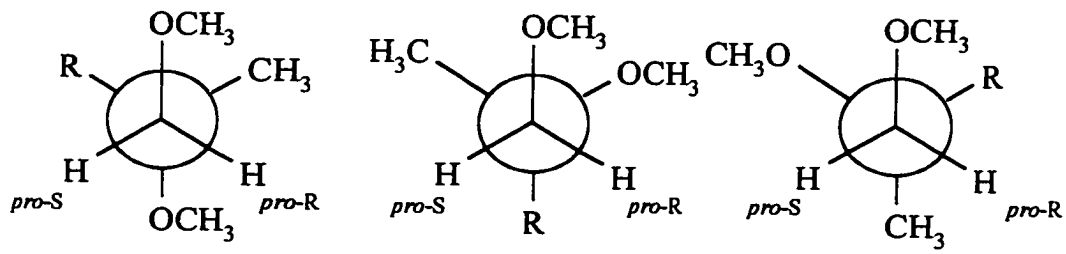

a g g'

Figure 2.6 Conformers of 1,2-dimethoxy-2-methylpropane (R=CH_3) (**4**) and 1,2-dimethoxypropane (R = H) (**5**). Note that for (**4**), the *gauche* and *gauche'* conformations are identical.

Table 2.6 Conformational Energies of Diethers Containing O-C-C-O Units

Compound	ΔG° (exp) (kJ/mol)	ΔG° standard (kJ/mol)	$\Delta\Delta G^\circ$ MM3(94) (kJ/mol)	ΔG° new (kJ/mol)	$\Delta\Delta G^\circ$ MM3(94) (kJ/mol)
1,2-dimethoxyethane	-0.4 to-0.8[a]	2.7	3.3	-2.0	-1.4
1,2-dimethoxyethane (rotational barrier)	39.8[b]	32.5	7.3	40.3	-0.5
trans-1,2-dimethoxycyclohexane	0.46[c]	7.7	7.2	1.8	1.3
1,2-dimethoxy-2-methylpropane	-2.2[d]	3.8	6.0	-1.2	1.0
1,2-dimethoxypropane	1.6[e]	0.8	0.8	5.9	4.3
	0.5[f]	-2.6	-3.1	2.2	1.7
5-methoxy-2-isopropyl-1,3-dioxane	-4.4[g]	1.8	6.2	-8.0	-3.6
	-5.2[h]	1.8	7.0	-8.0	-2.8
1,3,5,7-tetraoxadecalin	2.5[i]	-7.7	10.2	7.2	4.7
	19.6[j]	20.8	1.2	28.3	8.7
cis-6-methoxymethyl-2-methoxytetrahydropyran	2.5[k]	-2.8	-5.3	2.0	0.5
	4.7[l]	-8.6	-3.6	6.4	-1.7
Ave. $\lvert\Delta\Delta G^\circ\rvert$ (kJ/mol)			5.1		2.6

[a] For the equilibrium, *aga* ⇌ *aaa* by *ab initio* methods, see text. [b] By an MP3/6-311+G//HF/6-311+G* calculation.[84] [c] For the equilibrium, **(2e)** ⇌ **(2a)** in pentane at 193 K. [d] For the equilibrium *g* ⇌ *a* in cyclohexane.[100] [e] For the equilibrium *a* ⇌ *g* in cyclohexane-d_{12}, see text. [f] For the equilibrium *a* ⇌ *g'* in cyclohexane-d_{12}, see text. [g] For the equilibrium **(3a)** ⇌ **(3e)** in hexane.[92] [h] For the equilibrium, **(3a)** ⇌ **(3e)** corrected to the gas phase.[92] [i] For the equilibrium, *trans* ⇌ *cis*-in calculated at the MP2/6-31G*//6-31G* level,[69] see text. [j] For the equilibrium, *trans* ⇌ *cis*-out calculated at the MP2/6-31G*//6-31G* level,[69] see text. [k] For the equilibrium, *a* ⇌ *g* calculated at the HF/6-31G* level,[101] corrected for polarization and electron correlation, see text. [l] For the equilibrium, *a* ⇌ *g'* calculated at the HF/6-31G* level,[101] corrected for polarization and electron correlation, see text.

2.2.3.3 1,2-Dimethoxypropane (5)

As can be seen in the first and last columns of Table 2.7, the new parameters do not stabilize the *gauche* conformations of 1,2-dimethoxypropane (**5**) (see Figure 2.6) sufficiently to match the reported[102] experimental results. However, there is considerable uncertainty about the experimental determination of the conformational mixture present for **5**, which was calculated from $^3J_{H,H}$ values from gas phase NMR spectra of the derivative of **5** with the methoxy groups deuterated.[102] The experimental spectrum pictured in Figure 3 of that paper,[102] which shows the ABC part of the $ABCX_3$ pattern, is not very well resolved, thus there is significant error associated with their iterative solution. Also clearly visible in the experimental spectrum but not reproduced in the simulated spectra were bulges on the inside

Table 2.7 Relative Free Energies of 1,2-Dimethoxy-2-methylpropane (**4**) and 1,2-Dimethoxypropane (**5**) Conformers

Compound	Conformer	ΔG° (exp)[a] (kJ/mol)	ΔG° (exp)[b] (kJ/mol)	ΔG° (exp)[c] (kJ/mol)	ΔG° standard MM3(94) (kJ/mol)	ΔG° new MM3(94) (kJ/mol)
4	OCCO *a*		0.0[d]		3.8	0.0
	OCCO *g*		2.2[d]		0.0	1.2
	OCCO *g'*		2.2[d]		0.0	1.2
5	OCCO *a*	0.0	0.0[e]	0.0	0.0	0.0
	OCCO *g*	3.4	3.7[e]	1.6	0.8	5.9
	OCCO *g'*	-2.1	0.0[e]	0.5	-2.6	2.2

[a] In the gas phase.[30] [b] From data in cyclohexane-d_{12}. [c] In cyclohexane-d_{12} using coupling constants derived from the equation of Haasnoot *et al.*[103] [d] From ref. 100. [e] Derived using coupling constants from ref. 102.

and outside of the two large central peaks of the BC part of the pattern. The broadness of the lines and the inaccuracy of the simulation casts doubt on the coupling constants obtained.[102]

To obtain more reliable values for the coupling constants of **5**, an ^{1}H NMR spectrum in cyclohexane-d_{12} (0.08 M) was recorded at 500 MHz. The resulting $ABCX_3$ pattern was then analysed with the iterative program LAME8.[104] The final iteration included 110 of the 123 transitions and 99.9% of the total intensity. Figure 2.7 shows the agreement achieved and the results of this analysis are found in Table 2.8. Note that the conventional labelling for the spin system (e.g., the highest frequency is labelled A) has been used, not the system used previously.[102] The previous analysis had $^3J_{AB} > {}^3J_{AC}$ by 1.3-1.8 Hz at different temperatures. In the current results, $^3J_{AB}$ is equal to $^3J_{AC}$ within the calculated uncertainty. Simulation of the gas phase spectrum using the coupling constants obtained for the cyclohexane-d_{12} solution and chemical shifts from the gas phase spectrum reproduced the 345 K spectrum shown very well including the bulges evident on the central peaks that were not reproduced in the original simulation.[102]

Table 2.8 ^{1}H NMR (500 MHz) Data for (*R*)-1,2-Dimethoxypropane (**5**) in Cyclohexane-d_{12} (0.08 M)[a]

	Chemical Shifts (δ)[b]		Coupling Constants (Hz)		
Proton(s)	Shift (ppm)	Uncertainty		Coupling	Uncertainty
A (methine)	3.346	0.005	$^3J_{AB}$	5.53	0.037
B (*pro*-S)	3.328	0.005	$^3J_{AC}$	5.55	0.034
C (*pro*-R)	3.130	0.005	$^3J_{AX}$	6.27	0.021
X_3 (methyl)	1.060	0.005	$^2J_{BC}$	-9.41	0.037

[a] Data obtained from iterative fitting using LAME8.[104] [b] The chemical shifts of the methoxy groups were 3.276 and 3.252 ppm.

The new coupling constants were then used to determine the fractions of each conformer present in solution using equations 6-8, where the *f* values are the mole fractions of the three conformations, A is the methine proton, and B and C are the *pro-S* and *pro-R* methylene protons, respectively, in the *R* enantiomer of **5**. Miyajima *et al.* used 9.1 Hz as the value for both *anti* couplings and 2.6 Hz for all *gauche* couplings.[102] These values were taken from NMR studies on the conformationally hindered 1-methoxy-2-propanol.[105] When these values were used with the new experimental coupling constants, the populations of the *a*, *g'*, and *g* conformers were 45, 45, and 10%, respectively.

$$^3J_{AB} = f_a\,^3J_{AB_a} + f_g\,^3J_{AB_g} + f_{g'}\,^3J_{AB_{g'}} \quad (6)$$

$$^3J_{AC} = f_a\,^3J_{AC_a} + f_g\,^3J_{AC_g} + f_{g'}\,^3J_{AC_{g'}} \quad (7)$$

$$1 = f_a + f_g + f_{g'} \quad (8)$$

Haasnoot *et al.*[103] have developed an equation for calculating vicinal coupling constants involving terms for both torsional angles and electronegativities of the substituents. The H-C-C-H torsional angles for the three conformers were obtained from the MM3(94) results. These angles and the Huggin's electronegativities[106] for the substituents were used to calculate all $^3J_{H,H}$ values for each conformation with the help of a computer program incorporating the equation. The torsional angles and coupling constants obtained are shown in Table 2.9. These new coupling constants were then used to obtain the rotamer mole

fractions using equations 6-8, above. The populations of the *a*, *g'*, and *g* conformers derived were 43%, 35%, and 22%, respectively.

Table 2.9 Calculated Torsional Angles[a] and Coupling Constants[b] for 1,2-Dimethoxypropane Conformers

Conformer	*a*	*g*	*g'*
θ_{AB}	63.2°	-50.2°	168.4°
θ_{AC}	-177.9°	67.7°	-72.8°
$^3J_{AB}$	4.70 Hz	1.48 Hz	9.10 Hz
$^3J_{AC}$	10.48 Hz	1.96 Hz	1.86 Hz

[a] From MM3 calculations. [b] From the equation of Haasnoot *et al.*[103] using the calculated geometry.

The relative free energies of the conformers using both sets of coupling constants are found in Table 2.7. The results obtained from both approaches agree with the order of conformational energies obtained using the new parameters but not that obtained with the standard parameters. The best agreement is with the relative stabilities obtained from the coupling constants calculated from the equation of Haasnoot *et al.*[103] However, for this molecule, the *anti* conformation is somewhat overstabilized.

2.2.3.4 1,3,5,7-Tetraoxadecalin (6)

The relative stabilities of the conformations of the 1,3,5,7-tetraoxadecalin (**6**) isomers shown in Figure 2.8 potentially provide excellent tests of O-C-C-O torsional parameters because they contain three O-C-C-O units that adopt different geometries in each conformer. Three chair-chair conformers need be considered: the O-C-C-O units are present in 2 *aag* and 1 *gag'* arrangements in the *trans*-diastereomer **6t**; in the *O*-inside conformer **6ci** of the *cis*-

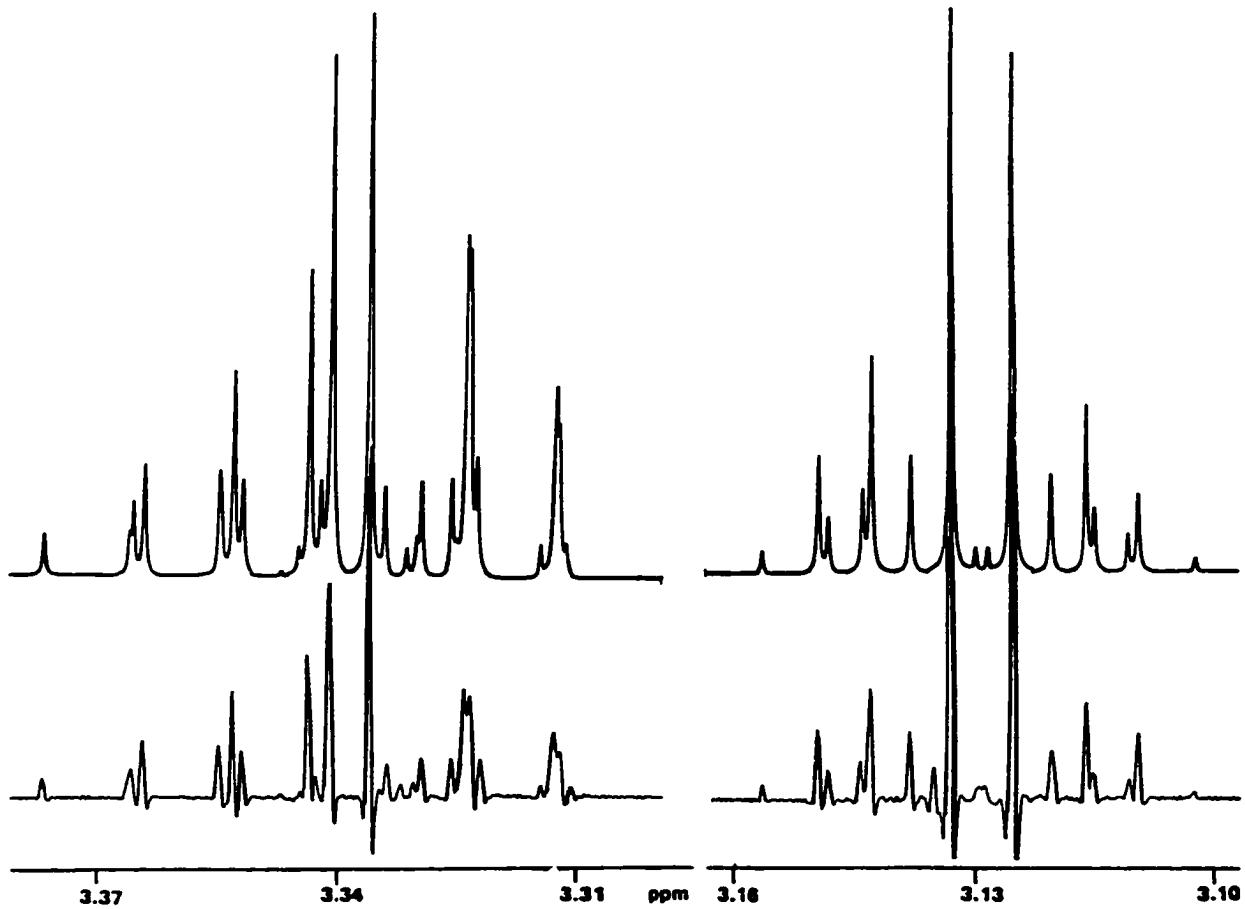

Figure 2.7 Top: simulation of the $ABCX_3$ pattern in the 500 MHz ^1H NMR spectrum of 1,2-dimethoxypropane (**5**) in cyclohexane-d_{12} (0.08 M); on the left, the AB portion; on the right, the C portion. Bottom: the experimental spectrum; on the left, the signals of the methine proton, H2 and the *pro-S* H1 proton (in the R-enantiomer); on the right, the signal of the *pro-R* H1 proton. The heights of the left and right portions are not on the same scale.

diastereomer, they are in 2 *agg* and 1 *ggg* arrangements; while in the *O*-outside conformer **6co**, they are in 3 *gag* arrangements (see Figure 2.8). Unfortunately, there are no good experimental data for this system. Fuchs and coworkers[69] suggest that **6t** is more stable than **6ci** based on fragment analysis and demonstrate that **6ci** is the only populated conformation for the *cis* isomer. They have performed MP2/6-31G*//6-31G* calculations on these conformations that confirm the above stability order. The standard MM3(94) parameters yield the wrong stability order, where **6t** is 7.7 kJ/mol less stable than **6ci**, when the *ab initio* calculations indicate that it is 2.5 kJ/mol more stable.[69] Our results (Table 2.10) are in the same order as the *ab initio* results and **6co** is similarly by far the least stable, although the differences are considerable.

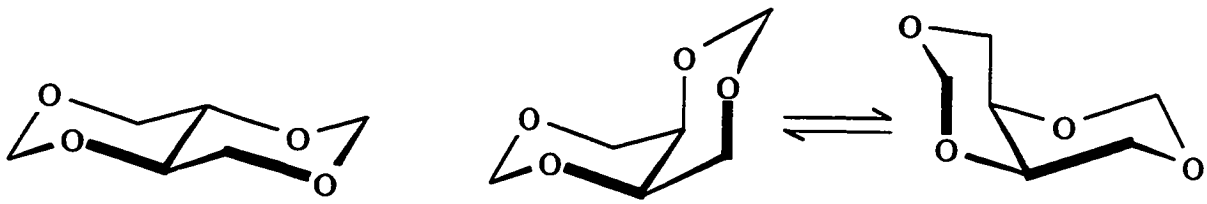

trans (**6t**) *cis*-O-inside (**6ci**) *cis*-O-outside (**6co**)

Figure 2.8 1,3,5,7-Tetraoxadecalin (**6**) conformers

Table 2.10 Stabilities (ΔH°) of 1,3,5,7-Tetraoxadecalin Conformers (kJ/mol)

Source	*trans* (**6t**)	*cis*-in (**6ci**)	*cis*-out (**6co**)
ab initio MP2/631G*//6-31G*[69]	0.0	2.5	19.6
Standard MM3(94)	0.0	-7.7	20.8
New MM3(94)	0.0	7.2	28.3

2.2.3.5 *cis*-6-Methoxymethyl-2-methoxytetrahydropyran (7)

The relative stability of rotamers about C5-C6 bond in hexopyranosides has attracted considerable attention because of its importance in the conformations of biologically significant 1,6-linked oligosaccharides.[107,108] This feature of carbohydrates has been modelled with mixed results.[107,108] A model compound for this conformational problem, *cis*-6-methoxymethyl-2-methoxytetrahydropyran (7), has recently been studied by *ab initio* methods at the HF/6-31G* level.[101] Results are compared with the enthalpy differences among the three exocyclic rotamers (see Figure 2.9) calculated by MM3 in Table 2.11. Raising the level of calculation to the MP2/6-311 +G(3df)//6-311+G(3df) caused the greater stability of the *aaa* conformer of 1,2-dimethoxyethane with respect to the *aga* conformer to decrease to 0.19 from 1.40 kcal/mol.[69] It is expected that the same effect would apply to 7. Correction of the difference between the *anti* and *gauche* conformations of 7 obtained from the 6-31G* calculations[101] for this elevation in level of theory brings the MM3 results using the new parameters into almost exact agreement with the corrected *ab initio* results as shown in Table 2.11. The standard MM3 parameters do not perform well for this molecule.

After the basis set correction mentioned above was used, higher level calculations by Tvaroška and Carver appeared in the literature.[109] As shown in Table 2.11 the corrected values were almost *exactly the same as* the ACM/dzvp//6-31G* calculations, validating the estimate and showing that the C5-C6 rotation in carbohydrates is controlled by the same factors that control 1,2-dimethoxyethane. The reproduction of the *ab initio* values by the new O-C-C-O torsional parameters was encouraging with respect to modelling carbohydrates.

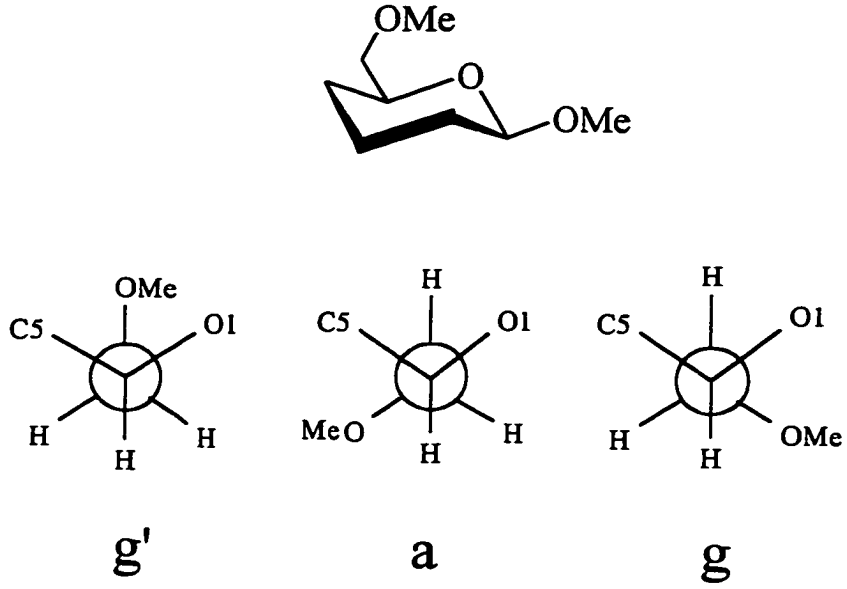

Figure 2.9 Structure of *cis*-6-methoxymethyl-2-methoxytetrahydropyran (7) and Newman projections of the exocyclic rotamers in 7.

Table 2.11 Relative Enthalpies of *cis*-6-Methoxymethyl-2-methoxytetrahydropyran (7)

OCCO Angle	$\Delta H^{o\,a}$ (calc) (kJ/mol)	$\Delta H^{o\,b}$ (calc) (kJ/mol)	$\Delta H^{o\,c}$ (calc) (kJ/mol)	$\Delta H^{o\,d}$ Std. (kJ/mol)	$\Delta\Delta H^{o\,d,e}$ Std. (kJ/mol)	$\Delta H^{o\,f}$ New (kJ/mol)	$\Delta\Delta H^{o\,e,f}$ New (kJ/mol)
a	0.00	0.00	0.00	0.00		0.00	
g	7.5	2.5	2.8	-2.8	5.6	2.0	0.8
g'	9.7	4.7	5.4	1.1	4.3	6.4	-1.0

[a] HF/6-31G*.[101] [b] Low level *ab initio* results[101] corrected by 5.0 kJ/mol for the difference between the *aaa* and *aga* conformers of 1,2-dimethoxyethane at this level of theory and at the highest level reported,[69] including MP2 electron correlation. [c] ACM/dzvp//6-31G*.[109] [d] Using standard MM3(94) parameters. [e] With respect to the ACM/dzvp//6-31G* enthalpies. [f] Using the new MM3(94) parameters.

2.2.4 Applications of the New Parameters to Systems with Significant Hydrogen Bonding

2.2.4.1 2-Methoxyethanol (8)

In addition to the factors considered for the ethers, intramolecular hydrogen bonding is important in determining conformational stabilities for both 1,2-vicinal methoxy alcohols[110-112] and carbohydrates. The two monomethoxy analogs of **1** (2-methoxyethanol (**8**)) and **2** (*trans*-2-methoxycyclohexanol (**9**)) were examined to explore the ability of the new parameters to model O-C-C-O systems with intramolecular hydrogen bonding. Microwave[113] and infrared data[114-117] are available for **8**, and two groups, Lii and Allinger [67]and Gil and Teixeira-Dias[115,116] have performed high level calculations on **8**. Four conformers are considered to have significant populations, the *aaa*, *aag*, *ggg'*, and *agg'* conformers. Here the first letter refers to the MeOCC rotamer and the last letter refers to the HOCC rotamer. The *agg'* and *ggg'* conformers contain intramolecular hydrogen bonds. Lii and Allinger obtained a value of 8.45 kJ/mol for the equilibrium *agg'* ⇌ *aaa* at the 6-31G** level.[67] Gil and coworkers' calculation at the MP2/6-31G* level gave 14.6 kJ/mol for this equilibrium, but they pointed out that the *anti* conformations become destabilized at higher levels of theory and that a second *gauche* conformer, the *ggg'* is intermediate in stability between the *agg'* and conformers with the O-C-C-O unit *anti*.[115,116] However, several infrared studies indicate that even the highest level *ab initio* calculations overestimate the *anti-gauche* energy difference; in dilute solution in non-polar solvents, various ΔH° values for equilibria between the hydrogen-bonded (O-C-C-O *gauche*) and non-hydrogen bonded conformers were

measured; 7.5 ± 1.0 kJ/mol,[114] 9.2 ± 2.0 kJ/mol[117], and 7-10 kJ/mol.[115,116] ΔG° values should be less because the hydrogen bonded conformers are more restricted.

2.2.4.2 *trans*-2-Methoxycyclohexanol (9)

trans-2-Methoxycyclohexanol (**9**) has been studied with FT-IR techniques.[112] These showed that intramolecular hydrogen bonding was important at low concentrations in non-polar solvents but the results were not quantitative. In order to obtain accurate data regarding this equilibrium (see Figure 2.10), **9** was synthesized and low temperature NMR spectra were measured in various solvents and analysed as for **2**. The results are listed in Table 2.12. Because it was not possible to measure the equilibria at low concentrations, the species on which the equilibria were measured were probably aggregates. In agreement with this conclusion, ^{1}H NMR spectra of **9** at 193 K were broad in CS_2 and THF.

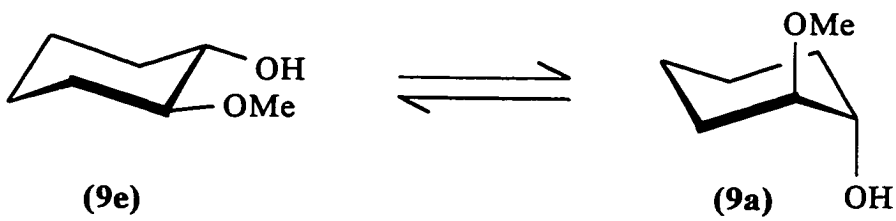

(9e) **(9a)**

Figure 2.10 The equilibrium between the diequatorial (e) and diaxial (a) conformations of *trans*-2-methoxycyclohexanol (**9**).

Table 2.12 Conformational Equilibria for *trans*-2-Methoxycyclohexanol (**9**)

Solvent	ϵ		% Dieq (**9e**)	$\Delta G^{o\,a,b}$ (kJ/mol)
	298 K	193 K[c]		
Pentane	1.8	2.0	89.8	3.5 (±0.2)
Toluene-d_8	2.4	2.7	95.2	4.8 (±0.4)
CS_2	2.6	2.9	96.5	5.3 (±0.5)
THF-d_8	7.6	10.1[d]	93.9	4.4 (±0.3)
CD_2Cl_2	8.9	15.0	>99	>7
Acetone-d_6	20.7	32.5	97.1	5.6 (±0.6)
Methanol-d_4	32.7	54	97.3	5.8 (±0.6)

[a] For 0.5 M solutions at 193 K. [b] For the equilibrium (**9e**) ⇌ (**9a**). [c]Calculated from data in ref. 91. [d] Temperature dependence adjusted using slope for dimethyl ether.

The diequatorial conformer was stabilized to a greater extent for **9** than for **2** in all solvents. At low concentrations (<0.002 M) in carbon tetrachloride or carbon disulfide, infrared spectroscopy has shown that, at room temperature, **9** exists as a mixture of the intramolecularly hydrogen-bonded diequatorial conformer and a minor, non-hydrogen bonded form.[112] It seems likely that at the higher concentrations used here aggregates will be important, particularly in non-polar solvents as they are for other ethers with hydroxyl groups on adjacent carbons.[118-120] The effect of solvent polarity on the equilibria supports this idea; plots against ϵ or E_T are not nearly as linear as for **2** and also show a lessened dependency on solvent polarity. For instance, using the ϵ values at 193 K and omitting the values for toluene and dichloromethane, $\Delta G^o = 0.0169\epsilon + 0.483$, with $r = 0.73$. Presumably this plot includes the effect of erratic lessening of aggregation as solvent polarity increases.

The parameters developed here were used to calculate ΔG° values for 2-methoxyethanol and *trans*-2-methoxycyclohexanol. The results are compared with *ab initio* results and experimental results in Table 2.13. The calculated value for **8** using the new parameters was considerably smaller than either the best *ab initio* results or results from MM3(94) using standard parameters. This arises from the large V_1 term, which as for **1**, reduces the stability of the *gauche* conformer. The difference between the results for **8** from the standard parameters and the new parameters are about the same as for **1**. The value obtained for the O-C-C-O torsional angle in the *agg'* conformer was 66.3° using MM3(94) with the new parameters, in comparison to Lii and Allinger's value of 62.1° [67] and the microwave value of 57(3).[113] The H-O-C-C torsional angle was 54°, larger than the uncertain microwave[113] value, 45(5)°. Not surprisingly, the new parameters give moments of inertia that are farther from the microwave values than the standard parameters[67] do: I_x 6.3716 (1.4% off), I_y 31.3277 (2.4%), I_z 34.4532 (1.3%).

Table 2.13 Conformational Energies of Compounds **8** and **9**

Compound	ΔG° (exp) (kJ/mol)	ΔG° standard MM3(94) (kJ/mol)	ΔG° new MM3(94) (kJ/mol)
2-methoxyethanol (**8**)	14.6[a,b], 7.5[a,c]	6.9	1.7
2-methoxyethanol (**8**)	6.3[d]	7.6	7.8
2-methoxycyclohexanol (**9**)	3.51[a,e]	14.9	9.3

[a] For the equilibrium *agg'* ⇌ *aaa*. [b] From MP2/6-31G*//6-31G* calculations.[115,116] [c] From dilute solutions by infrared spectroscopy.[114] [d] For the equilibrium *agg'* ⇌ *ggg'* from MP2/6-31G*//6-31G* calculations.[115,116] [e] For the equilibrium (**9e**) ⇌ (**9a**) from current results in pentane at 193 K.

The standard MM3(94) parameters are very poor in duplicating the experimental energy difference between conformers **9e** and **9a**. The new terms give significantly better agreement but the deviation is still large (5.8 kJ/mol). However, the direction of the deviation is opposite to that for **8**, that is, the conformer with the O-C-C-O unit *gauche* where hydrogen bonding is possible is now calculated to be more stable than observed experimentally.

2.2.4.3 Carbohydrates

Rotation about the C5-C6 bond in hexopyranosides was studied for methyl α-D-glucopyranoside (**10**), methyl α-D-galactopyranoside (**11**), and methyl 4-deoxy-α-D-*xylo*-hexopyranoside (**12**) and the results are compared with those from experimental studies[108] and MP2/6-31G* *ab initio* studies[121] in Table 2.14 (see Figure 2.11). Free energy differences between rotamers were obtained by modifying the enthalpy differences between pairs of most stable C6-O6 rotamers (those in position for hydrogen bonding) for the entropy of mixing contributions from the other C6-O6 rotamers. The MM3 calculations were performed at a dielectric constant of 80, similar to that of water, the solvent from which the NMR data is taken. A large ϵ value removes any intramolecular hydrogen bonding but does not duplicate the steric effects or electrostatic effects of solvation of the various hydroxyl groups. For all three compounds, the *tg* conformer is calculated by MM3 using the modified parameters to be much more stable than observed in water.[108]

It would appear on initial examination, that this deviation is due to the fact that the new parameters underestimate the stability of acyclic *gauche* isomers when intramolecular hydrogen bonding is involved. This, no doubt, contributes to the results, but it appears other factors are also at work.

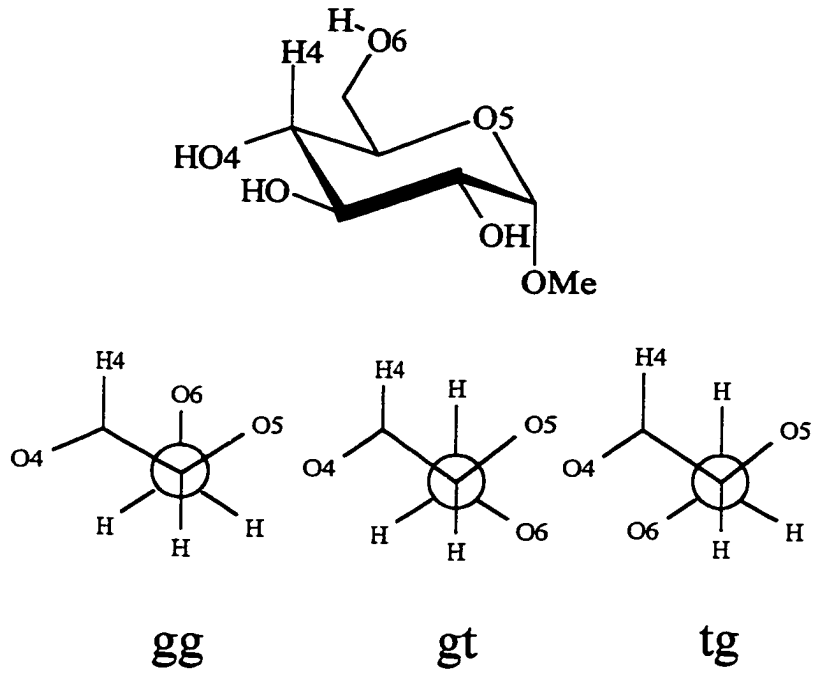

Figure 2.11 The structure and C5-C6 rotamers for methyl α-D-glucopyranoside (**10**). For methyl α-D-galactopyranoses (**11**), H4 and O4 exchange positions. For (**12**), O4 is replaced by an H.

The *ab initio* results also overestimate the stability of the *tg* rotamer to a similar extent and greatly underestimates the stability of the *gt*.[121] The standard MM3 parameters and the new parameters both overestimate the stability of the *gt* rotamer in all three cases. These two observations indicate that the poor replication of the experimental results is not entirely due to shortcomings in the parameterization. It may also include solvent effects or possible electronic effects that are not accounted for in the calculations.

It is possible that there may be significant solvent effects on the 1,3-synaxial interactions that control the stability of the *tg* and *gg* rotamers in **10** and **11** respectively. Evidence in support of this comes from the success in reproducing the rotamer populations of compound **7**, where the 1,3-synaxial interactions are absent. Experimentally, the importance of such interactions can be evaluated by considering the 4-deoxy derivative of **10**

or **11**, methyl 4-deoxy-α-D-*xylo*-hexopyranoside (**12**), for which data[108] is presented in Table 2.13. If these interactions were significant, their removal would stabilize the conformation in which they are present, *tg* for **10** and *gg* for **11**. For both **10** and **12**, the population of the *tg* conformer is too low to be evaluated accurately, so a comparison is not meaningful. The

Table 2.14 Relative Energies of Hydroxymethyl Rotamers in Methyl α-D-Glucopyranoside (**10**), Methyl α-D-Galactopyranoside (**11**), and Methyl 4-Deoxy-α-D-*xylo*-hexopyranoside (**12**) in Water

Compound	Rotamer	ΔG° (exp)[a] (kJ/mol)	ΔE[b] (kJ/mol)	ΔG°[b] (kJ/mol)	ΔG° standard MM3(94) (kJ/mol)	ΔG° new MM3(94) (kJ/mol)
10	*gg*	0.00	0.00	0.00	0.00	0.00
	gt	0.33	2.27	2.95	-3.14	-1.8
	tg	>10	-0.09	1.01	5.77	0.17
11	*gg*	3.85			5.21	6.15
	gt	0.0			0.0	0.0
	tg	5.29			6.69	1.51
12	*gg*	0.45			2.59	3.05
	gt	0.0			0.0	0.0
	tg	9.95			6.65	1.38

[a] By ^{1}H NMR in water-d_2 solutions.[122,123] [b] By *ab initio* calculations at the MP2/6-31G* level on α-D-glucopyranoside.[121]

relative stabilities of the *gg* and *gt* can be compared for **11** (*gt* 3.85 kJ/mol more stable) and for **12** (*gt* 0.45 kJ/mol more stable). In this case, the direction of change is consistent with this explanation but the size of the difference in the changes (3.4 kJ/mol) is not sufficient to explain the difference between the calculated and the experimental results, either by MM3 or by the *ab initio* method.[121] In fact, the experimental (3.4 kJ/mol) and MM3 calculated

changes (3.1 kJ/mol) are almost the same, suggesting that solvation of hydroxyl groups is not the cause of the difficulty.

Other possible mechanisms for solvent effects that would stabilize the *gg* rotamer in D-glucose could be either direct hydrogen bonding or hydrogen bonding involving one water molecule acting both as a hydrogen bond donor and as a receptor (OH6···O-H_{water}···O5) to complete a seven-membered ring. If this occurred, the 6-*O*-methyl derivative of **10** would be expected to have drastically different rotamer populations; in fact, the observed populations are almost identical to that of **10**.[108] Another possible mechanism has one water molecule acting as a hydrogen bond donor to both *gauche* oxygen atoms (O6···H-O-H···O5). If this effect were important, the position of these equilibria would be different in methanol; again, the experimental results in CD_3OD are almost identical to those in water.[108]

There does not appear to be a good explanation for this extra stability of the O-O *gauche* C5-C6 conformers with respect to the *trans* conformer in polar solvents at this time. It appears that there are specific interactions that either destabilize the *tg* conformer more than predicted and/or stabilize the *gg* and *gt* conformers. A more in-depth discussion of the factors affecting the C5-C6 rotation in D-hexopyranosides (including solvent effects) is presented in Chapter 3. The possibility of an electronic effect involving the coupling of the *gauche* effect to the anomeric effect is also discussed.

2.3 Conclusion

Using low-temperature NMR techniques, the conformational energies for the equilibria between the axial and equatorial conformers of **2** and **9** have been determined in solvents with a range of polarities. The values for **2** were then used in conjunction with theoretical and experimental data for **1** to determine new O-C-C-O torsional parameters for MM3(94). These new parameters are considerably better than those in the standard MM3(94) parameter set for reproducing experimental results on ethers. The agreement is less satisfactory when reproducing systems involving intramolecular hydrogen bonding. MM3(94) calculations, using the new parameters reproduce high level *ab initio* results for C5-C6 rotation for a model compound, but for methyl α-D-glucopyranoside fail to reproduce experimental results in which the *gg* and *gt* conformers are much more stable than the *tg* conformer. This is believed to be due to effects not accounted for in the force field.

2.4 Experimental

2.4.1 General Methods

1,2-Dimethoxyethane was dried and distilled over CaH_2 prior to use. Anhydrous methanol was obtained by reflux and distillation over $Mg(OMe)_2$. Cyclohexene oxide, ^{13}C-labelled methyl iodide, and 1,2-dimethoxypropane were purchased from Aldrich and used without further purification. *trans*-1,2-Cyclohexanediol was previously prepared by oxidation of cyclohexene with formic acid and hydrogen peroxide[124] and was recrystallized twice from ethyl acetate before use. Vacuum distillation and concentration were done under the vacuum produced by a water aspirator.

NMR spectra for identification purposes were measured on a Bruker AMX-250 spectrometer. Proton and carbon assignments were confirmed using HETCOR and COSY experiments. Chemical shifts are expressed in ppm relative to internal TMS (0.03%), or the central line of the solvent, chloroform-*d* (77.0 ppm), acetone-d_6 (^1H 2.04 ppm, ^{13}C 29.8 ppm), dichloromethane-d_2 (53.8 ppm), toluene-d_8 (20.4 ppm), methanol-d_4 (49.0 ppm), or THF-d_8 (67.4 ppm). The CS_2 sample was referenced to the CS_2 peak at 192.8 ppm and the pentane spectrum was referenced to the methyl peak of pentane at 13.7 ppm.

NMR samples for conformational analysis (0.5 M, unless otherwise specified) were prepared in 5 mm NMR tubes. The ^{13}C NMR spectra of labelled *trans*-1,2-dimethoxycyclohexane were measured on a Bruker AMX-400 with a 56° pulse, and inverse gated decoupling with a delay time of 5 s. The spectra of *trans*-2-methoxycyclohexanol were measured on a Bruker AC-250 spectrometer using a 56° pulse and an 8 s pulse delay. Temperatures on Bruker AC-250 and AMX-400 spectrometers were maintained with Bruker

B-VT 1000 and B-VT 1000E units, respectively. Processing of the spectra including automatic deconvolution (fitting the peaks to a Lorentzian function) was performed using Bruker software.

The initial structures for input into MM3 were obtained with PCMODEL. Then, either through modification of the PCMODEL files or by MM3 dihedral driving of the Me-O-C-C torsional angle, input files of all unique rotamers were created. The final energies of all conformers were obtained using full matrix Newton Raphson minimization and none had imaginary infrared frequencies. All saddlepoints had one imaginary frequency.

2.4.2 *trans*-1,2-Di[^{13}C]methoxycyclohexane (2)

trans-1,2-Cyclohexanediol (1.98 g, 17 mmol) was dissolved in dry 1,2-dimethoxyethane (35 mL). The solution was stirred and cooled in an ice bath. Excess sodium hydride (1.15 g, 48 mmol) was added slowly over 10 minutes and the mixture was stirred for 3 h. [^{13}C]methyl iodide (99%)(5.0 g, 35 mmol) was added via a syringe and stirring was continued for 12 h. An equal volume of water (35 mL) was added slowly to avoid frothing and the resulting aqueous solution was extracted with pentane (3 x 30 mL). The pentane fractions were combined, dried over $MgSO_4$, and concentrated. The concentrate was fractionally distilled to obtain *trans*-1,2-di[^{13}C]methoxycyclohexane (0.40 g, 16%) as a clear colourless liquid, bp 65-67°C/3.1 kPa (lit.[125] 75 °C/4.4 kPa). ^{1}H NMR (250 MHz, acetone-d_6) δ 1.22 (m, 4H, H-3_{ax}, H-4_{ax}, H-5_{ax}, H-6_{ax}), 1.57 (m, 2H, H-4_{eq}, H-5_{eq}), 1.87 (m, 2H, H-3_{eq}, H-6_{eq}), 2.83 (m, 2H, H-1, H-2), 3.32 (d, $^2J_{CH}$ 140 Hz, 6H, methoxy); ^{13}C NMR (62.9 MHz, acetone-d_6) δ 82.2 (C-1,6), 57.0 (2 x OMe), 28.9 (C-2,5), 23.4 (C-3,4).

2.4.3 *trans*-2-Methoxycyclohexanol (9)

trans-2-Methoxycyclohexanol was made by a literature method[126] and fractionally distilled as a clear colourless liquid, bp 80-82°C/3.2 kPa (lit.[126] 72.5-73.2/1.3 kPa). ^{1}H NMR (250 MHz, $CDCl_3$) δ 1.23 (m, 4H, H-3_{ax}, H-4_{ax}, H-5_{ax}, H-6_{ax}), 1.70 (m, 2H, H-4_{eq}, H-5_{eq}), 1.98 (m, 1H, H-6_{eq}), 2.10 (m, 1H, H-3_{eq}), 2.94 (ddd, 1H, $^3J_{12}$ 8.85 Hz, $^3J_{2,3e}$ 4.27 Hz, $^3J_{2,3ax}$ 10.68, H-2), 3.11 (bs, 1H, OH), 3.40 (m, 1H, H-1), 3.41 (s, 3H, OCH_3); ^{13}C NMR (62.9 MHz, $CDCl_3$) δ 23.8 (C-4), 23.9 (C-5), 28.2 (C-3), 32.0 (C-6), 56.1 (OMe), 73.4 (C-1), 84.8 (C-2).

Chapter 3
Conformational Analysis of Rotation About the C5-C6 Bond in D-Glucopyranosides

3.1 Introduction

Carbohydrates can be broadly defined as chiral polyhydroxy compounds. They have at least one stereogenic center and most have three or more. The majority contain at least one carbonyl functional group (e.g., ketone, aldehyde, carboxylic acid). Some carbohydrates contain other elements such as nitrogen, sulfur, and halogens.

These features allow nature to construct a wide array of structures from carbohydrate building blocks. The polyfunctionality of carbohydrates accommodates structures that involve branching and allows a wide variety of structures to be exploited.

Carbohydrates play a very important role in many biological systems. They are found in structural polymers such as cellulose (poly[(1→4)-β-D-glucopyranose]) and chitin (poly[(1→4)-2-acetamido-2-deoxy-β-D-glucopyranose]). D-Glucose is of paramount importance in metabolism; starch (amylose) (poly[(1→4)-α-D-glucopyranose]) and amylopectin (amylose with (1→6)-α-D-glucopyranose branches) are the primary store of energy in plants. In animals, D-glucose is stored as glycogen, a polysaccharide structurally identical to amylopectin except that the frequency of (1→6) branching is 10% rather than 3%. Carbohydrates also play a significant role in cell interactions.[9,127] Sperm-egg recognition is influenced by the presence of oligosaccharides in glycoproteins on the surface of the egg.[128]

A particular pentasaccharide structure which makes up about 1% of the polysaccharide heparin has been found to be responsible for its blood clotting effects.[129] Many functions of the immune system such as antibody-antigen interactions on bacterial cell walls, and blood type recognition are mediated by oligosaccharide epitopes.[130]

These interactions are rooted in the structure of the oligosaccharides. The biological response is induced after the carbohydrate moiety binds directly to another compound (i.e., a protein)[128,129] or the carbohydrate assists in the binding (e.g. in the antibiotic, vancomycin).[131] In both cases, the success of the binding is dependent on the structure of the oligosaccharide, especially the conformation adopted by the oligosaccharide. Thus, to understand the biology of these processes, or to develop new methods of enhancing or preventing these biological signals, an understanding of three dimensional carbohydrate structure is required.

The most common carbohydrates are hexoses and pentoses. These aldoses exist primarily in three isomeric forms: open chains, furanoses and pyranoses (see Figure 3.1). The pyranose forms are most common but some pentoses are regularly found in the furanose form. The most well known furanoses are the fructose moiety in sucrose, ribofuranose (in RNA) and 2-deoxyribofuranose (in DNA).

3.1.1 Conformation of Oligosaccharides

Many of the biologically important oligosaccharides that mediate interactions are composed of hexoses in their pyranose form. In order to consider the three-dimensional shape of an oligosaccharide, the points of attachment on each monosaccharide and the anomeric configuration must be known. Once these are established, there are four major points of conformation that must be determined: ring conformations, the *endo*-anomeric configurations,

the torsional angles defining the glycosidic linkages, and in the cases of hexopyranoses, the hydroxymethyl rotations.[62,132]

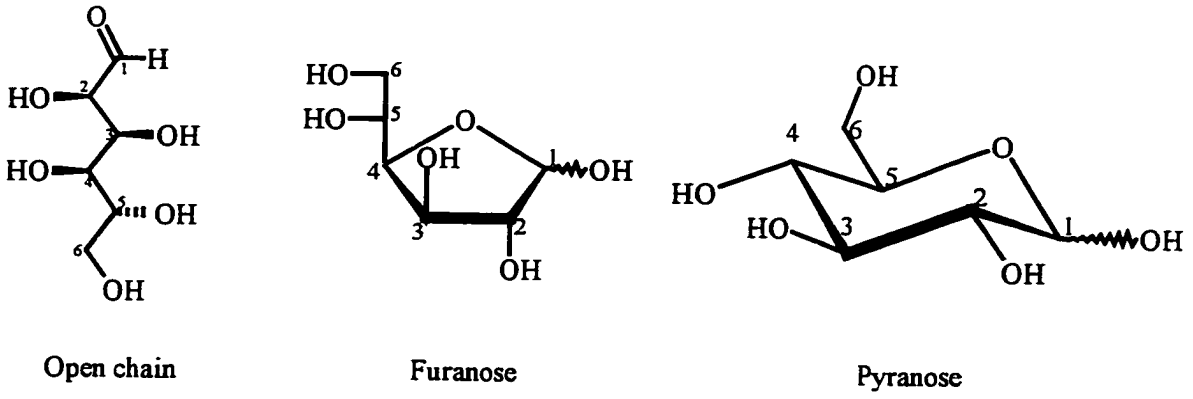

Figure 3.1 The three isomeric forms of carbohydrates illustrated by D-glucose.

Ring conformation is an internal structural feature of each monosaccharide unit. There are two possible chair conformations for a pyranose ring. They are termed the $^4C_1$ and $^1C_4$ conformations, where the numbers and their positions refer to which carbon atoms are above and below the plane defined by the other four atoms including the ring oxygen, in the chair form (see Figure 3.2). In some special cases, an envelope or skew form is favoured. The main factor in determining which of the two chair forms is the most populated is the number and size of 1,3-synaxial interactions between the substituents on the ring.

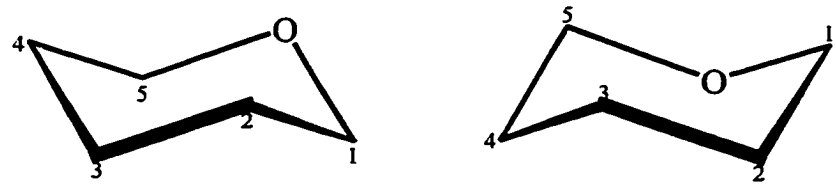

$^4C_1$ $^1C_4$

Figure 3.2 The two chair conformations of pyranose rings including the atom numbering system for pyranose sugars.

The anomeric effect is a stereoelectronic effect that occurs at carbons with geminal electronegative groups such as at C1 of an aldopyranose ring.[63,133] It is an internal property of a single monosaccharide unit. In D-aldopyranoses, the anomeric effect is an enhanced stability of the configuration at C1 where the oxygen is axial (see Figure 3.3). This enhanced stability is caused by the interaction of the nonbonding electrons of the ring oxygen with the antibonding orbital of the C1-O1 bond.[134] This is called the *endo*-anomeric effect because it takes place within the pyranose ring.

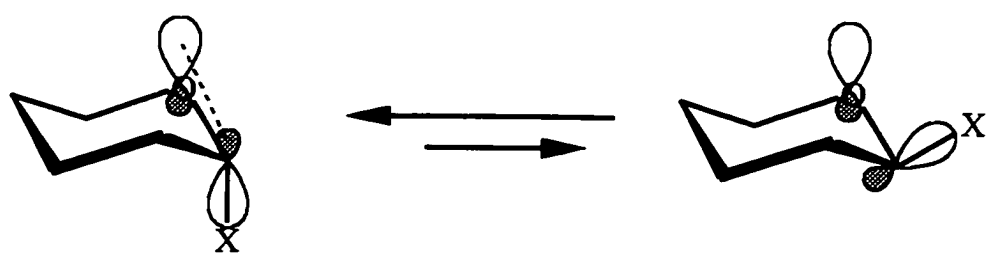

Figure 3.3 The *endo*-anomeric effect is caused by molecular orbital interactions in the axial isomer. The geometry of the orbitals in the equatorial isomer precludes stabilizing interactions.

The *endo*-anomeric effect and the $^1C_4$ and $^4C_1$ equilibrium are primarily aspects of the individual monosaccharide units in oligosaccharides. The bonds that link the monosaccharides are keys to the overall conformation of an oligosaccharide. The conformation about this linkage is defined by three torsional angles if the linkage involves a primary oxygen atom and two if the linkage involves a secondary oxygen atom (see Figure 3.4).[62]

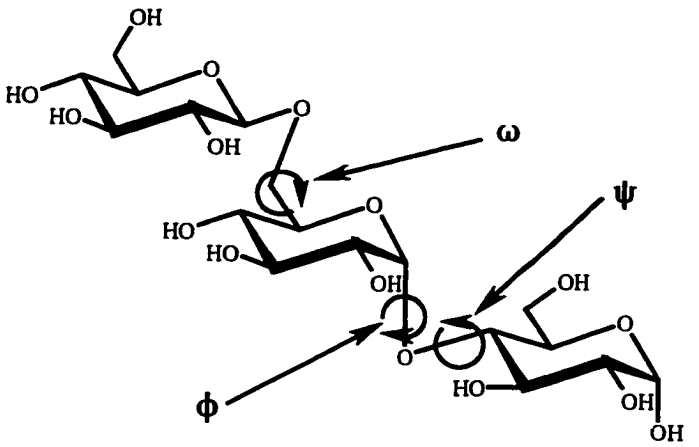

Figure 3.4 A simple D-glucose trisaccharide showing the various torsional angles of importance in determining oligosaccharide conformation.

The torsional angle ϕ is determined largely by the *exo*-anomeric effect. The *exo*-anomeric effect determines the favoured orientation of substituents on O1 in pyranoses. The nonbonding electrons on O1 interact with the antibonding orbital of the ring oxygen and C1 (see Figure 3.5). This results in an enhanced stability like that of the *endo*-anomeric effect and because of this, substituents on O1 prefer to adopt a conformation where the C-O-C-O torsional angle (ϕ) along the O1-C1 bond is *gauche* if the substituent is axial (α) and *gauche'* if the substitution is equatorial (β) in the $^4C_1$ conformation of a D-sugar. The angle ψ is a C-O-C-C torsional angle which is controlled largely by steric effects.

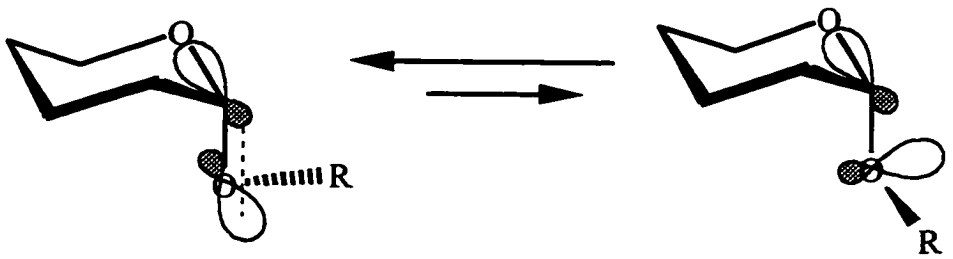

Figure 3.5 The *exo*-anomeric effect is caused by the interaction of orbitals on an exocyclic group with an antibonding orbital in the ring.

The angle ω involves both an O-C-C-C and O-C-C-O torsion. The central bond in these torsional angles is the C5-C6 bond in aldohexopyranoses. Since this angle is the primary focus of the work that follows, it will be discussed in greater detail in the following section.

3.1.2 The Hydroxymethyl Group

The C5-C6 torsional angle in D-aldohexopyranosides can assume three minimum energy values (see Figure 3.6). They are commonly named using a two-letter nomenclature system: *g* for *gauche* and *t* for *trans* (*anti*). The first letter refers to the torsional relationship between O6 and O5 (O6-C6-C5-O5). The second letter refers to the relationship between O6 and C4 (O6-C6-C5-C4). The two hydrogens on C6 are prochiral and they can be distinguished from one another using ^{1}H NMR spectroscopy. This is very important for studying the conformational equilibria of these systems. The hydrogens are labeled as shown in Figure 3.6, where "S" indicates a pro-*S* relationship and "R" is a pro-*R* relationship.

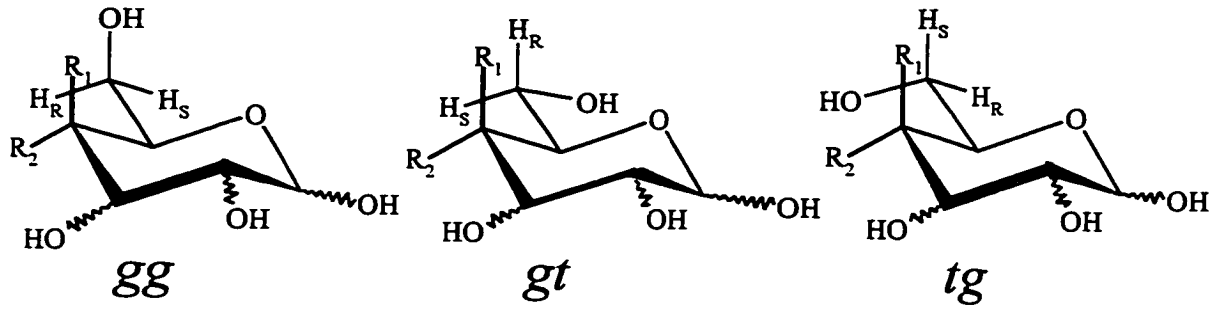

Figure 3.6 The three possible staggered rotamers of the hydroxymethyl group of a D-aldopyranose. When R_1 = H, R_2 = O the structure is *gluco*-like; when R_1 = O, R_2 = H the structure is *galacto*-like.

3.1.2.1 Experimental Methods of Rotamer Analysis

A number of experimental techniques have been used to examine the rotamer populations of hexopyranosides. The most common technique is NMR spectroscopy. Other techniques include statistical analysis of X-ray crystal data, and optical techniques such as optical rotation and circular dichroism.

3.1.2.1a X-Ray Crystallography

Statistical analyses of the X-ray crystal structures of glucose-type molecules showed *gg*:*gt*:*tg* rotamer distributions of 60:40:0 (101 molecules),[135a] and 56:43:1 (370 molecules).[135b] Similar analyses of galactose structures gave population distributions of *gg*:*gt*:*tg* = 8:58:34 (24 molecules),[135a] and 7:61:32 (84 molecules).[135b] Although this method is valuable and the results have been found to be in agreement with other techniques, it is not necessarily applicable to solution populations.

The populations determined from the statistical analysis may not reflect the relative stability of a given conformer due to crystal packing forces. For example, the crystal structure

of native ramie cellulose (I)[136] revealed that the hydroxymethyl group was only present as the *tg* rotamer. This result was due to the enhanced stability obtained when the *tg* OH group hydrogen bonded to the O2 of a neighboring glucose residue and possibly due to the fact that in the *tg* conformation, the cellulose is present in a flat ribbon-like shape that would be disrupted by other rotamer structures.[136,137]

3.1.2.1b Chiroptical Methods

Optical rotation has been used by Lemieux and coworkers[138,139] to examine the rotamer population of various hexopyranoside analogues and derivatives. They concluded that in polar solvents, the favoured rotamer for both *galacto*- and *gluco*-type sugars was *gt*. In a non-polar solvent (1,2-dichloroethane), the *tg* rotamer of *gluco*-type derivatives with OH6 free, was favored due to intramolecular hydrogen bonding to O4.[138] This result was supported by infrared spectroscopy. ^{1}H NMR spectroscopic results were found to support these findings.

Circular dichroism (CD) has been used recently to determine the rotamer populations.[140-142] In this technique, the carbohydrate is derivatized with a chromophore at O6 and at least one other site in the molecule. The couplings in the CD spectra are related to the rotamer population. This technique is qualitative and shows that the favoured rotamer for *gluco*-type sugars is *gg* followed by *gt*. As in X-ray analysis, the results are not necessarily applicable to biological systems because the chromophorically substituted compounds are not necessarily good models of unsubstituted carbohydrates.

3.1.2.1c Nuclear Magnetic Resonance Spectroscopy

The most common method used for the experimental determination of the rotamer populations is NMR spectroscopy.[108,143-149] The optical methods mentioned above both use ^{1}H

NMR spectroscopy as a supporting technique to confirm their results. The NMR spectra obtained are complex and analysis is performed with the help of iterative computer programs such as LAME8.[104] The most important data of interest are the coupling constants between H5 and the two prochiral protons (H6R and H6S). Some researchers have used NOE's to determine rotamer populations.[150,151]

The spectral coupling constants ($^3J_{5,6R}$ and $^3J_{5,6S}$) are time averages of values from each of the rotamers. These values can be related to the rotameric populations by the following set of equations (9-11) similar to Equations 6,7 and 8 (see Section 2.2.3.3), where f_x is the fractional population of a particular rotamer, and $^3J_{5,6(x)}$ is the limiting value of the coupling constant for a particular rotamer (x).

$$^3J_{5,6R} = f_{gg}\,{}^3J_{5,6R(gg)} + f_{gt}\,{}^3J_{5,6R(gt)} + f_{tg}\,{}^3J_{5,6R(tg)} \qquad (9)$$

$$^3J_{5,6S} = f_{gg}\,{}^3J_{5,6S(gg)} + f_{gt}\,{}^3J_{5,6S(gt)} + f_{tg}\,{}^3J_{5,6S(tg)} \qquad (10)$$

$$1 = f_{gg} + f_{gt} + f_{tg} \qquad (11)$$

In order to solve these equations, the limiting values ($^3J_{5,6(x)}$) must be obtained. The values of these "conformationally frozen" coupling constants can be determined by examining coupling constants of model compounds[108] where rotation is restricted or by calculating the values with Karplus type equations (see Section 1.2.3).[103,108,143,152] Model compounds are not

used often, due to the fact that torsional angles in the model compound would most certainly vary from the free rotamer. Also, the structural factors which restrict the rotation may have other effects on the coupling constants, for example bond angle distortion, which has been shown[153] to have an effect on the magnitude of coupling constants.

Karplus type relations are used to calculate the coupling constants of a given rotamer. The most used equation in the analysis of proton spectra is the Haasnoot-Altoona equation.[103] The major feature of this equation is the introduction of empirical correction terms to the traditional Karplus relation.[23] The correction terms are influenced by the number, position and electronegativity of substituents in the system.

The choice of angles used to obtain limiting values from the Karplus equation is also critical. Values derived from conformationally fixed or restricted compounds could be influenced by strain or substituent effects not present in the carbohydrates being studied. The angles derived from crystal data[143] may not necessarily be applicable to rotamers in the solution phase. One can also assume simple staggered relationships (60°, 180°, or 300°) for the torsional angles but this is an oversimplification. The best method is perhaps, the use of molecular modeling techniques.[143] The compound being studied is modeled and from the geometry of the minimum energy conformation, the torsional angles are obtained. Molecular modelling could also be used to determine the Boltzmann distribution of the coupling constants and then the weighted average of these coupling constants could be used.

Use of the NMR method requires that the spectrum be analyzed properly. An important factor in this is the identification of the two prochiral protons. In the past, chemical shift arguments were used based on assumed rotamer populations, but this method has been

shown to be unreliable in cases where the oxygens are substituted.[154] Ohrui and coworkers have successfully synthesized stereospecifically deuterated compounds by photochemical bromination followed by reduction in order to determine the correct assignment.[155,156] This results in unequivocal determination of the chemical shift assignment of the prochiral protons.[143,145,147,148,157-162] Other means of determining the correct assignment includes the NOE[149,151] and selective decoupling experiments.[163]

If compounds that are ^{13}C-substituted at the C4 position are used, $^{3}J_{CH}$ values can be used to determine the rotational populations.[164-166] The Karplus relations for these compounds are not nearly as well parameterized as those of ^{1}H-^{1}H couplings,[165] but ^{13}C-^{1}H coupling constants can be used to confirm the results of ^{1}H NMR methods and are very useful as a tool in assigning the H6S and H6R resonances.[165,166]

3.1.2.2 Values for the Rotamer Populations

The rotamer populations determined by ^{1}H NMR spectroscopy are fairly consistent. For *gluco*-type structures, the *gg:gt:tg* is 70-45:55-30:25-0.[108,142,143,147,148,159,161,162,167-169] Similar results are obtained for both glucose and mannose derivatives.[144,145,149,170-172] For *galacto*-type structures, the ratio is 20-10:70-60:30-10.[108,144,146-148,158,160,168-170,173,174] These ranges are a result of variations which occur due to differences in methods for the calculation of limiting values and in spectral resolution and analysis. They are also the result of structural variation and other variables explained below.

3.1.2.3 Factors Affecting The Hydroxymethyl Group Rotamer Population

The factors that determine the populations of the rotamers around the C5-C6 bond are varied.[108] The *gauche* effect[64] is believed to play a large role in determining the rotamer

populations. The constitution and configuration at C4[161,171,172] play a very significant role as does the configuration at the anomeric center.[174] Intramolecular hydrogen bonding can affect the stability of a rotamer.[138,139,163,175] The polarity of the solvent can also affect the rotamer populations by enhancing or diminishing dipole-dipole and coulombic interactions.

3.1.2.3a 1,3-Synaxial Interactions

1,3-Synaxial interactions between O6 and O4 are the most obvious factors affecting the rotamer populations. This can be seen in the low populations of the rotamers that have strong 1,3-diaxial interactions, the *tg* in *gluco*-type structures and *gg* in *galacto*-type structures. Bock and Duus[108] compared the populations of methyl α-D-glucopyranoside (**10**) with methyl α-D-*xylo*-hexopyranosid-4-ulose(hydrate) (**13**)(see Figure 3.7) and found that the additional hydroxy group destabilized the *gg* by 3.3 kJ/mol, but this is not sufficient to explain the negligible population of the *tg* rotamer in glucose derivatives.

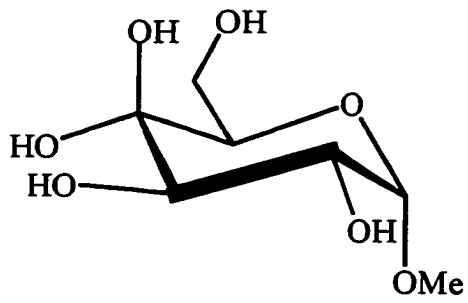

Figure 3.7 Methyl α-D-*xylo*-hexopyranosid-4-ulose(hydrate) (**13**)

3.1.2.3b The *Gauche* Effect

The work of Bock and Duus[108] and others[142,146,168,174] strongly supports the idea that the major determinant of the *gg* and *gt* rotamer population is the *gauche* effect.[63,64] The *gauche* effect is an electronic effect that stabilizes (or destabilizes, depending on the substituent), the

gauche conformations of compounds containing vicinal electronegative atoms. The effect can be described as the result of molecular orbital interactions similar to those in the anomeric effect. The specific interaction involved in the *gauche* effect of X-C-C-X moieties is the interaction between the bonding orbital of a C-H bond and the antibonding orbital of the C-X bond.[65,133,176,177] In the *anti* rotamer there are no C-H bonds antiperiplanar to a C-X bond. In both of the *gauche* rotamers there are two C-H bonds in position for maximum interaction.

3.1.2.3c Substituent Effects

The nature of the substituent on C6 is an important factor in determining rotamer populations. These effects are not unique unto themselves but are the results of modifying the steric and *gauche* effects mentioned above. Bock and Duus[108] showed that, when pH sensitive substituents such as phosphates or amines were present on C6, the rotameric populations were pH dependent. The source of this dependency could not be ascertained due to the large number of influences on the hydroxymethyl rotation such as hydrogen bonding, steric effects, *gauche* effects, and solvation. Jansson *et al.* studied the rotamer population of a series of (1→6)-linked disaccharides and found that the D-glucose disaccharides generally had higher populations of the *gg* rotamers than the monosaccharides.[178] A similar trend was discovered for D-galactose disaccharides with both the *gg* and *tg* rotamers being more stable in the disaccharides.[178]

The effects of substitution at sites adjacent to the hydroxymethyl group were also observed. Amino substitution at C4 induced pH dependency as did substitution of O5 with an sp^3 hybridized nitrogen atom. NMR spectroscopy on *N*-linked oligosaccharides[171] and

glucose trisaccharides[161,162] showed that large substituents at O4 had significant influence on the relative stabilities of the *gg* and *gt* rotamers.

3.1.2.3d Anomeric Effect

The configuration at the anomeric center has a significant effect on the position of the rotameric equilibria. In *gluco*-like structures, α anomers tend to have larger *gg* populations than β anomers.[108,178] This has been attributed to the effect of a through space interaction between O1 in the α position and H5. In the hyperconjugative model of the *gauche* effect, H5 is represented as a proton in the resonance structure for the *gg* rotamer the α oxygen stabilizes this proton via a through space electrostatic interaction and thus the *gg* rotamer is stabilized.

A recent circular dichroism study of β-glucopyranosides by Morales and coworkers[142] examined the effect of chiral aglycons on the rotamer populations. The results indicated that the amount of *gg* rotamer decreased as the *exo*-anomeric effect for β-glucosides increased (with increasing pK_a of the aglycon). Their work also indicated that rotamer population differences resulting from enantiomeric aglycons were the products of a similar mechanism. Due to steric effects, aglycons with the *S* configuration resulted in stronger *exo*-anomeric effects, thus decreasing the *gg* population.

Buck and de Vries[146,174] obtained evidence that the β anomer has a higher *tg* population than the α anomer in galactose derivatives. They postulated that the difference was attributable to a modulation of the *gauche* effect by the anomeric effect. They also demonstrated that the *tg* population was dependent on the pK_a of the aglycon, where a higher pK_a resulted in a higher *tg* population.

3.1.2.3e Solvent Effects

Solvent effects and hydrogen bonding are interrelated and thus are difficult to resolve into two separate interactions. Most NMR studies have been performed almost exclusively in aqueous solutions or in polar solvents such as methanol, DMSO or acetonitrile. Other examinations of solvent effects considered only the hydrogen bonding properties of solvents and only used H_2O or DMSO as solvents.[108,168,175]

The effects of solvent on the rotamers of galactose have been examined by de Vries and Buck. They used ^1H NMR spectroscopy to analyze the rotamer populations for methyl 2,3,4-tri-*O*-methyl-α- (**14a**) and β-D-galactopyranoside 6-(dimethyl phosphate) (**14b**)[146] and the 1→6 glycosidic linkage in the α (**15a**) and β (**15b**) anomers of methyl 2,3,4-tri-*O*-methyl-6-*O*-(2,3,4,6-tetra-*O*-acetyl-β-D-galactopyranosyl)-D-galactopyranoside (see Figure 3.8).[174]

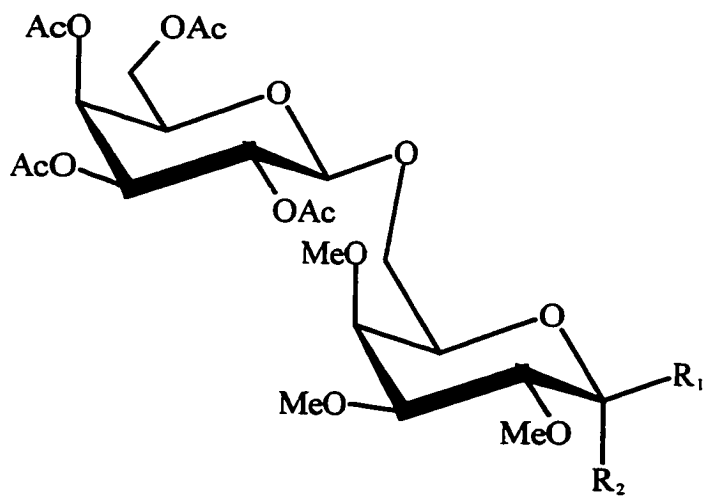

Figure 3.8 α (R_1=H, R_2=OMe) and β (R_1=OMe, R_2=H) anomers of methyl 2,3,4-tri-*O*-methyl-6-*O*-(2,3,4,6-tetra-*O*-acetyl-β-D-galactopyranosyl)-D-galactopyranoside (**15**).

Rotamer populations were studied in a wide range of solvents from CCl_4 to water-d_2. The results showed that as solvent polarity went up, the population of the *gg* rotamer (whose

population is largely determined by 1,3-synaxial interactions) stayed constant. The populations of the other two conformers (*gt* and *tg*) varied as the polarity changed. The *gt* rotamer increased in stability as polarity increased at the expense of the *tg* rotamer. This was attributed to increased electrostatic interactions in non-polar solvents between O6 and O5 in the *gt* rotamer. These results indicated that there is a strong, solvent effect which is not related to hydrogen bonding.

There has not been a comprehensive study of solvent effects on glucose derivatives. Nishida used deuterated glucose derivatives[143] in polar and non-polar media but only three solvents were evaluated (water, DMSO, and chloroform). The non-polar experiments were performed with acetylated and benzoylated derivatives; thus substituent effects on the rotamer equilibrium could not be eliminated. The results of these experiments did not indicate the presence of any significant solvent effects; but due to the possibility that substituent effects compete with solvent effects, the results are not unambiguous.

Hydrogen bonding involving OH6 has not been fully examined. Bock and Duus[108] explored hydrogen bonding with ^{1}H NMR spectroscopy in polar solvents and did not find significant amounts. A study of glucose in DMSO by Angyal[175] also pointed to this conclusion. Intramolecular hydrogen bonding is important because it can play a role in the stability of the *tg* population in *gluco*-like structures. Infrared spectroscopy, optical rotation and NMR spectroscopy[138,139,163] showed that in pyran and cyclohexane models of *gluco*-like carbohydrates, there was significant intramolecular hydrogen bonding in non-polar solvents.

3.1.2.4 Theoretical Analysis of the Hydroxymethyl Rotation

Theoretical calculations have been performed on glucopyranoses to examine the factors affecting the hydroxymethyl rotation. The three major techniques used are *ab initio* molecular orbital calculations, semiempirical molecular orbital calculations and molecular dynamics (MD). Some molecular mechanics studies have been performed,[59,179-181] but, due to the empirical nature of the technique, they are not applicable to the following discussion.

Ab initio calculations on D-glucose were first performed by Polavarapu and Ewig.[182] Their calculations were performed at the 4-31G and 6-31G* levels. The results showed that, on the basis of electronic energies alone, the most favored rotamer of α-D-glucose was *tg* followed by *gg*. Incorporation of entropies and temperature correction gave populations of *gg*≈*tg*>*gt* in the gas phase. Similar results were obtained by Brown and Wladkowski[121], who used higher level basis sets (from 6-31G* to 6-311G**, with and without electron correlation). They found that the *gg* rotamer was 4.23 kJ/mol more stable than the *tg* and 8.16 kJ/mol more stable than *gt*. The difference from experimental values was attributed to solvent effects that were not accounted for in the calculation.

Due to computational constraints, other calculations concentrate only on the *gt* and *tg* rotamers.[60,183] Salzner[183] found *tg*>*gt* by 0.84 kJ at the HF/6-31G* level. Solvent effects were invoked to explain the discrepancy from experiment. Barrows *et al.*[60] performed high level calculations (cc-pVTZ) on the two rotamers and found that *gt*>*tg*. When solvent effects were included, the results showed that the population of *tg* was dependent on solvent. The energy of the *tg* rotamer increased by 2.5 kJ on going from a *n*-hexadecane environment to an aqueous environment. Other *ab initio* calculations on substituted pyrans[184] showed that the

most favored conformations were *gt* and *gg* with intramolecular hydrogen bonding occurring in both conformers.

Recently, Tvaroška and Carver have presented an *ab initio* study of methyl 2,3,4-trideoxy-α- and methyl 2,3,4-trideoxy-β-D-*glycero*-hexopyranoside and their 6-*O*-methyl derivatives (compound 7 and its *trans*-isomer, see Section 2.2.3.5).[109] The results of the calculations suggest that the *gauche* effect does not play a role in determining the rotamer populations around the C5-C6 bond. They found that the *gg* and *gt* rotamers were the most stable because of intramolecular hydrogen bonding to O5 and that this stability was reduced when solvent effects were introduced.

The main use of semiempirical calculations has been the analysis of solvent effects on the rotamer equilibrium. Tvaroška[185,186] has performed PCILO (Perturbative Configuration Interaction using Localized Orbitals) calculations in various solvents. These simulated solvents contained cavities in which the solute was placed. The cavities had properties that were specific for each solvent. The results are very close to the experimental values and showed a strong dependence on the polarity of the solvent. For α-D-glucopyranose in non-polar solvents, the *gg* conformer dominates, but as the solvent polarity increases the *gg* population decreases and that of *gt* increases. For β-D-glucopyranose, the *gg* rotamer dominates, but as the solvent polarity increases, the population of the *gg* rotamer increases at the cost of *tg* rotamer while that of the *gt* rotamer stays constant. These trends were explained as the result of solvent polarity decreasing coulombic repulsions. Cramer and Truhlar[187] concluded from their AM1 calculations that the *tg* rotamer is favored in the gas phase but in aqueous solution, the rotamer is destabilized by 2.1 kJ.

Another important method for the theoretical calculation of rotamer population is molecular dynamics. Although the force fields employed are empirically parameterized, they have the advantage of being capable of modeling solvent effects.

Brady's initial analysis of glucose in the gas phase[188] produced rotamer populations of *gt>tg>gg* where intramolecular hydrogen bonding played an important role in stabilizing the *tg* rotamer. Later simulations in aqueous solution[189] indicated that *tg* was the only significant rotamer. This result was interpreted as a result of weaknesses in the force field. Kroon[190] ran molecular dynamics of methyl β-D-glucoside in water and *in vacuo*. The results showed that the *tg* rotamer was most stable in the gas phase but in aqueous solution this rotamer became less stable than the *gt* by 15 kJ/mol. Other molecular dynamic experiments[191-194] were in excellent agreement with experimental data. These calculations also showed that solvation was a very important factor in determining the rotamer population.

3.1.3 Summary

Many factors influence the rotameric population of the hydroxymethyl group, including 1,3-synaxial interactions, the *gauche* effect, hydrogen bonding and solvent effects. For *galacto*-like molecules, there appears to be a significant solvent effect based on solvent polarity. For *gluco*-like molecules, the effect of solvent on the population has not been as thoroughly analyzed experimentally. The experiments performed seem to point to the absence of solvent effects but the evidence is not unambiguous. Theoretical calculations are not clear on how much of a role, solvent and hydrogen bonding have on the rotamer stabilities. Most calculations indicate that intramolecular hydrogen bonding and solvation are very important in determining the rotamer populations.

The goal of this project is to unambiguously determine the effect of solvent on the rotamer population of the hydroxymethyl group in *gluco*-like structures. Solvent polarity effects and solute-solvent interactions will be examined as well as the importance of intramolecular hydrogen bonding on the rotamer population. This work will contribute to a better understanding of the conformations of oligosaccharides and will provide information for the production of better models of carbohydrates.

3.2 Results and Discussion

The goal of this research was to quantify and examine the effect of solvent on the rotamer population about the C5-C6 hydroxymethyl group in D-glucose. ^{1}H NMR spectroscopy and infrared spectroscopy were used to determine rotamer populations and the extent of hydrogen bonding. The experimental systems examined were chosen so as to limit the number of variables in order to understand the many complex interactions taking place that affect the hydroxymethyl rotation.

3.2.1 Non-Hydrogen Bond Solvent Effects

3.2.1.1 Choice of Compound

The influences of different anomeric effects in glucose on the rotamer populations were eliminated, as were the effects of differing aglycons by choosing to work exclusively with a derivative of methyl α-D-glucopyranoside (**10**). Methyl α-D-glucopyranoside could not be used as a model compound in this analysis because it is not very soluble in non-polar solvents. One of the goals of the research was to examine the rotamer population over a wide range of solvent polarity, especially in non-polar solvents. Also, the presence of the four secondary hydroxyl groups would make any results regarding solvent polarity ambiguous due to the possibilities for extensive hydrogen bonding. In order to overcome these difficulties, derivatization of **10** was performed. This, however, introduces a complication in that substitution may have an effect on rotamer stabilities.

In order to eliminate differences in rotamer population due to different substituents one derivative was chosen as a model compound. The derivative chosen was methyl 2,3,4,6-tetra-*O*-methyl-α-D-glucopyranoside (**16**). It is ideal for this experiment in many respects. It

has sufficient solubility in non-polar and polar solvents (including water!) for study. Methyl groups do not produce large electronic effects that could significantly affect the rotamer equilibrium. Methyl groups are small, inert substituent groups and thus steric effects on the rotation are minimized. Compound **16** is easy to synthesize from readily available starting materials.

The use of compound **16** however created problems of its own, specifically, in the ^1H NMR spectra. The signals of all protons (except the anomeric protons) including the methoxy protons are found between 3 and 4 ppm. To simplify this problem, it was decided to synthesize compound **16** having deuterated methoxy groups. For ease of synthesis, the anomeric methoxy group was not deuterated but the resulting signal did not significantly affect the analysis of the spectra.

3.2.1.2 Synthesis of Methyl 2,3,4,6-Tetra-*O*-[$^2H_3$]methyl-α-D-glucopyranoside (16a)

Methyl 2,3,4,6-tetra-*O*-[$^2H_3$]methyl-α-D-glucopyranoside (**16a**) (see Figure 3.9) was synthesized by removal of the hydroxy protons of **10** with NaH followed by reaction with [$^2H_3$]methyl iodide via the method of Brimacombe *et al.*[195] NMR samples of compound **16a** were prepared in a variety of solvents and 400 or 600 MHz ^1H NMR spectra were run.

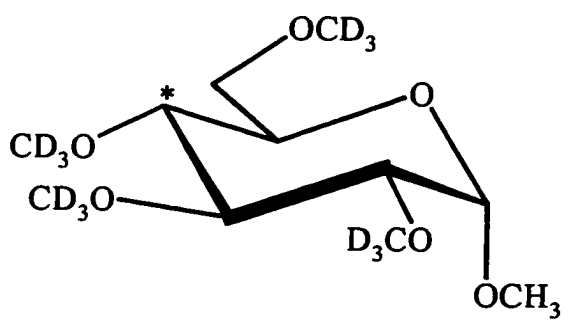

Figure 3.9 Methyl 2,3,4,6-tetra-*O*-[$^2H_3$]methyl-α-D-glucopyranoside (**16a**); methyl 2,3,4,6-tetra-*O*-[$^2H_3$]methyl-α-D-[4-^{13}C]glucopyranoside (**16b**) is identical except that the starred carbon is ^{13}C enriched.

3.2.1.3 NMR Spectroscopy of Compound (16a)

The 7 spin patterns in the ^{1}H NMR spectra due to H1, H2, H3, H4, H5, H6R and H6S were analyzed as follows. The results of hand analyses were simulated using the program NMRSIM. If the results resembled the experimental spectra, iterative simulation was performed using the program LAME8. The complete results are presented in Appendix Tables A.1 and A.2. In Table 3.1 the specific results for the H6's are presented. The table also includes the population of the various rotamers obtained by using Equations 11-13. The limiting values for the equations were determined by using molecular mechanics (MM3(94)) derived torsional angles in the Haasnoot-Altona modification of the Karplus equation.

$$^3J_{5,6R} = 1.61f_{gg} + 9.47f_{gt} + 4.11f_{tg} \qquad (12)$$

$$^3J_{5,6S} = 2.25f_{gg} + 2.09f_{gt} + 10.61f_{tg} \qquad (13)$$

The angles used in the calculation are found in Table 3.2. The angles were determined by calculating the geometry of the three rotamers of **16** using a modified version of MM3(94) (see Chapter 2) where the O-C-C-O torsional term was reparameterized. The calculation was simplified by assuming that the ring methoxy groups were oriented counterclockwise around the ring. For each rotamer, the calculations were only performed on the conformer with the Me-O6 bond *anti* to the C5-C6 bond.

The solvents used were chosen to provide as wide a range of polarities as possible. Most of the spectra were recorded at 600 MHz. The 400 MHz spectra in toluene-d_8 and cyclohexane-d_{12} were found to be relatively easy to analyze, so their 600 MHz spectra were

Table 3.1 NMR[a] Data for H6R and H6S and Rotamer Populations of (**16a**).

Solvent	ϵ (debye)	Chemical Shift (ppm)		Coupling Constant (Hz)		Rotamer Population[b,c] (%)		
		H-6R	H-6S	$^3J_{5,6R}$	$^3J_{5,6S}$	*gg*	*gt*	*tg*
C_6D_{12} [d]	2.0	3.52	3.38	4.49	1.64	68 (64)	39 (36)	-6
$C_6D_5CD_3$ [d]	2.4	3.55	3.47	4.79	1.48	65 (60)	43 (40)	-8
CS_2	2.6	3.43	3.34	4.90	1.70	62 (58)	44 (42)	-6
$CDCl_3$	4.8	3.59	3.57	4.02	2.42	67	30	3
THF-d_8	7.6	3.51	3.45	4.94	1.82	61 (58)	44 (42)	-4
CD_2Cl_2	8.9	3.53	3.51	4.52	2.21	63	37	0
$(CD_3)_2CO$	20.7	3.51	3.49	4.80	2.08	60 (60)	41 (40)	-1
CD_3OD	32.7	3.57	3.54	4.66	1.96	63 (61)	40 (39)	-3
CD_3CN	37.5	3.49	3.48	4.75	2.48	58	39	3
D_2O [d]	78	3.51	3.53	4.64	2.43	59	38	3

[a]All determined from 600 MHz spectra unless otherwise noted [b] Determined using equations 11-13. [c] Values in parentheses calculated assuming *tg* is unpopulated. [d] Recorded at 400 MHz

Table 3.2 Torsional Angles Used to Calculate the Limiting Coupling Values for **16a**

Rotamer	Torsional Angle[a]	
	H5-C5-C6-H6R	H5-C5-C6-H6S
gg	51.9°	293.9°
gt	190.6°	71.7°
tg	294.2°	175.9°

[a] Angles calculated using a modified form of MM3(94).(see Chapter 2)

not recorded. The spectrum of **16a** in water-d_2 was run at 600 MHz but its spectrum was quite broad and a 400 MHz spectrum was recorded in order to aid in analysis of the spectrum.

The signals of H1, H2, H3 and H4 were found to consist of first order subspectra which were very easy to analyze. The prochiral protons and H5 subspectra were of higher order and not as easily solved. The signals of these protons and H4 generally formed either ABCX or ABMX subspectra. An example of the fit obtained using LAME8 is presented in Figure 3.10.

One interesting feature of these spectra is that a long range coupling appeared in CD_3OD and THF-d_8. This small (~0.3 Hz) splitting was found in the H5 subspectra. It could not be simulated as a higher order effect in the ABCX or ABMX subspectra. The coupling was determined to be to H3 by examination of the spectra and noticing a slight line broadening for the H3 signal. The appearance of this splitting is most likely a result of higher resolution in these two solvents and not a solvent effect.

3.2.1.3a Assignment of 6S and 6R Protons

Unambiguous identification of the H6R and H6S protons came from examination of ^{13}C-C-C-H coupling constants. The $^3J_{CH}$ values were determined from NMR spectra of methyl 2,3,4,6-tetra-*O*-[$^2H_3$]methyl-α-D-[4-^{13}C]glucopyranoside (**16b**). Compound **16b** was synthesized by Fischer glycosidation[196] of D-[4-^{13}C]glucose (**17**) to obtain methyl α-D-[4-^{13}C]glucopyranoside (**1a**). This was followed by methylation with [$^2H_3$]methyl iodide.[197] The NMR spectra were analyzed as above (see Figure 3.11). Analysis of the NMR spectra was made difficult by the additional spin which was coupled to 6 of the 7 protons. The data for

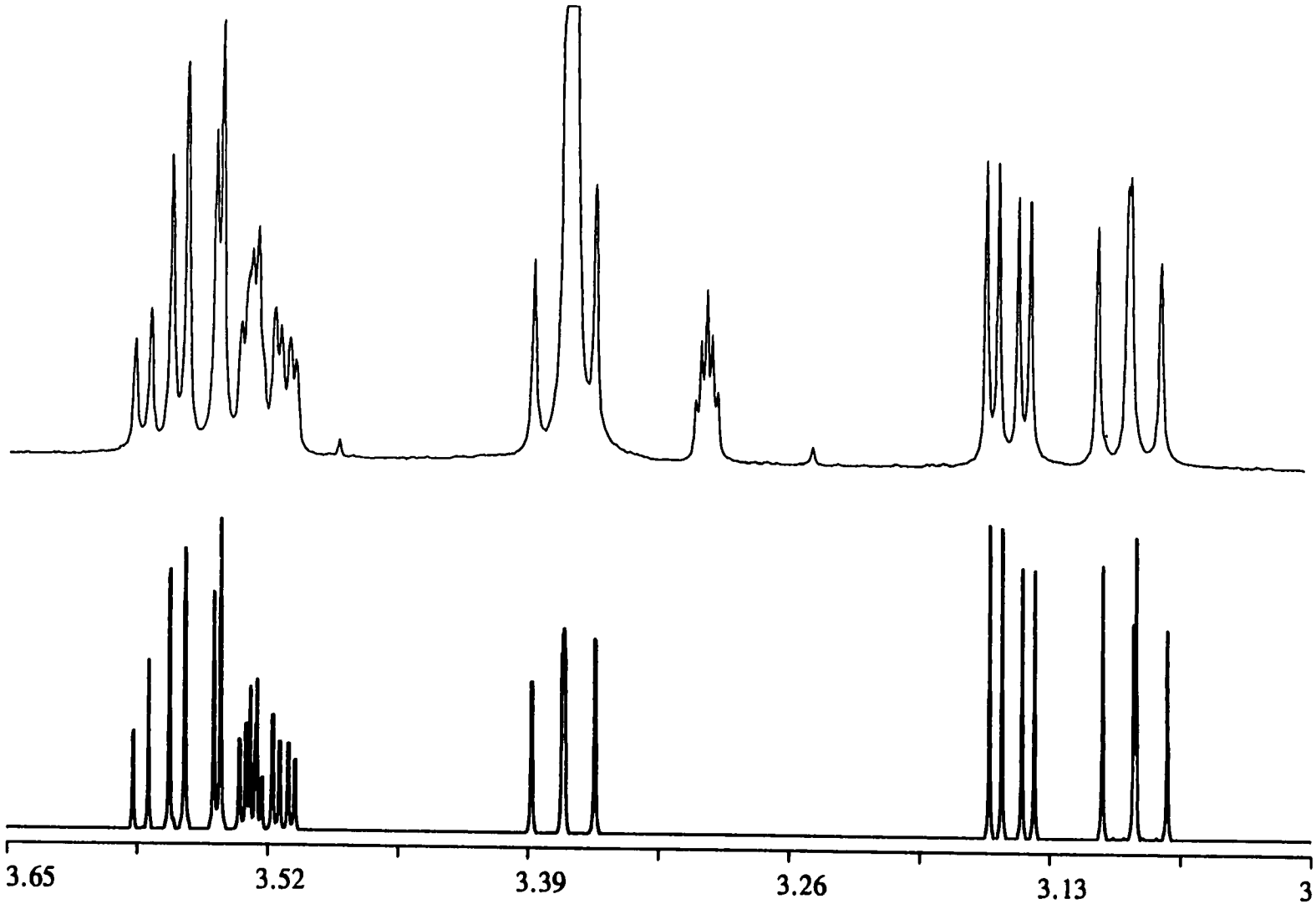

Figure 3.10 The experimental and simulated ^{1}H NMR spectra for compound **16a** in MeOH-d_4. Top: Experimental spectrum (600 MHz). Note that also present in the experimental spectrum are peaks for the anomeric OMe (3.37 ppm) and CD_2HOD (3.30 ppm) Bottom: Simulated spectrum (NMRSIM) using results from LAME8 iterative simulations.

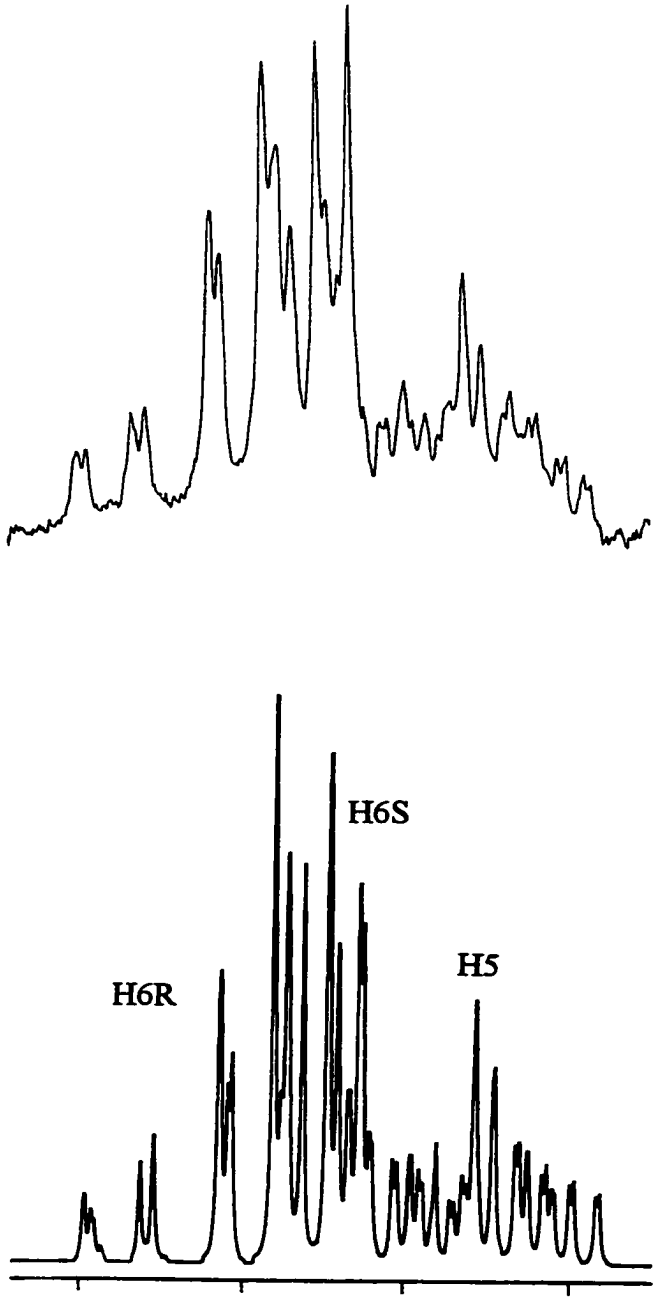

Figure 3.11 The experimental and simulated ^{1}H NMR spectra for the H5, H6S and H6R protons of the ^{13}C-labelled compound **16b** in MeOH-d_4. Top: Experimental spectrum (400 MHz) Bottom: Simulated spectrum (NMRSIM) using results from LAME8 iterative simulations.

the entire spectral analysis is in Appendix Tables A.3 and A.4 and the data pertaining to the prochiral H6's are found in Table 3.3.

Table 3.3 NMR Data from the Analysis of the Spectra of Compound **16b**

Solvent	Dielectric Constant ϵ	Chemical Shift (ppm)		Coupling Constants[a] (Hz)			
		H-6R	H-6S	$^3J_{5,6R}$	$^3J_{5,6S}$	$^3J_{C4,H6R}$	$^3J_{C4,H6S}$
C_6D_{12}	2.0	3.52	3.38	4.37	1.56	0.01	3.20
$C_6D_5CD_3$	2.4	3.56	3.48	4.59	1.72	0.36	3.09
CD_3OD	32.7	3.57	3.54	4.62	2.03	0.76	3.16

[a] As determined from LAME8 iterative analysis.

The assignment was made by examining the consequence of making both possible assignments of H6R and H6S in the proton spectrum. For example, using the data for **16a** in methanol (Table 3.1), one obtains two possible rotamer populations; assigning H6R as the high frequency proton and H6S as the low frequency proton gives a *gg*:*gt*:*tg* ratio of 61:39:0. For the reverse assignment, the ratio is 72:0:28, respectively. Using the $^3J_{CH}$ values from Tvaroska[165] ($^3J_{C4,H6R}$ (*gg*/*gt*/*tg*) = (0.73 Hz/0.73 Hz/ 7.92 Hz); $^3J_{C4,H6S}$ (*gg*/*gt*/*tg*) = (7.90 Hz/1.89 Hz/ 1.26 Hz)), the values for $^3J_{C4,H6R}$ and $^3J_{C4,H6S}$ are calculated for each assignment. The first assignment gives calculated $^3J_{C4,H6R}$ and $^3J_{C4,H6S}$ of 0.73 and 5.56 Hz respectively and the second assignment 2.75 and 6.04 Hz, respectively. There is definite agreement between the values for the first assignment and the experimental $^3J_{CH}$ coupling constants.

The assignment of H6R and H6S for compound **16a** in water-d_2 is anomalous. Initially, the H6 assignments for solvents other than those in Table 3.3 were based on the observation that in other solvents the larger $^3J_{H5,H6}$ is the coupling constant to H6R. If this

assignment is made for the water-d_2 data, the order of the chemical shifts is flipped; H6S appears at a higher frequency. This assignment was confirmed by recording the spectrum of compound **16b** in water-d_2. The resulting spectrum could not be fully analyzed due to broadening. Instead, spectra were simulated with both assignments for H6R and H6S and the resulting calculated spectra were compared with the experimental spectrum (see Figure 3.12). The assignment shown in Table 3.1 gave the best result.

For almost all glucose derivatives, the signal of H6S appears at a higher frequency than that of H6R. In all solvents other than water-d_2, the signal of H6R appears at a higher frequency than that of H6S for compound **16b**. Interestingly, for methyl 2,3,4-tri-*O*-[$^2H_3$]methyl-α-D-glucopyranoside (**18**), (see below) the H6 signals are in the normal order for glucose derivatives. This seems to indicate that the chemical shift reversal in **16a** is a substituent effect of some sort. It is not a direct substituent effect however, because, in the ^{1}H NMR spectrum of 6-*O*-methyl-α-D-glucose, the signal of H6S appears at a higher frequency than that of H6R.

A study of acetylated carbohydrates in chloroform-*d* by Rao and Perlin showed a similar chemical shift exchange (H6R at higher frequency).[154] However, when either O6 only or O4 only was acetylated, the chemical shifts were not reversed. The results were interpreted as the result of the magnetic anisotropy of acetyl groups on O6 *and* O4. As indicated above, similar results (higher frequency H6R) were obtained for the permethylated compound in all solvents but water-d_2. The reason for the chemical shift exchange for **16a** is obviously not the same as was theorized for the peracetylated compounds.[154]

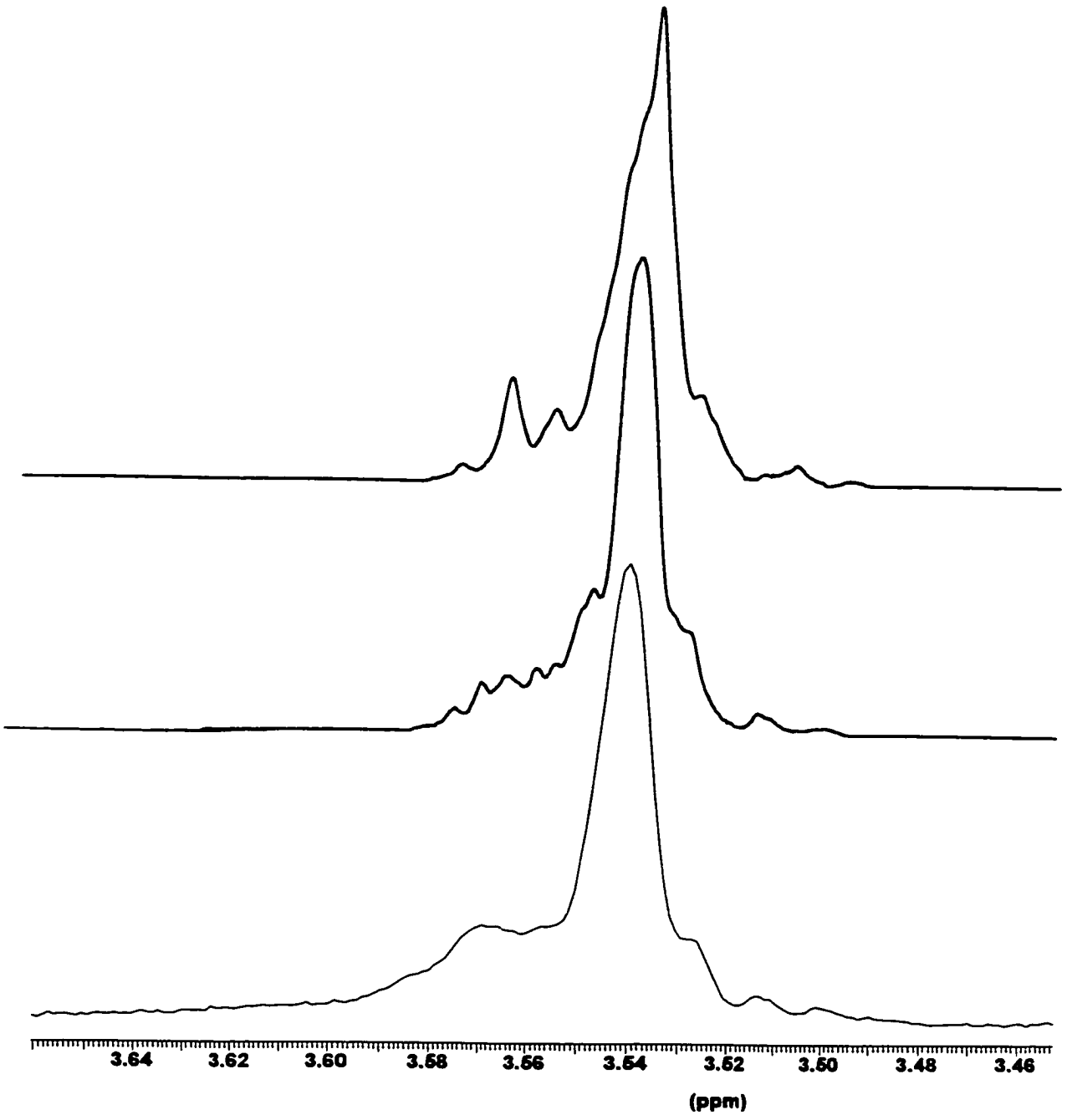

Figure 3.12 Comparison of the two simulated (NMRSIM) ^{1}H NMR spectra of **16b** in water-d_2 with the experimental spectrum in water-d_2. Top: Simulation with H6S at a lower frequency than H6R. Middle: Simulation with H6S at a higher frequency than H6R. Bottom: Experimental (400 MHz) spectrum.

The chemical shift reversal is a solvent effect modulated by the size of the substituents involved. Rao and Perlin have demonstrated that the chemical shift reversal requires that both O4 and O6 be acetylated and that benzoylation does not result in the shift reversal. Unfortunately, all of their measurements of the 4,6-*O*-acetylated compounds are in one solvent, chloroform-*d*. The results here confirm the need for 4,6-di-*O*-substitution but also show that the relative positions of the two hydrogen signals is solvent sensitive. It seems, therefore, that the shift reversal is a solvent effect that occurs when small substituents such as -Me and -Ac are substituted on O4 and O6. A possible mechanism for this effect is presented in the next Section.

3.2.1.4 Solvent Effects on the Rotameric Equilibria

A casual examination of the rotamer populations in the various solvents reveals that there is no large solvent effect on the rotamer equilibria. Similarly, none of the NMR parameters appear to have any significant solvent effect. A more quantitative analysis requires the use of a polarity scale.

There are a wide variety of polarity scales available.[94,198-200] They range from the simple dielectric constant to scales involving electron transitions (E_T, π^*). The scale used for this analysis is the Kirkwood function (ϵ_K, see Equation 14), which was developed for examining solvent effects on neutral polar molecules.[200] The function uses the dielectric constant (a ground state property) of the solvent as a variable. This polarity scale was chosen because the rotation of the hydroxymethyl group is a ground state phenomenon and thus any solvent effects should be reflected in the relation between rotamer population and the Kirkwood

function. Abraham *et al.* have used ϵ_K as a solvent polarity in their analysis of the rotational equilibrium of chloroethanes.[201,202]

$$\epsilon_K = \frac{\epsilon - 1}{2\epsilon + 1} \tag{14}$$

Statistical analysis of the rotamer populations and the free energy of the *gg*⇌*gt* equilibrium versus solvent polarity showed no significant solvent effects (see Figure 3.13). Other than toluene, none of the solvents appeared to have any unique solvent effect. In toluene, there were high frequency shifts of H3, H4, and H5. This is due to the particular

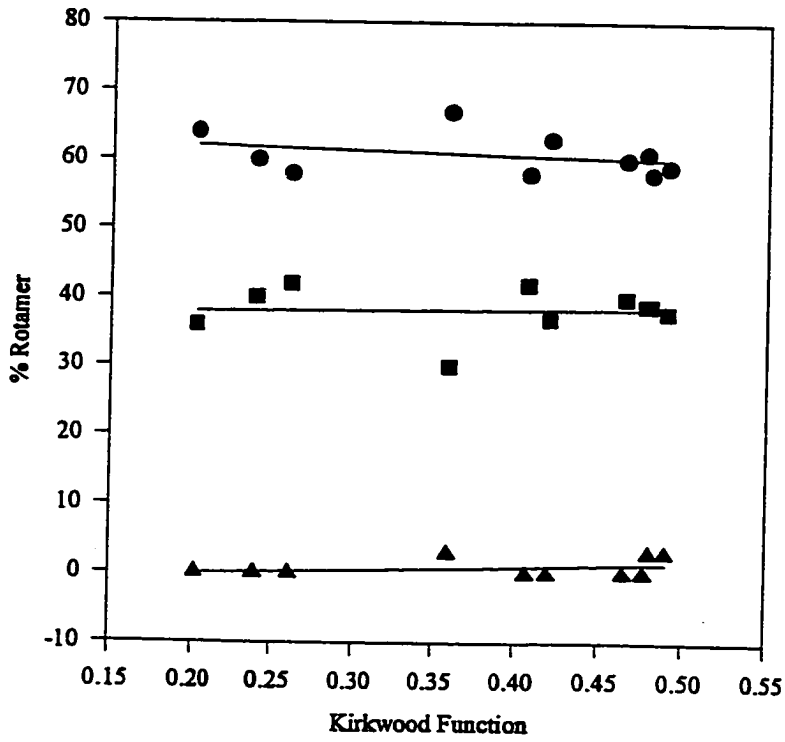

Figure 3.13 Plots of rotamer population (%) vs. the Kirkwood function (ϵ_K) (see Equation 14). (●) *gg* rotamer; (■) *gt* rotamer; (▲) *tg* rotamer.

solvation of aromatic compounds. Surprisingly, this solvation did not appear to have an effect on the rotamer equilibria.

Two parameters were found to have fair correlation to solvent polarity, the chemical shift of the anomeric proton (R^2=0.728) and the difference in chemical shift of the two prochiral protons (R^2=0.821). The regression data for these analyses and for literature data are found in Table 3.4.

The chemical shift of the anomeric proton is shifted to higher frequency with increasing solvent polarity. Possible explanations for this phenomenon include: *i*) the inductive effects of O5 and O1 are increased by electric fields caused by the polar solvents,or *ii*) as the solvent polarity increases the potency of the anomeric effect is diminished and this then has a deshielding effect on the anomeric proton. Neither explanation is likely because if the effect were the result of modulation of the anomeric effect or inductive effects it could be expected to occur in galactose where the effects should be similar. The chemical shift of the anomeric proton of methyl 2,3,4,6-tetra-*O*-methyl-α-D-galactopyranoside (**19**)[204] was not correlated with solvent polarity.

The second correlation, between the chemical shift difference between H6S and H6R and solvent polarity, is a stronger correlation and seems to account for the chemical shift reversal in water-d_2. As solvent polarity increases there is a decrease in the chemical shift difference between the two prochiral protons. An obvious question is: how are the respective chemical shifts affected as polarity increases? A regression analysis of the data indicates that H6S is moving to a higher frequency and H6R is remaining fixed (3.52 ±0.09 ppm). As the

Table 3.4 Regression Data for Solvent Dependent NMR Parameters

Solvent	Solvent Polarity (ϵ_K)	Chemical Shift (ppm)							
		Compound **16a**				Cpd **19**[a]	Compound **14a**[b]		
		H1	H6R	H6S	$\Delta\delta^c$	H1	H6R	H6S	$\Delta\delta^c$
C_6D_{12}	0.202	4.58	3.52	3.38	0.131	--	--	--	--
CCl_4	0.226	--	--	--	--	4.61	4.186	4.249	-0.063
C_6D_6	0.240	--	--	--	--	4.79	--	--	--
$C_6D_5CD_3$	0.240	4.60	3.55	3.47	0.087	--	--	--	--
CS_2	0.261	4.54	3.43	3.34	0.087	--	--	--	--
$CDCl_3$	0.359	4.82	3.59	3.57	0.018	4.86	4.167	4.181	-0.014
THF-d_8	0.407	4.69	3.51	3.45	0.053	--	--	--	--
CD_2Cl_2	0.420	4.75	3.53	3.51	0.015	4.78	--	--	--
$(CD_3)_2CO$	0.465	4.75	3.51	3.49	0.020	--	4.090	4.140	-0.050
CD_3OD	0.477	4.80	3.57	3.54	0.033	--	4.164	4.201	-0.037
CD_3CN	0.480	4.75	3.49	3.48	0.003	--	--	--	--
DMF-d_7	0.480	--	--	--	--	4.79	--	--	--
D_2O	0.490	4.82	3.51	3.53	-0.022	5.00	3.910	4.020	-0.110
R^2		0.728	0.009	0.445	0.821	0.466	0.357	0.486	0.049

[a] Methyl 2,3,4,6-tetra-*O*-methyl-α-D-galactopyranoside data from ref [203] [b] Methyl 2,3,4-tri-*O*-methyl-α-D-galactopyranoside 6-(dimethyl phosphate) data from ref. [146]. [c] δH6R -δH6S

solvent polarity reaches its maximum in water-d_2 H6S has shifted beyond H6R and it appears as though a reversal of the chemical shifts has occurred (see Figure 3.14).

The curious observation that $\Delta\delta$ is linearly related to solvent polarity but the correlation coefficient for δH6S and solvent polarity is much poorer, is probably caused by the variation in calibration of chemical shifts in the different solvents. The shift of H6S relative to H6R is possibly a result of H6S being present on the α face of the glucose molecule in both of the dominant rotamers (*gg* and *gt*). Its relatively fixed location means that its solvation environment is stable and thus solvent effects such as polar deshielding effects[205] would be magnified. The H6R proton is present on both the α and β faces and thus its solvation environment changes more dramatically from the *gg* to *gt* rotamers. This hypothesis is supported by the results for the galactose derivatives where both protons shift from the α to β faces and there is no evidence of either chemical shift having any significant solvent effect. A similar mechanism would apply equally to the peracetylated case.[154] The fact that the feature is not observed for larger substituents is due to the larger solvent shell and in the case of benzoyl substitution the perturbation of the solvent shell caused by rotation of the large non-polar phenyl ring. In these situations H6S and H6R would have similar solvent effects.

Aside from the above mentioned solvent effects, no other solvent effects were noted. The populations of the *gg*:*gt*:*tg* rotamers stayed essentially fixed at approximately 60:40:0 as solvent polarity increased.

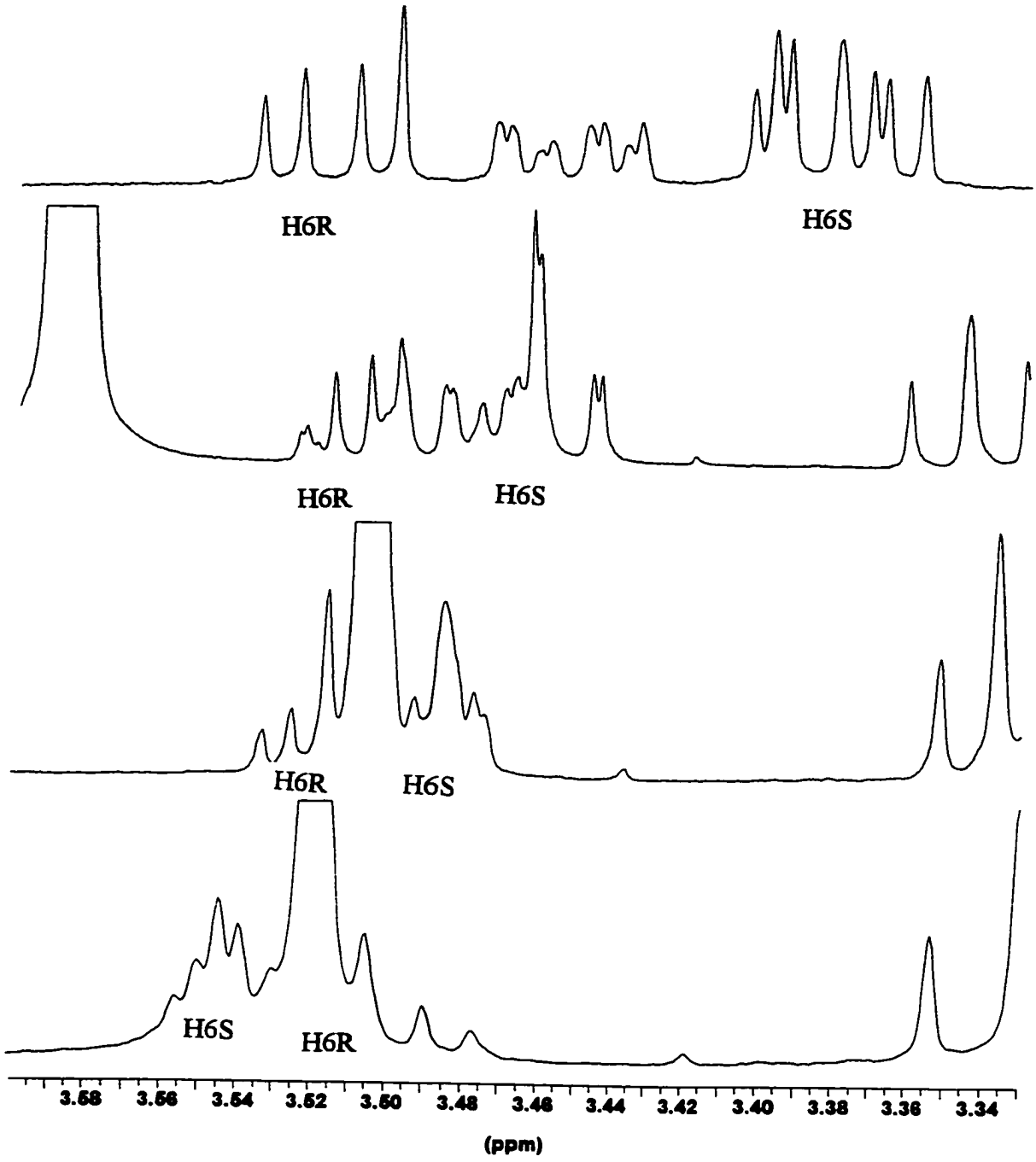

Figure 3.14 The ^{1}H NMR spectra of **16a** in the region containing H6S and H6R showing the change in relative chemical shift as solvent polarity changes. From top to bottom: in cyclohexane-d_{12} (400 MHz), in THF-d_8 (600 MHz),in acetone-d_6 (600 MHz),in water-d_2 (400 MHz).

3.2.2 Hydrogen Bonding Solvent Effects

Hydrogen bonding has been implicated as a major factor in determining the rotamer population of the hydroxymethyl group in carbohydrates. According to theoretical calculations,[109,121,183,185-187,190,194] the solute-solvent interactions between glucose and water are the determining factors in the stability of the *tg* rotamer. This explanation, however, has not been thoroughly tested experimentally with a carbohydrate derivative. Both intra- and intermolecular hydrogen bonding are solvent-sensitive phenomena and in non-polar solvents intramolecular hydrogen bonding should dominate. The most important functionality in glucose in determining hydrogen bonding effects on the rotamer populations is OH6. The experiments presented here examine OH6 separately from the other hydroxyl groups in glucose and determine the solvent effects on the rotamer populations when OH6 is free to form both intra- and intermolecular hydrogen bonds.

3.2.2.1 Choice of Compound

In order to examine the effect that hydrogen bonding had on the rotamer populations, a model compound was synthesized. Specific hydrogen bonding of OH6 could not be examined with the parent compound (**10**) because of possible interferences from the secondary hydroxyl groups. Methyl 2,3,4-tri-*O*-[$^2H_3$]methyl-α-D-glucopyranoside (**18**) was chosen as a suitable model compound to examine hydrogen bonding involving OH6. As with (**16a**), deuterated methyl groups were used to make analysis of the NMR spectra easier.

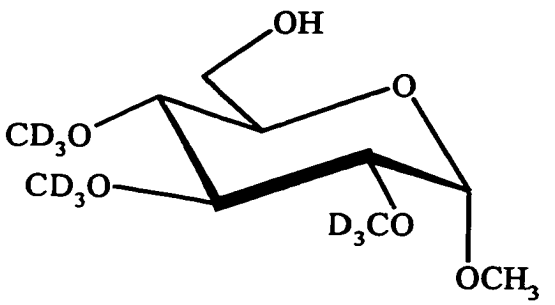

Figure 3.15 Methyl 2,3,4-tri-*O*-[$^2H_3$]methyl-α-D-glucopyranoside (**18**)

3.2.2.2 Synthesis of Methyl 2,3,4-tri-*O*-[$^2H_3$]methyl-α-D-glucopyranoside (18)

Methyl 2,3,4-tri-*O*-[$^2H_3$]methyl-α-D-glucopyranoside (**18**) (see Figure 3.15) was synthesized by a three step route (see Figure 3.16). Starting from methyl α-D-glucopyranoside (**10**), the primary hydroxyl on C6 was protected with a *tert*-butyldimethylsilyl (TBDMS) group by reaction of **10** with *tert*-butyldimethylsilyl chloride in pyridine.[206] The reaction was highly selective for the primary oxygen of the hydroxymethyl group but the yield obtained was poor (53%) compared to literature procedures. Methyl 6-*O*-TBDMS-α-D-glucopyranoside (**20**) was methylated with NaH and [$^2H_3$]methyl iodide by the same procedure as for **16a**.[197] It is interesting that other workers[207,208] have had difficulty retaining TBDMS groups during base-catalyzed methylation and the yield obtained here was relatively low (30%) The final step was reaction of methyl 2,3,4-tri[$^2H_3$]methyl-6-*O*-TBDMS-α-D-glucopyranoside (**21**) with fluoride ion to remove the silyl group to obtain compound **18**.[206]

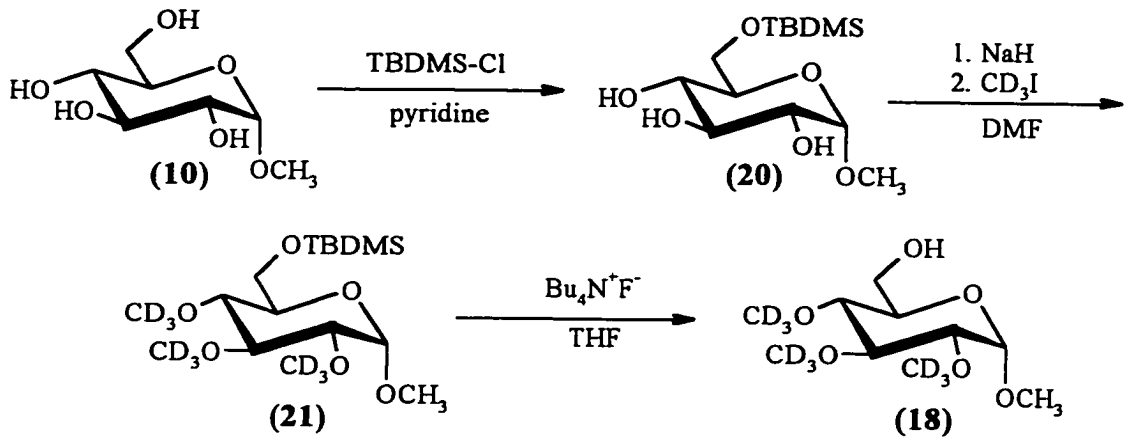

Figure 3.16 Synthesis of methyl 2,3,4-tri-*O*-[$^2H_3$]methyl-α-D-glucopyranoside (**18**)

3.2.2.3 NMR Spectroscopy of 18

As for compound **16a** the spectra of **18** were run in a variety of solvents in order to examine solvent effects on the hydrogen bonding of OH6. The spectra were run at 500 MHz except where noted. The spectra were solved by a combination of first and second order techniques combined with computer iteration (see Figure 3.17). The spectra from CS_2 and cyclohexane-d_{12} solutions could not be analyzed in the region containing the H6R/H6S/H5 subspectra due to broadening caused by coupling to the hydroxyl proton.

This problem was solved by exchanging the hydroxyl proton with a deuteron by repeatedly shaking a sample of **18** in water-d_2 followed by azeotropic removal of the water. The spectra of these deuterated samples (**18a**) were then recovered and the simplified spectra were solved. The complete data for all solvents can be found in Appendix Tables A.5 and A.6. The data for the prochiral protons are given in Table 3.5.

The procedure for rotamer calculation was identical to the procedure for **16a** using Equations 11, 15 and 16. The limiting values in equations 15 and 16 were determined by

combined use of MM3 geometries and the Haasnoot-Altona equation. The geometries (see Table 3.6) were calculated on molecules of **18** where the hydroxyl proton was *anti* to the C5-C6 bond.

$$^{3}J_{5,6S} = 2.16f_{gg} + 1.94f_{gt} + 10.59f_{tg} \quad (15)$$

$$^{3}J_{5,6R} = 1.61f_{gg} + 9.47f_{gt} + 3.97f_{tg} \quad (16)$$

3.2.2.3a Assignment of the 6R and 6S Protons

The assignment of the prochiral protons on C6 is rationalized by two facts. First, in nearly all *gluco*-like structures, the signal of H6S appears at a higher frequency than that of H6R.[108] The assignment for **16a** is anomalous, just as is the case for molecules where O4 and O6 are acetylated.[154] Other glucose derivatives that are only partially methylated do not have this reversal of chemical shift.[108]

Second, in the case of cyclohexane-d_{12}, where intramolecular hydrogen bonding would be most favored and the *tg* rotamer would be most stable, the coupling constants are nearly identical and thus the assignment of the protons is irrelevant with respect to determining the rotamer population in cyclohexane-d_{12}. The low frequency H6S assignment gives a *gg*:*gt*:*tg* rotamer ratio of 73:18:9, respectively. The opposite assignment gives 75:12:13, respectively. Thus, the assignments for chemical shifts in more polar solvents should be such that the *tg* population is approximately 13% or less. The result of this assignment is that in all solvents the signal of H6S appears at a higher frequency than that of H6R.

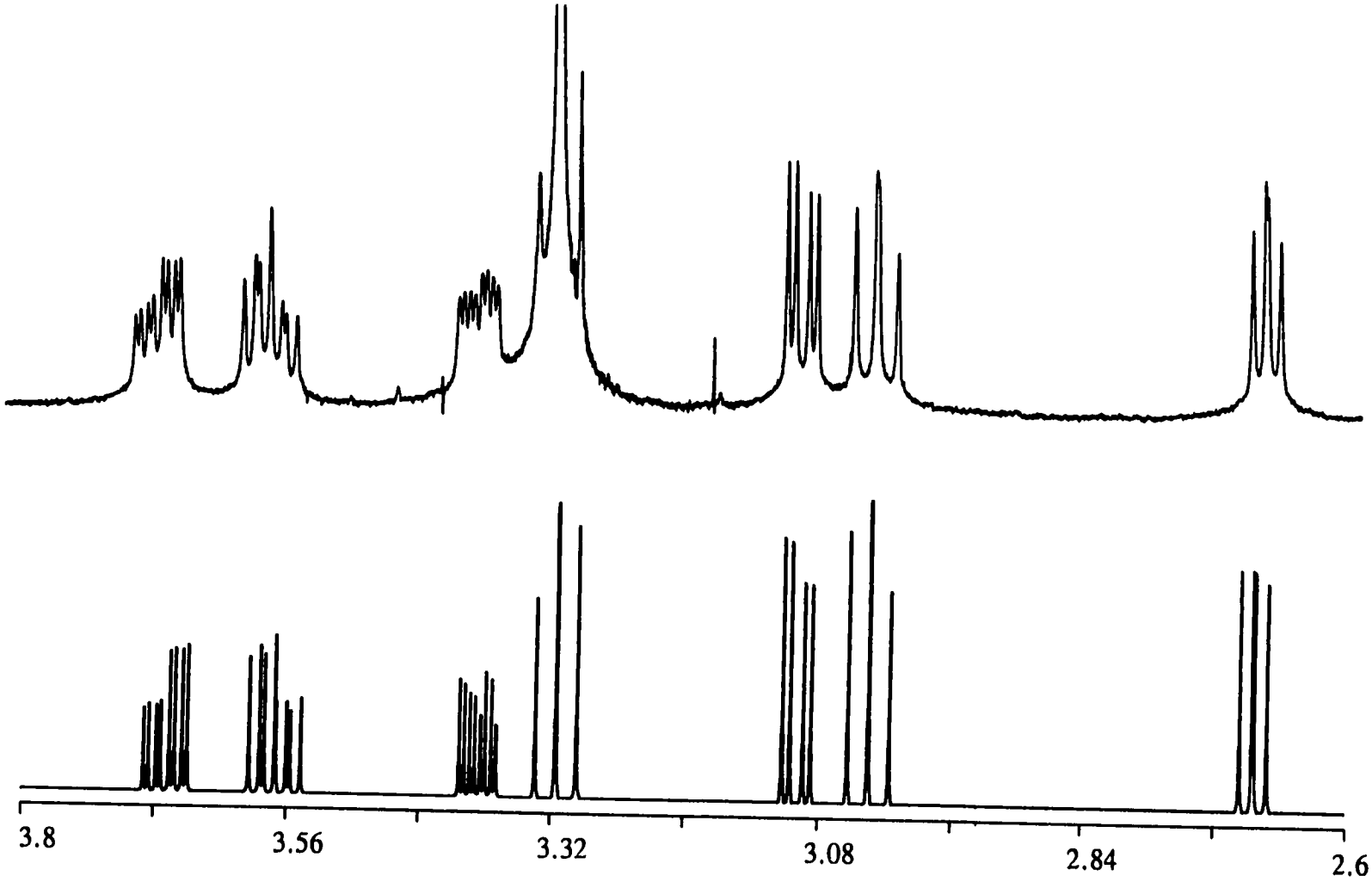

Figure 3.17 The experimental and simulated ^{1}H NMR spectra for compound **18** in acetonitrile-d_3. Top: Experimental spectrum (500 MHz) Bottom: Simulated spectrum (NMRSIM) using results from LAME8 iterative simulation.

Table 3.5 500 MHz NMR[a] Data for H6R and H6S and Rotamer Populations of **18**.

Solvent	∈ (debye)	Chemical Shift (ppm)		Coupling Constant (Hz)		Rotamer Population[b,c] (%)		
		H-6R	H-6S	$^3J_{5,6R}$	$^3J_{5,6S}$	*gg*	*gt*	*tg*
C_6D_{12}[d]	2.0	3.58	3.65	3.25	2.86	73	18	9
CS_2[d]	2.6	3.81	3.91	4.00	2.78	68	28	4
$CDCl_3$	4.8	3.75	3.84	4.14	3.09	60	28	12
$(CD_3)_2CO$	20.7	3.62	3.71	4.61	2.06	63	37	0
CD_3OD	32.7	3.66	3.72	4.66	2.06	62	38	0
CD_3CN	37.5	3.57	3.67	4.85	2.16	59	40	1
DMSO-d_6	46.7	3.47	3.57	5.48	1.13	58 (52)	53 (48)	-11
D_2O	80.2	3.55	3.64	4.84	1.90	61 (60)	41 (40)	-2

[a] All spectra run at 500 MHz unless noted otherwise. [b] Determined using eqns 10, 14, and 15. [c] Values in parentheses are corrected values assuming *tg* equals 0. [d] Recorded at 400 MHz.

Table 3.6 Torsional Angles Used to Calculate the Limiting Coupling Values for **18**

Rotamer	Torsional Angle[a]	
	H5-C5-C6-H6R	H5-C5-C6-H6S
gg	51.4°	293.4°
gt	191.5°	72.5°
tg	293.3°	175.9°

[a] Angles calculated using a modified form of MM3(94).(see Chapter 2)

3.2.2.4 NMR Spectroscopy of the Hydroxyl Proton

The other NMR parameter that can reveal information on the state of hydrogen bonding in the molecule is the coupling constant of the OH proton to the prochiral protons of C6. The magnitude of the coupling constants between the hydroxyl proton and the prochiral protons can be related to their respective torsional angles (H-O-C-H) via the Karplus equation.[209,210] The torsional angles show how the hydroxyl proton is oriented and thus help determine the amount of hydrogen bonding. There are three possible staggered rotamers (see Figure 3.18). The results in Table 3.7 were determined assuming perfectly staggered geometries and used the Karplus relation of Fraser *et al.* for the H-O-C-H torsional angle.[210]

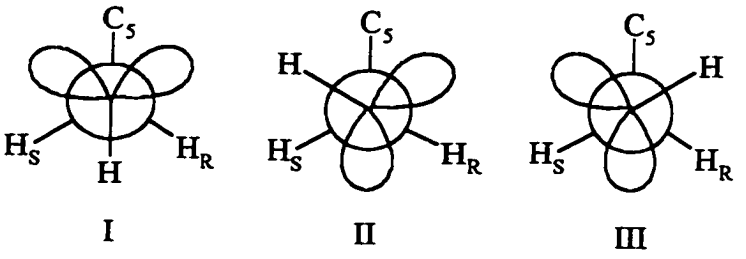

Figure 3.18 The three staggered rotamers of the primary OH group of a hexopyranoside.

3.2.2.5 Infrared Spectroscopy of 18

The presence of hydrogen bonding was also examined by infrared spectrometry. The infrared spectrum was recorded in anhydrous hexane over a range of concentrations from 5-20 mM. No changes in the spectrum were noted over this concentration range. The spectrum of **18** (Figure 3.19) shows a sharp peak and very broad peak. The narrow peak at 3613 cm^{-1} was assigned as the non-hydrogen bonded signal. The very broad peak was assigned to the

Table 3.7 NMR Data[a] for the OH Proton of **18**

Solvent	Chemical Shift (ppm)	Coupling Constant (Hz)		Rotamer Populations[b] (%)		
		$^3J_{OH,H6R}$	$^3J_{OH,H6S}$	I[c]	II[c]	III[c]
$CDCl_3$	1.85	7.71	4.77	17	56	27
$(CD_3)_2CO$	3.55	7.10	5.44	16	50	34
CD_3CN	2.68	6.72	5.51	19	46	35
$(CD_3)_2SO$	4.67	6.29	5.60	23	42	35

[a] Determined from 500 MHz spectra. [b] Determined using equations 9-11 using values for H-O-C-H coupling.[210] [c] See Figure 3.18.

OH stretch of different hydrogen bonds. The extinction coefficient of the various O-H stretching peaks could not be determined directly. Estimates of the extinction coefficient for the non-hydrogen bonded peak from the literature[139,163] allow the amount of non-hydrogen bonded compound to be calculated. These results indicate that 70-96 % of the molecule was hydrogen bonded. If it is assumed that all the hydrogen bonding is intramolecular and that it only occurs in the *tg* rotamer, this result does not match the results from NMR spectroscopy. However, the calculated value for the amount of OH involved in hydrogen bonding is not unreasonable if hydrogen bonding takes place in rotamers other than the *tg* rotamer. The infrared spectrum of **18** in acetonitrile was also run (see Figure 3.19) and intramolecular hydrogen bonding was also noted there. This is not surprising given that, even in DMSO, weak intramolecular hydrogen bonds are present.[175] Furthermore, the NMR results for acetonitrile (see Table 3.5) indicate very little *tg* rotamer was present. Acetonitrile is not an

especially good hydrogen bond acceptor.[199] Therefore, the strong hydrogen-bonded O-H stretch in acetonitrile must be due to intramolecular hydrogen bonding in the other rotamers.

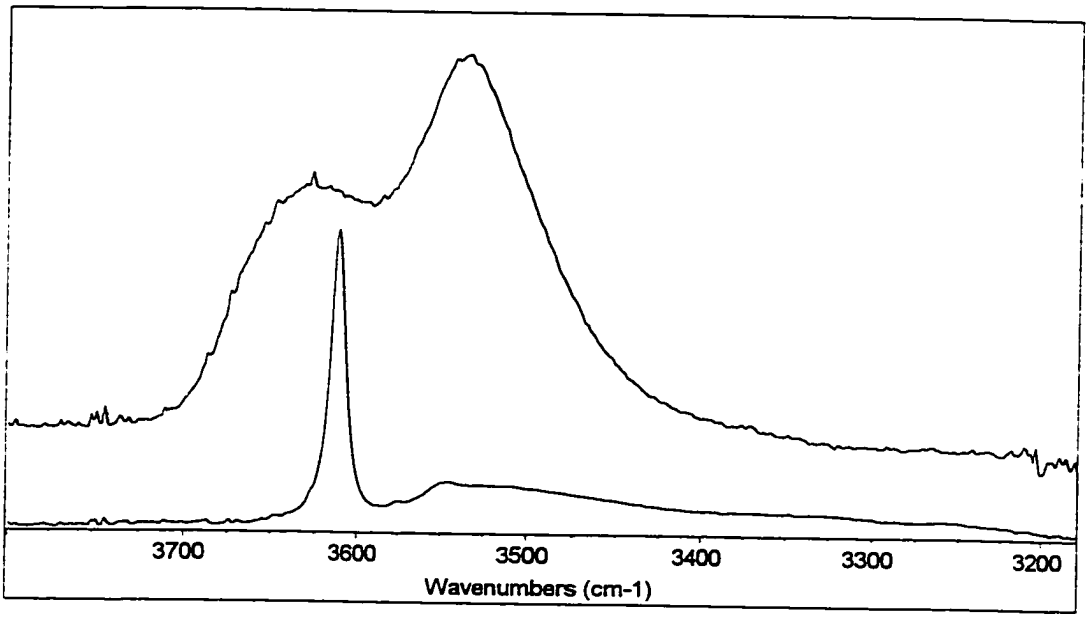

Figure 3.19 Infrared spectrum of **18** in *n*-hexane (bottom) and acetonitrile (top) showing the OH stretching region. The free O-H stretch is not visible in the acetonitrile spectrum due to masking by residual water in the solvent.

3.2.2.6 Solvent Effects on the Rotamer Population for Compound 18

A qualitative examination of the data in Table 3.5 reveals that there is a small but significant difference in rotamer populations when going from a non-polar to a polar solvent (see Figure 3.20). Two trends were noted. The amount of the *tg* rotamer increased as solvent polarity decreased from negligible to slight.

A quantitative examination of the data was performed by a statistical analysis of the NMR parameters similar to that for **16a**. In addition to the Kirkwood polarity scale (ϵ_K) used previously, two additional parameters were used, the Kamlet-Taft β_{KT} and α_{KT} parameters.[199] The β_{KT} parameter is a measure of a solvent's ability to accept a hydrogen bond while the α_{KT} parameter is a measure of a solvent's ability to donate a hydrogen bond.

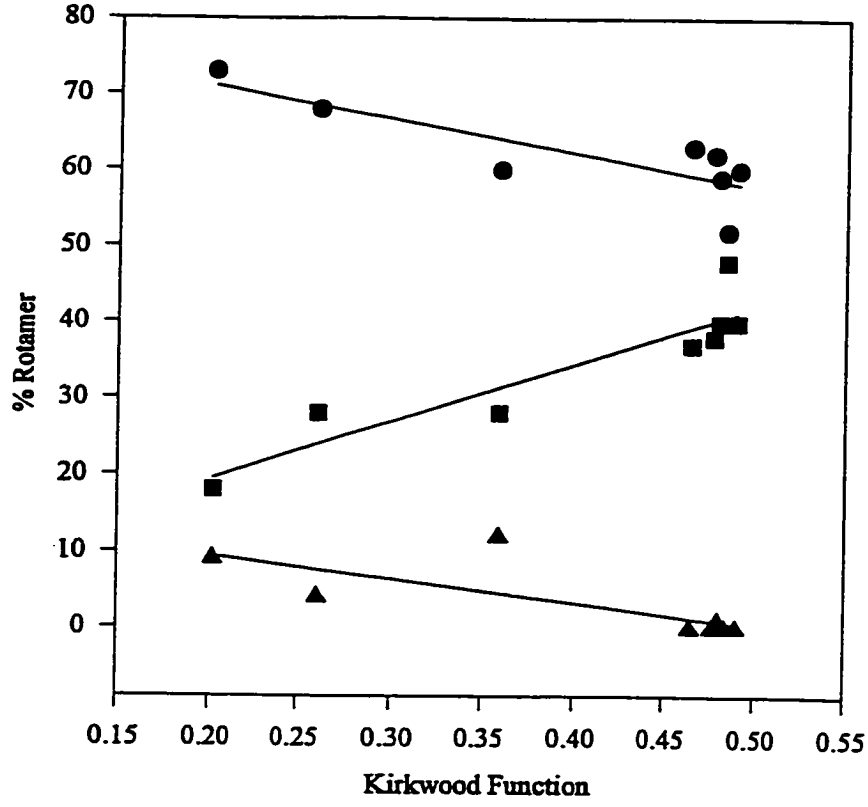

Figure 3.20 Plots of rotamer population of **18** (%) vs. the Kirkwood function (ϵ_K) (see Equation 14). (●) *gg* rotamer; (■) *gt* rotamer; (▲) *tg* rotamer.

The chemical shift data for the carbohydrate protons showed no correlation to any polarity scale. The only non-OH related coupling constant that showed a correlation to polarity was $^3J_{5,6R}$. This correlation (R^2=0.831) manifested itself in the relative populations

of the *gt* and *tg* rotamers. Interestingly, these populations showed a correlation (R^2=0.847) only to the Kirkwood function, not the Kamlet-Taft hydrogen bonding parameters.

The *tg* population (if dependent on intramolecular hydrogen bonding) should be best correlated to β_{KT}. In fact, ϵ_K shows a much better correlation to the amount of *tg* rotamer and thus to intramolecular hydrogen bonding. This result is probably a statistical artifact due the very low populations of the *tg* conformer in polar solvents and the asymptotic values of ϵ_K for polar solvents.

Unlike compound **16a**, there was no relationship between solvent polarity and the chemical shift difference of H6R and H6S. This is consistent with the results for acetylated compounds[154] where both O4 and O6 had to be substituted. The result is also consistent with the proposed mechanism in Section 3.2.1.4. In compound **18**, the hydroxyl group would require a different solvation shell for different rotamers. Thus, despite the fact that H6S spends most of its time on the α side of the molecule like in **16a**, the solvation shell changes as the rotamers interconvert and H6S is no more sensitive to solvent than H6R.

The correlations with the hydroxyl NMR parameters are much more informative with respect to the hydrogen bonding situation. As would be expected, there is a very good (R^2 = 0.985) correlation between the chemical shift of the hydroxyl proton and β_{KT}, the hydrogen bond acceptor parameter. The populations of rotamers II and III (see Figure 3.18) correlate very well with ϵ_K but this could be a product of the small data set and the asymptotic values of ϵ_K for polar solvents. The population of rotamer I shows no correlation to any of the solvent parameters.

The three rotamers of the OH group each have different potentials to hydrogen bond. Rotamer I cannot participate in any intramolecular hydrogen bonding (see Figure 3.18). This rotamer should be most favoured when intermolecular bonding dominates. This can be seen when the solvent changes to DMSO which increases the population from approximately 17% to 23%. Rotamers II and III are capable of intramolecular or intermolecular hydrogen bonding depending on the geometry around the C5-C6 bond (see Figure 3.21).

Determination of which of the hydroxyl rotamers can hydrogen bond in which C5-C6 rotamers was done by molecular modeling. Rotamer II is the rotamer that would be most stable when OH6 is intramolecularly hydrogen bonded to O5 and O4, in the *gg* and *tg* rotamers, respectively (see Figure 3.21). In rotamer III, OH6 can hydrogen bond to the ring oxygen (O5) in the *gt* conformation. There is NMR evidence for the latter contribution in the solvent dependence of the populations of the rotamers. As the *gt* population increases with solvent polarity so does the population of III. At the same time, there is a decrease in the *tg* and *gg* population and a corresponding decrease in the population of II. These results are consistent with intramolecular hydrogen bonding occurring to some extent in all rotamers.

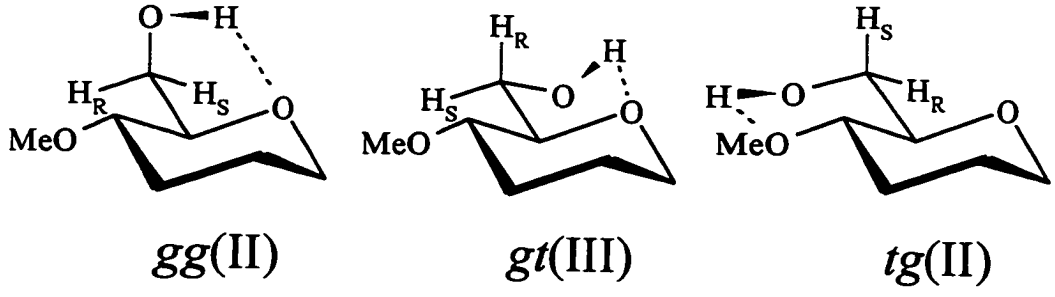

Figure 3.21 Figure showing C6-O6 rotamers in which intramolecular hydrogen bonding can take place for each of the C5-C6 rotamers. The Roman numerals refer to the rotamers in Figure 3.18.

3.2.3 Discussion

3.2.3.1 Systems Without Hydrogen Bonding

The solvent effects presented above for compound **16a** are in sharp contrast to results for galactose.[146,174] In the work of Buck and de Vries,[146,174] the *gt* population of galactose increased at the expense of the *tg* population as the solvent polarity went up (see Figure 3.6 for rotamer structures of galactose). This has been explained as the result of decreasing electrostatic repulsions in the *gt* rotamer in polar solvents[146] which results in it being stabilized by 1.0-2.5 kJ with respect to the *tg* rotamer. It has been stated that the *gg* population is unaffected by changes in solvent because the population is determined largely by steric rather than electronic interactions.[146,174] Another possible explanation is that the electrostatic interaction between the 1,3-dipoles is less than the one in the *gt* because they are more distant. Thus, solvent effect are intermediate in magnitude and its population does not change.

The absence of a solvent effect for compound **16a** is due to a number of factors. In non-polar solvents, both the *gg* and *gt* rotamers are favoured due to the *gauche* effect and the *tg* rotamer is disfavoured due to its higher dipole moment (2.72 D versus 1.35 D and 1.90 D for the *gg* and *gt* rotamers respectively) and electrostatic and steric interactions with O4. In polar solvents, the destabilization caused by the electrostatic and higher dipole moment in the *tg* rotamer is reduced.

The *tg* rotamer population surprisingly does not appear to increase in polar solvents. However, the population of the *tg* rotamer is generally below the level of detection. It is quite possible that there is a solvent effect that stabilizes the *tg* rotamer but that the changes cannot be observed due to the low populations involved. It is also possible that the reduction in

electrostatic repulsions in polar solvents is unequal in the three rotamers and that the repulsions in the *gg* and *gt* rotamers are reduced more in polar solvents than the *tg* rotamer due to the smaller distances involved. This could make up for additional stabilization of the *tg* rotamer due to its larger dipole moment Another source of stabilization for the *gg* and *gt* rotamers is a solvent effect on the *gauche* effect.

Such a solvent effect is possible given that the *gauche* effect is an electronic effect and thus should be sensitive to dielectric constant of the surrounding medium. Examination of the solvent effects on systems containing O-C-C-O does show that the stability of the *gauche* conformer increases as solvent polarity increases,[92,93,95] but whether this is due only to dipolar effects or a combination of dipolar and *gauche* effects has not been shown.

The *gauche* effect has been implicated as a major factor in determining the rotamer equilibria.[108] In Chapter 2, (2.2.3.3) NMR spectral data about the rotamer stability of 1,2-dimethoxypropane (**5**) was presented. This molecule is an excellent model to examine the magnitude of the other factors that determine the rotamer populations besides the *gauche* effect. Compound **5** is structurally identical to the methoxymethyl moiety of the pyranose ring in compound **16a**. In compound **5**, the only factor affecting the *gg* and *gt* rotamer stabilities is the *gauche* effect. Therefore, any difference in the rotamer stabilities is due to structural differences such as the presence of O4 and the anomeric effect in **16a**.

In Table 2.7, the relative energies of the three rotamers of **5** are presented. The data indicate that the *a* (*tg*) rotamer is the most populated and the *g'* conformer (an analogue of the *gt* rotamer) is more stable than the *g* rotamer (an analogue of the *gg* rotamer). Similar results (*gt*>*gg*) are found in pyran derivatives with methoxymethyl groups.[139] In the results presented

here for both the fully and partially methylated glucose, the order of rotamer populations is *gg*≥*gt*. The *gg* rotamer is stabilized by 2 kJ/mol more in glucose derivative **16a** than in **5**; the *tg* rotamer is destabilized by over 10 kJ/mol. The anomeric effect is a strong candidate for being the determining factor in the relative stability of the *gg* and *gt* rotamers.

Support for this conclusion comes from studies on the effect of modifications at the anomeric center on the rotameric populations. The rotamer populations in both galactose[146] and glucose[142] derivatives are sensitive to changes in the aglycon on the anomeric oxygen. An increase in the pKa of the aglycon stabilizes the *gt* and *tg* rotamers in glucose and galactose derivatives, respectively. The α-configuration at the anomeric center stabilizes the *gg* conformer relative to the *gt* rotamer in glucose derivatives,[108] making it slightly more stable, a similar effect is noted for galactose, where the *gt* rotamer is favoured relative to the *tg* rotamer.[108,142,146,174] This dependence on the anomeric effect points to the conclusion that the stability of the *gg* and *gt* rotamers is linked to the anomeric effect.[146]

There is an interesting trend relating the relative populations of the *gg* and *gt* rotamers to the structure of the substituent at C4 (see Table 3.8). α-D-Glucose derivatives in water with a free hydroxyl group at C4 (first three entries in Table 3.8) have rotamer populations such that *gt* ≥ *gg* while derivatives that have O4 methylated (compounds **16** and **18**) have rotamer populations showing the trend *gg* > *gt*.

This trend appears to be related to the nature of the substituent at C4. Hydrogen, hydroxyl and amino groups have higher relative *gt* populations. Methoxy, thiol, and ammonium groups give higher relative *gg* populations. The cause of this effect is not clear.

Table 3.8 Rotamer Populations of D-Glucose Derivatives with Different Substitution at C4.[a]

Compound	Rotamer Population (%)[b]			Reference
	gg	*gt*	*tg*	
α-D-glucopyranose	42	50	8	108
Me α-D-glucopyranoside (**10**)	48	48	4	108
6-*O*-Me-α-D-glucopyranose	46	52	2	108
Me 2,3,4,6-tetra-*O*-methyl-α-D-glucopyranoside (**16**)	61 (60)	41 (40)	-2	here
Me 2,3,4-tri-*O*-methyl-α-D-glucopyranoside (**18**)	59	38	3	here
Me 4-deoxy-α-D-glucopyranoside	33	55	12	108
Me 4-amino-4-deoxy-α-D-glucopyranoside	48	47	5	108
Me 4-ammonio-4-deoxy-α-D-glucopyranoside	48	33	19	108
Me 4-deoxy-4-thio-α-D-glucopyranoside	57	43	0	108

[a] Determined in water. [b] Calculated using Equations 11-13 or 11,15-16 where appropriate.

3.2.3.2 Systems with Hydrogen Bonding

The results for compound **18** shed light on the effects of hydrogen bonding in determining the rotamer populations. Hydrogen bonding is important and a significant solvent effect does exist. In non-polar solvents, hydrogen bonding occurs in the *tg* conformer sufficiently to stabilize this rotamer with respect to the others by at least 6-8 kJ and to give it a small but significant population. The other rotamers also show a differential solvent effect; the *gg* rotamer population decreases and the gt rotamer population increases as solvent

polarity increases. There is evidence that these rotamers are also stabilized by intramolecular hydrogen bonding.

The infrared spectra of compound **18** (see Figure 3.19) support this conclusion. The very broad peak in the hydrogen bonded O-H stretching region of **18** in hexane indicates that there is more than one type of intramolecular hydrogen bond present. In acetonitrile, the hydrogen bonded O-H stretching peak appears narrower and is centered at the largest intramolecular hydrogen bonding frequency, indicating that some types of hydrogen bonding have disappeared. This is consistent with the ^{1}H NMR evidence which indicates a decrease in the populations of the hydrogen-bonded rotamers of the *tg* and *gg* rotamers with increasing solvent polarity.

The solvent effects are most likely due to weakening of the hydrogen bonds in polar environments. The population trends in polar solvents are due to the rotamer populations returning to their non-hydrogen bonded population levels. The rotamer populations in water are identical to those in the permethylated derivative **16a** where no hydrogen bonding is present.

The small population of hydrogen-bonded *tg* rotamer is in marked contrast to the results of Beeson *et al.*[163] In chloroform, (1S,2R,4S)-4-*tert*-butyl-2-(hydroxymethyl)-1-methoxycyclohexane (**22**) (see Figure 3.22) was present in the hydrogen-bonded *tg* rotamer to an extent of 74%. The lower *tg* population in **18** reflects the ability of the other rotamers to participate in hydrogen bonding.

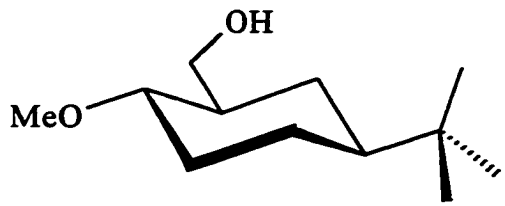

Figure 3.22 (1S,2R,4S)-4-*tert*-butyl-2-(hydroxymethyl)-1-methoxycyclohexane (**22**)

Beeson's work[163] showed that the amount of *tg* rotamer (and thus hydrogen bonding) was related to the β_{KT} of the solvent and to a lesser extent, the solvent parameter E_T. The results presented here indicate a weaker correlation to β_{KT} and a strong correlation to ϵ_{KT}. Beeson *et al.* discussed their results with respect to dielectric constants of protein binding sites.

3.2.3.3 Effect of Environmental Polarity on Carbohydrate Conformation

The importance of environmental polarity as measured by the dielectric constant (ϵ) in protein binding sites is of considerable interest.[211,212] Often the solution conformation of an oligosaccharide is not the conformation in the binding site and local ϵ values could be a determining factor. The dielectric constant of a carbohydrate recognition domain (CRD) in a protein varies depending on how one defines the dielectric constant.[212] The overall ϵ for a protein has been estimated at 2 D. This value however is not at all accurate in CRDs where many polar or ionic functionalities are concentrated. Estimates including functional group effects estimate ϵ to be anywhere from 4 to 80 with a value of approximately 10 being most representative.[211,212]

Beeson *et al.*[163] pointed out that the strong correlation of intramolecular hydrogen bonding to β_{KT} and lack of correlation to ϵ_K could mean that dielectric constant of a protein binding site was not important in determining hydrogen bond strength. This implies that the

protein dielectric constant is irrelevant in determining the population. Instead, the hydrogen bond basicity of a particular residue in the binding site would determine the rotamer population at the binding site. The results for compound **18** point to the opposite conclusion, if no specific electrostatic interactions stronger than hydrogen bonding are present, then the dielectric constant of the binding site will determine the amount of intramolecular hydrogen bonding and thus the conformation of the carbohydrate.

It is also of interest to examine the effect that CRD dielectric constant may have on glucose and galactose units in oligosaccharides with a substituent on O6, especially (1→6)-linked disaccharide units. The results here show that the rotamer population in glucose-containing units should not be sensitive to the change in dielectric constant going from water to the CRD but those in galactose-containing units should have a shift to more *tg* rotamer and less *gt* rotamer. This trend is useful if one is studying the conformational changes a carbohydrate would undergo when it is bound to a protein.

3.2.3.4 Comparison of Results to *Ab Initio* Calculations

The MP2/6-31G* calculations of α-D-glucopyranose by Brown and Wladkowski gave ΔG° values for the gas phase which result in *gg*:*gt*:*tg* rotamer energies of 0.0:1.95:1.01 kJ/mol respectively. Earlier calculations on β-D-glucopyranose by Barrows *et al.* at higher levels of theory level gave results with a ΔG° for the *gt* and *tg* rotamers of 2.4 kJ/mol in favour of the *gt* rotamer. This is in much better agreement with the experimental results. They also calculated, that in the aqueous phase, the *tg* rotamer was further destabilized by 3.8 kJ/mol by solvent effects. Applying the solvent destabilization to the results of Brown and Wladkowski yields energies which give *gg*:*gt*:*tg* rotamer populations of 62:30:8 respectively.

These results are much closer to the experimental results and they point to the importance of solvent effects in determining rotamer populations when hydrogen bonding is possible but they still result in detectable populations of the *tg* rotamer, thus indicating an underestimation of the *tg* destabilization. The solvent effect for a non-polar environment was found to be 2.5 kJ/mol less than that for an aqueous environment. This is much less than the amount estimated from the results for compound **18** (>5 kJ/mol).

3.3 Conclusions

The solvent dependence of the C5-C6 rotation of D-glucose has been determined by examination of two model compounds. The results were obtained through NMR spectroscopy and infrared spectroscopy. They indicate that, unlike galactose derivatives, glucose rotamer equilibria are not dependent on solvent dielectric constant when the hydroxyl proton is not present on O6. The rotamer population is unchanged with increasing dielectric constant. In cases where hydrogen bonding can take place, there is a change in rotamer population; however once the solvent is of sufficiently high polarity, intramolecular hydrogen bonding in the *tg* rotamer ceases to be significant and the rotamer populations are identical to the populations when hydrogen bonding is not structurally possible.

It has been shown through infrared and ^{1}H NMR analysis that significant intramolecular hydrogen bonding takes place in all rotamers, and that this intramolecular hydrogen bonding is present (although weakened) even in polar environments such as acetonitrile. A new explanation has been presented for the observed "reversed" chemical shifts in permethylated and peracetylated glucose derivatives. This chemical shift reversal is the result of a solvent effect, not a magnetic anisotropic effect.

The cause of the lack of a solvent effect for compound **16a** was not unequivocally shown but it has been theorized that it is due to an equal stabilization in all the rotamers as polarity increases. The stabilization of the *tg* rotamer is due to reduced electrostatic repulsions and favourable solvent-solute interaction (the *tg* rotamer has the highest dipole moment). The other rotamers are also stabilized by reduced electrostatic repulsions and a favourable solvent effect on the *gauche* effect.

The stability of the rotamers in the glucose derivatives were compared to that in a model compound (**5**) and it was theorized that the relative stabilities of the C5-C6 rotamers is due to enhancement of the *gauche* effect by the anomeric effect and by a substituent effect at C4. *Ab initio* results from the literature are in agreement with the results here but they tend to overestimate the stability of the *tg* rotamer.

3.4 Experimental

3.4.1 Spectroscopy

All NMR spectra were run at 300 K in high quality 5mm NMR tubes on a Bruker AMX-600, 500 or 400 MHz instrument. The samples were made up in concentrations between 10 and 15 mM in deuterated solvents (except CS_2). Chemical shifts are given parts per million (ppm)(±0.01 ppm) relative to TMS (chloroform-*d* and CS_2), or referenced to a solvent line as an internal standard as follows: cyclohexane-d_{12} 1.38 ppm (singlet), toluene-d_{12} 2.05 ppm (quintet), tetrahydrofuran-d_{12} 1.73 ppm (singlet), dichloromethane-d_2 5.32 ppm (triplet), acetone-d_{12} 2.05 ppm (quintet), methanol-d_4 3.31 ppm (quintet), acetonitrile-d_3 1.94 ppm (quintet), dimethyl sulfoxide-d_{12} 2.50 ppm (quintet) and water-d_2 4.63 ppm (singlet). Spectra were solved initially by first or second order[213-215] analysis followed by iterative simulation with the program LAME8.[104] The iterations gave results where the largest absolute error in chemical shift between the experimental and calculated spectra was 0.5 Hz or less. The accuracy of the coupling constants obtained from the iteration was ±0.05Hz. The populations calculated from these coupling constants have an accuracy of ±3% (absolute). Infrared spectra were recorded on a Nicolet 510P FTIR spectrometer using NaCl solution cells with lead spacers for solutions.

3.4.2 General Synthetic Techniques

Sodium hydride was purchase from Aldrich as a 60% dispersion in mineral oil. It was purified by repeated washing with pentane in an argon atmosphere. *N,N*-Dimethylformamide was dried over $MgSO_4$ for 48 hours followed by vacuum distillation and stored over 4Å molecular sieves. Pyridine was dried by reflux and distillation over calcium hydride.

Anhydrous methanol was obtained by reflux and distillation over $Mg(OMe)_2$. Anhydrous THF was obtained by predistillation over P_2O_5 followed by relux and distillation over Na/benzophenone. Amberlite IR-120(+) ion exchange resin was purchased from Aldrich and prepared for use in the H^+ form by gentle stirring for 24 hours in 1.0 M HCl, filtration and rinsing with anhydrous methanol. All solvents used for extraction and recrystallization were distilled before use. Mass spectra were run on a Dupont-CEC 21-110 (EI) double focusing mass spectrometer with an EI energy of 70.0 eV.

Melting points were determined with a Fisher-Johns melting point apparatus and are uncorrected. Specific rotations were measured on a Perkin-Elmer model 141 polarimeter. Thin layer chromatography was performed on 0.20 mm thick Merck silica gel 60F-254 aluminum plates. Components were visualized by spraying with a 2% ceric sulfate solution in 1 M H_2SO_4 followed by heating on a hot plate until discoloration occurred. Dry flash-column chromatography was performed on TLC grade silica gel using a gradient elution from hexane to ethyl acetate.

3.4.3 Synthesis

3.4.3.1 Methyl 2,3,4,6-Tetra-*O*-[$^2H_3$]methyl-α-D-glucopyranoside (16a)

Methyl α-D-glucopyranoside (**10**) (1.51 g, 7.8 mmol) was methylated using the technique of Brimacombe *et al.*,[197] but instead of methyl iodide, [$^2H_3$]methyl iodide (99%) was used as a methylating reagent. Methylene chloride was used as an extraction solvent and after evaporation the organic residue was distilled using a bulb to bulb distillation apparatus to give 1.48 g (72%) of **16a** as a clear oil: bp 98°/1.3 kPa, lit bp145°/1.8 kPa;[216] ^1H NMR (see

Appendix Tables A.1 and A.2); EI-MS: calcd for $C_{11}H_{10}O_6{}^2H_{12}$ *m/z* 262, found *m/z* 231 $(M\text{-}OCH_3)^+$.

3.4.3.2 Methyl α-D-[4-^{13}C]glucopyranoside (10a)

D-[4-^{13}C]Glucopyranoside (99%)(17)(248.9 mg, 1.37 mmol) was converted to methyl α-D-[4-^{13}C]glucopyranoside (70 mg, 26%) by the method of Bollenback:[196] mp. 165-166°, lit:166-167°.[196]

3.4.3.3 Methyl 2,3,4,6-Tetra-*O*-[$^2H_3$]methyl-α-D-[4-^{13}C]glucopyranoside (16b)

Compound **10a** was methylated as for **10** above. The clear oil (30.2 mg, 35%) was not distilled. ^{1}H NMR (see Appendix Tables A.3 and A.4); EI-MS: calcd for $C_{10}H_{10}O_6{}^{13}C^2H_{12}$ *m/z* 263, found *m/z* 232 $(M\text{- }OCH_3)^+$.

3.4.3.4 Methyl 6-*O*-*tert*-Butyldimethylsilyl-α-D-glucopyranoside (20)

Compound **10** (3.88 g, 20 mmol) and *tert*-butyldimethylsilyl chloride (3.32, 22 mmol) were dissolved in pyridine (40 mL) and stirred overnight at room temperature. Water (25 mL) was added and the mixture was extracted with ether (5 x 40 mL). The combined extracts were dried ($MgSO_4$) and concentrated to a solid residue that was recrystallized from hexane-ether to give **20** (3.08 g, 50%) as a colorless solid: mp 155-156° lit 155-157°;[206] ^{1}H NMR spectrum identical to that of Franke and Guthrie;[206] ^{13}C NMR (62.9 MHz, chloroform-*d*) 99.2 (C1), 74.5 (C3), 72.1 (C5), 71.7 (C2), 71.0 (C4), 63.8 (C6), 55.1 (OMe), 25.9 (-C(CH_3)$_3$), 18.3 (-**C**(CH_3)$_3$).

3.4.3.5 Methyl 2,3,4-Tri-*O*-[$^2H_3$]methyl-6-*O*-*tert*-butyldimethylsilyl-α-D-glucopyranoside (21)

Compound **20** was methylated by the method used to prepare **16a** and **16b**. The title compound (**21**) was purified by dry-column flash chromatography to give a clear oil (1.07 g, 30%); ^1H NMR spectrum identical to that reported by Franke and Guthrie;[206] ^{13}C NMR (62.9 MHz, $CDCl_3$) 97.3 (C1), 83.6 (C3), 81.8 (C2), 79.1 (C4), 71.4 (C5), 62.1 (C6), 54.9 (OMe), 25.9 (-C(CH_3)$_3$), 18.3 (-C(CH_3)$_3$).

3.4.3.6 Methyl 2,3,4-Tri-*O*-[$^2H_3$]methyl-α-D-glucopyranoside (18)

Compound **21** (1.07 g, 3 mmol) was desilylated by the method of Franke and Guthrie[206] to give **18** after chromatography as a colorless oil (226.9 mg, 30%): ^1H NMR (see Appendix Tables A.5 and A.6); EI-MS: calcd for $C_{10}H_{11}O_6{}^2H_9$ *m/z* 245, found *m/z* 214 (M- OCH_3)$^+$; ^{13}C NMR (62.9 MHz, $CDCl_3$) 97.6 (C1), 83.3 (C3), 81.8 (C2), 79.6 (C4), 70.5 (C5), 62.0 (C6), 55.2 (OMe).

Chapter 4
Conformational Analysis of Crown Thioethers

4.1 Introduction

For several years there has been growing awareness of the role that conformation plays in multidentate ligands with respect to the formation, stability and properties of their metal complexes whether these be large, naturally occurring metalloproteins or comparatively simpler small molecules.[217-224] For example, the rapid electron transfer kinetics of Type I or "blue" copper enzymes has been attributed to the coordination sphere geometry imposed on copper by its protein ligand which is in turn a consequence, at least in part, of the secondary structure of that ligand.[225,226] A key aspect of this ligand geometry is the presence of sulfur-copper coordination.[227,228]

Crown thioethers (see Figure 4.1) are particularly interesting ligands because most of these compounds prefer to adopt conformations that have their sulfur atoms exodentate in the wrong orientation for binding.[229,230] They are important ligands, particularly for late transition metal complexes. Crown thioethers have a variety of other important uses as well as being used as models for metalloproteins. The use of tri- and tetraaza-macrocycles[231] for delivery of radioactive isotopes for both diagnostic and therapeutic purposes has led the way for the possible use of crown thioethers to deliver rhenium and rhodium radionuclides.[232,233] It is also possible that crown thioethers could be used as a treatment for cases of heavy metal

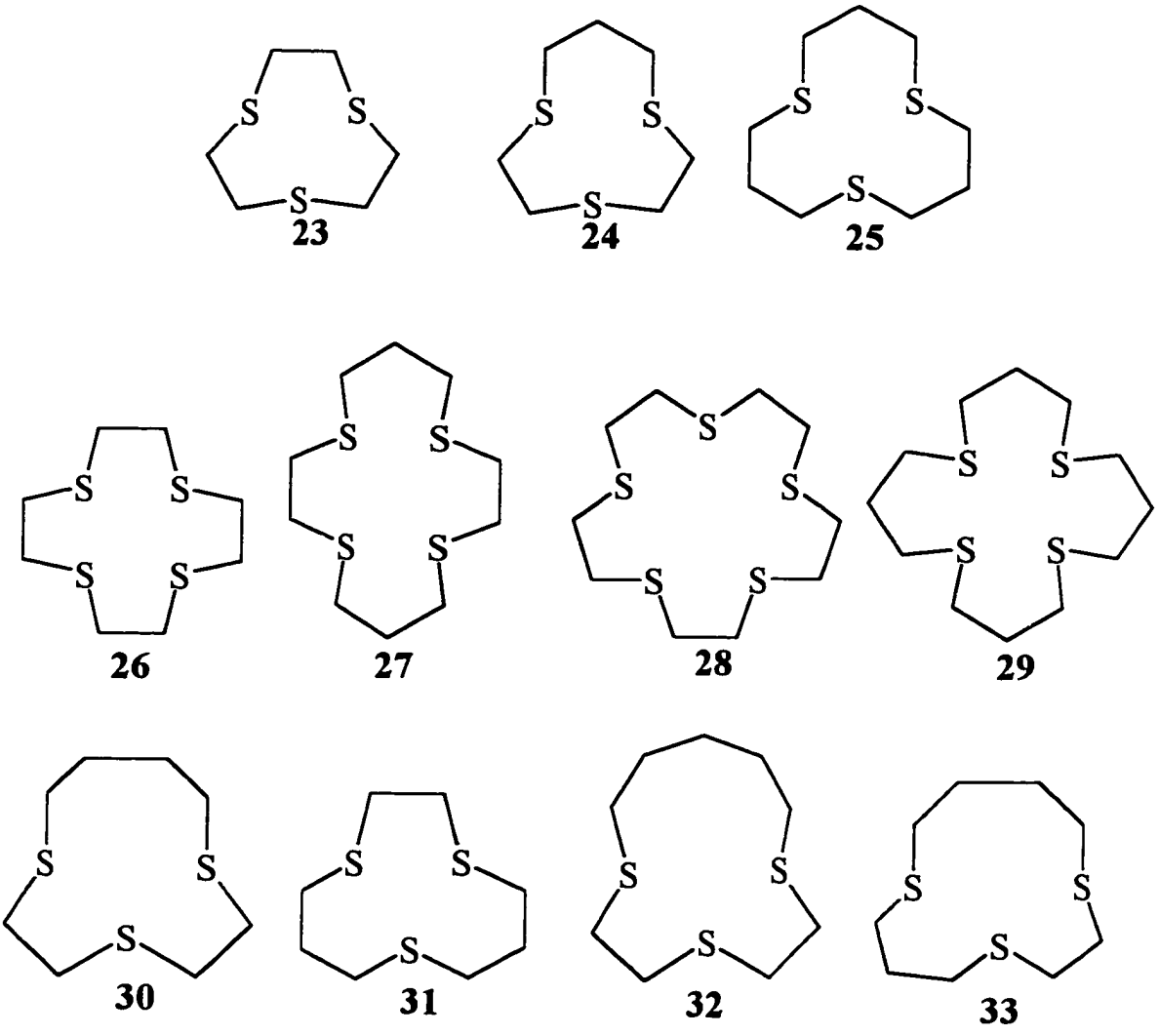

Figure 4.1 Structures of various crown thioethers considered in this study: 1,4,7-trithiacyclononane (**23**), 1,4,7-trithiacyclodecane (**24**), 1,5,9-trithiacyclododecane (**25**), 1,4,7,10-tetrathiacyclododecane (**26**), 1,4,8,11-tetrathiacyclotetradecane (**27**), 1,4,7,10,13-pentathiacyclopentadecane (**28**), 1,5,9,13-tetrathiacyclohexadecane (**29**), 1,4,7-trithiacycloundecane (**30**), 1,4,8-trithiacycloundecane (**31**), 1,4,7-trithiacyclododecane (**32**), 1,4,8-trithiacyclododecane (**33**).

poisoning.[234] They have been examined as possible constituents of molecular devices.[235] The strong complexing behaviour of crown thioethers to late transition elements could be used to extract heavy metals from the environment or to extract economically important metals for commercial use. An example of this type of use has been presented by Guyon *et al.*[236] who found that crown thioethers were very effective at recovering palladium from waste solutions produced during the recovery of plutonium and uranium from spent nuclear fuel rods.

Although acyclic thioethers are not especially good binders,[237] the crown thioethers complex surprisingly well. They have also been found to have interesting complexing properties. They are able to stabilize rare or unstable oxidation states of metals such as cobalt(II)[238], iron(II),[239] platinum(III)[240] and rhodium(II).[241,242] They can stabilize low spin states of cobalt(II) and iron(II).[239,243] Crown thioethers also appear to have large ligand field strengths[242,244] and their complexes have unusual electrochemical properties.[218]

The unusual properties of macrocyclic polythioether ligands and their complexes have been attributed to assumed conformational preferences based on conformations observed in X-ray studies of the ligands and their complexes in the solid state.[222,229,230,241,242,245,246] Knowledge of the relative stabilities and structures of all conformers for crown thioethers would allow understanding of the relationship between binding properties and conformation and prediction of the binding properties of new compounds. It was felt that careful molecular modelling could markedly improve understanding of this area. The compounds considered are shown in Figure 4.1.

4.1.1 Conformational Trends for Crown Thioethers

Based on concepts originally proposed by Dale to account for conformational preferences of medium and large rings,[28,247] Cooper and his coworkers presented a rationalization for the exocyclic orientation of non-bonding pairs of electrons on sulfur atoms that were observed in the crystal structures of most crown thioethers that contained SCH_2CH_2S units.[248] This conformational preference of crown thioethers is opposite to that found in crown ethers. It has also been observed in other types of sulfur-containing systems such as thiophenophanes, thiacyclophanes, macrocycles with heteroatoms in addition to sulfur, and even in acyclic species.[220-222,249-252] Cooper's rules can be summarized as follows; C-S-C-C units prefer to be *gauche* and S-C-C-S units prefer to be *anti*. On this basis, the two S-C-C-S sections in an S-C-C-S-C-C-S unit prefer to be *anti* and a turn at the central S allows the two 2 C-S-C-C sections to be *gauche* resulting in an overall "bracket"-shape for the 7 atom segment (see Figure 4.2).[248]

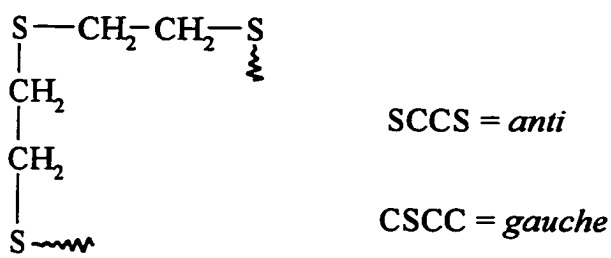

Figure 4.2 The "bracket" substructure of crown thioethers resulting from application of Cooper's rules.

Unambiguous assignment of conformation to a crown thioether ligand has been most commonly performed by X-ray crystallographic study of solid samples of the free ligand. The question then arises as to whether the observed conformation of the free ligand is due to

intramolecular interactions as suggested by Cooper or because of intermolecular interactions that are peculiar to the solid state. This question has been at least partially addressed by comparisons between the conformation of ligands in their free and complexed states. If the forces controlling conformation are mainly intramolecular, one could expect similar conformations in both states and this has been observed in several instances.[241,246,253-255]

Results such as these are in agreement with the concept of preorganization.[17,256-258] Cram and coworkers[256] stated that the stability of a complex depended on whether or not the ligand was preorganized for bonding. This involves two criteria: a) the conformation of the ligand should be the same or similar to that in the metal-ligand complex prior to actual complexation; and b) the binding sites in the ligand should not be solvated. In other words, if the conformation found in the complex was also significantly populated and not solvated in a solution of the free ligand then the complex would be more stable due to the fact that the ligand would not have to alter its conformation and desolvate and thus create unfavourable enthalpy and entropy of formation. Lehn has discussed the effects of preorganization on complexation of crown ethers.[259]

However, there are also examples in the literature in which the solid state conformations of free and complexed ligands are different or variable and this suggests that preorganization and the source of conformational control are not always as simply defined as they may have seemed.[221,222,245,246,254,255,260-262] This conclusion is reinforced by results from a small number of studies that attempt to compare conformations in the solid state with those in the gas phase or solution and which often find significant differences between states.[221,263-266]

4.1.2 Molecular Mechanics as a Tool for Conformational Analysis

In order to develop better crown thioether ligands, it would be helpful to have a rational design strategy. To do this, a knowledge of the effects of preorganisation or lack thereof is required. If preorganisation is a major factor, then syntheses should be directed toward ligands that favour conformers with endodentate sulfurs. If other, more subtle, factors are involved then different synthetic targets should be examined. A complete knowledge of the conformational energy surface for the free ligand is necessary in order to determine effects of preorganization, if any, on a known ligand or a synthetic target. The best available technique to examine conformational energy surfaces is molecular mechanics combined with conformational search routines.

Molecular mechanics computer programs, particularly those with class II force fields such as MM3,[42] are now accurate enough that the prediction of relative conformational stability can be performed with small tolerances for hydrocarbons. The introduction of heteroatoms is also handled well.[66,267,268] Even when different types of compounds are studied, the agreement with experiment is excellent; for instance, using MM3(89), the standard deviation between calculated and experimental heats of formation for 52 hydrocarbons was 1.8 kJ/mol,[42] that for 39 ethers was 1.6 kJ/mol,[66] and for 24 sulfides was 1.8 kJ/mol.[267] Accurate force fields are only one requirement for conformational searching. A method for searching the conformational space is also required.

4.1.2.1 Methods for Conformational Searching

There are a variety of methods for complete searching of conformational space. These algorithms allow the location of the many conformations that are available to medium and

large ring molecules.[269-273] These methods involve the random or systematic modification of an input structure followed by subsequent energy minimization. The chief difference in the various methods is the type of modification made and the amount of CPU time required for a complete search.

Random or stochastic methods[269,274] are generally considered the most effective for searching conformational space.[270,272] In these methods, particular features of a molecule such as torsional angles or the coordinates of atoms are randomly altered. The MM3(94) program contains such a method for conformational searching. The program uses the stochastic search routine of Saunders.[269] The stochastic search method starts from an initial conformation, then moves each Cartesian coordinate for each atom a random distance obtained by multiplying the allowed maximum move (an adjustable parameter) by a random number between 0 and 1. The new conformation is then minimized and the process repeated starting from this new conformation.

4.1.2.2 Molecular Mechanics Analyses of Crown Thioethers

Conformational analyses using molecular mechanics have been performed on 1,4,7-trithiacyclononane (**23**)[275] and 1,4,7-trithiacyclodecane (**24**)[245,276]. These searches found 13 conformations for **23**[275] using molecular dynamics, systematic and random search methods with the CHARMm force field; and 24 conformations for **24**[245,276] using a method of systematic modification of previously determined conformers of cyclodecane with the MM2 force field. The results of these calculations were interpreted in terms of their relationship to the structure of the ligands in the solid state complexes but a comprehensive examination of the relationship

between conformer population of the free ligand and the conformation in the complex was not performed.

4.1.3 Summary

The conformation of the ligand plays an important role in determining the stability of crown thioether complexes. Previous work has particularly emphasized the conformation of the free ligand in the solid state. This is an oversimplification of the problem because experimental work for **23** indicates that free ligands in the gas phase are much more complex conformationally.[17] A more complete examination of the conformations of the free ligands using computational techniques, and extending the results to the solution phase, is required to fully determine the effect that the constitution of these conformational mixtures have on the stability of complexes.

4.2 Results and Discussion

4.2.1 Molecular mechanics

4.2.1.1 Parameterization for Sulfur-Containing Molecules

Molecular mechanics calculations were performed using a slightly modified version of the program MM3(94).[42,66] The original MM3(89) parameter set has undergone several modifications to improve agreement between calculations and observation for sulfides[267] and now gives good agreement for heats of formation and geometries for these types of compounds as well as for hydrocarbons. However, there are several subtle conformational features that for our purposes were not satisfactorily reproduced with the MM3(94) parameter set. Experimentally, ethyl methyl sulfide (**34**) slightly prefers the *gauche* conformation[277-280] while a slight *anti* preference is calculated; the calculated A-value for the thiomethyl group is about 2 kJ/mol bigger than the experimental value.[281,282] Therefore, a limited reparameterization was undertaken in order to improve the agreement for a range of simpler model compounds before the crown thioethers were examined.

The three torsional terms involving sulfur and carbon in the crown thioethers examined here, i.e. the C-S-C-C, S-C-C-C, and S-C-C-S terms, were among the few terms that could be changed without influencing the performance of the force-field to a major extent. The strategy adopted for parameter development was to choose small molecules for which reasonably accurate data was available and that had features that were sensitive to changes in the parameter of interest and then to develop improved parameters. The resulting improved parameters were tested against data for other small molecules not used in parameter development.

4.2.1.1a C-S-C-C Parameterization

The simplest compound containing the C-S-C-C torsional unit is ethyl methyl sulfide (**34**). Early experimental results[283,284] qualitatively showed that the *gauche* and *anti* conformers were approximately equal in stability. More recent studies were able to give a more quantitative picture of the *gauche/anti* equilibrium. Electron diffraction results for ethyl methyl sulfide indicate that the *gauche* conformer is favoured by 0.75 kJ/mol at room temperature[277] and infrared and Raman studies[278-280] gave a preference of 0.19-0.13 kJ/mol in the gas phase, and 0.59 kJ/mol in the liquid phase. The original parameters in MM3(94) favoured the *anti* conformer by 0.54 kJ/mol. The C-S-C-C parameters were slightly altered (Table 4.1) in order to favour the *gauche* conformer of this compound as outlined in Table 4.2 and also to better fit the conformational energies for diethyl sulfide (**35**).[285]

Table 4.1 Revised Torsional Parameters (kcal/mol)

Torsional Angle		V_1	V_2	V_3
C-S-C-C	Old	-0.44	-0.26	0.60
	New	-0.63	-0.32	0.60
S-C-C-C	Old	0.00	0.20	0.40
	New	-0.50	0.15	2.00
S-C-C-S	Old	1.25	-0.30	0.00
	New	3.13	-2.00	1.00

4.2.1.1b S-C-C-C Parameterization

No molecule that contained S-C-C-C units where the sulfur atom was not incorporated in a ring was included in the paper describing sulfur parameter development for MM3.[267] Here, the A-value for (methylthio)cyclohexane (**36**)[281,282] and the energy difference between *gauche* and *anti* conformers of 1-propanethiol (**37**)[286] were used for this purpose. The A-value for SMe (4.19-4.48 kJ/mol) had been determined by low temperature NMR spectroscopy in CS_2.[281,282] The *anti* conformer of propanethiol was found to be 1.7 kJ/mol more stable than the *gauche* by examination of the infrared and Raman spectra combined with measurements of heat capacity and entropy in the gas phase.[286]

The resulting parameters (Table 4.1) differed most markedly from the original parameters by the addition of a substantial V_1 term. Adding this term improved the agreement considerably with experimental results both for the two molecules used for parameter development as shown in Table 4.2 and for the test molecules to be discussed.

4.2.1.1c S-C-C-S Parameterization

The original parameters[267] for the torsional terms for the S-C-C-S unit were based on electron diffraction[287] and microwave data[288] for 1,2-ethanedithiol (**38**). 1,2-Ethanedithiol, however, has the complication of intramolecular hydrogen bonding, which makes the relative stability of the *gauche* and *anti* conformers due to torsional effects alone difficult to ascertain. To overcome this difficulty, 1,2-bis(methylthio)ethane (**39**) was used as the model compound. The relative stability of the *ggg* and *gag'* conformers (4.6 kJ/mol), determined by infrared spectroscopy,[289] was chosen as the target for parameterization. It was felt that a second model compound would allow for a more accurate parameterization. An ideal compound for

Table 4.2 Results from Parameterization with Model Compounds

Torsion	Compound	Experiment	ΔG^{o} Exp.[a] (kJ/mol)	Method	Ref.	ΔE^{b} Std. (kJ/mol)	ΔG^{o}-ΔE (kJ/mol)	ΔE^{c} New (kJ/mol)	ΔG^{o}-ΔE (kJ/mol)
C-S-C-C	ethyl methyl sulfide	*gauche* ⇌ *anti*	0.75	ED	277	-0.54	1.29	0.21	0.54
		equilibrium	0.19	IR-Raman	278	-0.54	0.73	0.21	-0.02
			0.13	IR-Raman	279	-0.54	0.67	0.21	-0.08
			0.59	IR-Raman(liq)	280	-0.54	1.13	0.21	0.38
	diethyl sulfide *aa*	*ag* ⇌ *aa*	1.9	IR-Raman	285	-0.46	2.36	0.29	1.61
	gg	*ag* ⇌ *gg*	0.17	IR-Raman	285	0.84	-0.76	0.04	0.13
S-C-C-C	1-propanethiol	*g* ⇌ *a*	-1.7	IR-Raman	291	-4.23	2.53	-2.72	1.02
	methylthiocyclohexane	ax ⇌ eq	-4.39	NMR	282	-6.32	1.97	-3.64	-0.75
S-C-C-S	1,2-bis(methylthio)ethane	*ggg* ⇌ *gag'*	-4.6	IR-Raman	292	-6.91	2.31	-6.57	1.97
	trans-1-thiomethyl-2-thiophenylcyclohexane	dieq ⇌ diax	-0.17	NMR	290	5.02	-5.19	0.04	-0.21

[a] For information about the measurement, see text. [b] Calculated using standard parameters. [c] Calculated using parameters in Table 4.1.

this purpose would be a *trans*-di-S-substituted cyclohexane ring. The only compound of this type in the literature for which accurate conformational energies had been determined was *trans*-2-methylthio-1-phenylthiocyclohexane (**40**). Zefirov *et al.*[290] performed low temperature ^{1}H NMR studies and determined that **40** slightly favoured the diaxial form by 0.42 kJ/mol in CCl_4 and the diequatorial form by 1.7 kJ/mol in CH_3CN. The experimental value in CS_2 (0.17 kJ/mol in favour of the diaxial) was used as the target for parameterization.

The S-C-C-S parameterization was performed using the same method used in Chapter 2 for the O-C-C-O parameters. V_1 and V_2 were systematically altered and calculations run on the *aaa* and *aga* conformations of *trans*-1,2-bis(methylthio)cyclohexane (**41**) and the *ggg* and *gag'* conformers of compound **39**, until satisfactory agreement with the experimental energy differences was obtained. Compound **41** was used as a computational model for **40** because the fewer number of atoms and higher symmetry of the methyl group made calculation simpler. The diaxial-diequatorial energy differences of **40** and **41** were assumed to be identical, based on the close similarity of the A-values for SMe and SPh groups (4.35[281,282] and 4.60 kJ/mol,[293] respectively). It was assumed that interactions between the phenylthio and methylthio group are minimal. Then V_3 was adjusted until satisfactory geometry about the S-C-C-S moiety was obtained for the *g'gg* conformer of 1,2-ethanedithiol (calculated 70.8° ; experimental 69.0° [288]). The new parameters are shown in Table 4.1 and the calculated energies are found in Table 4.2.

4.2.1.2 Parameter Testing

The new parameters were then used in various test cases to determine their accuracy for both energy and geometry. Tables 4.3 and 4.4 and Figure 4.3 show the results. The calculated difference in energy between the chair conformers of 3-methylthiane (**42**) having

the methyl group in axial or equatorial orientations (4.98 kJ/mol) agreed with the experimental result[294] within 0.9 kJ/mol. *cis*-3,4-Dimethylthiane (**43**) was considered to be particularly interesting because the observed free energy difference between conformers did not fit that calculated from values for the monosubstituted compounds, assuming additivity.[294] The calculated value using the new parameters was 0.42 kJ/mol different from the experimental value. For both these cases, the original parameters gave much poorer agreement. Further parameter testing was performed by calculating the torsional angles of various compounds. Table 4.4 shows calculated and experimental torsional angles for ethyl methyl sulfide,[277] thiane (**47**)[295] and 1,4-dithiane (**48**).[296] The agreement is about the same as for the original MM3 parameters.

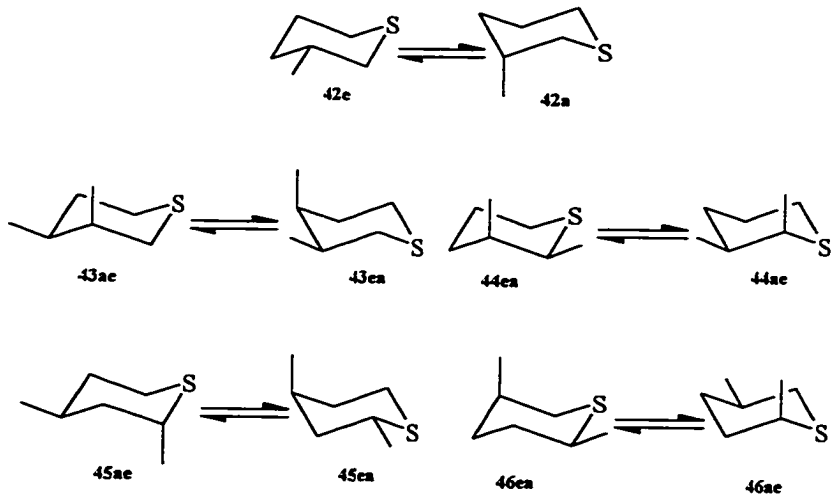

Figure 4.3 Conformational equilibria of 3-methylthiane (**42**), *cis*-3,4-dimethylthiane (**43**), *cis*-2,3-dimethylthiane (**44**), *trans*-2,4-dimethylthiane (**45**), *cis*-2,5-dimethylthiane (**46**) calculated in Table 4.3.

Table 4.3 Test of Parameters 1, Energy

Compound	ΔG^{o} Experimental[a] (kJ/mol)	ΔE Std. (kJ/mol)	ΔG^{o}-ΔE (kJ/mol)	ΔE New (kJ/mol)	ΔG^{o}-ΔE (kJ/mol)
42	5.86	6.69	-0.83	4.98	0.88
43	2.51	1.13	1.38	2.93	-0.42
44	0.67	-2.18	2.85	-1.26	1.93
45	1.59	3.22	-1.63	4.01	-2.42
46	0.08	-2.34	2.42	-1.51	1.59
Average $\lvert\Delta G^{o}$-$\Delta E\rvert$			1.82		1.44

[a] All data are for the equilibria shown in Figure 4.3 and are determined from low temperature ^{13}C NMR spectroscopy[294]

Table 4.4 Tests of Parameters 2, Torsional Angles

Compound	Method	Ref	Angles (°)		
			C-S-C-C	S-C-C-C	S-C-C-S
ethyl methyl sulfide	experimental	277	66	---	---
	old parameters		72.2	---	---
	new parameters		72.1	---	---
thiane	experimental	295	55.4	60.8	---
	old parameters		57.7	62.3	---
	new parameters		57.6	62.2	---
1,4-dithiane	experimental	296	---	---	69.5
	old parameters		62	---	70.5
	new parameters		62.6	---	71.3

It is interesting to compare the results of the parameterization with the generalizations used by Cooper *et al.*[248] to empirically determine the conformations of crown thioethers. Unlike the original parameterization, the new MM3 parameterization very slightly favours a *gauche* C-S-C-C torsion as stated in "Cooper's rules". The S-C-C-S torsion in the new parameterization fits the experimental energy better than the old parameters but both parameter sets give the same qualitative result as the rules, S-C-C-S favours the *anti* conformation.

4.2.1.3 Crown Thioethers

The stochastic search routine of Saunders[269] incorporated in MM3(94) was used to examine the conformational energy surfaces for eleven macrocyclic trithioethers with between 9 and 16 atoms in the ring. Calculations for each compound were performed using two different dielectric constants; 1.5 and 30 D, to simulate non-polar and highly polar environments. In the MM3 force field, changes in environmental polarity are simulated through the electrostatic energy term which has the dielectric constant in the denominator. Employment of a dielectric constant greater than 20 makes the magnitude of the electrostatic term insignificant in comparison with the other terms. Since macrocyclic thioethers seem to be relatively poorly solvated in general,[297] predictions of their conformations in solution based on calculations employing a relatively crude estimate of solvation effects via a bulk dielectric constant is probably fairly reliable, more so than for more heavily solvated analogs involving nitrogen or oxygen heteroatoms.

After each stochastic search run, the ten most stable conformers at each dielectric constant were reminimized using the other dielectric constant to confirm that the minima were

unique. All conformers were checked for negative infrared frequencies to establish unequivocally that they were minima. Boltzmann distributions of conformers at 298 K were calculated from conformer strain energies and entropies (calculated by the MM3 program) relative to those of the global minimum.

The lowest energy conformers for each compound were characterized using the conformers' symmetry, relative strain energy, dipole moment and mole fraction calculated at both dielectric constants. Since a large dipole moment indicates that most of the C-S bond moments are oriented in similar directions, it can be used to obtain a rapid evaluation of the likely binding properties of conformations. A large dipole moment requires that two or more sulfur atoms be exposed on the same side of the conformer, and as a result the conformer is likely to be a good binder. Dipole moments for S-containing molecules are slightly underestimated by MM3, for instance, thiane, observed 1.781 D[298], 1.71 D[299], calculated 1.58 D; allyl mercaptan, observed 1.331 D, calculated 1.24 D.[267] Conformers are numbered for each compound starting from the conformer with the smallest strain energy at a dielectric constant of 1.5 as conformer 1.

.4.2.2 1,4,7-Trithiacyclononane (23)

4.2.2.1 MM3 Conformational Analysis

Compound **23** has been the most studied of the crown thioethers largely because it readily forms stable complexes with late transition elements.[229,230] In the solid state, uncomplexed **23** is present in a C_3-symmetric conformation (see Figure 4.4, conformer 6) with the three sulfur atoms endodentate.[300] In most complexes, this C_3 conformer is the preferred structure of the ligand. It was long assumed that this predominance in both the free and bound

ligand meant that the C_3 conformer was also the most populated in solution.[225,229,230] Support for this assumption came from the gas phase photoelectron spectrum of **23** at 330 and 350 K which contained two broad bands in an approximately two to one intensity ratio separated by about 0.5 eV, due to loss of sulfur lone pair electrons.[264,301,302] This observation is qualitatively what would be expected from three equivalent sulfur lone-pair orbitals that interact through space. The original authors[264] considered this evidence an indication that only the symmetric C_3 conformer was present. However, the orbital energies of only two conformers were evaluated, not including the one calculated here and previously[17] to be the global minimum.

More recent information suggests that this simple picture does not describe the conformational situation correctly. An electron diffraction spectrum of the gas at 473 K was most consistent with C_1 or C_2 conformers, but the fit to the C_3 conformer was only slightly worse.[17] The spectrum observed was not compatible with a major contribution from the D_3 conformer.

More concrete evidence was provided by an infrared-Raman study of the solid, the liquid just over the melting point (78-81°C), and of a carbon tetrachloride solution. Comparison of these spectra indicated that the C_3 conformer of the solid was not present in the liquid or solution to any significant extent.[265,266] The spectra from the latter two phases were very similar and, in contrast to the conclusions of the electron diffraction study, were interpreted as being of the D_3 conformer.[265,266] However, the published spectra[265,266] of these phases, in which some of the intense lines from the C_3 conformer are absent, most notably the isolated band at 1455 cm^{-1}, appear to be much more complex than that expected for a single conformer, and are more consistent with a mixture of conformations.(see below) The ^1H

NMR spectra of **23** indicated that the SCH_2CH_2S units are largely fluxional in *gauche* conformations.[257,258]

Table 4.5 lists data calculated for the 13 conformers obtained for **23** in stochastic searches of the conformational energy surface using MM3(94) with the modified sulfur parameters described above. ATOMS diagrams of the seven conformers with the lowest strain energies are displayed in Figure 4.4. Comparison of the X-ray geometry with that calculated for the same conformation by MM3 is shown in Table 4.6 and 4.7 and it can be seen that the torsional angles calculated for the C_3 conformation are almost identical to those obtained from the solid.

These calculations indicate that a C_1 conformer is most stable, followed by a C_2 conformer, a D_3 conformer, and another C_1 conformer, with calculated mole fractions at 298 K of 0.79, 0.14, 0.006, and 0.046, respectively, using the default dielectric constant. The most important consequence of changing the dielectric constant is that the most polar conformation, the C_3 conformation present in the solid,[300] becomes much more stable in the more polar medium relative to the global minimum, moving from being the sixth to the third most stable conformer. However, because the solid-state C_3 conformation is disfavoured by entropy, it is only calculated to increase its fractional population from 0.2% to 3.8%, not large enough to be observed by any of the techniques used here. Conformers 1 to 4 are the same ones considered by Blom *et al.* in their analysis of electron diffraction data of **23**,[17] although the torsional angles derived in that study from MM2 calculations were fairly different from those obtained here, particularly for the global minimum C_1 conformer. Differences between

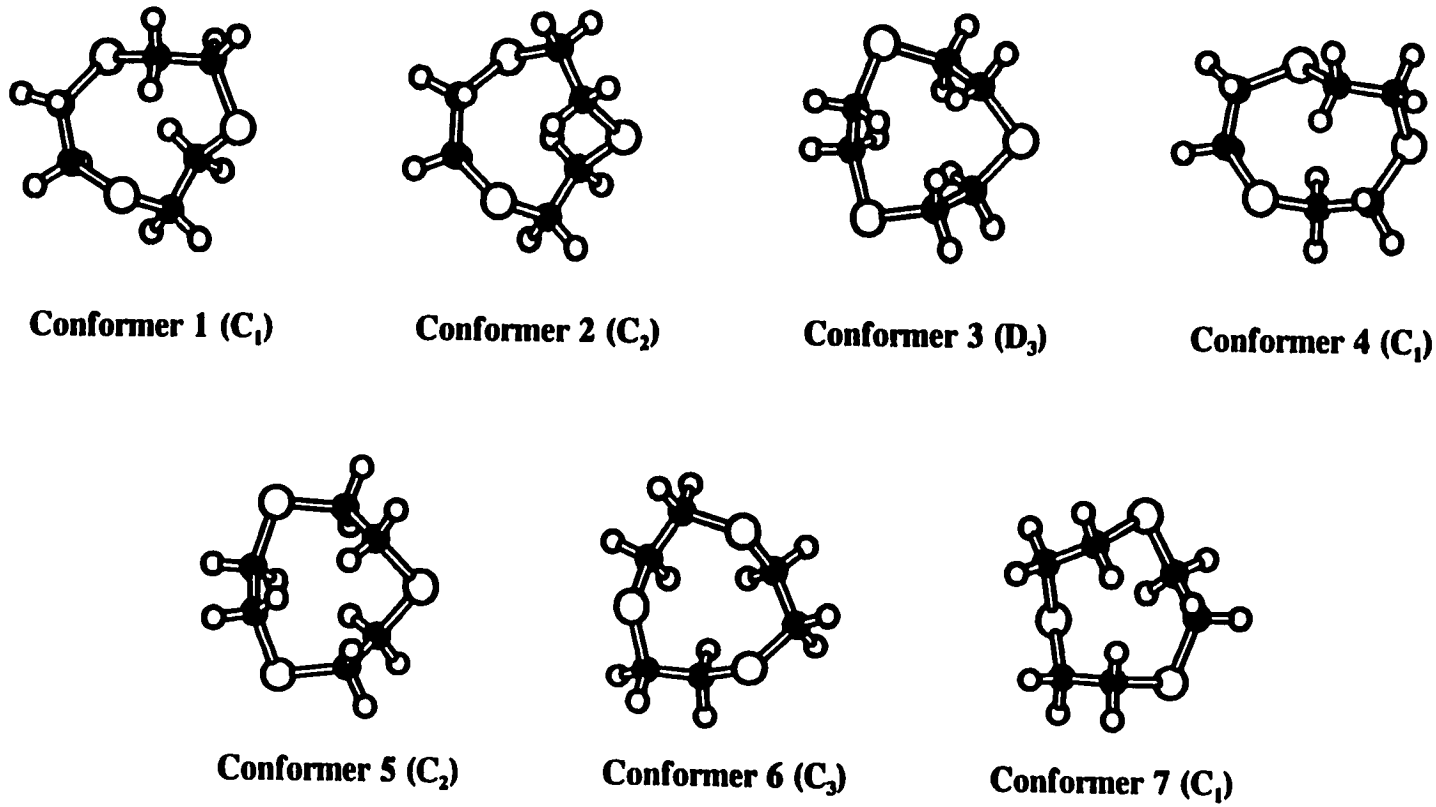

Figure 4.4 The seven most stable conformers of 1,4,7-trithiacyclononane (**23**).

Table 4.5 MM3(94) Results for 1,4,7-Trithiacyclononane (**23**)

Order[a] ϵ=1.5	Symmetry	Dipole Moment (D) (ϵ=1.5)	Strain Energy[b] (kJ/mol)	Mole Fraction (25 °C)	Order[a] (ϵ=30)	Dipole Moment (D) (ϵ=30)	Strain Energy[b] (kJ/mol)	Mole Fraction (25 °C)
1	C_1	1.51	0	0.79	1	1.51	0	0.79
2	C_2	1.32	1.53	0.14	2	1.32	1.86	0.12
3	D_3	0	5.26	0.006	4	0	3.91	0.009
4	C_1	1.54	8.48	0.046	5	1.53	8.17	0.018
5	C_2	0.013	9.44	0.007	6	0.009	9.06	0.007
6[c]	C_3	4.24	10.35	0.002	3	4.24	2.78	0.038
7	C_1	2.67	12.71	0.003	7	2.69	10.52	0.008
8	C_1	1.43	13.39	0.006	9	1.42	13.62	0.005
9	C_1	2.18	13.81	<0.001	8	2.22	13.11	0.002
10	C_1	2.75	16.06	0.001	10	2.78	14.3	0.002
11	C_1	4	27.43	<0.001	11	4.04	19.94	<0.001
12	C_2	1.57	65.91	$3x10^{-11}$	12	1.57	64.62	$4x10^{-12}$
13	C_1	1.2	70.42	$1x10^{-12}$	13	1.18	70.38	$4x10^{-13}$

[a] The numbers are the order of the conformations based on their strain energies at that dielectric constant. [b] With respect to the strain energy of the lowest energy conformation of this compound at this dielectric constant. [c] X-ray structure: ref. 300.

Table 4.6 Comparison of MM3 Torsional Angles (°) with X-Ray Torsional Angles (°)of **23**

Conformer	Symmetry	SCCS	CCSC	CSCC	SCCS	CCSC	CSCC	SCCS	CCSC	CSCC
X-Ray[a]	C_3	58.5	55.1	-131.1	58.5	55.1	-131	58.5	55.1	-131
1	C_1	-95.0	67.6	-122.5	66.8	70.8	-118.5	80.3	-90.1	134.7
2	C_2	70.5	-73.7	-73.7	70.5	58.9	-108.4	89.2	-108.4	58.9
3	D_3	-61.0	-61.0	141.3	-61.0	-61.0	141.3	-61.0	-61.0	141.3
4	C_1	-62.7	154.2	-91.8	73.4	-94.5	127.9	-117.9	97.0	-47.9
5	C_2	136.7	-81.6	91.3	-137.3	91.3	-81.6	136.7	-68.9	-68.9
6	C_3	58.6	55.7	-133.3	58.6	55.7	-133.3	58.6	55.7	-133.3
7	C_1	65.5	73.4	-70.4	-59.9	105.8	-88.7	124.8	-57.8	-76.0
8	C_1	-165.1	62.5	46.9	-109.1	114.0	-125.5	96.5	-54.4	96.1
9	C_1	-137.2	98.5	-105.3	59.4	58.8	-148.9	91.2	-55.0	102.1
10	C_1	69.1	-66.6	-59.0	149.9	-96.1	19.6	66.2	-146.6	54.4
11	C_1	-57.5	130.3	-114.9	57.1	39.7	-136.3	51.4	75.1	-60.0
12	C_2	57.1	-70.1	-70.3	57.1	51.3	2.0	-87.1	2.0	51.3
13	C_1	-118.9	113.9	-111.6	89.0	-37.8	-173.5	-167.7	-31.6	78.5

[a] X-ray results from ref. 300

Table 4.7 Comparison of MM3 Geometries with X-Ray Geometries of **23**[a]

	Bond Lengths (Å)			Bond Angles(°)		
Method	S-C1	S-C2"	C1-C2	C1-S-C2"	S-C1-C2	C1-C2-S'
X-Ray	1.820(5)	1.823(5)	1.510(6)	102.8(3)	113.0(4)	117.0(4)
MM3	1.8275	1.8341	1.5426	102.2	112.2	115.5

[a] X-ray results from ref. [300]

the torsional angles from MM2 and those calculated here for conformer 1 ranged from 5.1 to 19.6°.

The conformational analysis of **23** conducted by Beech *et al.*[275] gave results that are similar to those found in Table 4.5 in some respects. In their analysis of **23** using the Quanta/CHARMm 3.2 force field, they also found 13 minima, 10 of which were geometrically similar to our conformers 1-8 and 10-11 (see Table 4.5 and 6). However, the conformer order was different. Their lowest energy conformer was the sixth here, the C_3 conformer. Their second conformer was our first, their third conformer was our second, their fourth conformer was our fourth and their fifth conformer was our third. The higher energy conformers showed more variation in their order. The major difference between the two analyses is the fact that they found the C_3 conformer to be the global minimum. In fact it was calculated to be 1.30 kJ/mol lower in energy than the C_1 global minimum found in the current analysis. Based on their strain energies (that is, neglecting entropy effects) the population of the C_3 conformer was calculated to be 42%.

4.2.2.2 Spectroscopic Conformational Analysis

4.2.2.2a Photoelectron Spectra and Electron Diffraction

It will be shown that all experimental evidence is consistent with the results of the stochastic searches of the conformational energy space performed on **23** using MM3(94) as detailed above; that is, there are conformational mixtures in the gas phase and solution dominated by the global minimum C_1 conformer and the next one or two conformers. One piece of evidence which has been cited as supporting a C_3 conformer in the gas phase is the photoelectron spectrum at 330 K[264,301] which contains two bands at about 8.4 and 8.9 eV with intensity ratios of about 2:1.[264,301,302] Both bands in the published spectra[264,302] are broader than those in compounds containing SCH_2CH_2S units that exist in single conformations[264] and the 8.4 eV band is broader than the 8.9 eV band. At that temperature, the MM3 results predict that the mixture would consist of 77% conformer 1, 14% conformer 2, 6% conformer 4, 1% conformer 8 and lesser amounts of the others, including 0.3% of conformer 6 (C_3). The lone pair orbital energies for the six most stable (MM3) conformers were calculated using the implementation of AM1 present in HYPERCHEM and are listed in Table 4.8.

The spectra calculated for conformers 1, 2, 4 and for 6, the C_3 conformer, are all roughly in agreement with the observed spectra in that they contain two bands at 8.5±0.2 eV and one at 8.9±0.11 eV. The spectrum calculated for conformer 3, the D_3 conformer is not, and probably those of conformer 5 are also not consistent with observation. The presence of both conformers 1 and 2 is in agreement with the broad bands, the greater intensity at the lower energy and the fact that the lower energy band is broader.

Table 4.8 Photoelectron Spectra of 1,4,7-Trithiacyclononane (**23**)

Conformation[a]	Symmetry	Relative Stability (kJ/mol)[b]	Photoelectron	Spectral (eV)	Bands
Observed[c]			~8.4	~8.4	~8.9
Calculated[d]					
1	C_1	2.28	8.56	8.68	8.91
2	C_2	0	8.46	8.67	9.09
3	D_3	7.73	8.84	8.84	9.07
4	C_1	*e*	8.55	8.70	9.00
5	C_2	4.4	8.75	8.84	9.13
6	C_3	28.6	8.30	8.30	8.82

[a] Conformations numbered from the order of their MM3 stabilities. [b] Relative to the most stable conformation of that compound as calculated by AM1. [c] From references 264,302 [d] Calculated using AM1 [e] The fourth conformation of **23** slowly minimized to the first conformation. The photoelectron spectra were calculated using a single point calculation from the MM3 geometry. The initial stability of this conformation was 8 kJ/mol higher than those from conformer 1.

The electron diffraction study was conducted at 473 K.[17] At that temperature, the global minimum C_1 conformer is predicted here to constitute 64% of the mixture present, and other conformers are predicted to be present as follows: 2 (C_2), 3 (D_3), 4 (C_1) , 5 (C_2), 6 (C_3), 7 (C_1), 8 (C_1), 14%, 1.0 %, 13%, 2.2%, 0.8%, 1.8% and 3.6%, respectively. Our MM3 results are in agreement with the conclusion drawn from the electron diffraction study that the C_1 global minimum is most populated and the D_3 conformer is not significantly populated.[17]

4.2.2.2b Infrared Spectroscopy

The infrared spectra of solid **23** recorded here (see Figure 4.5) are very similar to those previously published.[265,266,303] The solution spectra obtained here in carbon disulfide, however, exhibited considerably better resolution than the published[265,266] spectra of the pure liquid phase. Based on AM1 calculations that indicated that the D_3 conformer was most stable by 5.3 kJ/mol, Park and Shurvell assigned the liquid phase infrared spectral lines to transitions calculated for the D_3 conformer.[266,285] Figure 4.5 compares regions of the spectra of the solution and solid. A table (A.7) containing a complete listing of experimental data and comparisons with frequencies calculated for several conformers is given in the Appendix.

The additional resolution obtained here makes it evident that the solution spectra contain many more lines than would be expected for a conformation of D_3 symmetry and also more than would be expected for a single conformation of C_1 symmetry. For instance, in the 800 to 1020 cm^{-1} region, the calculations predict 6 absorption lines for both the C_3 and D_3 conformers, but 9 for the global minimum and 8 for the C_2 conformer. Five lines were observed in the spectra of the solid but 12 in that of the solution (see Figure 4.5), consistent

with the presence of a mixture of the C_1 conformer with another conformer(s). Marked differences between solution and solid-state spectra were also observed in the CH stretching region.

The mostly solvent-free region from 600 to 1400 cm^{-1} of the infrared spectra of an acetonitrile solution was identical to that of the CS_2 solution after low intensity solvent bands had been subtracted. If the highly polar C_3 conformer had been much more populated in this polar medium than calculated (3.8%), some changes would have been observed; as the spectrum of the solid indicates, this conformer has several strong bands in the region.[265,266]

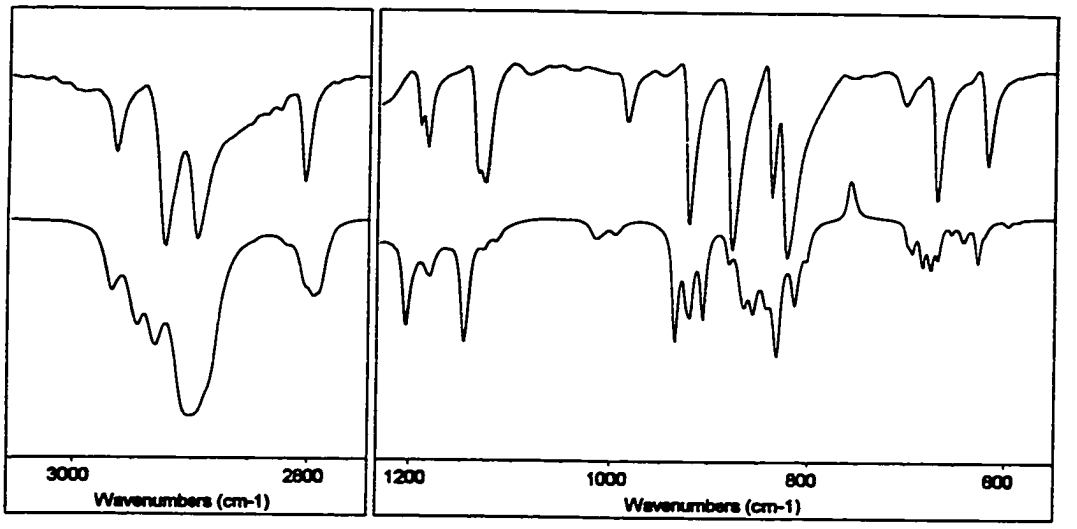

Figure 4.5 The 600 to 1200 and 2750 to 3050 cm^{-1} regions of the infrared spectra of 1,4,7-trithiacyclononane (**23**): top, of the solid, bottom, of the CS_2 solution.

4.2.2.2c NMR Spectroscopy of Compound 23

The AA'BB'X patterns in the ^{13}C satellite signals of the ^{1}H NMR spectra from chloroform-*d* and acetone-d_6 were analysed by sub-spectral analysis, then simulation using the program LAME8.[104] The results from both solvents, shown in Table 4.9, are very similar to those from chloroform-*d* solutions analysed by Lockhart and Tomkinson,[257] who concluded that these observations were consistent with *gauche* SCH_2CH_2S units of the C_3 conformer oscillating between + and - *gauche* orientations and used this as support for their conclusion that their molecular dynamics calculations were indicative of an inversion of the C_3 conformer.[257] If the highly polar C_3 conformer were a minor component of the mixture present in chloroform-*d*, its proportion would increase markedly in the much more polar solvent acetone and the observed coupling constants would change (see below).

Table 4.9 Experimental and Calculated ^{1}H NMR Results for 1,4,7-Trithiacyclononane (**23**)

Solvent	Experimental[a]			
	δ (ppm)	$^3J_{2,3} = {}^3J_{2',3'}$ (Hz)	$^3J_{2,3'} = {}^3J_{2',3}$ (Hz)	$^1J_{C,H}$ (Hz)
$CDCl_3$	3.14	2.52	8.16	139
$(CD_3)_2CO$	3.12	2.66	8.14	136
Conformer	Calculated[b]			
1, C_1		1.73	8.67	
2, C_2		1.98	8.63	
4, C_1		2.79	8.13	
6, C_3		3.72	7.85	

[a] By analysis of the ^{13}C satellites, see text. [b] By averaging *J* values calculated for the different environments using the Haasnoot-Altona equation, see text.

The average J values for the three most populated conformers calculated at the default dielectric constant and for the C_3 conformer as shown in Table 4.9 were calculated as follows. In each SCH_2CH_2S unit of each fixed conformer, two hydrogens can be classed as being in equatorial orientations and two in axial orientations (see Figure 4.6). Ring inversion exchanges axial and equatorial orientations. For each SCH_2CH_2S unit, J_{aa} and J_{ee} values were calculated using the Haasnoot-Altona equation.[103] Initial calculations, using Huggins' value of electronegativity for sulfur in SR groups did not yield values in accord with observation either for **23** or for 1,4-dithiane (**48**). To correct this discrepancy, the value of the electronegativity used for the SR group was increased from 2.6 to 2.85 and the ^3J values for 1,4-dithiane were recalculated to give $J_{ee} = 4.47$ Hz, $J_{aa} = 12.18$ Hz, and $J_{ae} = 2.13$ Hz. The two former numbers yield an inversion averaged value for J_{trans} of 8.32 Hz, which is similar to the experimental value for **48** of $J_{trans} = 8.2$ Hz, and the calculated J_{ae} value is exactly equal to the experimental J_{cis} value.[304,305]

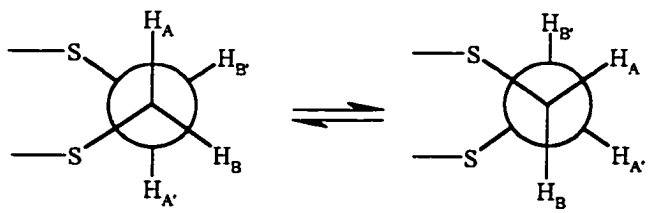

I

$J_{ea} = J_{A'B}(I) = J_{AB'}(II)$

$J_{ae} = J_{AB'}(I) = J_{A'B}(II)$

$J_{23} = J_{23'} = 1/2 * (J_{ea} + J_{ae})$

II

$J_{ee} = J_{BB'}(I) = J_{AA'}(II)$

$J_{aa} = J_{AA'}(I) = J_{BB'}(II)$

$J_{23} = J_{23'} = 1/2 * (J_{aa} + J_{ee})$

Figure 4.6 The various relationships between vicinal coupling constants in an inverting SCH_2CH_2S unit.

The calculated coupling constants in Table 4.9 were determined as follows. The J_{aa}, J_{ee}, J_{ae} and J_{ea} values for each SCH ĢH Ş unit of each low energy conformer of **23** were calculated using the electronegativity value for SR of 2.85. Then, the three sets of J_{aa},J_{ee} values and J_{ae}, J_{ea} values arising from the three different SCH_2CH_2S units in each conformer were averaged. The results shown in Table 4.9 are in general agreement with the conformational mixture suggested by the calculations, given the uncertainty associated with the electronegativity treatment above, and factors not taken into account when the Haasnoot-Altona equation[103] was derived, such as bond-angle effects.[153,306] The values calculated for the individual conformers given in Table 4.9 indicate that if the population of the C_3 conformer were significant, the observed coupling constants would change on increasing the polarity of the medium. The absence of change again indicates that the C_3 conformer is not significantly populated.

Figure 4.7 shows the ^{13}C NMR spectrum of **23** in chloroform-*d* solution and a ^{13}C CP/MAS spectrum of the solid; the former spectrum contains one signal at 35.0 ppm. The solid state spectrum shows two signals at 25.9 and 31.7 ppm, consistent with the C_3 symmetry of the crystal which results in two environments for the carbon atoms.[300] The marked difference between the solution value and the solid state values clearly demonstrates that the C_3 conformation of the solid is not the major conformer in solution. ^{13}C NMR spectra of compounds that adopt the same conformation in both the solid state and in solution have chemical shifts that are identical within 1-2 ppm.[307] The ^{13}C NMR chemical shift in a polar solvent, acetonitrile-d_3, was 35.4 ppm. The fact that this value is almost identical to the chloroform-*d* value and very different from the average of the solid state values (28.8 ppm),

again supports the conclusion that the C_3 conformer does not constitute a significant proportion of the conformational mixture present in solution.

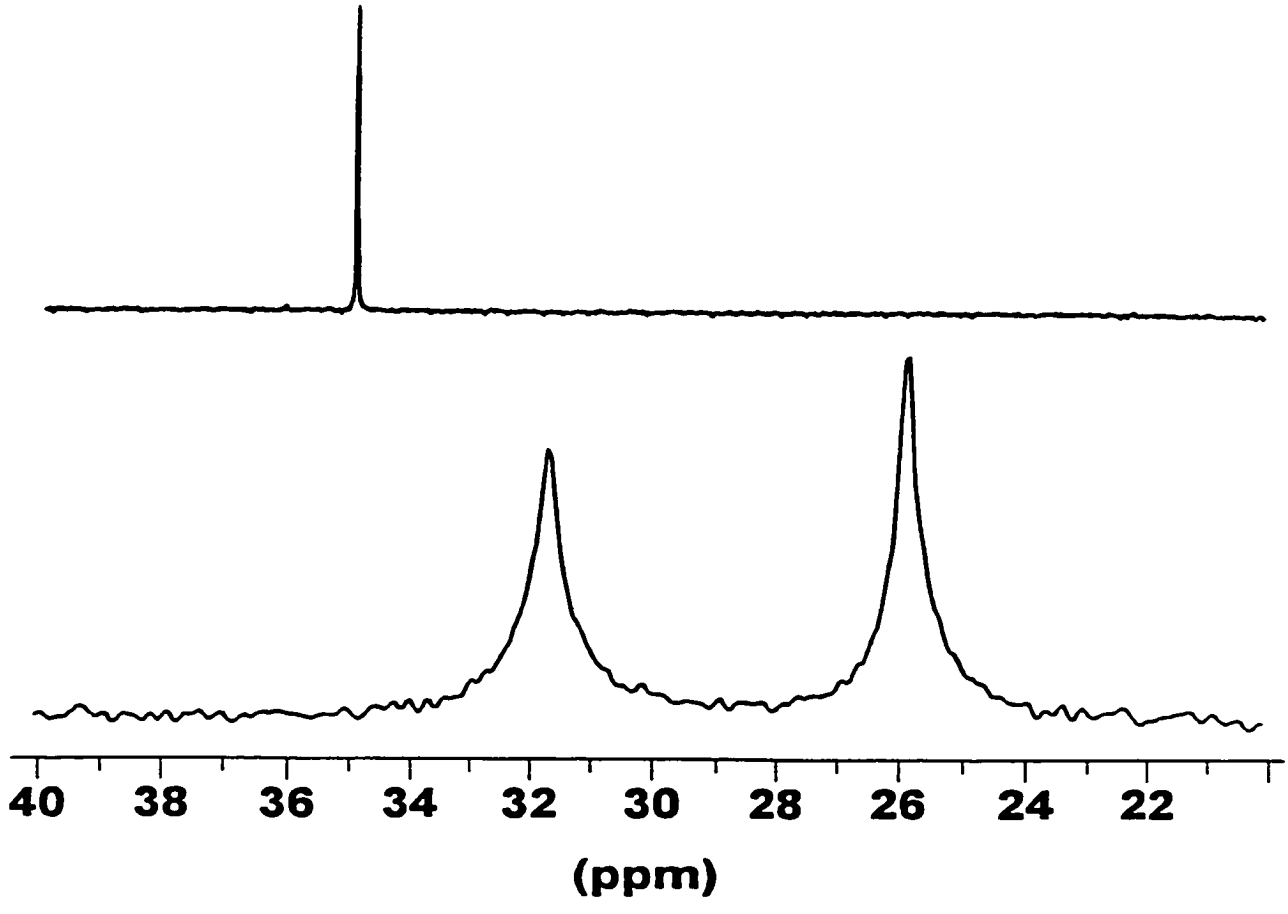

Figure 4.7 The ^{13}C NMR Spectra of 1,4,7-trithiacyclononane (**23**): top, in chloroform-*d* solution, bottom, CP/MAS spectrum of the solid.

Recent theoretical work using the *ab initio* IGLO (Individual Gauge for Localized Molecular Orbital) method successfully calculated the effects of geometrical relationships on α-, β-, γ-, and δ-effects on ^{13}C NMR chemical shifts.[308,309] γ-Effects are most important and

affect both the terminal and internal carbon atoms in each C-C-C-C or C-S-C-C unit. Of the two different carbon atoms in the C_3 conformer in the solid, one is terminal in two γ-*gauche* relationships and internal in a *gauche* and a -131.1° torsional angle while the other is terminal in two γ-relationships of -131.1° and internal in two *gauche* relationships. A γ-relationship over a -131.1° torsional angle is calculated to shift the signal to a higher frequency by about 4 ppm more than the *gauche* relationships for the terminal carbons.[308,309] For the internal carbons, the *gauche* relationship causes the carbon atoms to be shifted to a lower frequency by about 1 ppm more than the -131.1° angle. The geometric relationships involving β-effects are about the same for the two carbons; therefore, the chemical shift difference in the solid is predicted to be about 7 ppm, very similar to the 6 ppm difference observed. No such marked differences are expected for the global minimum C_1 conformer.

4.2.2.3 Conformer Interconversion

In addition to determining the global and local minima on a conformational energy surface, it is also very useful to examine the transition states between these minima to see how they interconvert. In order to obtain information about the pathways available for conformational interconversion for **23**, several stochastic searches were run from different starting conformations using only full-matrix Newton-Raphson minimization of the conformations generated in each push. This procedure locates many more saddlepoints than the normal minimization procedure. Saddlepoints were identified by the presence of one imaginary vibrational frequency and confirmed as saddlepoints by reminimization using the block-matrix/full-matrix Newton-Raphson minimization sequence. Information about those

saddlepoints that were found to be within 42 kJ/mol of the global minimum are shown in Table 4.10; less stable saddlepoints are listed in the Appendix Table A.8.

The minima closely related to each saddlepoint were identified in the following way. The MM3(94) program was altered to permit an option in which pushes of random sizes always start from the same conformation, in this case, a particular saddlepoint. Maximum push sizes were chosen, usually 0.5 or 0.6 Å, that resulted in minimization to one or two conformations. For instance, a push size of 0.5 Å from the saddlepoint 18.9 kJ/mol above the global minimum resulted in the C_1 conformer 4, 31 times out of 100 and a second C_1 conformer, 8, 43 times. Since the geometry of a saddlepoint connecting two conformers should resemble those of the connected conformers more closely than that of any other conformer, this process allows identification of the conformers related by the saddlepoint. This is a new procedure for identifying conformational interconversion pathways but is related to Saunders "small kick" method.[29] An alternative method uses eigenvector-following techniques.[273]

Examination of these saddlepoints and their related minima indicate that all of the ten lowest energy minima can be interconverted via saddlepoints less than 55 kJ/mol above the global minimum, in agreement with low temperature NMR evidence that indicates that conformational interconversion between populated conformers is facile.[261] From this data it is possible to construct a hypothetical pathway by which the global minimum can be interconverted to the C_3 binding conformer (see Figure 4.4).

Interestingly, the global minimum conformer (1) and the C_3-symmetric conformer (6) have six consecutive torsional angles of identical sign and similar magnitudes with the

Table 4.10 Identification of Saddlepoints for 1,4,7-Trithiacyclononane (**23**)[a]

Conf.	Dipole Moment (D)	Imag. Freq. (cm^{-1})	Energy Difference (kJ/mol)[b]	Connected Conformers			
				Conf[c]	Frequency[d]	Conf[e]	Frequency[d]
S1	1.48	-42	8.64	S1	47	1	39
S2	2.17	-10.8	13.8	1	84	4	5
S3	0.75	-61.3	15.2	5	80	8	9
S4	2.1	-36.2	18.93	8	43	4	31
S5	1.29	-105	30.87	10	56	2	30
S6	3.42	-98.6	33.8	7	58	11	29
S7	1.1	-119	33.9	3	61	10	29
S8	1.47	-125	38.38	5	65	1	19
S9	3.38	-141	41.11	10	56	6	30
S10	1.04	-125	41.59	8	58	1	35
S11	1.79	-198	41.7	1	57	4	31
S12	2.49	-173	42.91	1	42	4	31
S13	2.88	-175	42.93	10	51	7	44
S14	1.39	-83	43.8	10	78	2	17

[a] All saddlepoints had one imaginary infrared frequency and C_1 symmetry. [b] With respect to the global minimum. [c] The most common conformer obtained from this saddlepoint. See Table 4.5 for conformer identity. [d] The number of times this conformer was found out of 100 pushes each starting from the saddlepoint indicated. [e] The second most common conformer obtained from this saddlepoint. See Table 4.5 for conformer identity.

remaining three, centered by angles with an absolute value of 134±1°, but having reversed signs (see Table 4.6). It would thus seem reasonable that interconversion could take place by a simple "flipping" of these angles to the other side of the plane of the molecule. Driving this torsional angle from conformer 6 to the value in conformer 1 and holding the other angles

>|118°| at an average value midway between the sizes in the two conformers gave a barrier of about 98 kJ/mol. This is considerably higher than the highest barrier (50.1 kJ/mol) on the lowest energy pathway (1 → 2 → 10 → 6) depicted in Figure 4.8 for interconversion between conformers 1 and 6. Thus, these calculations indicate that more complex interconversion pathways of conformers 1 and 6 would be preferred by **23** over the conceptually appealing "corner flapping" pathway.

4.2.2.4 Complex Formation

In most complexes of **23**, the nine-membered ring adopts the C_3 "crown" conformation of the free ligand in the solid state which presents the three sulfur atoms in favourable orientations for tridentate complexation to the same cation.[229,230] In three complexes, **23** forms only one bond to individual metal atoms.[225,310,311] Although it might be expected that the most stable conformation would be adopted in monodentate complexes, the conformations observed are not the one calculated here to be the global minimum.

4.2.2.4a Complexes With Monodentate Ligands

One molecule of **23** in the binuclear copper-**23** complex ($[Cu^{I}_{2}\mathbf{23}_{3}]$) (**23a**) bridges between the two Cu(I) atoms and adopts a conformation very close to that of the C_2 conformer 2, with an average difference in torsional angles between the X-ray structure and that calculated here of 3.8° with the largest being 6.5°.[310] In the gold complex $[Au(\mathbf{23})_2]^{2+}$(**23b**), the monodentate ligand also adopts the C_2 conformer 2.[311] In the two independent complexes in the unit cell, the average deviations of the monodentate ligand from the torsional angles calculated for conformer 2 were 2.6 and 3.7°. In $[Cu^{I}\mathbf{23}_2]^{+}$ PF_6^- (**23c**),

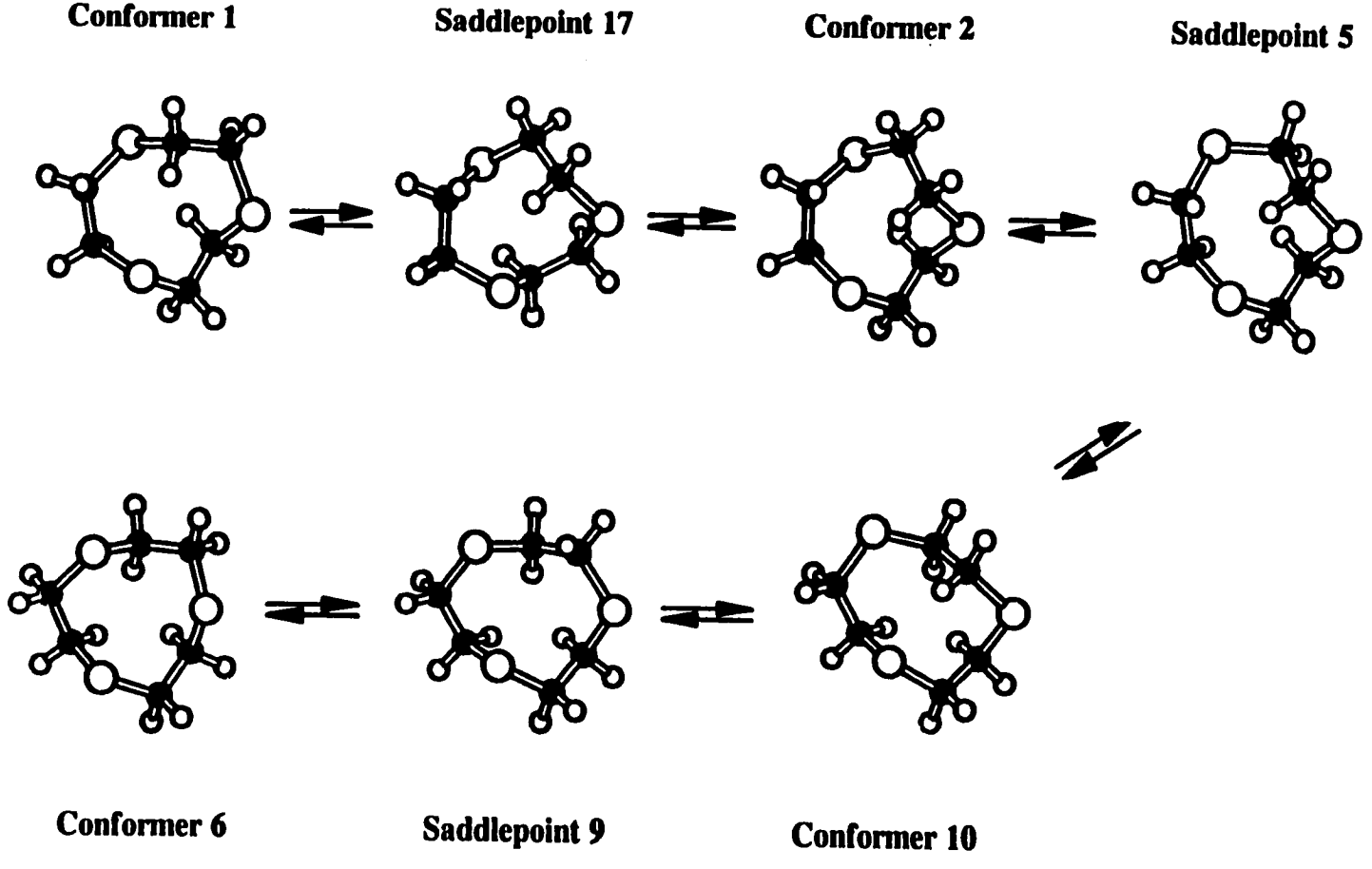

Figure 4.8 The lowest energy pathway for interconversion of conformers 1 and 6 of 1,4,7-trithiacyclononane (**23**); conformer 1 (μ, 1.52 D) via saddlepoint 17 (μ 1.77 D, 50.1 kJ/mol above 1) to conformer 2 (μ 1.32 D) via saddlepoint 5 (μ 1.29 D, 30.9 kJ/mol above 1) to conformer 10 (μ 2.75 D) and on to conformer 6 (μ 4.24) via saddlepoint 9 (μ 3.38, 41.1 kJ/mol above 1).

one molecule of **23** is tridentate, the other monodentate.[225] In the two independent molecules in the unit cell, the monodentate rings both adopt conformer 7, with average deviations from calculated torsional angles of 3.1 and 4.0°. Interestingly, conformer 7 is derived from the same cyclononane conformation as conformer 2, a TBC (twist-boat-chair) or [12222] conformation (this conformational representation [12222] describes the number of bonds in each "side' of the conformer;[247] in this case the conformation has 5 "sides" 4 of which contain 2 bonds). For conformer 7, the sulfur atoms are moved in comparison to conformer 2 so that no S atom lies on the C_2 axis (See Figure 4.4).

An explanation for this absence of certain low energy conformers in complexes lies in the observations of Hendrickson.[312] Hendrickson found that there were two types of positions for exocyclic substituents on medium ring conformations (in addition to an equatorial position) where introduction of a substituent caused little increase in strain.[312] The two positions are: on the isoclinal position of a C_2 symmetric conformer or on the position adjacent to the bow position in the boat segment of a conformer (see Figure 4.9). In both environments, the atom being substituted is a central atom in two *gauche* torsional angles of the same sign. In these positions, the substituent is *gauche* to a ring carbon on one side but close to *anti* to the ring carbon on the other side, so that large substituents like metals, particularly if they are weakly bonded, can bend away from the *gauche* carbon, resulting in a large bond angle from the metal to the carbon on the *gauche* side and a small bond angle on the other side.

Four of the six bonding situations for the monodentate rings in molecules **23a**, **23b**, and **23c** have sulfur atoms placed in conformations so that the metal atoms can assume this type of position. In the other two bonding situations, the sulfur atom is part of torsional angles that are approximately *gauche*, but of opposite signs, and the metal is in an approximately equatorial orientation. The point of attachment to the metal is different for the two independent molecules of **23c**; in one molecule, the attached S atom in one molecule is the central atom in C-S-C-C torsional angles of 76 and 60°. This pattern of C-S-C-C torsional angles is common, being 70.1 and 72.5° at one site in **23a**, -73.9 and -65.8° for one molecule in **23b**, and 72.1 and 70.9° in the other. Further evidence of the pattern suggested by Hendrickson is also observed; for example, the sulfur atom in **23a** that lies in the center of the two *gauche* torsional angles has its attached Cu atom *gauche* to one carbon and *anti* to the other. The Cu-S-C bond angle on the gauche side is 108.9° but is 100.6° on the other.

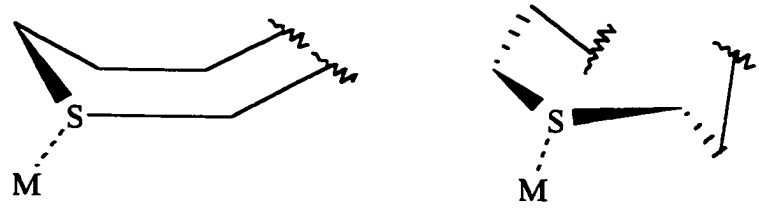

Figure 4.9 The two positions (besides equatorial) that a substituent can be added to a medium sized ring with minimal strain. Left: the "boat" position; Right: the isoclinal position.

An attractive explanation for the fact that none of the conformations adopted by the three monodentate or bidentate ligands in the solid state is the conformation calculated to be the global minimum is that particular conformations are selected because they provide favourable complexation environments. Of course, this explanation is responsible for the fact

that the tridentate ligands adopt the C_3 conformation. Can it also explain the conformations adopted by the monodentate ligands? Conformer 1 (the global minimum) has no sulfur atoms as central atoms in two *gauche* torsional angles of the same sign, neither does conformer 4. Conformer 3, the D_3 conformer does, but this conformer is strongly disfavoured on entropy grounds. Metals bound to the sulfur atoms in the global minimum conformer could adopt equatorial orientations, but for each sulfur atom in conformer 1, one of the flanking torsional angles is about 120° or greater, making the equatorial orientation more hindered than normal.

4.2.2.5 Summary for 1,4,7-Trithiacyclononane (23)

All evidence clearly indicates that the solid-state conformer is not significantly populated in solution, in agreement with the MM3 molecular mechanics calculations here. The clearest support for this assertion is provided by the infrared spectra and the comparison of the solution and solid phase ^{13}C NMR spectra. Infrared spectra, electron diffraction results, and photoelectron spectra demonstrate that the D_3 conformer is not populated in solution or in the gas phase. The infrared spectra demonstrate that a mixture is present. Although it cannot be shown conclusively that the populated conformers are those calculated to be most stable, a mixture of conformers 1 and 2 is in accord with all the evidence currently available.

4.2.3 1,4,7-Trithiacyclodecane (24)

4.2.3.1 MM3 Conformational Analysis

Compound **24** is a low melting solid (mp 18°C) that has not been studied by X-ray diffraction. It has been used extensively in complexation studies. Eighty conformers were found in the stochastic search for compound **24**. Information about the 10 lowest energy

conformers of **24** and about the four most stable conformers with large dipole moments are listed in Table 4.11. ATOMS diagrams of the four lowest energy conformers are shown in Figure 4.10. A C_1 conformer is calculated to be most populated but only to the extent of 59% of the total mixture at 25 °C; a second C_1 conformer contributes 24% and a C_2 conformer is calculated to make up 9% of the mixture. As for **23**, increasing the dielectric constant markedly stabilizes conformations having large dipole moments. However, for **24**, these more polar conformers are much less stable relatively than is the C_3 conformer of **23**. The most populated polar conformer (26), is 19.3 kJ/mol less stable than conformer 1 at a dielectric constant of 1.5 and contributes 0.05% of the mixture present. At a dielectric constant of 30, it is 11.7 kJ/mol less stable than conformer 1, but is still only 1.2% of the mixture.

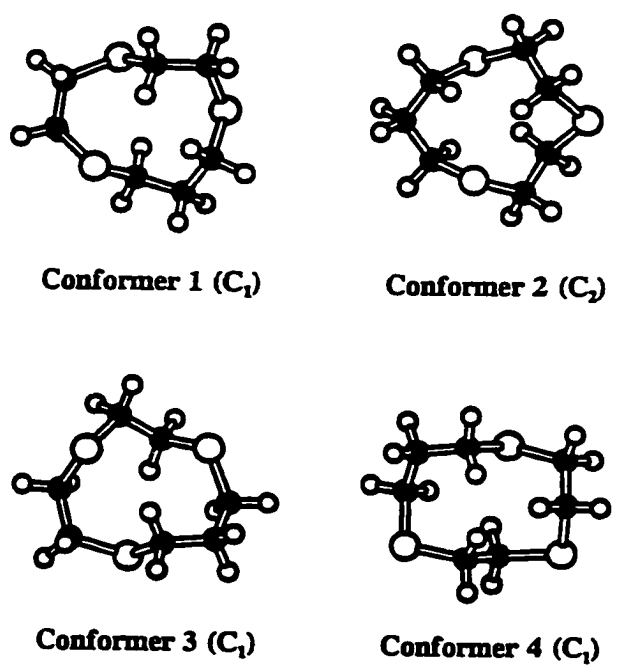

Figure 4.10 The four most stable conformers of 1,4,7-trithiacyclodecane (**24**).

Table 4.11 MM3(94) Results for 1,4,7-Trithiacyclodecane **(24)**

Order[a] (ϵ=1.5)	Symmetry	Dipole Moment (D) (ϵ=1.5)	Strain Energy[b] (kJ/mol)	Mole Fraction (25 °C)	Order[a] (ϵ=30)	Dipole Moment (D) (ϵ=30)	Strain Energy[b] (kJ/mol)	Mole Fraction (25 °C)
1	C_1	1.58	0	0.59	1	1.58	0	0.62
2	C_2	1.17	1.74	0.092	3	1.17	3.02	0.06
3	C_1	1.61	2.28	0.24	2	1.617	2.77	0.22
4	C_1	2.17	7.35	0.017	4	2.17	6.99	0.02
5	C_1	1.74	10.25	0.012	6	1.73	11.37	0.008
6	C_1	1.71	12.34	<0.001	9	1.71	11.77	0.006
7	C_1	1.44	12.54	0.01	18	1.43	13.59	0.004
8	C_1	2.41	12.9	<0.001	11	2.41	12.22	0.003
9	C_1	1.93	12.92	0.01	15	1.93	13.38	0.006
10	C_1	1.99	13.09	<0.001	16	2.01	13.47	0.003
24	C_1	4.32	18.25	<0.001	5	4.35	10.45	0.008
26	C_1	4.14	19.33	<0.001	8	4.17	11.71	0.011
27	C_1	4.38	19.53	<0.001	10	4.41	11.84	0.006
33	C_s	4.41	22.43	<0.001	14	4.12	15.12	0.001

[a] The numbers are the order of the conformations based on their strain energies at that dielectric constant. [b] With respect to the strain energy of the lowest energy conformation of this compound at this dielectric constant.

An MM2 study of the conformations of **24** by Setzer *et al.* found 24 conformers starting from the five most stable cyclodecane conformers. The 24 conformers included the global minimum found here and the second most stable conformer, the C_2 conformer.[276] However, conformer 3, a [2233] conformer calculated to be the second most populated conformer was not found previously. This result highlights the difficulty of finding all stable conformers for these complex systems if random searching techniques are not used. The current force field suggests that conformer 2 is closer in stability to the global minimum than previously[276] calculated. Molecular dynamics calculations of **24**, using the CHARMm force field, starting from the [2323] endodentate conformation found in $[Fe(\mathbf{24})_2](ClO_4)_2$ resulted in only conformers with endodentate configurations.[257] None of the low energy conformers found here and previously,[245] were found.

4.2.3.2 Spectroscopic Conformational Analysis

4.2.3.2a NMR Spectroscopy

The NMR spectral data for compound **24** were recorded in four solvents having a wide range of polarity and the results are shown in Tables 12. These spectra consisted of an AA'BB' or AA'XX' (depending on the field strength) pattern and an AA'A''A''''XX' pattern for the SCH_2CH_2S and $SCH_2CH_2CH_2S$ units, respectively (see Figure 4.11). In all spectra but those in benzene-d_6, the signals of one of the CH_2 units from the SCH_2CH_2S group and those of the SCH_2 protons from the $SCH_2CH_2CH_2S$ group overlap, making analysis of the latter pattern difficult. However, those in benzene-d_6 are resolved and are shown in Figure 4.11. All AA'BB' and AA'A"'A""XX' patterns were analysed as for **23** using iterative

simulation by means of the program LAME8[104] to refine initial hand analyses. The results for the AA'BB' pattern are similar to those obtained by Lockhart and Tomkinson in $CDCl_3$.[257]

Table 4.12 ^1H NMR Results for 1,4,7-Trithiacyclodecane (**24**).

SCH_2CH_2S Section

Solvent	$\delta H_{2,2'}$ (ppm)	$\delta H_{3,3'}$ (ppm)	$^2J_{2,2'}$ (Hz)	$^3J_{2,3} = {}^3J_{2',3'}$ (Hz)	$^3J_{2',3} = {}^3J_{2,3'}$ (Hz)	$^2J_{3,3'}$ (Hz)
C_6D_6	2.697	2.523	-14.52	3.44	8.04	-14.52
$CDCl_3$	3.133	2.932	-14.28	3.46	8.08	-14.63
$(CD_3)_2CO$	3.088	2.887	-14.59	3.71	7.99	-14.59
CD_3CN	3.070	2.876	-14.62	3.60	7.97	-14.62

$SCH_2CH_2CH_2S$ Section

Solvent	$\delta H_{8,8'}$ (ppm)	$\delta H_{9,9'}$ (ppm)	$^2J_{8,8'}$ (Hz)	$^3J_{8,9} = {}^3J_{8',9'}$ (Hz)	$^3J_{8',9} = {}^3J_{8,9'}$ (Hz)	$^2J_{9,9'}$ (Hz)
C_6D_6	2.911	1.481	-12.34	3.79	8.32	-10.18
$CDCl_3$	3.152	1.841	---	3.80	8.33	---
$(CD_3)_2CO$	3.090	1.792	---	3.99	8.14	---
CD_3CN	3.077	1.805	---	3.95	8.25	---

The results for the AA'BB' pattern in chloroform-*d* are very similar to that previously obtained.[257] Changes in vicinal coupling constants with solvent polarity were less than 0.1 Hz and there was no relationship to solvent polarity. Thus, consistent with the molecular mechanics results, polar solvents appear to have little effect on the makeup of the

conformational ensemble present. Similarly, the ^{13}C NMR chemical shifts (see Figure 4.12) are independent of solvent polarity. Vicinal coupling constants were calculated using the Haasnoot-Altona equation as for **23** for the four conformers calculated to be most populated (Table 4.13). Again, the calculated values are in general agreement with the predicted mixture; the larger size of $^3J_{ae}$ in the SCH_2CH_2S segment observed than calculated for conformers 1 and 3 suggests that conformer 4 may contribute more than calculated.

Table 4.13 Calculated Coupling Constants for **24**

	SCH_2CH_2S Section		$SCH_2CH_2CH_2S$ Section	
Conformer	$^3J_{ae} = {}^3J_{ea}$ (Hz)	$(^3J_{aa} + {}^3J_{ee})/2$ (Hz)	$^3J_{ae} = {}^3J_{ea}$ (Hz)	$(^3J_{aa} + {}^3J_{ee})/2$ (Hz)
1 (C_1)	2.57	8.23	2.77	8.52
2 (C_2)	1.68	8.78	4.26	7.58
3 (C_1)	1.79	8.64	3.5	8.08
4 (C_1)	7.06	5.82	3.08	8.44
Obs. Ave.	3.55	8.02	3.88	8.26

4.2.3.2b Photoelectron Spectra

Photoelectron spectra of **24** also show two maxima in the lone-pair region (8.41 and 8.83 eV [301] or 8.38 and 8.75 eV [302]) with the lower energy band being somewhat more intense. In comparison to the spectrum of **23**, the splitting (0.4 eV) is smaller and the two bands are broader and closer to being of the same intensity.[302] The photoelectron spectra of the four lowest energy conformers were calculated using AM1 and the results are shown in Table 4.14. This method indicates that the two most stable C_1 conformers (1 and 3) would

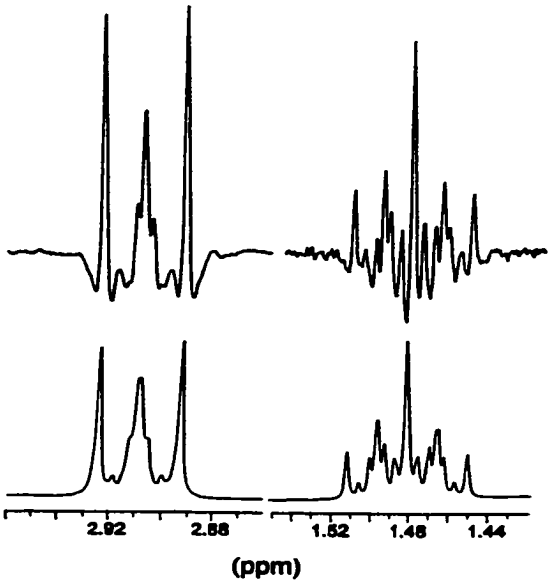

Figure 4.11 The parts of the ^{1}H NMR spectrum of 1,4,7-trithiacyclodecane (**24**) in benzene-d_6 due to the $CH_2CH_2CH_2$ segment: top, experimental spectrum; bottom, LAME8 simulation.

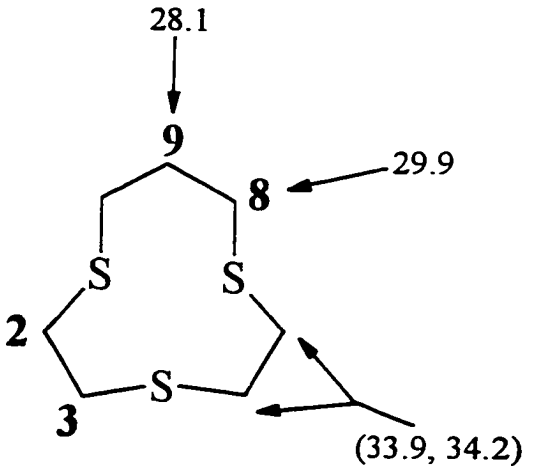

Figure 4.12 Numbering of compound **24** for NMR purposes and the ^{13}C NMR chemical shifts of the indicated carbons (in ppm).

give similar photoelectron spectra, each with two bands close together centered on 8.5 eV and with a third band at about 8.9 eV. The observed spectrum has about the same separation between the two bands as that calculated for conformers 1 and 3 but the calculated energies are about 0.1 to 0.15 eV too large. In addition, the bands appear to be broader than is calculated to be observed for a mixture of 1 and 3. The C_2 conformer 2 is calculated to have three widely separated bands one of which occurs at a lower energy than those of conformers 1 and 3, another of which lies halfway between the two areas predicted for 1 and 3. At 330 K, it is calculated that the mixture present would contain 55% 1, 25% 3, 9% 2, and 2% 4. The presence of this amount of conformer 2 would explain the broadened appearance of the spectrum.

Table 4.14 Photoelectron Spectra of **24** Calculated by AM1

Conformer[a]	Symmetry	Relative Stability (kJ/mol)[b]	Photoelectron	Spectral (eV)	Bands
Observed			8.41[c]		8.83[c]
			8.38[d]		8.75[d]
Calculated					
1	C_1	2.92	8.46	8.51	8.91
2	C_2	2.72	8.34	8.74	8.92
3	C_1	0	8.47	8.55	8.87
4	C_1	3.55	8.58	8.61	9.04

[a] Conformations numbered from the order of their MM3 stabilities. [b] Relative to the most stable conformation of that compound as calculated by AM1. [c] From reference 301 [d] From reference 302.

4.2.3.2c Infrared Spectroscopy

The infrared spectrum of **24** in CS_2 is listed in the Appendix Table A.9 along with spectra calculated for the three lowest conformers. The spectrum contains about as many lines as calculated for a C_1 conformer but the similarity of frequencies calculated for different conformations does not allow conformational information to be obtained from the spectrum. There were no marked differences between this spectrum and one recorded in acetonitrile other than those due to solvent subtraction.

4.2.3.3 Complex Formation

In complexes with molybdenum tricarbonyl, compound **24** is tridentate in a C_1 [1333] conformation.[244] In a palladium complex, $[Pd(\mathbf{24})_2](PF_6)_2 \cdot 2CH_3NO_2$, each ring is also tridentate[313] and a similar conformation of these rings is adopted in $[Pd(\mathbf{24})_2](PF_6)_2 \cdot 2CH_3CN$.[260] In both complexes, compound **24** is in a [2233] form. One intersecting aspect of these palladium complexes is that due to the lack of an axis of symmetry through the middle of the free ligand chiral complexes can be formed.[313] In the iron complex, $[Fe(\mathbf{24})_2] \cdot (ClO_4)_2$, the two ligands take on tridentate [2323] conformations.[245]

A molecular dynamics simulation of **24** seemed to show that conformers prearranged for tridentate complexation were populated to a large extent in solution.[257] In contrast, the molecular mechanics calculations presented here and previously show that the lowest energy conformer is a [1333] conformer that is not in a tridentate conformation. None of the low energy conformers calculated here can form tridentate complexes. This is in agreement with Setzer *et al.*, who have stated that in order to bind successfully, compound **24** must alter its conformation.

4.2.4 1,5,9-Trithiacyclododecane (25)

4.2.4.1 MM3 Conformational Analysis

The conformational situation for compound **25** provides a marked contrast to that of **23** (see Table 4.15). Compound **25** is calculated to be relatively homogeneous conformationally, both in polar and non-polar media, although 231 conformers were found in stochastic searches. The calculated global minimum is the conformation observed in the solid by X-ray crystallography for both **25** alone[253] and in three complexes in which the metal

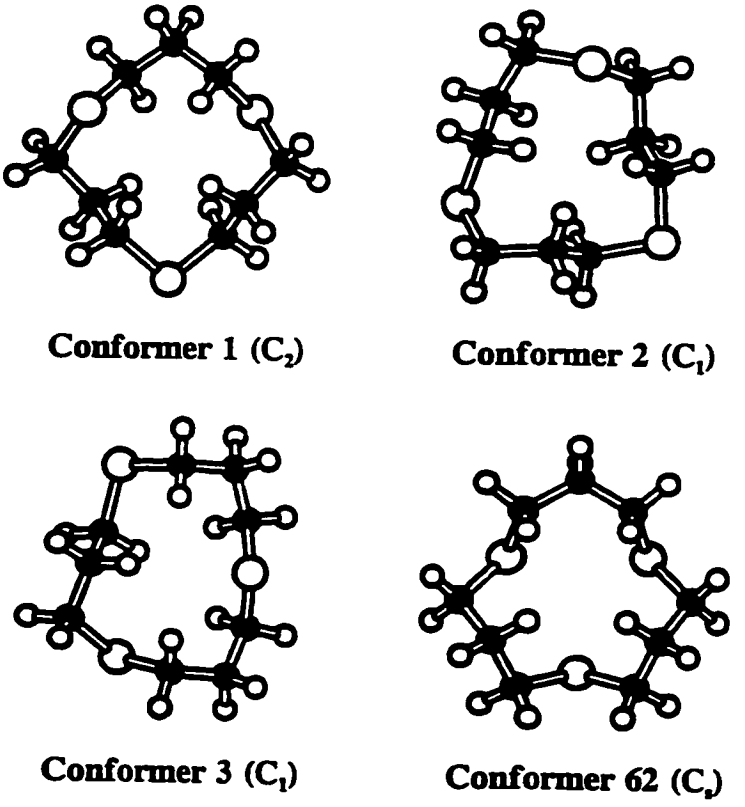

Figure 4.13 The three most stable conformers of 1,5,9-trithiacyclododecane (**25**) and of the most stable polar conformer.

ion is complexed to only one sulfur atom: the 1:1 complex it forms with copper(II) chloride,[253] in $Ru_5(CO)_{13}(\mu\text{-}\eta^1\text{-}\mathbf{25})(\mu_5\text{-}C)$,[314] and in $Os_4(CO)_{13}(\mathbf{25})$.[315] Interestingly, in the copper complex the metal is bonded to a "side" sulfur in the C_2 conformer, while in the other two it is bonded to the "corner" sulfur (for definition of "side" and "corner" atoms see below).

ATOMS diagrams of the three most stable conformers and the most stable polar conformer are shown in Figure 4.13. The global minimum has C_2 symmetry and the conformation in the solid[253] is very close to being C_2 symmetric with torsional angles similar to those calculated by MM3(94) (see Tables 4.16 and A.10). The global minimum is calculated to be more stable than the next most stable conformation by 9.2 kJ/mol but there are a large number of conformations that lie between 9 and 20 kJ/mol above it. Thus, conformer 1, although by far the most populated, is calculated to constitute only about 88% of the mixture present. The most stable highly polar conformation, the sixty-seventh conformation, is calculated to be much less stable than the global minimum, by 39.7 kJ/mol and 29.2 kJ/mol at dielectric constants of 1.5 and 30.0 kJ/mol, respectively.

4.2.4.2 Spectroscopic Conformational Analysis

The infrared spectra of **25** from the solid phase and from a solution in carbon disulfide are virtually identical (see Figure 4.14), in marked contrast to the same comparison for **23**. Thus, as calculated, the major conformation present for compound **25** in this CS_2 solution is conformation 1. A complete listing of the experimental spectra and the calculated spectra see Table A.11 in the Appendix.

Table 4.15 MM3(94) Results for 1,5,9-Trithiacyclododecane **(25)**

Order[a] (ϵ=1.5)	Symmetry	Dipole Moment (D) (ϵ=1.5)	Strain Energy[b] (kJ/mol)	Mole Fraction (25 °C)	Order[a] (ϵ=30)	Dipole Moment (D) (ϵ=30)	Strain Energy[b] (kJ/mol)	Mole Fraction (25 °C)
1[c]	C_2	1.06	0	0.88	1	1.05	0	0.83
2	C_1	1.28	9.19	0.056	2	1.27	8.27	0.075
3	C_1	1.11	9.42	0.037	4	1.1	10.15	0.027
4	C_s	2.49	12.4	<0.001	3	2.49	10.01	0.009
5	C_s	1.7	12.54	<0.001	5	1.7	10.7	0.021
6	C_1	0.89	13.35	0.01	8	0.88	12.54	0.01
7	C_s	1.2	13.96	<0.001	6	1.19	12.48	0.005
8	C_s	2.26	14.83	<0.001	7	2.26	12.51	0.003
9	C_1	1.54	15.48	<0.001	9	1.54	13.46	0.007
10	C_1	1.06	16.89	<0.001	11	1.05	17.44	0.002
62	C_s	4.45	39.74	$1x10^{-7}$	34	4.45	29.24	$7x10^{-6}$
66	C_s	4.42	41.04	$1.x10^{-7}$	40	4.41	30.34	$2x10^{-5}$
81	C_{3v}	4.4	44.12	$1.x10^{-9}$	57	4.39	33.83	$2x10^{-6}$

[a] The numbers are the order of the conformations based on their strain energies at that dielectric constant. [b] With respect to the strain energy of the lowest energy conformation of this compound at this dielectric constant. [c] X-ray structure: reference 253.

Table 4.16 Comparison of MM3 Torsional Angles (°) with X-Ray Torsional Angles (°): 1,5,9-Trithiacyclododecane (**25**)

Conformer	CSCC	SCCC	CCCS	CCSC	CSCC	SCCC	CCCS	CCSC	CSCC	SCCC	CCCS	CCSC
X-Ray[a]	-65	172.6	-67.7	-75	156.6	-66.1	-66	162.5	-76	-70.8	167.6	-64
MM3												
1	-67.7	172.1	-63.6	-77	159.7	-66.9	-67	159.7	-77.2	-63.6	172.1	-68
2	-67.5	169.8	-56.4	-60	150	-171	58.1	68.4	-91.1	-60.7	179	-64
3	-61.8	-173	-56.7	-75	148.2	-61.2	-60	158	-164.4	59.9	70.1	-87

[a] X-ray results from reference [253].

The ^{13}C NMR spectra from solution and the solid are given in Figure 4.15. The chemical shifts from the solution spectrum are 26.4 and 28.3 ppm and from the solid-phase spectrum: 26.2, 27.3, 28.4, 30.7, and 32.2 ppm. The crystal structure (similar to conformer 1 in Figure 4.13) is roughly a square with one S atom and three CH_2 groups at the corners with a slight deviation from C_2 symmetry. It is not clear whether the five chemical shifts fothe solid represent the five environments of C_2 symmetry or if there are actually a larger number of distinct signals. In the discussion following, it has been assumed that there are only five signals but little difference would result if some signals were split in two by small amounts (<2 ppm).

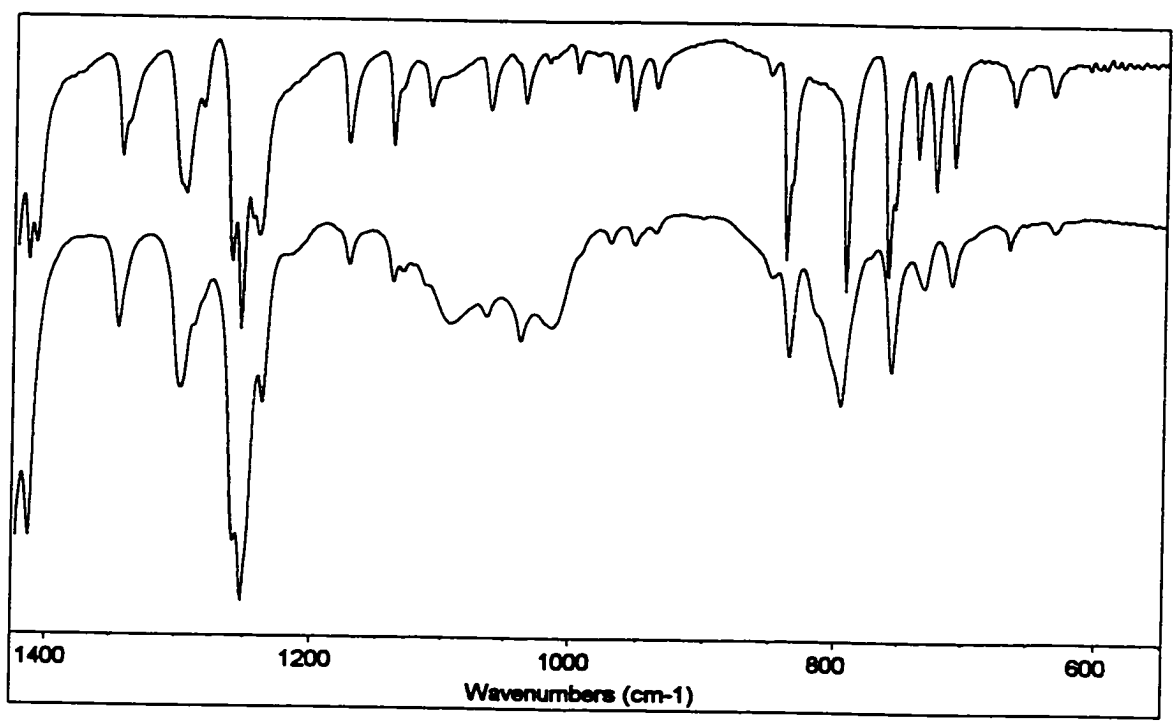

Figure 4.14 The 600 to 1400 cm^{-1} region of the infrared spectra of 1,5,9-trithiacyclododecane (**25**): top, of the solid, bottom, of the CS_2 solution.

In the solid, one of the three central atoms in the three CCH_2C units is in a corner while the other two are in symmetry-related side positions. The torsional angles around this ring are close to those of normal *gauche* and *anti* relationships. The peaks in the solid can be assigned using γ-substituent effects similar to those used for compound **23**. Going from an *anti* to a *gauche* relationship, for instance in methylcyclohexane, results in both the terminal and internal carbons being shielded by about 5 ppm and it will be assumed that the same sizes of change are observed in the C-S-C-C units here.[316] Corner atoms are central in

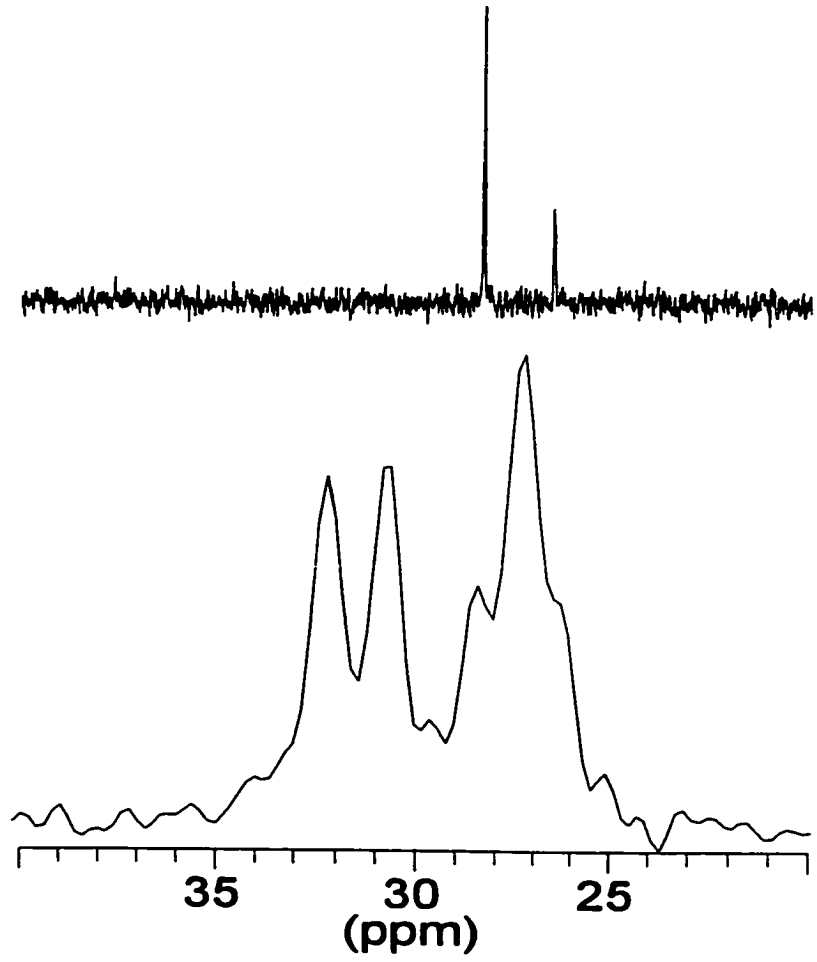

Figure 4.15 The ^{13}C NMR spectra of 1,5,9-trithiacyclododecane (**25**): top, in chloroform-*d* solution, bottom, CP/MAS spectrum of the solid.

two *gauche* relationships but terminal in two *anti* relationships. Side atoms in three atoms sides are terminal in two *gauche* relationships but central in one *gauche* and one *anti* relationship. Thus, side atoms should be shifted to a lower frequency by about 5 ppm relative to the corner carbons.

On this basis, the two signals at 32.2 and 30.7 ppm in the solid are assigned to corner carbons, while the signals at 28.4, 27.3, and 26.2 are assigned to the side carbons. Averaging the chemical shifts at 32.2 (2 C), 28.4 (2 C) and 27.3 (2 C) and at 30.7 (1 C) and 26.2 (2 C) gives values of 29.3 and 27.7 ppm, about 1 ppm greater than the solution values of 28.3 and 26.4 ppm for the SCH_2 and CCH_2C carbons. Slight differences would be obtained if different assignments were made but it is clear that the average chemical shifts from solution are about the same as averaged values from the solid state, consistent with the same conformer being present in both phases. The ^1H NMR spectrum of **25** in $CDCl_3$ consisted of a triplet (2.70 ppm) and a low frequency pentet (1.89 ppm) with splittings of 6.64 Hz.

4.2.4.3 Complex Formation

Compound **25** forms a 2:1 complex with Rh^{3+} in which the rhodium ion is complexed to all 6 S atoms of the two crown thioether molecules. Each molecule is disordered, but each adopts polar conformations with the three sulfur atoms oriented towards the same side.[241] The electrochemistry of the rhodium complex supports the idea that this complex is unstable because of the large enthalpic destabilization of the conformation of the ligand needed for complexation. It also forms similar complexes with ruthenium ions[317] and with ruthenium atoms in ruthenium carbonyl clusters.[314,315,318] These compounds also undergo facile reactions with carbon monoxide in which the crown thioether is replaced. Similar reactions were not

reported for complexes of **23**, supporting the weakness of tridentate binding of **25**. Further support for this conclusion comes from the stability of Fe^{2+} complexes; although $[Fe(\mathbf{23})_2]^{2+}$ is stable in water, $[Fe(\mathbf{25})_2]^{2+}$ decomposes instantly on contact.[317]

4.2.5 1,4,7,10-Tetrathiacyclododecane (26)

4.2.5.1 MM3 Conformational Analysis

Two previous molecular mechanics studies of 1,4,7,10-tetrathiacyclododecane (**26**) have been performed.[301,319] One was simply a series of calculations on four conformers derived from cyclododecane[319], the other was a random search using the TRIPOS and MM2 force fields which found 96 unique conformers.[301] The results for the search performed here are in Table 4.17. The higher symmetry of **26**, compared to the other twelve-membered rings studied here, results in fewer possible conformers, and only 108 were found, the smallest number for the twelve-membered rings. ATOMS diagrams of the global minimum and some of the polar conformations for 12S4 are shown in Figure 4.16. According to these calculations and in general accord with the previous calculations,[301,319] the D_4 symmetric global minimum is 13.1 kJ/mol and 13.8 kJ/mol more stable than the next conformer at dielectric constants of 1.5 and 30.0, respectively. This stability translates into a population at 25°C of 95-96%. This D_4 conformer has all of its sulfurs exodentate, which would seem to indicate that this ligand may be a poor ligand. The most stable highly polar conformer has C_4 symmetry and a calculated dipole moment of 5.9 D, but it is 27.8 or 19.4 kJ/mol less stable than the global minimum at dielectric constants of 1.5 and 30.0, respectively. These are heavy enthalpic penalties that must be overcome if endodentate complexation to this conformer is to take place.

The crystal structure of compound **26** has been reported.[248,320] The conformation adopted in the solid is the same as that predicted to be the global minimum by molecular mechanics (see Tables 4.18 and A.12). The unit cell contains two different molecules that are both slightly distorted from D_4 symmetry. This exodentate-D_4 conformation is the ideal example of the rules of Cooper[248] governing the conformations of crown thioethers; in fact the conformation of **26** is simply that of two overlapping S-C-C-S-C-C-S "brackets".(See Figure 4.3). This would also explain the high calculated stability of this conformer, in that it is the "ideal" model conformer of a crown thioether.

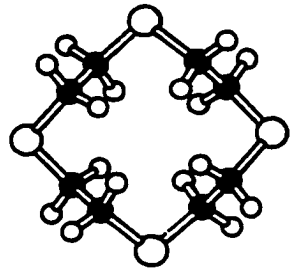

Conformer 1 (D_4)

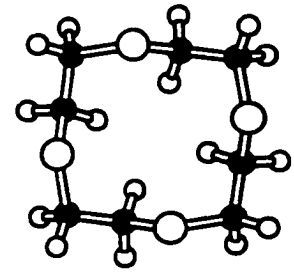

Conformer 12 (C_4)

Figure 4.16 ATOMS diagrams of the D_4 and C_4 conformers of 1,4,7,10-tetrathiocyclododecane (**26**)

4.2.5.2 Spectroscopic Conformational Analysis

The photoelectron spectra of **26** show only one peak assigned to lone pairs;[301,302] this is consistent with the MM3 calculations. The infrared spectra of solid **26** and a solution of **26** in CS_2 are presented in Figure 4.17. The two spectra are virtually identical. This supports the calculated result that the favoured conformer is the same as that in the solid phase.

The ^1H NMR spectrum of **26** was examined by means of its ^{13}C satellites. The only

Table 4.17 MM3(94) Results for 1,4,7,10-Tetrathiacyclododecane (**26**)

Order[a] (ϵ=1.5)	Symmetry	Dipole Moment (D) (ϵ=1.5)	Strain Energy[b] (kJ/mol)	Mole Fraction (25 °C)	Order[a] (ϵ=30)	Dipole Moment (D) (ϵ=30)	Strain Energy[b] (kJ/mol)	Mole Fraction (25 °C)
1[c]	D_4	0.000	0.000	0.950	1	0.000	0.000	0.965
2	C_2	0.098	13.105	0.016	2	0.104	13.885	0.011
3	C_1	0.345	14.656	0.013	3	0.352	15.575	0.0080
4	C_{2h}	0.000	15.759	0.012	4	0.000	16.968	0.0078
5	C_1	1.950	17.554	0.0073	5	1.948	17.849	0.0061
6	C_2	1.589	22.965	0.0007	9	1.572	25.806	0.0002
7	S_4	0.000	23.560	0.0003	7	0.000	24.384	0.0002
8	C_1	2.699	25.779	0.0004	13	2.713	28.905	0.0001
9	C_1	3.504	27.132	0.0002	10	3.524	26.576	0.0002
10	C_1	1.972	27.320	0.0002	11	1.971	28.040	0.0001
11	C_1	4.809	27.762	0.0001	8	4.834	25.257	0.0003
12	C_4	5.919	27.770	8×10^{-6}	6	5.919	19.397	0.0002

[a] The numbers are the order of the conformations based on their strain energies at that dielectric constant. [b] With respect to the strain energy of the lowest energy conformation of this compound at this dielectric constant. [c] X-ray structure: ref. 248,320

Table 4.18 Comparison of MM3 Torsional Angles with X-Ray Torsional Angles: 1,4,7,10-Tetrathiacyclododecane (**26**)

Conformer	CSCC	SCCS	CCSC	CSCC	SCCS	CCSC	CSCC	SCCS	CCSC	CSCC	SCCS	CCSC
X-Ray[a]	-72.2	173.1	-73.7	-72.5	172.7	-72.2	-71.0	174.1	-71.5	-76.1	173.8	-68.2
(2nd)	-73.2	173.8	-71.1	-69.3	173.2	-75.8	-71.0	173.7	-71.0	-72.0	173.1	-74.2
MM3												
1	-71.9	174.0	-71.9	-71.9	174.0	-71.9	-71.9	174.0	-71.9	-71.9	174.0	-71.9
2	-77.0	166.8	-77.0	-79.1	172.2	-83.3	98.5	-172.4	98.5	-83.3	172.2	-79.1
3	-80.5	155.7	-79.9	146.2	-175.2	65.3	-101.0	173.8	-71.5	-74.0	177.2	-75.1
4	-82.7	169.9	-93.3	93.3	-169.9	82.7	82.7	-169.9	93.3	-93.3	169.9	-82.7
7	-75.1	169.0	-107.8	75.1	-169.0	107.8	-75.1	169.0	-107.8	75.1	-169.0	107.8
12	-69.6	-66.4	164.9	-69.0	-66.4	164.9	-69.0	-66.4	164.9	-69.0	-66.4	164.9

[a] From ref. 248.

NMR parameter that could be obtained was the time-averaged value of the vicinal coupling constants (8.16 Hz) and $^1J_{CH}$ (141 Hz). The ^{13}C NMR spectrum in solution and the CP/MAS spectrum of solid **26** (see Figure 4.18), also provided evidence in support of the molecular mechanics result. The solid phase spectrum shows 6 distinct peaks. There appears to be a shoulder between the two low frequency peaks and it is not unlikely that the lowest frequency peak is the result of two overlapping signals making a total of at least 8 peaks. This is consistent with the X-ray results where two different molecules are present in the unit cell and both are close to D_4 symmetry. The average chemical shift of the 6 distinct peaks is 28.97 ppm, only 0.55 ppm higher frequency than the solution spectrum signal (28.43 ppm). If one were to include the other two postulated peaks (see above) then the fit would be even closer. It would seem that according to the ^{13}C spectra, the solution conformation is fairly similar to the solid conformation (unlike compound **23**).

4.2.5.3 Complex Formation

Compound **26** forms 1:1 complexes in which it acts as a tetradentate ligand. The most stable conformer of the free ligand is not capable of tetradentate binding because it has its sulfur atoms exodentate. In order to form, the ligand must alter its conformation to an endodentate conformer. In Pt(**26**)Cl_2,[218] the ligand takes on a C_4 crown conformation in the complex with the Pt(II) ion at the centre of a planar square of S atoms separated by 3.20 Å. In Pt(**26**)$(PF_6)_2$, the Pt is still square planar, but the ligand adopts a C_1 conformation. In Bi(**26**)Cl_3,[262] it takes on a highly distorted C_4 geometry. The lowest energy C_4 conformer calculated here was at least 19 kJ/mol higher in energy than the global minimum in polar medium. The complexes formed are quite stable[218] despite the fact that **26** has to pay a high

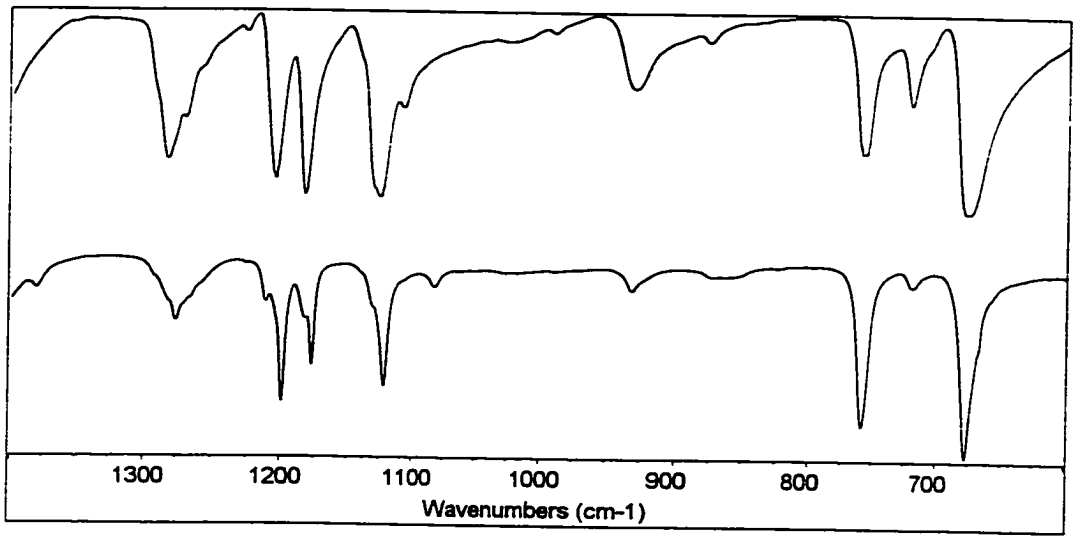

Figure 4.17 Infrared spectra of compound **26**; top: solid phase spectrum; bottom: solution spectrum in CS_2.

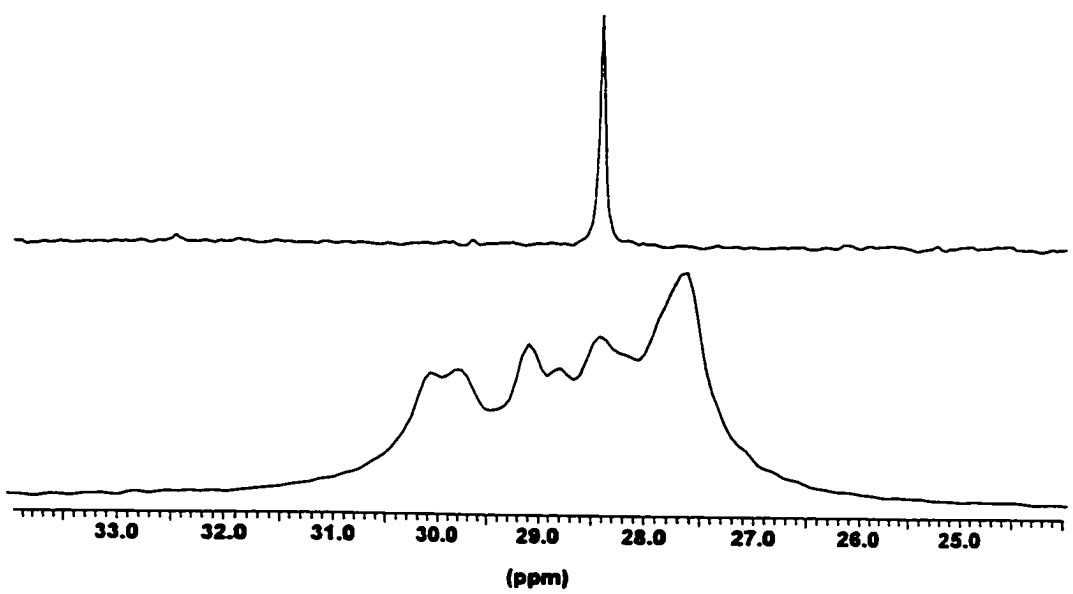

Figure 4.18 ^{13}C NMR spectra of **26**; top: spectrum of $CDCl_3$ solution; bottom: CP/MAS spectrum.

enthalpic price for endodentate binding. However, the D_4 global minimum conformation is adopted in a complex to $Al(Me)_3$, in which the aluminum is complexed to one S atom.[320] This is a result of the fact that $Al(Me)_3$ has only one binding site and that the global minimum is quite stable and will readily form a monodentate complex.

4.2.6 1,4,8,11-Tetrathiacyclotetradecane (27)

4.2.6.1 MM3 Conformational Analysis

Compound **27** has been obtained in two crystalline forms; the α form contained molecules in conformations with C_{2h} symmetry, the β form contained unit cells with molecules in equal amounts of two conformations, the β_1 molecules were in a conformation similar to

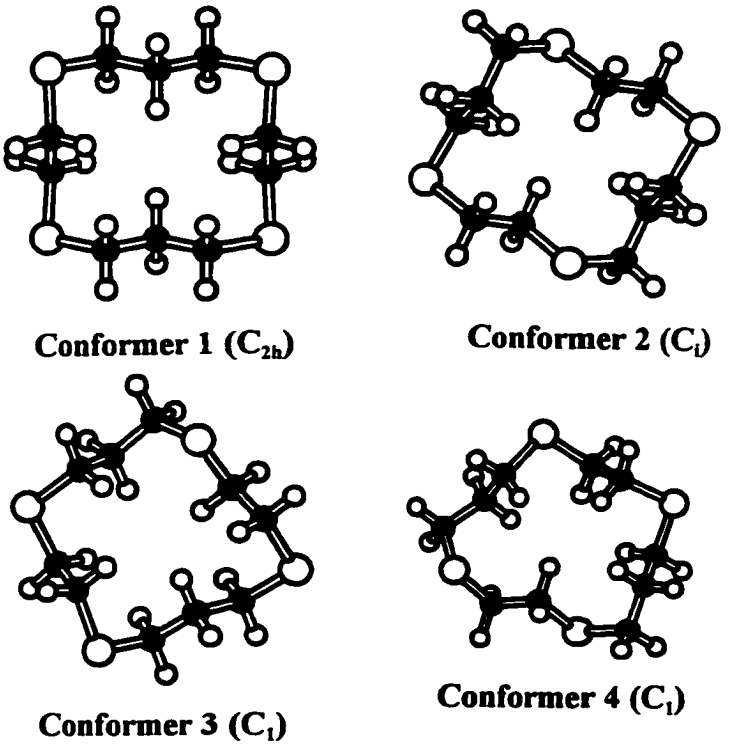

Figure 4.19 ATOMS diagrams of the four most stable conformers of 1,4,8,11-tetrathiacyclotetradecane (**27**).

that of the α form, the β_2 molecules were also similar but were disordered in the ethano bridges.[246] The MM3 calculations (see Table 4.19) indicate that the C_{2h} conformation is indeed the most stable, but unlike the compounds just considered, several other conformers are only slightly less stable, including a C_i conformer with almost identical stability at a dielectric constant of 1.5 but 3.6 kJ/mol less stable at a dielectric constant of 30.0. ATOMS diagrams of several of the most stable conformers are shown in Figure 4.19. A comparison of the MM3 geometries and the x-ray structures can be found in Tables 4.20 and A.13. The larger ring size here again increases the possibilities; a total of 697 conformers were found.

4.2.6.2 Spectroscopic Conformational Analysis

The photoelectron spectra of **27** also show only one peak assigned to lone pairs.[301,302] The infrared spectra of **27** are shown in Figure 4.20. The spectrum of a CS_2 solution is broader and more complex than the solid phase spectrum especially in the region between 1400 and 600 cm^{-1}. The ^{13}C NMR spectra of solid **27** and of a solution of **27** in benzene-d_6 are presented in Figure 4.21. The solution spectrum shows three peaks at 31.5, 30.3, and 30.0 ppm. These were assigned as the ethano bridge carbons, the terminal propyl carbons, and the CCH_2C carbons respectively.[321] There are 5 distinct peaks in the CP/MAS spectrum of the solid, two more than would be expected for the C_{2h} symmetry. The additional peaks in the CP/MAS spectrum are most likely due to the fact that the sample used to obtain the spectrum was a mixture of the α and β crystals The chemical shifts are significantly different from the solution values. This supports the results of the MM3 calculation that the solution mixture should be heterogenous.

Table 4.19 MM3(94) Results for 1,4,8,11-Tetrathiacyclotetradecane (27)

Order[a]	Symmetry	Dipole Moment (D) (ϵ=1.5)	Strain Energy[b] (kJ/mol)	Mole Fraction (25 °C)	Order[a] (ϵ=30)	Dipole Moment (D) (ϵ=30)	Strain Energy[b] (kJ/mol)	Mole Fraction (25 °C)
1[c]	C_{2h}	0	0	0.103	1	0	0	0.223
2	C_i	0	0.1	0.227	2	0	3.637	0.121
3	C_1	2.101	2.944	0.184	3	2.103	4.66	0.208
4	C_1	1.383	5.195	0.113	4	1.365	8.692	0.06
5	C_1	1.845	7.901	0.023	10	1.853	10.841	0.016
6	C_2	1.304	8.252	0.027	14	1.311	12.17	0.012
7	C_2	1.799	9.094	0.01	8	1.801	10.456	0.012
8	C_2	2.431	9.099	0.013	5	2.43	9.583	0.023
9	C_1	0.445	9.339	0.032	6	0.438	10.117	0.011
10	C_1	2.48	9.45	0.163	7	2.481	10.249	0.058
11	C_1	2.25	9.617	0.069	13	2.26	11.953	0.013
12	C_1	1.02	9.916	0.147	16	1.012	13.148	0.02
14	C_1	3.431	10.38	0.011	9	3.431	10.612	0.021

[a] The numbers are the order of the conformations based on their strain energies at that dielectric constant. [b] With respect to the strain energy of the lowest energy conformation of this compound at this dielectric constant. [c] X-ray structure: reference 246.

Table 4.20 Comparison of MM3 Torsional Angles (°) with X-Ray Torsional Angles (°): 1,4,8,11-Tetrathiacyclotetradecane (**27**)

Conformer	CSCC	SCCS	CCSC	CSCC	SCCC	CCCS	CCSC	CSCC	SCCS	CCSC	CSCC	SCCC	CCCS	CCSC
X-Ray[a]														
α	-67	-176	-60	-62	178	177	63	67	176	60	62	-178	-177	-63
β_1	-65	-175	-60	-64	176	-180	66	65	175	60	64	-176	180	-66
β_2	129	179	113	-74	177	179	80	-129	-179	-113	74	-177	-179	-80
MM3														
1	62.1	174.2	62.1	63.2	179.2	-179	-63	-62.1	-174	-62.1	-63.2	-179	179.2	63.2
2	-61	178.9	-176	67	57.2	175.9	58	60.9	-179	176.3	-67	-57.2	-176	-58
3	64.8	172.8	71.6	71.2	174.7	58.6	71.6	-167	176.1	-56.3	-52.7	179.5	-177	67.7
4	-75	-171	-80.6	-74	-168	-60.9	-68	109.8	-175	-169	-55.5	-58.5	-180	-76

[a] X-ray results from ref. 246.

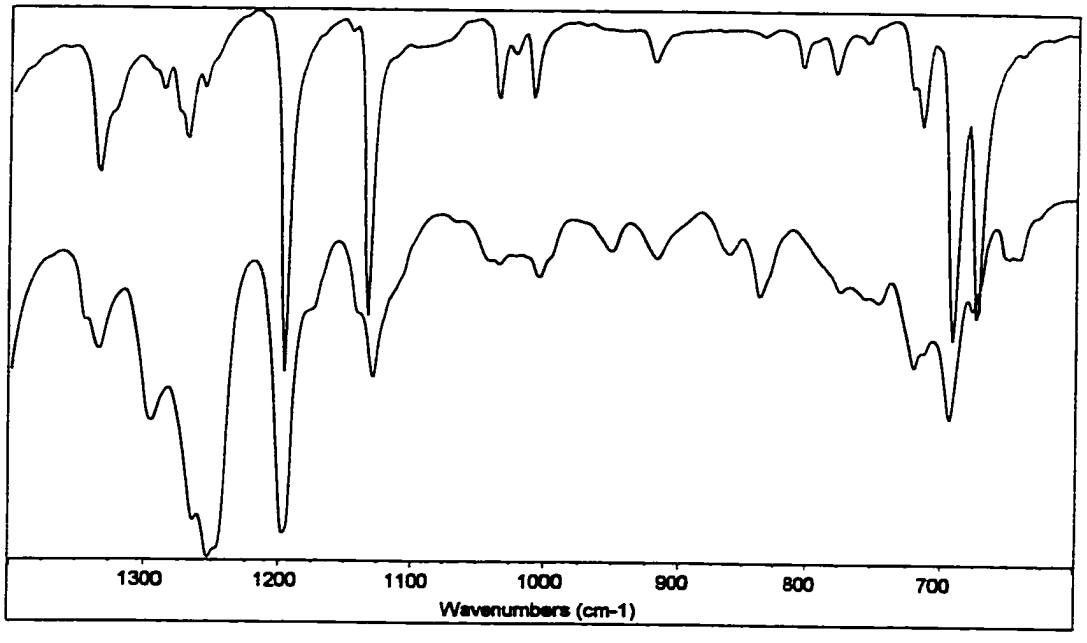

Figure 4.20 The infrared spectra of 1,4,8,11-tetrathiacyclotetradecane (**27**). Top: solid spectrum Bottom: spectrum in CS_2

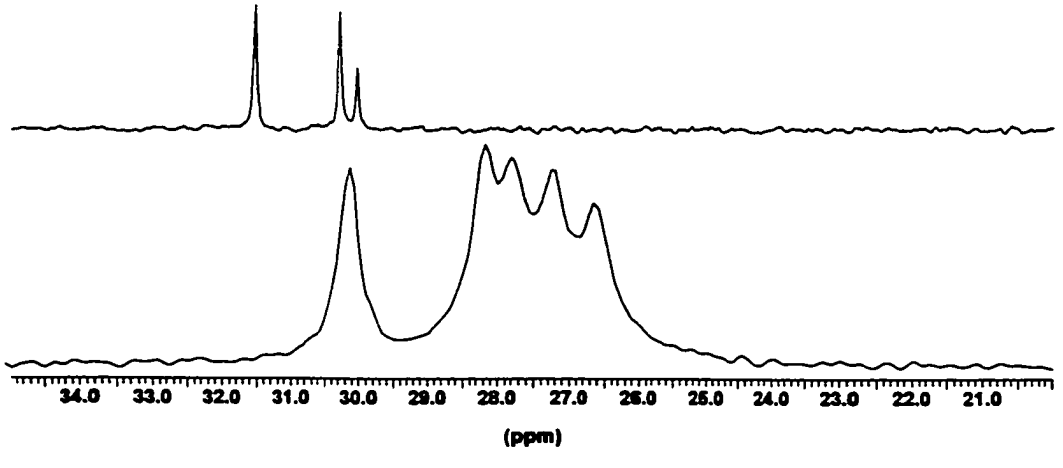

Figure 4.21 The ^{13}C NMR spectra of 1,4,8,11-tetrathiacyclotetradecane (**27**). Top: spectrum in benzene-d_6 Bottom: CP/MAS spectrum of the solid.

4.2.6.3 Complex Formation

Compound **27** commonly takes one of two conformations when it binds to a metal (see Figure 4.22).[229] These two conformations are referred to as the *anti* and *syn* conformations.[229] Neither of these conformations is calculated to be a low energy conformer in the MM3 results. The ligand takes on the *anti* conformation with $Cu(\mathbf{27})^{2+}$ and $Ni(\mathbf{27})^{2+}$ cations.[322,323] In nitromethane solution, the Ni complex converts to an approximately 50:50 mixture of the *anti* and *syn* conformations.[229] The larger metals tend to favour the *syn* conformation for their ligands. For example, Rh(I) and Ru(II) form *syn* complexes.[229] Spectral analyses of the $W(CO)_3(\mathbf{27})$ in solution supported a *syn* conformation also.[321] As has been seen with other crown thioethers, compound **27** also forms exodentate ligands that act as bridges between metals. In the case of the $(NbCl_5)_2(\mathbf{27})$, complex the ligand is exodentate and acts as a bridge between the two $NbCl_5$ units.[324] Its conformation is similar to the crystal structure, which is also the global minimum.

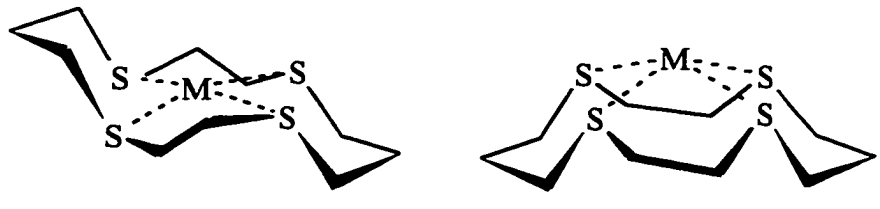

anti *syn*

Figure 4.22 The two common conformations of complexes involving compound **27**.

4.2.7 1,4,7,10,13-Pentathiacyclopentadecane (28)

4.2.7.1 MM3 Conformational Analysis

The stochastic search results for 1,4,7,10,13-pentathiacyclopentadecane (**28**)(see Table 4.21) indicate that there are at least 467 unique conformations of **28**. The search found that at least 30 conformers are calculated to be within 10 kJ/mol of the global minimum, at both dielectric constants. The calculations suggest that the lowest energy conformer has D_5 symmetry, with all S-C-C-S torsional angles *anti*. ATOMS diagrams of several of the most stable conformers are shown in Figure 4.23. Thus, although the D_5 conformer may be the single most populated conformer, particularly at low temperatures, solutions of this conformer will contain an ensemble of conformers, with none dominating.

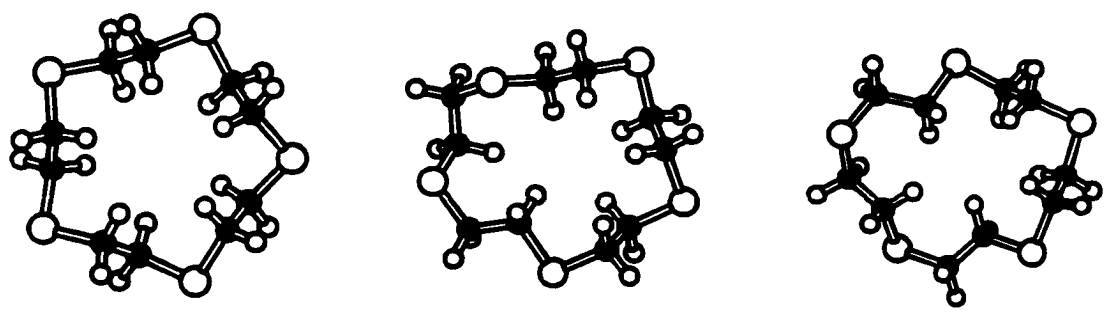

Conformer 1 (D_5) **Conformer 2 (C_1)** **Conformer 3 (C_1)**

Figure 4.23 ATOMS diagrams of the three most stable conformers of 1,4,7,10,13-pentathiacyclopentadecane (**28**)

Table 4.21 MM3(94) Results for 1,4,7,10,13-Pentathiacyclopentadecane[a] **(28)**

Order[b]	Symmetry	Dipole Moment (D) (ϵ=1.5)	Strain Energy[c] (kJ/mol)	Mole Fraction (25 °C)	Order[b] (ϵ=30)	Dipole Moment (D) (ϵ=30)	Strain Energy[c] (kJ/mol)	Mole Fraction (25 °C)
1	D_5	0	0	0.033	1	0	0	0.052
2	C_1	1.865	2.944	0.05	2	1.887	3.714	0.057
3	C_1	0.299	4.336	0.111	8	0.292	6.514	0.074
4	C_1	2.035	5.053	0.03	4	2.016	5.536	0.038
5	C_2	2.009	5.226	0.036	26	2.002	8.948	0.013
6	C_1	2.012	5.341	0.05	7	2.033	6.352	0.051
7	C_1	0.205	5.479	0.093	12	0.212	7.089	0.076
8	C_1	0.222	5.481	0.041	3	0.227	5.513	0.06
9	C_2	0.365	5.969	0.005	6	0.371	6.081	0.008
10	C_1	0.298	6.022	0.019	16	0.296	7.87	0.014
11	C_1	1.902	6.366	0.039	13	1.913	7.221	0.043
12	C_1	1.726	6.453	0.015	18	1.736	8.094	0.012
26	C_1	3.416	8.882	0.002	11	3.438	6.897	0.007

[a] X-ray structure: ref. 248, conformer in the solid-state is not one of the ten conformers calculated to be most stable. [b] The numbers are the order of the conformations based on their strain energies at that dielectric constant. [c] With respect to the strain energy of the lowest energy conformation of this compound at this dielectric constant.

At a dielectric constant of 1.5, the first conformer with a dipole moment greater than 3 D was the 26th, 8.9 kJ/mol above the minimum, the first greater than 4 D was the 145th, 19.4 kJ/mol above the minimum, the first greater than 5 D was the 172nd, 21.1 kJ/mol above the minimum and the first above 6 D was the 388th, 36.3 kJ/mol above the minimum. At a dielectric constant of 30, the corresponding initial conformers were 11th (6.9 kJ/mol), 94th (16.4 kJ/mol), 119th (18.4 kJ/mol) and 168th (22.1 kJ/mol), respectively.

The solid-state conformation of compound **28** has been determined to be a C_1 conformer.[248] This conformation was not among the conformations calculated to be of low relative energy by MM3 and it incorporates a feature that is not found in any of the low energy conformations of any of these thiocrown ethers, namely + and - signs for the *gauche* torsional angles about one sulfur atom, S4 (see Table 4.22). Normally, low energy conformations have two *gauche* torsional angles of the same sign about the sulfur atoms, resulting in a square corner (see Figure 4.3). In the crystal structure, only four of the five SCCS angles are *anti*. A photoelectron spectrum should be able to differentiate between these conformers, (the crystal structure and the low energy conformers) because the *gauche* relationship should result in splitting but unfortunately, the photoelectron spectrum has not been recorded. Data for the geometry of the crystal structure and the MM3 global minimum can be found in Tables 4.22 and A.14.

4.2.7.2 Spectroscopic Conformational Analysis

The infrared spectra of **28** in the solid phase and in CS_2 solution are presented in Figure 4.24. The ^{13}C NMR spectrum of a $CDCl_3$ solution and the CP/MAS spectrum are

Table 4.22 Comparison of MM3 Torsional Angles (°)with X-Ray Torsional Angles (°): 1,4,7,10,13-Pentathiacyclopentadecane (**28**)

Conf	CSCC	SCCS	CCSC	CSCC	SCCS	CCSC	CSCC	SCCS	CCSC	CSCC	SCCS	CCSC	CSCC	SCCS	CCSC
X-Ray[a]	-76.1	-171.9	-121.9	91	174.4	82.8	113.8	-63.9	-88.5	84.3	166.6	-156	-78.4	167	-80.9
MM3															
1	78.1	168.2	78.1	78.1	168.2	78.1	78.1	168.2	78.1	78.1	168.2	78.1	78.1	168.2	78.1
2	169.4	176.3	74	-149.5	69.8	76.1	-177	-175	-70.7	-71.5	-174	-77.7	-83.7	178	-84
3	162	-170.9	99.9	-63.2	-175.4	-168	-72.3	-176	-75.1	-77.3	173.7	-66.8	-147	177.1	-74.9
4	-76.9	-175.9	-69	-68.7	-178.4	176.2	73.8	74.5	-102	-75.5	-166	-76.8	-75.7	-164	-70.6

[a] X-ray results from ref. 248.

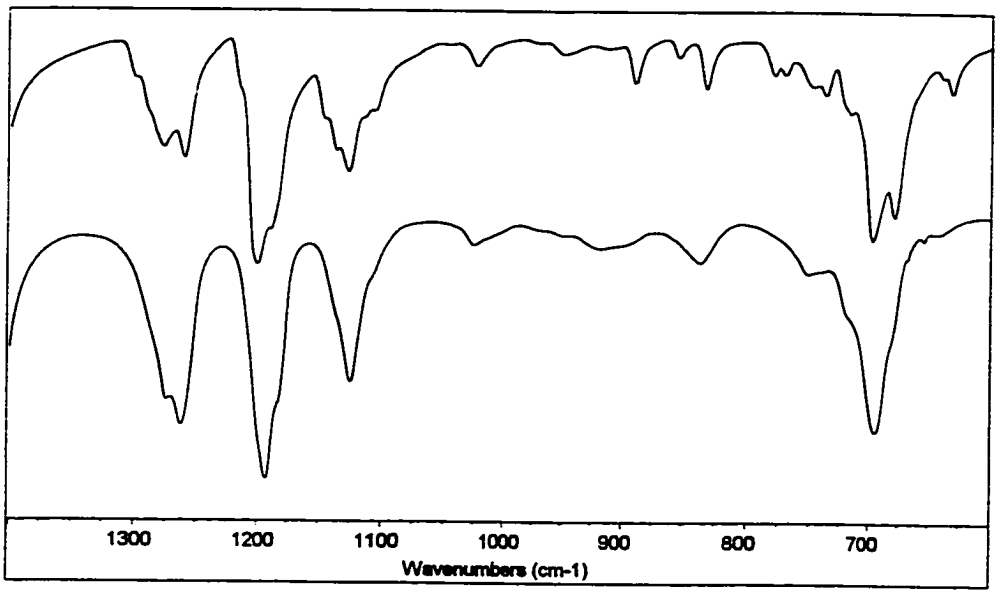

Figure 4.24 The infrared spectra of 1,4,7,10,13-pentathiacyclopentadecane (**28**) Top: solid phase spectrum Bottom : spectrum in CS_2

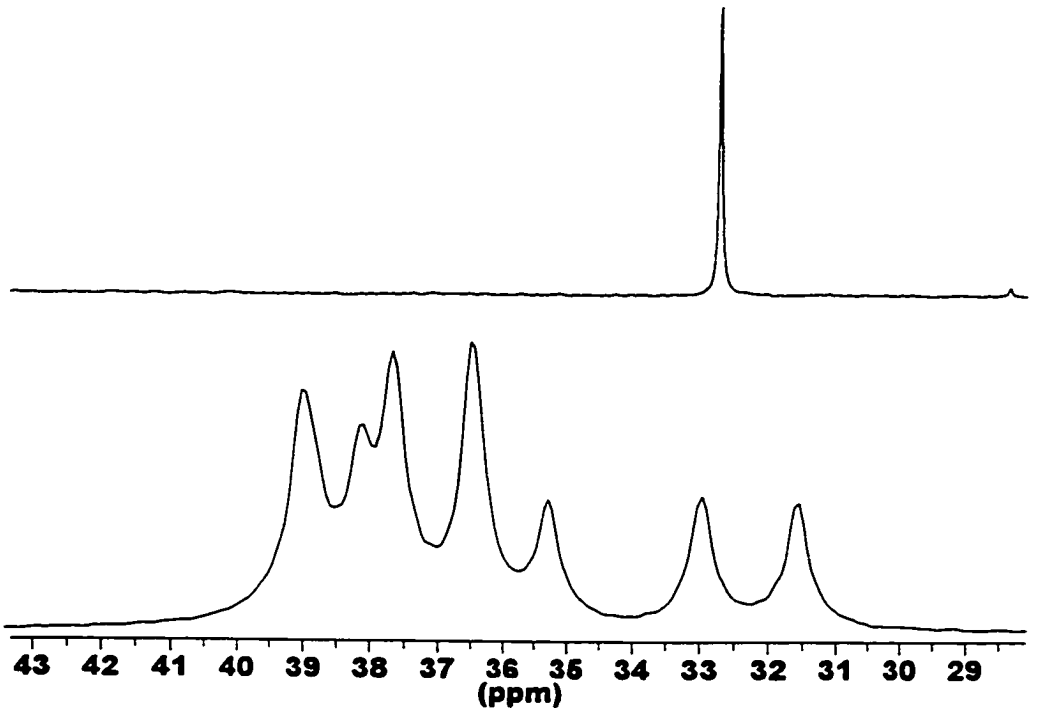

Figure 4.25 The ^{13}C NMR spectra of 1,4,7,10,13-pentathiacyclopentadecane (**28**) Top: spectrum in $CDCl_3$ Bottom : CP/MAS spectrum

shown in Figure 4.25. The infrared spectra are similar especially with respect to the stronger absorptions, but the weaker signals at lower frequencies are different. The NMR spectra indicate that the solution conformers are similar but not identical to the solid phase. The CP/MAS spectrum only contains 7 distinct peaks but three of these peaks are about twice the size of the others, perhaps due to signal overlap. These three hidden signals would thus account for the ten separate carbons in the crystal structure of **28**. The chemical shift in solution is 32.85 ppm. The average of the 7 signals in the CP/MAS spectrum is 35.88 ppm.

4.2.7.3 Complex Formation

The complexes of **28** have the ligand in a wide range of conformations. The complexes differ according to the type of metal and its oxidation state. In Re(I) complexes, only two of the sulfurs are coordinated, in Pd(II) and Pt(II) complexes, four of the five sulfurs are coordinated.[230] The $Hg(\mathbf{28})^{2+}$ and $Cu(\mathbf{28})^{2+}$ cations have all five sulfurs coordinated to the metal and the resulting conformation of the ligand contains a mirror plane.[325,326] The metals in both of these complexes both have square pyramidal coordination spheres. Upon reduction of $Cu(\mathbf{28})^{2+}$ to the $Cu(\mathbf{28})^{1+}$ cation the metal coordination sphere becomes a distorted tetrahedron and one of the equatorial Cu-S bonds is removed. The conformation of the ligand changes to accommodate this by taking on a conformation with an approximate C_2 axis of rotation.[325] In $BiCl_3(\mathbf{28})$ all five endodentate sulfurs are bonded to the metal but the ligand **28** sits on top of the Bi atom like a cap and its conformation does not appear to be symmetrical in any way.[262] This situation is believed to be due to the relative inflexibility of the geometry of the $BiCl_3$ unit.[262] In the case of the $Ag_2(\mathbf{28})_2^{2+}$ cation the two asymmetric ligands are each coordinated differently by the two Ag atoms.[327] One of the atoms is

coordinated to two sulfurs of one ligand and to one of the other, the other atoms is tetrahedrally coordinated to three sulfurs of one ligand and one of the other. These results indicate, what Blake *et al.* refer to as the "coordinative flexibility" of compound **28**.[327]

4.2.8 1,5,9,13-Tetrathiacyclohexadecane (29)

4.2.8.1 MM3 Conformational Analysis

Blake and coworkers[328] performed molecular mechanics (MM2) calculations on a series of eight conformations of **29** derived from cyclohexadecane conformers. The stochastic search performed here produced 767 unique conformers. The low energy results of the search are in Table 4.23 and ATOMS diagrams of several of the most stable conformers of the 767 found are shown in Figure 4.26. The global minimum was found to be a C_{2v}-symmetric square with all four S atoms at the corners. The calculations also indicate that there is no conformer that dominates the conformational mixture. The result is that the calculations predict that a very complex conformational mixture will be present.

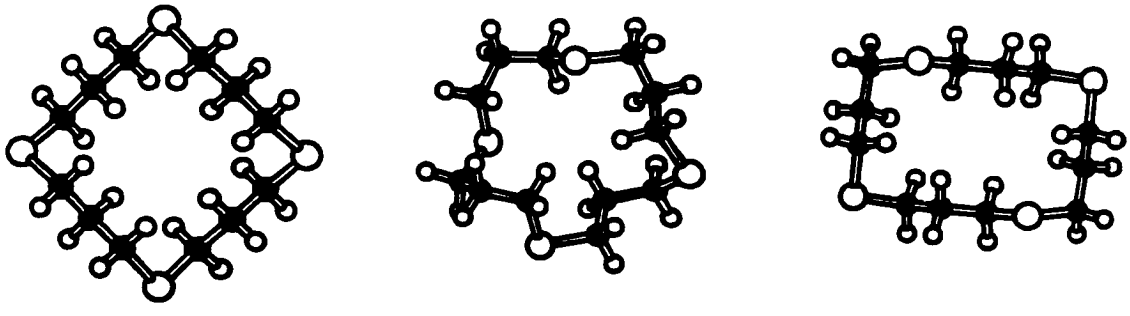

Conformer 1 (C_{2v}) **Conformer 2 (C_1)** **Conformer 3 (C_2)**

Figure 4.26 ATOMS diagrams of the three lowest energy conformers of 1,5,9,13-tetrathiacyclohexadecane (**29**)

Table 4.23 MM3(94) Results for 1,5,9,13-Tetrathiacyclohexadecane (**29**)

Order[a]	Symmetry	Dipole Moment (D) (ϵ=1.5)	Strain Energy[b] (kJ/mol)	Mole Fraction (25 °C)	Order[a] (ϵ=30)	Dipole Moment (D) (ϵ=30)	Strain Energy[b] (kJ/mol)	Mole Fraction (25 °C)
1	C_{2v}	0	0	0.045	1	0	0	0.206
2	C_1	2.197	0.224	0.034	3	2.18	6.158	0.015
3[c]	C_2	2.992	1.409	0.024	2	2.992	3.658	0.046
4	S_4	0	1.623	0.042	4	0	7.187	0.021
5	C_1	2.198	2.177	0.025	8	2.207	8.099	0.011
6	C_1	2.107	2.53	0.136	6	2.108	7.684	0.082
7	C_1	0.418	3.849	0.094	17	0.412	10.956	0.027
8	C_1	0.471	4.627	0.067	14	0.467	10.855	0.027
9	C_1	2.352	5.102	0.017	16	2.356	10.951	0.008
10	C_1	2.29	5.212	0.01	12	2.304	10.956	0.007
11	C_2	2.811	5.226	0.026	10	2.861	9.233	0.025
12	C_1	2.207	5.528	0.044	11	2.205	9.818	0.038
18	D_2	0	6.184	0.006	19	0	11.444	0.004

[a] The numbers are the order of the conformations based on their strain energies at that dielectric constant. [b] With respect to the strain energy of the lowest energy conformation of this compound at this dielectric constant. [c] X-ray structure: ref. 328.

The conformation present in the crystal structures of two forms of compound **29** is a C_2-symmetric rectangular [3535] conformation with two S atoms at the corners and two adjacent to corners.[328] A third crystal form exists but its structure has not yet been determined.[328] The C_2 conformation matches the third most stable conformer at a dielectric constant of 1.5 and was calculated to be slightly less stable than the global minimum, by 1.4 and 3.7 kJ/mol at dielectric constants of 1.5 and 30.0, respectively (see Table 4.24). A comparison of the MM3 geometry with the crystal structures can be found in Tables 4.24 and A.15.

4.2.8.2 Spectroscopic Conformational Analysis

Experimental photoelectron spectra of this compound differ in that one study reports two lone pair maxima, a large one at 8.35 eV and a much smaller one at 8.87 eV,[301] while the other study reports only a single broad peak with a maximum at 8.4 eV.[302] In the global minimum, the 4 S atoms are equivalent and too distant from each other to cause splitting. However, a C_1 conformer, with 4 different S atoms is only 0.2 kJ/mol less stable at a dielectric constant of 1.5, and as noted above, the solid-state conformer, with 2 different types of S atoms, is calculated to be only slightly less stable.

The infrared and ^{13}C NMR spectra of the solid and solution phase **29** are in Figures 27 and 28 respectively. Comparison of the infrared spectra from the solid and the CS_2 solution show that there is more complexity in the solution spectrum especially at low frequencies. This observation supports the MM3 results, which predict the presence of a complex heterogenous mixture in solution. The average of the eight distinct peaks in the CP/MAS spectrum (28.8 ppm) is 1.5 ppm lower frequency than the weighted average of the

Table 4.24 Comparison of MM3 Torsional Angles (°) with X-Ray Torsional Angles (°): 1,5,9,13-Tetrathiacyclohexadecane (**29**)

Conf	CSCC	SCCC	CCCS	CCSC	CSCC	SCCC	CCCS	CCSC	CSCC	SCCC	CCCS	CCSC	CSCC	SCCC	CCCS	CCSC
X-Ray[a]																
α	62.1	-175	69.2	74.6	-168	179	-178	62.9	66.6	-174	66.8	75	-166	-179	178.4	61.5
β	65.8	-173	68.2	76.7	-170	179.7	-178	60.1	61.6	-176	70.3	75.1	-168	178.2	-178	64
MM3																
1	62.7	178.2	-178	-62.7	-62.7	-178	178.3	62.7	62.7	178.3	-178	-62.7	-62.7	-178	-178	62.7
2	75.9	178.9	58.6	56.5	62.1	173.1	62.4	77.9	172.3	63.4	63.1	179.2	65.6	52.2	58	-159
3[b]	70.1	-176	61	71.1	-169	178.7	-177	68.2	70.1	-176	61	71.1	-169	178.7	-177	68.2
4	-176	179	-56.3	-62.9	176	-179	56.3	62.9	-176	179	-56.3	-62.9	176	-179	56.3	62.9
6	-175	174.6	-61	-61	174.6	-175	61	61	-175	174.6	-61	-61	174.6	-175	61	61

[a] X-ray data from ref. [328]; [b] The conformation present in both crystalline forms.

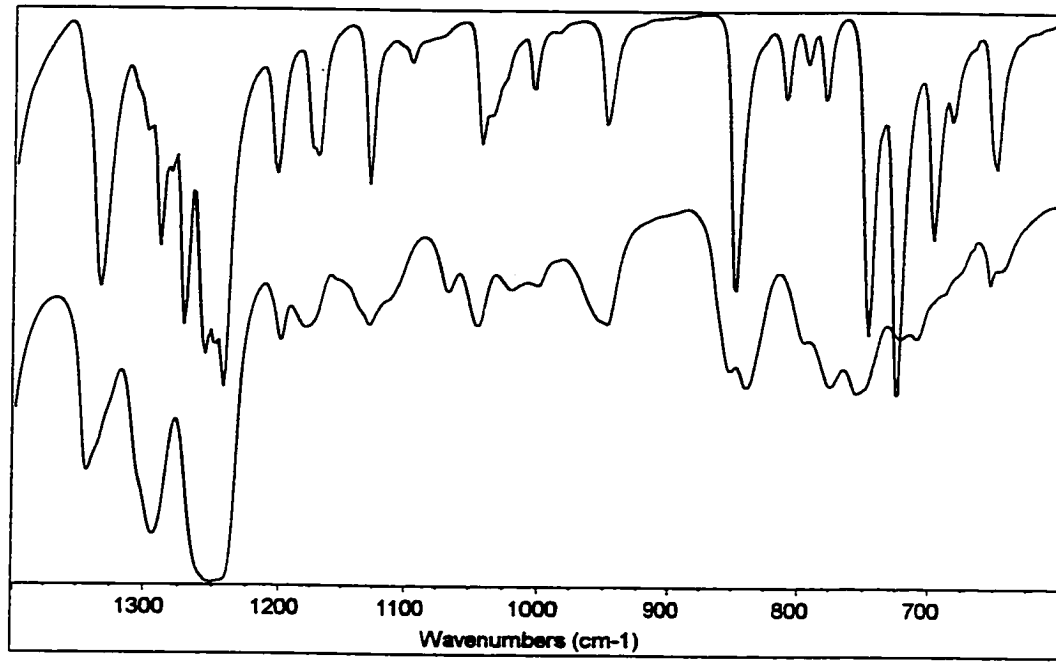

Figure 4.27 The infrared spectra of 1,5,9,13-tetrathiacyclohexadecane. Top: solid spectrum. Bottom: spectrum in CS_2.

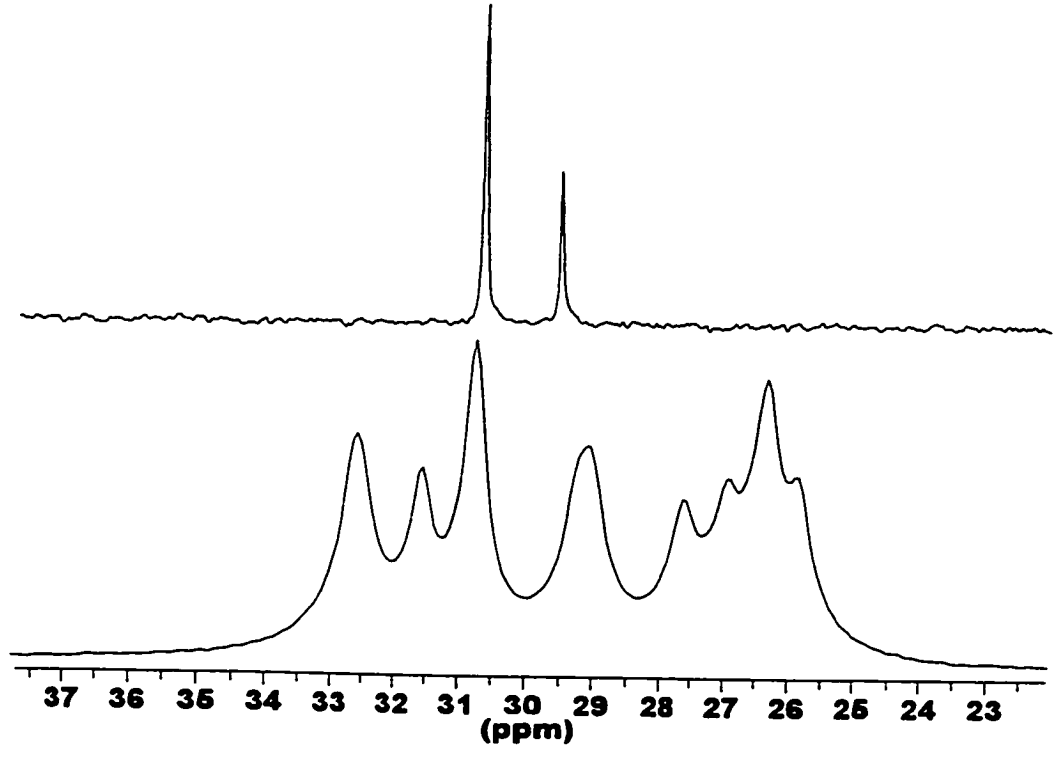

Figure 4.28 ^{13}C NMR spectra of 1,5,9,13-tetrathiacyclohexadecane.(**29**): top, in chloroform-*d* solution, bottom, CP/MAS spectrum of the solid.

signals in $CDCl_3$. The CP/MAS spectrum contains more peaks than would be expected for the crystal structure which has a C_2 symmetry. This is probably due to the fact that the sample used for the spectrum was not a single crystal form. It was most likely a mixture of the α and β forms of **29**.[328] In addition, it appears that the peaks at 32.6, 30.8, 29.1 and 26.35 ppm, which are broader or taller than the others, may be due to peak overlap. If this is correct, the CP/MAS spectrum contains 12 signals, which is consistent with two slightly different C_2 symmetric conformers or one or more pseudo-symmetric C_2 conformers.

4.2.8.3 Complex Formation

Compound **29** is present in an approximately C_s conformation when bound to the edge of a ruthenium cluster with two S atoms bound to two different Ru atoms.[318] This conformation does not appear to be one of the 20 most stable minima. In the $Hg(\mathbf{29})^{2+}$ and $Cd(\mathbf{29})^{2+}$ cations[329] the ligand takes on two different conformations. Both have C_2 axes of symmetry, but the directions the sulfurs point relative to the plane of the S atoms differs. In the Hg complex, the sulfurs are "up-down-up-down", while in the Cd complex they are "up-up-down-down". This last conformation (the Cd conformation) is also found in the $Cu(\mathbf{29})^{2+}$ cation.[330] An MM2 conformational analysis of the conformers in the Hg and Cd complexes indicated that the "up-down-up-down" conformation was 3.47 kJ/mol higher in energy than the global minimum and the "up-up-down-down" conformation was 23.1 kJ/mol higher in energy.[329]

4.2.9 MM3 Conformational Analyses of Potential Trithiacycloalkanes Ligands

A number of trithiacycloalkanes were examined to see whether any of these would be efficient complex formers. Results for all of these compounds are also given in Tables 25-27.

4.2.9.1 1,4,7-Trithiacycloundecane (30)

The increased degrees of freedom resulting from increasing ring size results in many more conformers than compound **23**; 158 were found in the stochastic search for compound **30**. The 3.1 kJ/mol gap between the global minimum conformer and the next conformer obtained by MM3 suggests that it would be the most populated conformer by a significant amount and indeed it is calculated to be about three times more populated than conformer 2. However, there are 18 other conformers that are calculated to be within 10 kJ/mol so the global minimum is calculated to make up only 34% of the conformational ensemble at 25 °C. The most stable conformer with a dipole moment > 4 D is the 38th conformer at a dielectric constant of 1.5, 16.2 kJ/mol above the global minimum. This conformer becomes 23rd most stable at a dielectric constant of 30.0, 12.5 kJ/mol above the minimum. Thus, compound **30** is unlikely to be a particularly efficient binder. Compound **30** has been synthesized[331] but no complexation studies have been reported. Figure 4.29 shows ATOMS diagrams of the two most populated conformers of **30**.

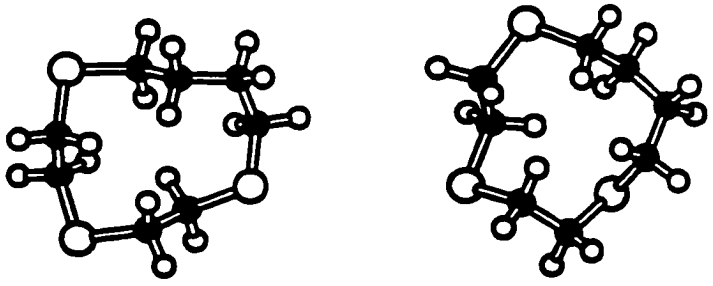

Conformer 1 (C_1) **Conformer 2 (C_1)**

Figure 4.29 The two most stable conformers of 1,4,7-trithiacycloundecane (**30**).

Table 4.25 MM3(94) Results for 1,4,7-Trithiacycloundecane (**30**)

Order[a]	Symmetry	Dipole Moment (D) (dielc 1.5)	Strain Energy[b] (kJ/mol)	Mole Fraction (25 °C)	Order[a] (die 30.)	Dipole Moment (D) (dielc 30.)	Strain Energy[b] (kJ/mol)	Mole Fraction (25 °C)
1	C_1	1.54	0	0.34	1	1.54	0	0.42
2	C_1	1.7	3.1	0.12	2	1.7	3.62	0.13
3	C_1	1.59	4.34	0.082	6	1.58	6.27	0.05
4	C_1	2.98	4.77	0.042	3	2.99	4.69	0.055
5	C_1	1.64	4.78	0.051	5	1.65	5.99	0.042
6	C_2	1.27	5.13	0.02	8	1.27	6.6	0.014
37	C_1	4.17	16.25	<0.001	23	4.19	12.54	0.003

[a] The numbers are the order of the conformations based on their strain energies at that dielectric constant.
[b]With respect to the strain energy of the lowest energy conformation of this compound at this dielectric constant.

4.2.9.2 1,4,8-Trithiacycloundecane (31)

As can be seen from Table 4.26, a considerable number of the 180 conformers found for compound **31** are close in stability to the global minimum. This compound is also calculated to have a number of conformers with quite large dipole moments not too much less stable than the minimum. At a dielectric constant of 30, one of these is found to be only 3.0 kJ/mol less stable than the minimum, very similar to the difference calculated between the C_3 conformer of **23** and its global minimum. The four most stable conformers plus this most stable polar conformer are shown in Figure 4.30. Thus, compound **31** is expected to be a good complexing agent. It has been prepared but its reactivity and the stability of its complexes have not been studied.[331]

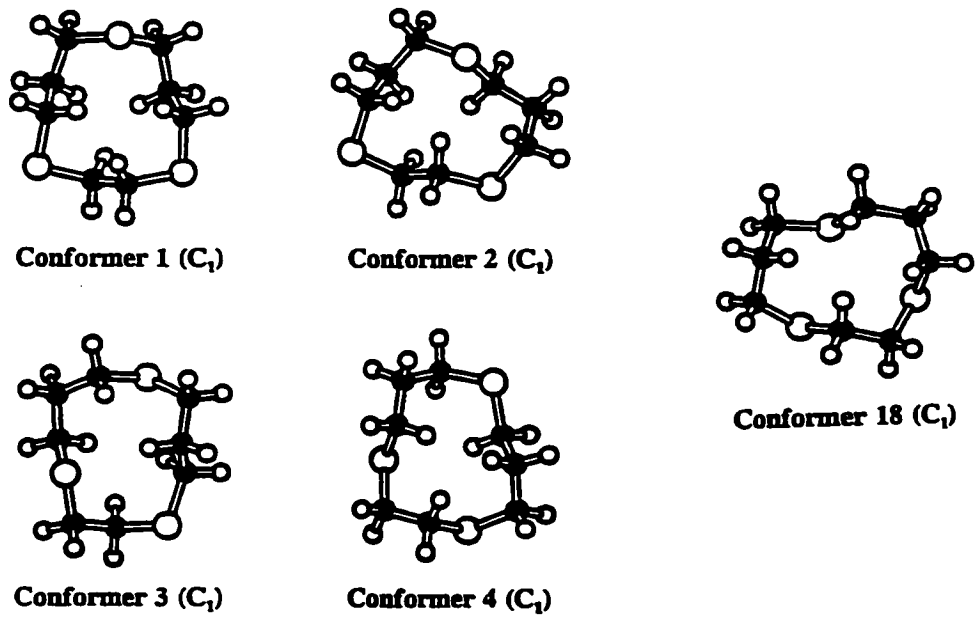

Figure 4.30 The four most stable conformers of 1,4,8-trithiacycloundecane (**31**) plus that of the most stable polar conformer.

Table 4.26 MM3(94) Results for 1,4,8-Trithiacycloundecane (**31**)

Order[a]	Symmetry	Dipole Moment (D) (dielc 1.5)	Strain Energy[b] (kJ/mol)	Mole Fraction (25 °C)	Order[a] (die 30.)	Dipole Moment (D) (dielc 30.)	Strain Energy[b] (kJ/mol)	Mole Fraction (25 °C)
1	C_1	1.79	0	0.23	2	1.78	1.17	0.15
2	C_1	1.78	0.41	0.24	1	1.78	0	0.19
3	C_1	1.23	1.52	0.13	3	1.24	1.59	0.11
4	C_1	2.12	2.56	0.077	4	2.14	1.59	0.093
5	C_1	1.88	2.91	0.114	5	1.88	1.64	0.16
6	C_1	1.42	3.73	0.036	8	1.43	4.18	0.026
18	C_1	4.5	11.43	0.003	7	4.51	3.03	0.057
31	C_1	4.42	17.28	<0.001	18	4.43	8.83	0.005

[a] The numbers are the order of the conformations based on their strain energies at that dielectric constant.[b] With respect to the strain energy of the lowest energy conformation of this compound at this dielectric constant.

4.2.9.3 1,4,7-Trithiacyclododecane (32)

In contrast to the previous two compounds, examination of Table 4.27 suggests that **32** will be relatively homogeneous conformationally, both in polar and non-polar solvents, although the larger ring size causes the total number of conformers to be increased, in this case to 353. The fourth most stable conformer at a dielectric constant of 1.5 is very polar with a dipole moment of 4.48 D and it becomes the second most stable conformer at a dielectric constant of 30.0, 6.3 kJ/mol above the global minimum. The four most stable conformers are shown in Figure 4.31. Thus, it might also be expected to be a good binder. It does not appear that a synthesis of compound **32** has been published.

4.2.9.4 1,4,8-Trithiacyclododecane (33)

A 4000 push stochastic search of the conformational energy surface yielded 638 conformers, of which 7 are within 10 kJ/mol of the global minimum at a dielectric constant of 1.5. The number of conformers is increased for **33** because of its lack of symmetry. ATOMS diagrams of the four that are least strained are shown in Figure 4.32. Although compound **33** was found to be quite inhomogeneous, the major conformer, a [3333] conformation, still constitutes nearly 70% of the mixture present at room temperature. This arrangement of sulfur atoms requires that at least one sulfur atom be endodentate in the most stable twelve-membered ring conformation, as in conformers 1 and 2. The most stable polar conformer is very much less stable than the global minimum, 32.2 and 20.2 kJ/mol at dielectric constants of 1.5 and 30, respectively. Thus, it is predicted that **33** would only form relatively unstable complexes. Synthetic and complexation studies for compound **33** have not yet appeared in the literature.

Table 4.27 MM3(94) Results for 1,4,7-Trithiacyclododecane (**32**) and 1,4,8-Trithiacyclododecane (**33**)

Compound	Order[a]	Symmetry	Dipole Moment (D) (dielc 1.5)	Strain Energy[b] (kJ/mol)	Mole Fraction (25 °C)	Order[a] (die 30.)	Dipole Moment (D) (dielc 30.)	Strain Energy[b] (kJ/mol)	Mole Fraction (25 °C)
	1	C_2	1.43	0	0.83	1	1.43	0	0.82
	2	C_1	1.34	7.15	0.058	3	1.35	7.3	0.054
	3	C_1	3.41	10.21	0.011	4	3.42	11.21	0.026
32	4	C_1	4.48	10.47	0.008	2	4.5	6.31	0.043
	5	C_1	2.64	11.827	0.011	6	2.63	12.91	0.007
	6	C_1	2.15	11.96	0.014	5	2.15	12.89	0.009
	17	C_1	4.43	17.22	0.001	7	4.44	13.31	0.007
	1	C_1	2.47	0	0.7	1	2.46	0	0.67
	2	C_1	1.5	2.76	0.088	2	1.51	2.81	0.082
	3	C_1	2.61	6.32	0.042	4	2.61	6.41	0.039
33	4	C_1	3.23	6.45	0.056	3	3.21	4.54	0.115
	5	C_1	2.12	9.4	0.016	5	2.11	10.15	0.011
	6	C_1	1.75	9.79	0.0078	6	1.75	10.95	0.005
	155	C_1	4.49	32.15	$6x10^{-6}$	53	4.53	20.21	0

[a] The numbers are the order of the conformations based on their strain energies at that dielectric constant.[b] With respect to the strain energy of the lowest energy conformation of this compound at this dielectric constant.

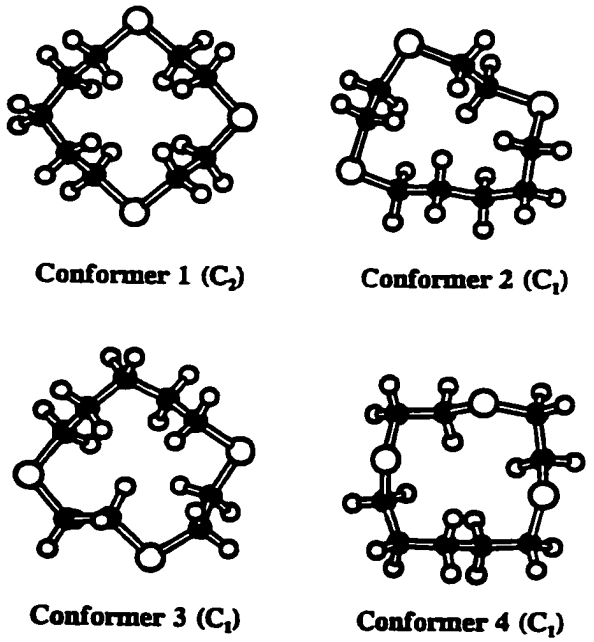

Figure 4.31 The four most stable conformers of 1,4,7-trithiacyclododecane (**32**).

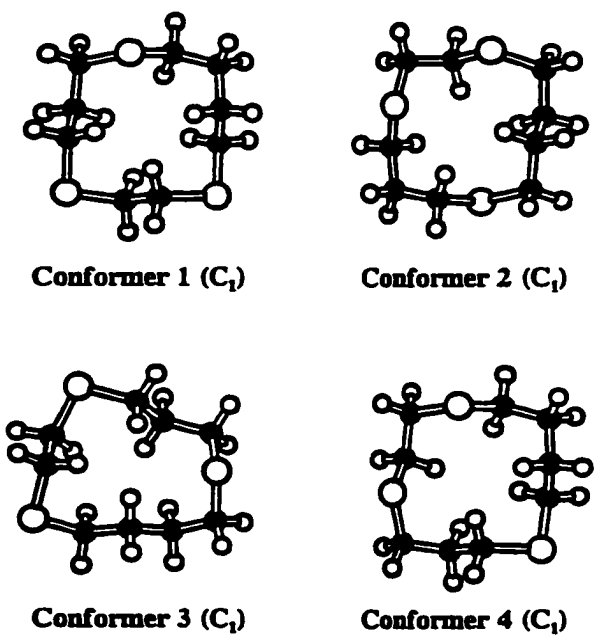

Figure 4.32 The four most stable conformers of 1,4,8-trithiacyclododecane (**33**).

4.2.10 Discussion of Crown Thioether Conformation

The results of these calculations can be compared to the predictions of the qualitative rules described by Cooper *et al.*[248] As described earlier, the energetic size of these preferences are relatively small; therefore, where other factors come into play, conformers not displaying the exodentate "bracket" configuration will be important. Thus, for the smaller ring sizes, ring strain makes it difficult to attain *anti* torsional angles about the S-C-C-S torsions. For **23**, the first conformer with a bracket arrangement is the third conformer, the D_3 conformer. For **24**, the first conformer following these rules is the fourth conformer. Only when the ring size becomes larger does this tendency become dominant; the smallest size ring in which the most stable conformer contains a bracket is the eleven-membered ring, and this feature is present in the global minimum for both isomers at this ring size. The rules work very well for the twelve-membered rings but the relatively small sizes of these preferences become more and more evident as the ring sizes get bigger.

The generalizations of Cooper *et al.*[248] were originally used to predict the conformations of uncomplexed crown thioethers which consisted of S-C-C-S units. They could be extended to include crown thioethers with propano bridges by simply adding that S-C-C-C units prefer to be *anti* whenever possible. This addition allows one to analyse compounds like 1,5,9-trithiacyclododecane (**25**). The global minimum and the crystal structure are the same and they both obey these rules by having as many *gauche* C-S-C-C torsional angles as possible while maximizing the number of *anti* S-C-C-C angles.

All of the ligands containing 4 or 5 sulfurs fit the general pattern outlined by Cooper in both the calculated global minimum and the crystal structure. The only major exception

to this is the single *gauche* S-C-C-S angle in 1,4,7,10,13-pentathiacyclopentadecane (**28**). It should also be noted that although both the calculated global minima and the crystal structures followed the trends above the actual structures often were different.

What is also of interest is that for many cases where the solid state structure of the free ligand is known from X-ray studies, it is not the global minimum energy conformer.[248,328] In fact, it appears that there is only a small range of ring-sizes where the crystal structure matches the calculated global minimum. The smaller rings, as stated above, are more strained and the rules will not apply. The larger rings, such as the 15- and 16-membered rings are interesting cases in that the calculated global minima for both of these molecules had very low dipole moments while the conformer present in the crystal structure for 1,5,9,13-tetrathiacyclohexadecane (**29**) is calculated to have a dipole moment of 3.0 D. It is possible that as ring flexibilty increases then the free ligand will prefer to adopt a conformation in the solid that is somewhat more strained than the global minimum but has a significant dipole moment which aids in aligning molecules during crystallization.

Comparison of the MM3 results with conformations found in complexes of the ligands shows that the complexed ligand normally adopts a conformation which is different from that of the lowest energy conformer[244,245,260,262] and in most cases, different from that of the free ligand as well.[261,262] The conformation of the complexed ligand is controlled by the steric and electronic requirements of the metal's coordination sphere.[262,325]

Furthermore, when thiamacrocycles bind as monodentate ligands, where their conformations are not controlled by geometric requirements of a metal's coordination sphere, the conformation adopted is often the same as in crystalline samples of uncomplexed

macrocycle. This is the case for $Cu(\mathbf{25})_2Cl_2$,[253] $Os_4(CO)_{13}(\mathbf{25})$,[315] and $(CH_3)_3Al(\mathbf{26})$,[320] for example, and it is even true for the mixed S,O heterocycle, 1,4,7,10-tetraoxa-13,16-dithiacyclooctadecane (18S2O4) which acts as a bidentate S-coordinated ligand in $[Hg(18S2O4)Cl_2]{\cdot}HgCl_2$.[252] It is also the case when a ring bridges two metal atoms and acts as a monodentate ligand to each as in $(NbCl_5)_2(\mathbf{27})$.[324] A notable exception occurs in $[Cu(\mathbf{23})_2](PF_6)$ where one ring is monodentate and adopts a different conformation.[225] This is probably due, however, to the small size of **23** and to the suitability of the binding site (see Section 4.2.2.4a) on a particular conformation, since it is known to adopt several different conformations in its various complexes.[229,261]

From these observations it may be concluded that conformations of macrocyclic ligands are determined by an interplay of steric demands by the metal to which the ligand is binding, intramolecular non-bonding interactions within the macrocycle and intermolecular forces that become particularly important in the solid state. Since there is considerable evidence of the influence from conformation on chemical and physical properties of both the ligand itself and its complexes, it is of interest to be able to predict ligand conformations.

The rules that have been proposed by Cooper *et al.* are satisfactory for predicting the conformation of free ligands within a certain range of ring sizes but not all molecules involving thioether sulfurs.[248] They do *not* allow prediction of the conformation of the complexed ligand, but this was never their purpose. Setzer, Glass and others have given examples of experimentally confirmed conformation predictions based on molecular modelling calculations for systems described by the Cooper rules as well as for others.[221-223,245,264] As will be explained in the following section the difference in the conformational energy of the free

ligand versus that of the complexed ligand can play a role in determining the stability of a complex.

Molecular mechanics is a much better method for evaluating conformational possibilities for a free ligand, especially in solution. As was shown for compound **23**, the crystal structure will often differ greatly from the solution. Since it is in solution where the greatest interest occurs concerning conformation and conformational change, and since macrocyclic thioethers seem to be relatively poorly solvated in general,[297] predictions of their conformations in solution that are based on calculations neglecting solvation effects may be fairly reliable unlike those for more heavily solvated analogs involving nitrogen or oxygen heteroatoms.

4.2.10.1 Preorganization

For a ligand to be preorganized for complexation as defined by Cram *et al.*[256] it must: a) be organized for binding *prior* to complexation, that is, the conformation of the ligand resembles the conformation of the complexed ligand; and b) the ligand is organized for low solvation, that is the amount of desolvation of the binding sites on the ligand is minimized. If these criteria are met then the complexes formed from such a ligand should be more stable than ones that do not.[256] In the case of the crown thioethers, the second criterion is unnecessary due to the fact that they are poorly solvated.[297] The first criterion can be easily determined by the sort of molecular mechanics calculations performed here. There are other factors involved, which may also play a role in determining the stability of a complex so although the rules of preorganization are experimentally valid they do not necessarily give the

whole picture. The complexity of the situation can be explained with a simple series of reactions.

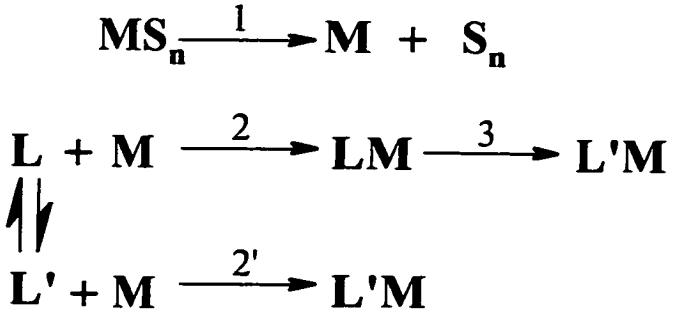

Figure 4.33 Figure illustrating the reactions involved in the formation of a metal complex from a ligand and a solvated metal species. M=metal species, S=solvent, L=ligand not organized for ideal binding, and L'=ligand organized for maximum binding.

A simplified illustration of the steps involved in formation of a ligand metal complex is found in Figure 4.33. The first step involves the desolvation of the metal. This step is enthalpically disfavoured and entropically favoured. The next step depends on the species involved, but involves the conformational equilibrium of the ligand. In some cases, where an organized conformation is part of an equilibrium, the metal will bind directly to the ligand as in step 2'.[219]

In most cases, step 2 takes place and the ligand forms a "non-ideal" complex (LM). This is then followed by a step where the metal acts as a template by which the ligand rearranges to its "ideal" binding conformation.[219] The thermodynamics of step 2 involve a negative entropy term and a variable but favourable enthalpy term. Step 3 is the step where preorganization effects are most important in crown thioethers complex formation. The thermodynamics of step three for most crown thioethers is very enthalpically disfavoured and

the goal is to pay the enthalpic cost of going from L to L' during synthesis rather than during formation of the complex.

The factors that affect complexation of the tetra- and pentathioethers have been well documented by a Rorabacher, Ochrymowycz and coworkers.[297,332] None of the ligands could be said to be preorganized, but the results of their work sheds much light on the factors at play in crown thioether complex formation. They explored the effects different sized rings had, on the kinetics of formation and the stability of Cu(II) complexes.

The results of their thermodynamic analysis of complex formation are summarized in Table 4.28.[297] It was found that as ring size increased for the tetrathioethers, the entropy change on complexation (entropy of complexation) decreased (the entropy for **27** and **29** were approximately equal). The entropy for **28** was anomalously high. The main factors determining entropy in complexation are the loss of solvation around the metal and the ligand and the change in disorder as the ligand alters its conformation. The loss of solvation changes with the complex. Cu(II) is present as $Cu(II)(H_2O)_6^{2+}$ initially and the number of water molecules removed depends on the number of sulfurs binding to the copper ion (see Equation 17).

$$Cu(H_2O)_6^{2+} + L \rightleftharpoons CuL(H_2O)_{6-n}^{2+} + nH_2O \qquad (17)$$

For 1,4,7,10-tetrathiacyclododecane (**26**), the crystal structure of the complex has square pyramidal Cu with one apical water molecule, thus n=5.[330] For compounds **27** and **29**, the Cu(II) atom is square planar with two apical water molecules and thus n=4.[330] For

1,4,7,10,13-pentathiacyclopentadecane (**28**), the Cu(II) atom is square pyramidal with no water molecules, and thus n=6.

Table 4.28 Thermodynamic Data for Crown Thioether-Cu(II) Complexes

Ligand	ΔG^{oa} (kJ/mol)	ΔH^{oa} (kJ/mol)	ΔS^{a} (J/mol/K)	Cu-S[b] (Å)	ΔH_{conf}[c] (kJ/mol)
26	-19.4	0.46±0.21	66.5±0.8	2.30-2.37	19.4
27	-24.8	-17.7±0.9	23±3	2.30	>10.6
28	-23.9	-12.6±0.3	38±1	2.31, 2.40	>16.4
29	-12.6	-5.99±0.38	22±1	2.33, 2.39	>9.2

[a] Thermodynamic values from reference 297. [b] Cu-S bond lengths from reference 297 [c] Difference in energy between the global minimum and lowest energy conformer with highest dipole.

The trend noted above fits the results of the calculations when the thermodynamics of metal desolvation are taken into account. It is important to note that the entropy changes above are for the entire complexation pathway so it includes the entropy gained by desolvation of the metal. If one assumes that the initial binding between the ligand and the metal takes place via the global minimum, compound **26** alters its conformation (according to the calculations) from a D_4 conformer to a C_4 conformer; since essentially only the D_4 conformer is populated, the conformational entropy change will largely reflect the entropies of the conformers and should be small and favourable. Thus the relatively large entropy of complexation (66.5 J/mol/K) compared to those of the larger thioethers (22.2-23.4 J/mol/K), reflects the small positive conformational entropy plus the large entropy for the loss of 5 H_2O molecules on complex formation. The entropies of conformational conversion for the larger

rings are large and unfavourable because they are going from a fairly heterogeneous mixture of asymmetric conformers to a single, relatively symmetric, conformation in the complex.

The entropy of complexation for compound **28** is 37.7 J/mol/K; this would appear to be quite high considering the heterogeneous conformational mixture calculated. This value is however, due to an increased entropy of desolvation as all five of the sulfurs are bonded to the metal.[297]

The enthalpies of complexation can also be interpreted in terms of the results of the calculations. While the enthalpies of complexation for most of the compounds are negative, that for **26** is small and positive. The magnitudes of the negative enthalpies are readily explained on the basis of cavity size ($|\Delta H^{\circ}|$ increases as Cu-S bond length decrease), but another factor may affect the result for **26**. Here, the difference in enthalpy between the populated D_4 conformer of the free ligand and the complexing conformer is large, at least 19 kJ/mol. The enthalpy of conformational change for **28** is also quite high, but it also has an additional Cu-S bond will help offset the conformational penalty.[325]

Preorganization has played an important role in the chemistry of compound **23**. The versatility and robustness of complexes with **23** as a ligand have led many workers to conclude that because the crystal structure is organized for binding, then in solution it is preorganized.[257,300,333,334] Previous work has attempted to show otherwise.[17] This study has conclusively demonstrated that the conformer of 1,4,7-trithiacyclononane (**23**) that is preorganized for complexation is not populated to a sufficient level to influence observed properties of **23**, even in polar solvents.

The question then arises: if compound **23** is not preorganized then how can one explain its properties? The difference between **23** and some of the other crown thioether ligands is that this polar conformer of **23** is present at a level just one order of magnitude below that required for observation, particularly in polar environments. For other trithiacycloalkane ligands that have been examined for binding properties, **24** and **25**, binding conformers are much less stable compared to the global minimum. This difference in stability is reflected in the complexation equilibrium constants.

In view of the calculated low population of conformer 6 in solution, it is of interest as to how tridentate complexes of **23** form so easily. One facile pathway would involve initial complex formation to conformer 2, which has two sulfur atoms suitably aligned for bidentate complexation. Then, motion of part of **23** to proceed over saddlepoint S5 (barrier 29 kJ/mol from conformer 2) to conformer 10, then over S9 (barrier 25 kJ/mol from conformer 10) leads to conformer 6 where a tridentate complex can form (see Figure 4 and Table 4.10). In addition, for **23** the two most populated conformers have two of the three sulfur atoms preorganized for complexation and reorganization to present the third sulfur atom is probably facile, particularly from the second most populated conformer. So although the concept of preorganization has proven useful in field of crown thioether ligands,[258,335,336] it does not explain the results of complexation involving compound **23**.

4.2.11 Differential Scanning Calorimetry of Crown Thioethers

Recently, Park and Shurvell published work on the temperature dependence of the infrared and Raman spectra of 1,4,7-trithiacyclononane (**23**).[266] They had previously examined the infrared and Raman spectra of **23** in the liquid phase and in the solid phase at room

temperature and above.[265] The crystal structure of **23** had been previously determined to be a conformation with a C_3 axis of symmetry.[300] They interpreted their results as a conformational change from the C_3 conformer in the solid to a D_3 conformer in the liquid phase. As shown above, (Section 4.2.2) this conclusion is not valid.

The work on compound **23** in the solid phase showed small anomalies in frequency versus temperature plots.[266] These anomalies and splittings in the infrared and Raman bands, as the temperature was lowered, were interpreted as indicating a phase transition near 225 K. These workers further concluded that this phase change in the solid as the temperature was lowered was due to a conformational change from the C_3 to a C_2 or C_{2v} symmetric conformation.[266] The changes observed were not very marked[266] so an examination of compound **23** and other crown thioethers was performed using differential scanning calorimetry (DSC) to determine whether the above interpretation was correct and also to obtain thermodynamic information to aid the conformational analysis of these compounds.

Differential scanning calorimetry is a method of thermal analysis that allows one to measure the enthalpy of a phase transition. These transitions include changes in crystal phases and heats of fusion. Because these transitions occur under equilibrium conditions, the following equation applies:

$$\Delta G_{trans} = \Delta H_{trans} - T\Delta S_{trans} = 0 \qquad (18)$$

This can then be rearranged to find the entropy of the transition:

$$\Delta S_{trans} = \frac{\Delta H_{trans}}{T} \qquad (19)$$

4.2.11.1 Results of the DSC Analysis

The results of the DSC experiments are shown in Table 4.29. All of the compounds were run at least twice and the values averaged. The scanning was done from 173 K to 10 K above the melting point of the compound. The runs were calibrated using an indium standard.

A particularly interesting feature of these results was the absence of a phase change at 225 K, claimed by Park and Shurvell.[266] In none of the runs for compound **23** was there any sign of a phase transition below the melting point. In fact, none of the crown thioethers showed a phase transition below room temperature. A detailed analysis of the phase transitions was not done. It is possible that the small transition for compound **27** may be the result of a transition from one crystal form to another due the fact that **27** exists in two slightly different crystal forms.[246] The transitions for **25** and **28** are not as easily explained however.

The entropy of fusion for a molecule comes from four sources: translational disorder, rotational disorder, conformational disorder, and entropy due to volume change.[337] Not all mechanisms are present in every system. The ΔS values for all of the compounds examined here are above normal for organic molecular crystals (50-60 J/mol/K).[337] However, only compounds **26** and **29** have values that can be considered extraordinarily large. The entropy of fusion for these molecules is approximately 120 J/mol/K. This is identical to the entropy of fusion for compounds such as *n*-decane, which has a value of 118.5 J/mol/K.[337]

Table 4.29 DSC Results for Crown Thioethers

Compound	T_{trans} [a] (K)	ΔH_{trans} [a] (kJ/mol)	ΔS_{trans} [a] (J/mol/K)	T_{melt} [b] (K)	ΔH_{melt} [b] (kJ/mol)	ΔS_{melt} [b] (J/mol/K)	ΔH_{tot} [c] (kJ/mol)	ΔS_{tot} [c] (J/mol/K)
23	--	--	--	354.6	29±3	81±8	29±3	81±8
25	348.0	11±1	31±3	373.1	16±2	44±4	27±3	75±7
26	--	--	--	499.8	60±6	121±12	60±6	121±12
27	343.7	2.7±0.4	8±1	392.7	33±3	83±8	36±4	91±9
28[d]	317.4	11±1	34±3	390.8	19±2	48±5	35±4	96±10
	339.3	4.7±0.5	14±2					
29	--	--	--	326.1	39±4	120±12	39±4	120±12

[a] Values refer to phase transitions before the melting point of the compound. [b] Values refer to melting transition of the compound. [c] Total of enthalpies and entropies for melting and all transitions. [d] Compound **28** had two pre-melting point transitions.

In the *n*-alkanes, this is interpreted as due to the large increase in the degrees of freedom of the molecule on going to the liquid phase. In other words, the increase comes from rotational and conformational disorder.[337] Can a similar argument be used here to explain the high values for the crown thioethers especially compounds **26** and **29**?

In fact, for all the compounds except **26**, conformational disorder can explain high the entropies of fusion. The entropies for the compounds are in the order **29** > **28** ≈ **27** > **23** > **25**. This order is similar to what one would expect qualitatively from the MM3 calculations, which show that compounds **29**, **28**, and **27** go from the conformationally homogeneous crystal state, to what are calculated to be complex conformational mixtures, a process that would have large entropies of mixing. The calculations for compound **23** show a less complex mixture (and therefore smaller entropy) and the calculations show that compound **25** is conformationally similar in the solid and liquid phases, thus accounting for its low entropy of fusion.

The entropy of fusion for compound **26** is much harder to explain in these terms. As described earlier (see Section 4.2.5), compound **26** adopts the same single conformer in the solid and in the liquid. Thus, **26** should have the smallest entropy of fusion or at least have a value close to the value for **25**. It is possible that the dominant factor in the entropy of fusion for compound **26** is the rotational term.

The entropy of fusion for rigid planar molecules is generally higher than expected and this is considered to be due to the tighter packing of these molecules that restricts rotation and is relieved upon melting.[338] Compound **26** can be described as a rigid planar molecule because the D_4 conformation is planar and very stable in the liquid phase. It is quite possible

that in the solid state **26** is very tightly packed in a very stable crystal lattice. This stability manifests itself in the high enthalpy of fusion, the high melting point and relative insolubility of **26** in a wide range of solvents. Thus, it is quite possible that the high entropy of fusion for compound **26** is due to the increased rotational entropy of the liquid phase.

4.3 Conclusions

It was demonstrated conclusively that 1,4,7-trithiacyclononane (**23**) exists in solution as a conformational mixture that probably consists of the C_1 and C_2 conformers but contains the solid-state conformation at a level somewhat below what is observable. Its more facile complexation than other crown thioethers is ascribed either to the relatively higher population of its complexing conformer or possibly to rapid interconversion of a partially complexed and more highly populated conformer to the conformer that can achieve tridentate complexation. The unusual conformers adopted by monodentate ligands arise because these conformers have more stable isoclinal-like sites for complexation.

1,5,9-Trithiacyclododecane exists predominantly in solution in the same conformation as in the solid. Its complexes are unstable because assumption of the complexing conformation adds a large enthalpic penalty to the complex. 1,4,7-Trithiacyclodecane is present as a mixture of conformations and complexing conformations are relatively unstable. 1,4,7,10-Tetrathiocyclododecane is calculated and shown to be primarily in a D_4 conformation in solution. 1,4,8,11-Tetrathiocyclotetradecane, 1,4,7,10,13-pentathiocyclopentadecane and 1,5,9,13-tetrathiocyclohexadecane have been calculated as heterogeneous mixtures in solution and the experimental results bear this out. Of the other compounds studied by MM3 calculations, 1,4,8-trithiacycloundecane and 1,4,7-trithiacyclododecane are predicted to be excellent complexing agents.

The DSC results have shown unequivocally that, contrary to literature conclusions,[266] 1,4,7-trithiacyclononane does not have a low temperature solid phase transition. The MM3 conformational analysis of the crown thioethers is consistent with the values for the entropies

of fusion of the crown thioethers. The anomalously large entropy of fusion for 1,4,7-tetrathiacyclododecane (**26**) can also be adequately explained in terms of the results of the conformational analysis.

4.4 Experimental

4.4.1 Materials

1,4,7-Trithiacyclononane (**23**), 1,4,7-trithiacyclodecane (**24**), 1,4,7,10-tetrathiacyclododecane (**26**), 1,4,8,11-tetrathiacyclotetradecane (**27**), 1,4,7,10,13-pentathiacyclopentadecane (**28**), and 1,5,9,13-tetrathiacyclohexadecane (**29**) were purchased from Aldrich. 1,5,9-trithiacyclododecane (**25**) was generously supplied by Professor R. D. Adams of the University of South Carolina.

4.4.2 Spectroscopy

NMR spectra were measured on Bruker AC-250, or AMX-400 spectrometers. AA'BB', AA'BB'X and AA'A"A"'XX' patterns were analysed by hand initially then iteratively simulated using the program LAME8.[104] CP/MAS ^{13}C NMR spectra were recorded on the Bruker AMX-400 spectrometer using 4 mm rotors spun at 6 kHz and were referenced to the secondary carbon peak of adamantane as 29.50 ppm. Infrared spectra were recorded on a Nicolet 510P FTIR spectrometer using KBr pellets for solids or NaCl solution cells with lead spacers for solutions.

4.4.3 Differential Scanning Calorimetry

Differential scanning calorimetry experiments were performed on a DuPont Instruments DSC 2910 system at atmospheric pressure on samples made up in aluminum pans. An indium standard was used for temperature calibration and an empty aluminium pan was employed as a reference. Scans were recorded from 173 K to 10 K above the melting point of the compound at a rate of 10 K/min unless otherwise stated. A DuPont Instruments

DSC Standard Data Analysis program was used for data analysis, including calculations of peak areas.

4.4.4 Molecular Mechanics Calculations

Evaluation of the conformational energy surface for the crown thioethers was performed using the stochastic search routine of Saunders[29,273] incorporated in MM3(94),[42,66] but slightly modified locally.[339] Changes were made to reduce the volume of output when stochastic searches were being run, to increase the number of conformations that could be stored during a stochastic search (NSTO) from 200 to 5000, and to allow an option that made the starting conformation the initial point for every random push in a stochastic search run.

Stochastic search runs, aimed at determining all conformations present, employed from 1000 to 20000 random pushes and maximum jump sizes between 1.5 and 2.2 Å. Minimization was normally performed using block-diagonal Newton-Raphson minimization followed by full-matrix Newton-Raphson minimization. Some of the conformations generated in this process were not minima or saddlepoints. A program for automatic detection of these false conformers and of saddlepoints, and for performing Boltzmann distribution calculations was used.[339] The program (BOLTZ) takes the output coordinates and energies from the stochastic search runs, then performs another block-diagonal followed by full-matrix Newton-Raphson minimization sequence. Conformations that have changed in strain energy or have negative infrared frequencies are not included in the subsequent Boltzmann calculation. For the Boltzmann calculation, strain energies and the entropies obtained by MM3(94) by statistical mechanical methods are calculated relative to those of the global minimum and are used to obtain free energy differences and equilibrium constants at selected temperatures.

These are then converted into mole fractions. In some cases, minimization was performed only by full-matrix Newton-Raphson minimization in order to locate saddlepoints, identified by the presence of one imaginary infrared frequency. Stochastic search runs aimed at determining which conformations were obtained from particular saddlepoints used 100 to 500 pushes and push sizes from 0.5 to 0.7 Å. AM1 calculations were done with HYPERCHEM, release 4.0. Three-dimensional representations were drawn using the ATOMS program using atomic coordinates generated by MM3(94).

Chapter 5
General Conclusions

The preceding chapters have presented the results of conformational analyses of compounds containing oxygen and sulfur. Molecular mechanics calculations were a theme running throughout the thesis. Much of the experimental work presented was performed in order to confirm the results of molecular mechanics calculations and in many cases, the most interesting experimental work was performed in response to calculations that were less than satisfactory.

Molecular mechanics provides a computational model that summarizes what is known about molecular structure. The model used is often somewhat imperfect due to the assumptions and simplifications used, such as the use of classical equations and empirical parameterization. When calculations are performed and the results are compared to experimental data or hypothetical expectations there are two possible outcomes: the calculated results will match the expected results within experimental uncertainty or they will not.

If they match, then one can explain the experimental results in terms of what is currently known about the structure and conformational energies as delineated in the molecular mechanics model. When the results of the calculations do not match the experimental or hypothetical data then other questions must be asked and more research must be done. The primary question is: are the unsatisfactory results caused by deficiencies in the

force field or are the experimental results inaccurate or wrong? In either case, more research must be performed to expand the current state of knowledge of the system being studied. Thus, molecular mechanics calculations, even when they give incorrect answers, allow one to test hypotheses and clarify our understanding of structure and conformational energy.

The work presented in Chapter 2 is an excellent example of this process. The reparameterization of the O-C-C-O torsional term in MM3(94) was undertaken due to the inability of the force field to simulate experimental results. The new parameters (developed from new experimental data and literature data) gave excellent results for ethers, which matched experimental data much better than those obtained using the standard MM3(94) parameters (see Sections 2.2.2 and 2.2.3). However, the new parameters were less successful when used to simulate systems containing intramolecular hydrogen bonds. This was most likely due to problems with the hydrogen bonding term in MM3(94), which needs to be reevaluated in a future cycle of improvements.

As stated above, when the calculations fail to reproduce the expected results then one must determine the source of this error. During the testing of the new O-C-C-O parameters, it was discovered that the experimental data for 1,2-dimethoxypropane were inconsistent with the calculated results (see Section 2.2.3.3). It was concluded that the current experimental data and analysis were inaccurate and that a new examination of this system was necessary (see Section 2.2.3.3). The new experimental spectra were better defined than the previous ones, which allowed precise analysis that yielded results in excellent agreement with the calculations.

Similarly, the inability of the new parameters to successfully reproduce experimental results for the C5-C6 rotation in α-D-glucopyranose derivatives led to the work in Chapter 3. The inconsistencies were initially believed to be due to weaknesses in the force field with respect to intramolecular hydrogen bonding and solvent effects. The literature data involving intramolecular hydrogen bonding and solvent effects were inconclusive, so the cause of the poor computational results could not be determined with confidence. Thus, an experimental examination of solvent effects in α-D-glucopyranose derivatives was performed.

The work presented in Chapter 3 demonstrates that solvent effects due to solvent polarity are insignificant except when intramolecular hydrogen bonding occurs (see Section 3.2.3). This indicated that the hydrogen bonding term in the force field was the weakness that caused the differences between experiment and calculation. The experimental work also showed a solvent effect on the chemical shift of the H6S proton. Previously, the changes in chemical shift were believed to be due to magnetic anisotropy, but here it was shown to be a solvent effect (see Section 3.2.1.4). It is important to note that the experiments in Chapter 3 that led to this discovery were performed because the MM3(94) calculations gave imperfect results and the literature data were not accurate enough to identify the source of the error in the calculations.

The work in Chapter 4 was performed in order to understand the conformational preferences of crown thioethers in solution, and how these preferences affect their ability to complex. For most of the compounds examined, the calculations and spectra in Chapter 4 and in the literature were in agreement in that they were consistent with complex conformational mixtures in solution. In two cases, 1,5,9-trithiacyclododecane (**25**) and

1,4,7,10-tetrathiacyclododecane (**26**), the molecular mechanics calculations successfully predicted conformational homogeneity in solution (see Sections 4.2.4.1 and 4.2.5.1). The most interesting case, however, was for 1,4,7-trithiacyclononane (**23**).

Most of the previous calculations and experimental results indicated that an endodentate C_3 conformer dominated conformational mixtures of **23** in solution. Other work suggested that C_1, C_2 or D_3 conformers were important. If the results of calculations had supported the presence of the C_3 conformer, then it is quite likely that much of the experimental work would have been less detailed. However, more experimental analysis of the conformation of **23** was performed and the literature results were reinterpreted. The results of the experiments showed that, in agreement with the MM3(94) calculations, the C_3 conformer was not a significant contributor to the conformational mixture in solution (see Section 4.2.2.1). The differential scanning calorimetry in Chapter 4 was performed to confirm the results of the calculations and to disprove claims in the literature. Although most of the data were consistent with calculated results, the most interesting piece of data was the large entropy of melting for compound **26**, which was attributed to a lack of internal rotation in the crystal (see Section 4.2.11.1).

This thesis spans a wide range of topics and experimental techniques. The unifying principle behind the work is the use of molecular mechanics as a tool for conformational analysis. Molecular mechanics calculations have been shown to be very important in interpreting experimental results and as a catalyst for further experiments that expand our knowledge. This capability of molecular mechanics presents itself when the calculations are both successful and unsuccessful, as shown in this thesis.

Appendix

Table A.1 ^{1}H NMR Results[a,b] (Chemical Shift) for Methyl 2,3,4,6-Tetra-*O*-[$^{2}H_3$]methyl-α-D-glucopyranoside (**16a**)

Solvent (dielectric constant)	Chemical Shift[d] (ppm)						
	H1	H2	H3	H4	H5	H6R	H6S
cyclohexane-d_{12} (2.0)[c]	4.58	2.99	3.38	3.02	3.45	3.52	3.38
toluene-d_8 (2.4)[c]	4.60	3.09	3.69	3.25	3.71	3.55	3.47
carbon disulfide (2.6)	4.54	2.93	3.24	2.89	3.34	3.43	3.34
chloroform-*d* (4.8)	4.82	3.21	3.49	3.18	3.59	3.59	3.57
tetrahydrofuran-d_8 (7.6)	4.69	3.05	3.34	3.01	3.47	3.51	3.45
dichloromethane-d_2 (8.9)	4.75	3.13	3.38	3.07	3.52	3.53	3.51
acetone-d_6 (20.7)	4.75	3.06	3.33	3.01	3.48	3.51	3.49
methanol-d_4 (32.7)	4.80	3.15	3.37	3.09	3.52	3.57	3.54
acetonitrile-d_3 (37.5)	4.75	3.09	3.29	3.01	3.48	3.49	3.48
water-d_2 (78)[c]	4.82	3.18	3.33	3.10	3.53	3.51	3.53

[a] Determined by manual analysis of the spectra followed by iterative simulation with LAME8.[104] [b] All spectra recorded at 600 MHz except where noted. [c] Recorded at 400 MHz. [d] Anomeric CH_3 signals at 3.3 ± 0.1 ppm.

Table A.2 ^{1}H NMR Results[a,b] (Coupling Constants) for Methyl 2,3,4,6-Tetra-*O*-[$^2H_3$]methyl-α-D-glucopyranoside (**16a**)

Solvent (dielectric constant)	Coupling Constant (Hz)						
	$^3J_{1,2}$	$^3J_{2,3}$	$^3J_{3,4}$	$^3J_{4,5}$	$^3J_{5,6R}$	$^3J_{5,6S}$	$^2J_{6R,6S}$
cyclohexane-d_{12} (2.0)[c]	3.58	9.38	9.09	10.06	4.49	1.64	-10.61
toluene-d_8 (2.4)[c]	3.54	9.44	9.35	9.70	4.79	1.48	-10.43
carbon disulfide (2.6)	3.62	9.30	9.00	10.14	4.90	1.70	-10.64
chloroform-*d* (4.8)	3.71	9.46	9.28	9.74	4.02	2.42	-10.52
tetrahydrofuran-d_8 (7.6)[d]	3.58	9.38	9.01	10.09	4.94	1.82	-10.76
dichloromethane-d_2 (8.9)	3.59	9.46	9.14	10.12	4.52	2.21	-10.70
acetone-d_6 (20.7)	3.70	9.24	9.08	9.62	4.80	2.08	-10.71
methanol-d_4 (32.7)[d]	3.64	9.76	9.18	10.05	4.66	1.96	-10.81
acetonitrile-d_3 (37.5)	3.59	9.48	9.08	9.56	4.75	2.48	-10.73
water-d_2 (78)[c]	3.69	9.64	9.46	9.53	4.64	2.43	-11.28

[a] Determined by manual analysis of the spectra followed by iterative simulation with LAME8.[104] [b] All spectra recorded at 600 MHz except where noted. [c]Recorded at 400 MHz. [d] The THF and MeOH spectra included another coupling constant determined to be $^4J_{3,5}$ with a value of 0.34 and 0.32 Hz respectively.

Table A.3 ^{1}H NMR Results[a,b] (Chemical Shift) for Methyl 2,3,4,6-Tetra-*O*-[$^{2}H_3$]methyl-α-D-[4-^{13}C]glucopyranoside (**16b**)

Solvent (dielectric constant)	Chemical Shift[c] (ppm)						
	H1	H2	H3	H4	H5	H6R	H6S
cyclohexane-d_{12} (2.0)	4.58	2.99	3.38	3.02	3.45	3.52	3.38
toluene-d_8 (2.4)	4.61	3.10	3.70	3.25	3.71	3.56	3.48
methanol-d_4 (32.7)	4.80	3.15	3.37	3.09	3.52	3.57	3.54

[a] Determined by manual analysis of the spectra followed by iterative simulation with LAME8.[104] [b] All spectra recorded at 400 MHz. [c] Anomeric CH_3 signals at 3.3 ± 0.1.

Table A.4 ^{1}H NMR Results[a,b] (Coupling Constants) for Methyl 2,3,4,6-Tetra-*O*-[$^{2}H_3$]methyl-α-D-[4-^{13}C] glucopyranoside (**16b**)

Solvent (dielectric constant)	Coupling Constant (Hz)						
	$^{3}J_{1,2}$	$^{3}J_{2,3}$	$^{3}J_{3,4}$	$^{3}J_{4,5}$	$^{3}J_{5,6R}$	$^{3}J_{5,6S}$	$^{2}J_{6R,6S}$
cyclohexane-d_{12} (2.0)	3.49	9.27	9.23	9.65	4.37	1.56	-10.58
toluene-d_8 (2.4)	3.54	9.53	8.91	10.23	4.59	1.72	-10.61
methanol-d_4 (32.7)[c]	3.59	9.52	9.16	9.99	4.62	2.03	-10.88
	$^{3}J_{C4,H2}$	$^{2}J_{C4,H3}$	$^{1}J_{C4,H4}$	$^{2}J_{C4,H5}$	$^{3}J_{C4,H6S}$	$^{3}J_{C4,H6R}$	
cyclohexane-d_{12} (2.0)	0.62	-5.02	142.86	-4.11	3.20	0.01	
toluene-d_8 (2.4)	0.98	-5.02	142.72	-3.79	3.09	0.36	
methanol-d_4 (32.7)	1.01	-5.09	143.62	-4.00	3.16	0.76	

Determined by manual analysis of the spectra followed by iterative simulation with LAME8.[104] [b] All spectra recorded at 400 MHz. [c] The MeOH spectrum contained showed an additional coupling constant. ($^{4}J_{3,5}$=0.20 Hz)

Table A.5 ^{1}H NMR Results[a,b] (Chemical Shifts) for Methyl 2,3,4-Tri-*O*-[$^{2}H_3$]methyl-α-D-glucopyranoside (**18**)

Solvent (dielectric constant)	Chemical Shift[e] (ppm)							
	H1	H2	H3	H4	H5	H6R	H6S	OH
cyclohexane-d_{12} (2.0)[c,d]	4.62	2.99	3.41	3.04	3.41	3.58	3.65	NA
carbon disulfide (2.6)[c,d]	4.92	3.27	3.60	3.26	3.63	3.81	3.91	NA
chloroform-*d* (4.8)	4.81	3.18	3.53	3.16	3.55	3.75	3.84	4.77
acetone-d_6 (20.7)	4.78	3.07	3.35	3.08	3.40	3.62	3.71	5.44
methanol-d_4 (32.7)	4.83	3.17	3.40	3.12	3.44	3.66	3.74	NA
acetonitrile-d_3 (37.5)	4.78	3.10	3.31	3.03	3.39	3.57	3.67	5.51
dimethyl sulfoxide-d_6 (46.7)	4.78	3.06	3.26	3.01	3.28	3.47	3.57	6.29
water-d_2 (78)	4.80	3.15	3.31	3.08	3.40	3.55	3.64	NA

[a] Determined by manual analysis of the spectra followed by iterative simulation with LAME8.[104] [b] All spectra recorded at 500 MHz except where noted. [c] Recorded at 400 MHz. [d] The cyclohexane and CS_2 samples were deuterated at OH6 for ease in analyzing the spectra. [e] Anomeric CH_3 siganals at 3.3 ± 0.1.

Table A.6 ^{1}H NMR Results[a,b] (Coupling Constant) for Methyl 2,3,4-Tri-*O*-[$^{2}H_3$]methyl-α-D-glucopyranoside (**18**)

Solvent (dielectric constant)	Coupling Constant (Hz)								
	$^{3}J_{1,2}$	$^{3}J_{2,3}$	$^{3}J_{3,4}$	$^{3}J_{4,5}$	$^{3}J_{5,6R}$	$^{3}J_{5,6S}$	$^{2}J_{6S,6R}$	$^{3}J_{OH,6R}$	$^{3}J_{OH,6S}$
cyclohexane-d_{12} (2.0)[c,d]	3.43	9.28	9.26	9.60	3.24	2.86	-11.76	NA	NA
carbon disulfide (2.6)[c,d]	3.81	9.43	8.95	9.36	4.00	2.78	-11.62	NA	NA
chloroform-*d* (4.8)	3.61	9.41	9.33	9.66	4.14	3.09	-11.67	7.71	4.76
acetone-d_6 (20.7)	3.54	9.40	9.47	9.94	4.60	2.06	-11.84	7.10	5.44
methanol-d_4 (32.7)	3.60	9.55	9.46	9.79	4.66	2.06	-11.89	NA	NA
acetonitrile-d_3 (37.5)	3.61	9.47	9.28	9.69	4.85	2.16	-11.82	6.72	5.51
dimethyl sulfoxide-d_6 (46.7)	3.50	9.51	9.36	9.48	5.48	1.13	-11.51	5.60	6.29
water-d_2 (78)	3.63	9.72	9.63	9.88	4.84	1.90	-12.35	NA	NA

[a] Determined by manual analysis of the spectra followed by iterative simulation with LAME8.[104] [b] All spectra recorded at 500 MHz except where noted. [c] Recorded at 400 MHz. [d] The cyclohexane and CS_2 samples were deuterated at OH6 for ease in analyzing the spectra.

Table A.7 Observed and Calculated Wavenumbers for the Infrared Spectra of 1,4,7-Trithiacyclononane (**23**)

Observed Solid C_3	C_3 Calculated[a] MM3	C_1 Calculated[a] MM3	C_2 Calculated[a] MM3	D_3 Calculated[a] MM3	Observed Solution (CS_2)
	3003.8(A,m)	2987.1(m)	3010.1(A,m)	2986.7(A_1,0)	2969.2(w)
2966.2(m)	2984.4(E,m)	2950.2(m)	3009.6(B,m)	2984.0(A_2,m)	2948.0(m)
	2984.4(E,m)	2935.2(m)	2936.3(B,m)	2971.7(E,w)	
2924.5(vs)	2925.1(E,m)	2932.4(m)	2935.6(A,m)	2971.7(E,w)	2933.0(m)
	2925.1(E,m)	2929.9(m)	2923.2(B,m)	2969.6(E,w)	
	2925.1(A,s)	2927.8(m)	2923.2(B,m)	2969.6(E,w)	
2896.4(vs)	2896.6(A,m)	2894.8(m)	2887.3(A,m)	2900.8(A_1,0)	2903.6(vs)
	2895.4(E,m)	2889.1(m)	2887.0(B,m)	2899.0(E,m)	
	2895.4(E,m)	2885.5(m)	2884.9(A,m)	2899.0(E,m)	
2804.0(m)	2874.2(A,vw)	2876.3(m)	2872.9(B,m)	2890.6(A_2,m)	2821.4(w)
	2874.0(E,m)	2874.5(m)	2871.4(A,vw)	2889.3(E,w)	2796.1(m)
	2874.0(E,m)	2873.1(m)	2871.4(B,m)	2889.3(E,w)	
1455.6(s)	1546.4(A,w)	1519.5(w)	1552.5(A,vw)	1526.7(E,w)	1413.5(vs)
1420.3(m)	1524.0(E,w)	1516.8(vw)	1552.2(B,w)	1526.7(E,w)	1405(sh)
	1524.0(E,w)	1514.8(w)	1536.4(A,w)	1523.2(A_1,0)	
	1520.4(A,w)	1511.7(w)	1536.0(B,w)	1520.7(A_2,m)	
1408.6(s)	1519.3(E,m)	1508.5(w)	1513.5(A,w)	1508.5(A_1,0)	1302.3(sh)
	1519.3(E,m)	1496.3(w)	1504.8(B,w)	1494.6(E,w)	1288.4(s)
1296.8(m)	1468.5(E,vw)	1466.2(w)	1491.9(A,vw)	1494.6(E,w)	1280.0(s)
	1468.5(E,vw)	1463.7(w)	1491.1(B,vw)	1485.6(E,w)	1271.3(s)
	1467.6(A,vw)	1456.1(vw)	1455.5(A,vw)	1485.6(E,w)	1265.1(s)
	1413.1(A,vw)	1409.0(w)	1440.1(B,m)	1426.9(E,m)	1205.4(m)
1281.6(s)	1411.3(E,m)	1403.0(w)	1440.1(A,w)	1426.9(E,m)	1182.0(m)
	1411.3(E,m)	1399.2(m)	1407.0(B,m)	1420.9(A_2,w)	1148.8(m)
1190.0(w)	1310.7(A,vw)	1305.4(vw)	1323.8(B,vw)	1302.7(E,w)	1132.3(w)
1184.3(m)	1308.7(E,vw)	1299.4(vw)	1323.2(A,vw)	1302.7(E,w)	1117.8(w)
	1308.7(E,vw)	1294.6(vw)	1301.7(A,vw)	1289.8(E,w)	
1135.5(m)	1281.6(E,vw)	1277.1(vw)	1289.6(B,vw)	1289.8(E,w)	
1129.2(m)	1281.6(E,vw)	1269.9(vw)	1287.4(A,vw)	1282.4(A_1,0)	
	1254.5(A,vw)	1263.8(vw)	1270.2(B,vw)	1266.8(A_2,w)	

continued on page 239

Table A.7 (continued) Observed and Calculated Wavenumbers for the Infrared Spectra of 1,4,7-Trithiacyclononane (**23**)

Observed Solid C_3	C_3 Calculated[a] MM3	C_1 Calculated[a] MM3	C_2 Calculated[a] MM3	D_3 Calculated[a] MM3	Observed Solution (CS_2)
986.4(w)	983.5(E,vw)	982.0(vw)	990.8(A,vw)	953.4(E,w)	1015.7(w)
	983.5(E,vw)	970.4(vw)	990.8(B,vw)	953.4(E,w)	997.8(w)
	966.9(A,vw)	963.0(vw)	955.0(A,vw)	948.5(A_1,0)	936.6(m)
922.8(s)	931.4(E,vw)	931.4(vw)	928.4(A,vw)	911.5(A_2,w)	922.2(m)
	931.4(E,vw)	920.4(vw)	917.7(B,w)	902.3(E,w)	907.9(m)
877.7(s)	928.7(A,w)	884.2(w)	897.4(A,vw)	902.3(E,w)	881.1(w)
838.7(m)	849.6(A,w)	866.9(vw)	864.0(B,vw)	841.0(A_1,0)	865.6(m)
823.3(s)	839.3(E,w)	861.1(w)	849.1(B,vw)	803.8(E,w)	856.7(m)
	839.3(E,w)	852.3(w)	848.8(A,w)	803.8(E,w)	843.8(m)
703.2(w)	671.0 (A,w)	657.4(w)	671.1(B,vw)	712.0(E,w)	833.6(s)
670.3(m)	649.9(E,w)	646.6(w)	662.7(A,m)	712.0(E,w)	815.9(m)
	649.9(E,w)	639.2(w)	634.8(B,w)	669.9(A_2,w)	804.6(sh)
	608.4(E,w)	616.8(m)	612.1(B,m)	640.9(A_1,0)	700(w,sh)
	608.4(E,w)	600.2(vw)	587.7(A,0)	638.0(E,m)	695.6(w)
619.3(m)	592.7(A,m)	584.1(w)	564.1(A,vw)	638.0(E,m)	684.8(w)
454.0(w)	398.3(A,vw)	398.9(w)	420.7(A,m)	359.4(A_2,w)	676.4(w)
414.0(m)	377.8(E,m)	387.7(m)	388.8(B,m)	331.1(E,w)	669.5(w)
	377.8(E,m)	379.4(w)	380.2(B,vw)	331.1(E,w)	654.9(w)
	331.9(A,0)	318.6(w)	320.3(B,m)	319.9(A_1,0)	643.4(w)
	284.5(E,vw)	293.8(vw)	298.9(A,vw)	305.6(A_1,0)	628.9(w)
	284.5(E,vw)	273.7(w)	285.4(A,vw)	258.1(E,w)	
	273.2(A,m)	232.9(w)	236.2(A,vw)	258.1(E,w)	
	180.4(E,w)	217.2(vw)	226.3(B,w)	244.7(A_2,m)	
	180.4(E,w)	164.7(vw)	158.1(A,vw)	173.9(E,w)	
	178.8(A,w)	138.4(w)	148.4(B,w)	173.9(E,w)	
	110.0(E,w)	100.6(w)	133.7(A,w)	148.6(E,w)	
	110.0(E,w)	87.7(w)	83.5(B,w)	148.6(E,w)	

[a] Infrared or Raman

Table A.8 Identification of Higher Energy Saddlepoints for 1,4,7-Trithiacyclononane(**23**).[a]

Conf	Dipole Moment[b]	Energy Difference (kJ/mol)[c]	Connected Conformers			
			Conformer[d]	No.of times found[e]	Conformer[f]	No.of times found[e]
S15	1.62	44.28	10	86	3	9
S16[g]	4.09	50.03	11	86	7	11
S17	1.77	50.13	2	49	1	36
S18[g]	4.3	50.2	11	89	6	7
S19	4.21	50.44	6	49	11	40
S20	1.45	53.1	7	53	8	39
S21	2.17	57.76	10	57	8	30
S22	2.99	59.58	7	52	1	30
S23	1.47	60.84	7	52	5	44
S24	3.3	62.5	11	39	1	31

[a] All saddlepoints had one imaginary infrared frequency and C_1 symmetry except where noted. [b] In D. [c] With respect to the global minimum. [d] The most common conformer obtained from this saddlepoint. See Table 4.5 for conformer identity. [e] The number of times this conformer was found out of 100 pushes each starting from the saddlepoint indicated. [f] The second most common conformer obtained from this saddlepoint. See Table 4.5 for conformer identity. [g] Saddlepoint had C_s symmetry.

Table A.9 Observed and Calculated Wavenumbers for the Infrared Spectra of 1,4,7-Trithiacyclodecane (**24**)

C_1 Conformer (1) Calculated[a] MM3	C_2 Conformer (2) Calculated[a] MM3	C_1 Conformer (3) Calculated[a] MM3	Observed Solution (CS_2)
2984.3(m)	2997.3(A,m)	2972.5(m)	
2959.6(m)	2996.8(B,m)	2971.0(m)	2957.5(m)
2948.0(m)	2957.4(A,m)	2940.7(m)	2949.9(m)
2932.2(m)	2957.1(B,m)	2936.8(m)	
2929.9(m)	2925.4(B,m)	2931.6(m)	
2927.8(m)	2925.4(B,m)	2929.3(m)	
2915.4(m)	2914.9(B,m)	2913.1(m)	2918.6(s)
2895.7(m)	2896.4(A,m)	2896.2(m)	2904.4(s)
2894.5(m)	2893.9(B,m)	2895.0(m)	
2890.6(m)	2886.6(A,m)	2886.2(m)	2864.9(w)
2884.4(m)	2886.4(B,m)	2886.0(m)	2837.9(m)
2875.8(m)	2872.4(A,vw)	2877.1(m)	2815.4(w)
2872.1(m)	2872.4(B,m)	2873.3(m)	2808.6(w)
2872.1(m)	2863.3(A,m)	2861.6(m)	2800.3(w)
1520.2(w)	1539.6(A,vw)	1519.9(w)	1455.8(w)
1519.6(w)	1539.5(B,w)	1518.0(w)	1451.8(w)
1517.9(w)	1526.2(A,w)	1511.9(w)	1428.8(s)
1513.6(w)	1525.8(B,vw)	1510.8(w)	1421.7(m)
1511.4(w)	1517.9(A,vw)	1509.9(w)	1407.9(s)
1505.5(w)	1517.2(B,w)	1507.8(w)	1373.5(w)
1480.6(w)	1488.8(A,vw)	1487.5(w)	1357.2(w)
1475.9(w)	1488.3(B,vw)	1476.8(w)	1343.6(w)
1471.1(vw)	1477.5(B,w)	1463.3(vw)	1320.3(w)
1455.0(vw)	1473.4(A,w)	1454.3(vw)	1304.9(w)
1420.2(m)	1439.5(B,m)	1420.9(w)	1285.5(m)
1418.0(w)	1439.4(A,w)	1409.0(w)	1274.4(s)
1403.4(w)	1413.1(A,w)	1402.3(m)	1264.1(s)
1390.7(m)	1396.1(B,m)	1401.6(m)	1253.7(s)
1300.1(vw)	1321.0(B,vw)	1303.6(vw)	1204.6(w)
1298.4(vw)	1319.8(A,vw)	1297.9(vw)	1194.3(w)
1294.1(vw)	1301.1(A,vw)	1287.5(vw)	1184.3(w)
1292.0(vw)	1300.1(B,vw)	1287.1(vw)	1150.1(w)
1282.9(vw)	1275.1(A,vw)	1278.3(vw)	1136.0(m)

continued on page 242

Table A.9 (continued) Observed and Calculated Wavenumbers for the Infrared Spectra of 1,4,7-Trithiacyclodecane (**24**)

C_1 Conformer (1) Calculated[a] MM3	C_2 Conformer (2) Calculated[a] MM3	C_1 Conformer (3) Calculated[a] MM3	Observed Solution (CS_2)
1266.6(vw)	1274.3(B,vw)	1272.6(vw)	1066.2(w)
1251.0(vw)	1252.6(A,vw)	1261.0(vw)	1048.3(w)
1037.1(vw)	1040.2(B,vw)	1044.4(vw)	1015.6(w)
991.6(vw)	975.5(A,vw)	988.3(vw)	971.5(w)
966.8(vw)	975.3(B,vw)	966.4(vw)	
951.7(w)	956.9(B,w)	955.9(w)	914.5(m)
950.8(w)	937.3(A,vw)	942.9(w)	906.5(w)
935.4(w)	918.8(A,0)	924.0(vw)	885.1(w)
926.2(w)	909.1(B,w)	913.7(w)	855.26(m)
869.3(w)	865.7(B,vw)	870.3(w)	826.3(w)
850.5(w)	864.6(A,w)	854.2(w)	815.0(m)
819.7(w)	813.4(A,w)	821.0(w)	779.9(m)
810.2(w)	803.8(B,w)	809.7(w)	764.8(w)
672.9(w)	663.1(B,vw)	661.4(w)	693.0(w)
662.6(w)	661.1(A,m)	650.2(w)	684.4(w)
640.4(vw)	652.1(A,vw)	640.0(w)	665.7(w)
627.7(w)	625.6(B,m)	625.0(w)	
618.0(w)	622.4(B,w)	614.5(w)	
591.8(w)	583.8(A,vw)	586.2(w)	
436.0(w)	434.9(A,vw)	440.1(w)	
409.9(w)	407.5(A,m)	392.8(w)	
372.6(m)	385.5(B,w)	377.6(m)	
341.6(w)	325.1(B,w)	337.8(w)	
300.9(w)	313.8(B,w)	308.4(w)	
295.0(vw)	301.8(A,vw)	294.3(w)	
274.1(w)	272.6(A,w)	279.2(w)	
234.2(w)	268.8(B,m)	243.0(w)	
218.7(w)	200.2(A,w)	211.9(w)	
198.6(vw)	191.5(B,w)	183.7(vw)	
152.8(w)	153.8(A,w)	149.8(vw)	
130.4(vw)	139.9(B,w)	132.0(w)	
115.0(w)	131.3(A,w)	99.3(w)	
72.5(w)	89.2(B,w)	88.5(w)	

[a] Infrared or Raman

Table A.10 Comparison of MM3 Geometries with X-Ray Geometries: 1,5,9-Trithiacyclododecane (**25**)

Bond Lengths (Å)

Method	Conformer	Symmetry	S-C	C-C	C-C	C-S	S-C	C-C
X-ray[a]			1.809(6)	1.518(8)	1.521(8)	1.811(6)	1.809(6)	1.521(8)
MM3	1	C_2	1.823	1.541	1.54	1.824	1.826	1.541

Bond Angles (°)

Method	Conformer	Symmetry	C-S-C	S-C-C	C-C-C	C-C-S	C-S-C	S-C-C	C-C-C
X-ray[a]			101.9(1)	115.2(4)	112.2(5)	113.9(4)	100.5(2)	110.9(4)	114.0(2)
MM3	1	C_2	100.7	113.1	113.4	112.3	100.2	111.7	114.7

[a] X-ray results from reference 253; the bond lengths and angles are averaged to C_2 symmetry

Table A.11 Observed and Calculated Wavenumbers for the Infrared Spectra of 1,5,9-Trithiacyclododecane (**25**)

Observed Solid	C_2 (1) Calculated[a] MM3	C_1 (2) Calculated[a] MM3	C_1 (3) Calculated[a] MM3	Observed Solution (CS_2)
	2969.5(A,m)	2999.5(m)	2978.2(m)	
2967.1(w)	2965.7(B,m)	2988.6(m)	2959.4(m)	
	2957.5(B,s)	2970.1(m)	2958.6(m)	
2954.4(m)	2955.4(A,m)	2965.5(m)	2953.3(m)	
2944.2(m)	2950.2(B,m)	2954.6(m)	2945.5(m)	2948.2(s)
	2950.2(A,w)	2944.2(m)	2942.4(m)	
2925.5(m)	2933.0(B,m)	2931.4(m)	2929.8(m)	
	2933.0(A,m)	2929.2(m)	2916.4(m)	
	2916.4(B,m)	2928.7(m)	2911.9(m)	
2918.0(m)	2895.9(A,m)	2905.8(m)	2896.4(m)	2916.4(s)
2914.5(m)	2894.6(B,m)	2896.3(m)	2894.5(m)	
2905.1(s)	2894.0(A,m)	2894.1(m)	2894.3(m)	
2877.2(m)	2891.4(B,m)	2886.6(m)	2890.0(m)	2873.9(w)
2843.9(m)	2887.1(B,m)	2885.4(m)	2885.3(m)	2843.2(m)
(area	2886.4(A,w)	2884.7(m)	2884.5(m)	
obscured	2876.1(B,m)	2875.8(m)	2873.4(m)	
by water	2875.7(A,w)	2874.0(m)	2864.4(m)	2832.6(m)
band)	2864.8(A,m)	2872.8(m)	2860.4(m)	2814.0(w)
1447.0(m)	1540.6(B,w)	1540.9(vw)	1542.9(w)	
	1529.0(A,vw)	1532.5(vw)	1531.3(w)	
1443.9(m)	1503.1(B,w)	1527.4(w)	1510.1(w)	
1433.7(m)	1502.7(A,vw)	1516.5(vw)	1505.6(w)	
1427.5(m)	1498.5(A,vw)	1509.2(vw)	1505.3(vw)	1427.3(m)
	1498.2(B,w)	1506.7(w)	1496.6(w)	
1416.7(m)	1490.8(A,w)	1496.4(w)	1496.1(vw)	1415.6(m)
	1479.8(B,w)	1491.9(vw)	1483.3(vw)	
1410.6(m)	1476.4(B,w)	1489.1(w)	1477.6(w)	
1345.1(w)	1475.1(A,w)	1480.1(vw)	1475.6(w)	1347.2(w)
	1468.3(A,w)	1467.3(vw)	1474.2(w)	
	1467.2(B,w)	1463.0(vw)	1467.3(vw)	
1296.9(w)	1425.2(B,w)	1435.0(w)	1438.5(w)	1299.6(w)
1284.5(w)	1423.8(A,w)	1428.5(w)	1432.3(w)	1289.5(vw)
	1419.0(A,w)	1426.3(vw)	1417.4(w)	

continued on page 245

Table A.11 (continued) Observed and Calculated Wavenumbers for the Infrared Spectra of 1,5,9-Trithiacyclododecane (**25**)

Observed Solid	C_2 (1) Calculated[a] MM3	C_1 (2) Calculated[a] MM3	C_1 (3) Calculated[a] MM3	Observed Solution (CS_2)
1262.7(m)	1395.2(B,m)	1391.3(m)	1406.7(m)	1260.1(w)
1255.5(m)	1384.9(A,m)	1388.7(m)	1394.8(m)	1253.7(m)
1247.8(m)	1382.2(B,m)	1372.9(m)	1386.5(m)	
	1304.8(B,vw)	1304.9(vw)	1313.8(vw)	
1242.6(m)	1299.6(A,vw)	1302.6(vw)	1304.5(vw)	1239.2(w)
1175.7(w)	1290.5(A,0)	1301.3(vw)	1290.4(vw)	1174.8(w)
	1285.7(B,vw)	1293.2(vw)	1290.1(vw)	
	1277.3(B,vw)	1291.4(vw)	1281.1(0)	
	1277.3(A,vw)	1288.8(vw)	1266.6(vw)	
1141.7(w)	1256.7(A,0)	1268.4(vw)	1262.1(vw)	1140.9(vw)
1113.6(w)	1249.6(B,vw)	1250.0(vw)	1252.8(vw)	1133.4(vw)
1096.3(bw)	1244.2(A,vw)	1240.8(vw)	1245.0(vw)	1096.9(bw)
1066.5(w)	1035.7(B,vw)	1027.7(vw)	1045.9(vw)	1068.3(w)
1039.5(w)	1020.5(B,vw)	1024.1(vw)	1034.1(vw)	1041.4(w)
1022.2(w)	1016.6(A,w)	1020.1(vw)	1019.3(vw)	1017.6(w)
999.8(vw)	979.1(A,vw)	978.4(vw)	980.9(w)	
971.9(vw)	974.3(B,w)	974.2(vw)	960.7(w)	973.6(vw)
958.0(w)	960.5(A,vw)	966.1(vw)	954.9(vw)	956.3(vw)
	947.7(B,w)	942.9(w)	949.7(vw)	
	943.7(A,vw)	937.3(w)	939.8(w)	
940.9(vw)	940.6(B,w)	935.4(vw)	934.0(w)	940.4(vw)
855.0(vw)	860.6(A,vw)	858.3(vw)	855.0(vw)	854.2(w)
841.6(m)	848.9(B,w)	844.5(w)	831.4(w)	838.5(w)
795.4(m)	833.5(B,w)	839.2(vw)	825.5(vw)	798.3(m)
761.7(m)	819.1(A,vw)	800.0(vw)	820.5(w)	
757.1(sh)	803.5(A,w)	791.1(w)	814.8(w)	758.4(w)
739.7(w)	794.2(B,w)	785.7(m)	794.5(w)	733.8(w)
725.4(w)	733.0(B,w)	729.6(w)	713.1(w)	
710.6(w)	691.6(A,w)	711.0(w)	692.6(w)	711.9(w)
	662.5(A,w)	683.3(w)	653.4(w)	
665.2(vw)	646.1(B,w)	648.7(vw)	650.9(w)	667.7(vw)
	645.5(A,vw)	639.2(w)	633.3(w)	
636.3(vw)	631.6(B,w)	602.9(w)	610.1(w)	634.2(vw)

continued on page 246

Table A.11 (continued) Observed and Calculated Wavenumbers for the Infrared Spectra of 1,5,9-Trithiacyclododecane (**25**)

Observed Solid	C_2 (1) Calculated[a] MM3	C_1 (2) Calculated[a] MM3	C_1 (3) Calculated[a] MM3	Observed Solution (CS_2)
	436.3(A,vw)	420.0(w)	449.9(vw)	
	405.1(A,m)	411.7(w)	432.1(vw)	
	399.8(B,w)	387.6(vw)	408.3(w)	
	356.8(B,w)	334.9(w)	369.4(w)	
	311.2(B,w)	311.0(w)	334.8(vw)	
	303.6(A,vw)	292.5(vw)	303.4(w)	
	294.3(A,vw)	282.3(w)	283.8(vw)	
	274.7(B,w)	271.3(w)	255.4(w)	
	245.5(A,w)	252.0(vw)	244.5(w)	
	236.7(A,w)	237.0(w)	235.4(w)	
	233.3(B,w)	233.7(w)	223.3(w)	
	203.5(B,w)	203.6(w)	199.9(w)	
	201.0(B,w)	187.1(vw)	196.7(w)	
	160.9(A,vw)	170.9(w)	147.4(vw)	
	151.7(A,w)	140.2(w)	142.5(w)	
	116.4(B,w)	115.9(vw)	108.0(w)	
	68.4(A,w)	67.3(w)	73.3(w)	
	43.2(B,)	44.3(w)	53.1(w)	

[a] Infrared or Raman

Table A.12 Comparison of MM3 Geometries with X-Ray Geometries: 1,4,7,10-Tetrathiacyclododecane (**26**)

Method	Conformer	Symmetry	Bond Lengths (Å)			Bond Angles (°)	
			S-C	C-S	C-C	C-S-C	S-C-C
X-ray[a]	Molecule 1	D_4	1.817(6)	1.814(6)	1.511(8)	101.3(3)	113.8
	Molecule 2	D_4	1.817(6)	1.817(7)	1.514(9)	101.3(3)	113.8
MM3	1	D_4	1.825	1.825	1.541	101.1	112.5

[a] From reference 248; bond lengths averaged to D_4 symmetry. [b] SCC bond angles calculated from atomic coordinates

Table A.13 Comparison of MM3 Geometries with X-Ray Geometries: 1,4,8,11-tetrathiacyclotetradecane (27)

Bond Lengths (Å)

Method	Conformer	Symmetry	S-C	C-C	C-S	S-C	C-C	C-C	C-S
X-ray[a]	α	C_{2h}	1.803(3)	1.504(4)	1.817(3)	1.812(3)	1.518(3)	1.505(3)	1.802(3)
	β_1	C_{2h}	1.792(9)	1.431(10)	1.877(9)	1.807(7)	1.500(9)	1.542(9)	1.790(7)
	β_2	C_2	1.933(10)	1.292(10)	2.035(10)	1.796(8)	1.526(9)	1.504(9)	1.812(8)
MM3	1	C_{2h}	1.824	1.539	1.824	1.823	1.538	1.538	1.823

Bond Angles (°)

Method	Conformer	Symmetry	C-S-C	S-C-C	C-C-S	C-S-C	S-C-C	C-C-C	C-C-S
X-ray[a]	α	C_{2h}	103.6(1)	114.1(2)	113.4(2)	102.2(1)	114.1(2)	111.6(2)	115.1(2)
	β_1	C_{2h}	106.1(4)	113.9(6)	113.4(7)	103.3(3)	114.6(5)	112.1(6)	114.7(5)
	β_2	C_2	97.5(3)	102.4(7)	101.9(8)	99.2(3)	114.6(5)	111.8(6)	114.5(5)
MM3	1	C_{2h}	102.6	112.9	112.9	102.6	113.3	111.9	113.3

[a] X-ray results from reference 246; the bond lengths and angles are averaged to C_2 symmetry.

Table A.14 Comparison of MM3 Geometries with X-Ray Geometries: 1,4,7,10,13-pentathiacyclopentadecane (**28**)

Bond Lengths (Å)

Method	Symmetry	S-C	C-C	C-S	S-C	C-C	C-S	S-C	C-C
X-ray[a]	C_1	1.820(6)	1.448(11)	1.821(6)	1.950(11)	1.449(12)	1.840(11)	1.817(6)	1.502(8)
MM3	D_5	1.822	1.54	1.822	1.822	1.54	1.822	1.822	1.54

Method	Symmetry	C-S	S-C	C-C	C-S	S-C	C-C	C-S
X-ray[a]	C_1	1.800(7)	1.813(5)	1.509(8)	1.819(5)	1.842(5)	1.483(8)	1.837(7)
MM3	D_5	1.822	1.822	1.54	1.822	1.822	1.54	1.822

Bond Angles (°)

	C-S-C	S-C-C	C-C-S	C-S-C	S-C-C	C-C-S	C-S-C	S-C-C	C-C-S
X-ray[a]	100.6(3)	112.9	114.7	102.5(4)	107.9	106.1	102.4(3)	113.2	116.7
MM3	101.7	111.7	111.7	101.7	111.7	111.7	101.7	111.7	111.7

	C-C-S	C-S-C	S-C-C	C-C-S	C-S-C	S-C-C	C-C-S
X-ray[a]	116.7	103.7(3)	113.4	110.5	98.8(3)	110.4	112.2
MM3	111.7	101.7	111.7	111.7	101.7	111.7	111.7

[a] X-ray results from reference 248; the SCC bond angles were calculated from the atomic coordinates.

Table A.15 Comparison of MM3 Geometries with X-Ray Geometries: 1,5,9,13-Tetrathiacyclohexadecane (**29**)

Bond Lengths (Å)

Method	Conformer	Symmetry	S-C	C-C	C-C	C-S	S-C	C-C	C-C	C-S
X-ray[a]	α	C_2	1.807(4)	1.524(5)	1.525(5)	1.811(5)	1.807(4)	1.515(5)	1.512(5)	1.816(4)
	β	C_2	1.798(19)	1.52(3)	1.53(3)	1.828(21)	1.82(5)	1.50(3)	1.50(3)	1.803(19)
MM3[b]	3	C_2	1.822	1.539	1.54	1.823	1.824	1.538	1.537	1.821

Bond Angles (°)

	Conformer	C-S-C	S-C-C	C-C-C	C-C-S	C-S-C	S-C-C	C-C-C	C-C-S
X-ray[a]	α	101.4(3)	114.6(7)	112.6(4)	114.0(3)	101.0(2)	110.1(4)	112.0(8)	114.4(5)
	β	101.9(12)	115.3(15)	112.7(15)	112.2(15)	100.4(12)	109.8(40)	111.4(20)	116.1(30)
MM3[B]	3	100.1	113.3	113.8	112.7	101.4	113.1	112.1	111

[a] X-ray data from reference 328; bond lengths and angles were averaged to C_2 symmetry. [b] From the C_2-symmetric third conformation.

References

1. Moss, G. P. *Pure Appl. Chem.* **1996**, *68*, 2193-2222.

2. Eliel, E. L.; Wilen, S. H.; Mander, L. N. *Stereochemistry of Organic Compounds*; John Wiley & Sons: New York, 1994.

3. Burkert, U.; Allinger, N. L. *Molecular Mechanics*; ACS: Washington, 1982.

4. Wiberg, K. B.; Murcko, M. A. *J. Am. Chem. Soc.* **1988**, *110*, 8029-8038.

5. Seeman, J. I. *Chem. Rev.* **1983**, *83*, 83-134.

6. Durig, J. R.; Liu, J.; Little, T. S.; Kalasinsky, V. F. *J. Phys. Chem.* **1992**, *96*, 8224-8233.

7. Goodwin, A. R. H.; Morrison, G. *J. Phys. Chem.* **1992**, *96*, 5521-5526.

8. Grootenhuis, P. D. J.; van Boeckel, C. A. A.; Haasnoot, C. A. G. *Trends Biotech.* **1994**, *12*, 9-14.

9. Lee, Y. C.; Lee, R. T. *Acc. Chem. Res.* **1995**, *28*, 321-327.

10. Stewart, R. F.; Hall, S. R. In *Determination of Organic Structures by Physical Methods*; Nachod, F. C., Zuckerman, J. J. Eds.; Academic Press: New York, 1971; Vol. 3, pp 74-132.

11. Lipscomb, W. N.; Jacobsen, R. A. In *Physical Methods of Chemistry Part IIID Optical, Spectroscopic and Radioactivity Methods.* Weissberger, A., Rossiter, B. W. Eds.; John Wiley & Sons: Toronto, 1972; Vol. 1, pp 1-124.

12. Cameron, A. F. In *Elucidation of Organic Structures by Physical and Chemical Methods Part I*; Bentley, K. W., Kirby, G. W. Eds.; John Wiley & Sons: Toronto, 1972; Vol. 4, pp 481-514.

13. Hastings, J. M.; Hamilton, W. C. In *Physical Methods of Chemistry Part IIID Optical, Spectroscopic, and Radioactivity Methods*; Weissberger, A., Rossiter, B. W. Eds.; John Wiley & Sons: Toronto, 1972; Vol. 1, pp 159-214.

14. Karle, J. In *Determination of Organic Structures by Physical Methods*; Nachod, F. C., Zuckerman, J. J. Eds.; Academic Press: New York, 1973; Vol. 5, pp 1-74.

15. Bartell, L. S. In *Physical Methods of Chemistry Part IIID Optical, Spectroscoopic and Radioactivity Methods*; Weissberger, A., Rossiter, B. W. Eds.; John Wiley & Sons: Toronto, 1972; Vol. 1, pp 125-158.

16. Flygare, W. H. In *Physical Methods of Chemistry Part IIIA Optical, Spectroscopy, and Radioactivity Methods*; Weissberger, A., Rossiter, B. W. Eds.; John Wiley & Sons: Toronto, 1972; Vol. 1, pp 439-498.

17. Blom, R.; Rankin, D. W. H.; Robertson, H. E.; Schröder, M.; Taylor, A. *J. Chem. Soc., Perkin Trans. II.* **1991,** 773-778.

18. Anet, F. A. L.; Anet, R. In *Determination of Organic Structures by Physical Methods*; Nachod, F. C., Zuckerman, J. J. Eds.; Academic Press: New York, 1971; Vol. 3, pp 344-420.

19. McFarlane, W. In *Elucidation of Organic Structures by Physical and Chemical Methods Part I*; Bentley, K. W., Kirby, G. W. Eds.; John Wiley & Sons: Toronto, 1972; Vol. 4, pp 225-322.

20. Keeler, J. K. *Chem. Soc. Rev.* **1990**, *19*, 381-406.

21. Saunders, J. K.; Easton, J. W. In *Determination of Organic Structures by Physical Methods*; Nachod, F. C., Zuckerman, J. J., Randall, E. W. Eds.; Academic Press: New York, 1976; Vol. 6, pp 271-334.

22. Wüthrich, K. *NMR of Proteins and Nucleic Acids*; John Wiley & Sons: New York, 1986.

23. Karplus, M. *J. Am. Chem. Soc.* **1963**, *85*, 2870-2871.

24. Averyanov, A. S.; Khait, Y. G.; Puzanov, Y. V. *J. Mol. Struct. (Theochem)* **1996**, *367*, 87-95.

25. Adalsteinsson, H.; Maulitz, A. H.; Bruice, T. C. *J. Am. Chem. Soc.* **1996**, *118*, 7689-7693.

26. Foresman, J. B.; Wong, M. W.; Wiberg, K. B.; Frisch, M. J. *J. Am. Chem. Soc.* **1993**, *115*, 2220-2226.

27. Anet, F. A. L. *J. Am. Chem. Soc.* **1990,** *112*, 7172-7178.

28. Dale, J. *Acta Chem. Scand.* **1973,** *27*, 1130-1148.

29. Saunders, M. *J. Comp. Chem.* **1991,** *12,* 645-663.

30. Tietze, L. F.; Geissler, H.; Fennen, J.; Brumby, T.; Brand, S.; Schulz, G. *J. Org. Chem.* **1994**, *59*, 182-191.

31. Ealick, S. E.; Babu, Y. S.; Bugg, C. E.; Erion, M. D.; Guida, W. C.; Montgomery, J. A.; Secrist III, J. A. *Proc. Natl. Acad. Sci. USA* **1991**, *88*, 11540-11544.

32. Watson, J. D.; Crick, F. H. C. *Nature* **1953**, *171*, 737-738.

33. Boyd, D. B. In *Reviews in Computational Chemistry*; Lipkowitz, K. B., Boyd, D. B. Eds.; VCH Publishers INC: New York, 1990; Vol. 1, pp 321-354.

34. Shi, Z.; Boyd, R. J. *J. Am. Chem. Soc.* **1989**, *111*, 1575-1579.

35. Davidson, E. R. In *Reviews in Computational Chemistry*; Lipkowitz, K. B., Boyd, D. B. Eds.; VCH Publishers INC: New York, 1990; Vol. 1, pp 373-382.

36. Wong, M. W.; Frisch, M. J.; Wiberg, K. B. *J. Am. Chem. Soc.* **1991**, *113*, 4776-4782.

37. Pople, J. A.; Santry, D. P.; Segal, G. A. *J. Chem. Phys.* **1965**, *43*, S129-S135.

38. Pople, J. A.; Segal, G. A. *J. Chem. Phys.* **1965**, *43*, S136-S149.

39. Stewart, J. J. P. In *Reviews in Computational Chemistry*; Lipkowitz, K. B., Boyd, D. B. Eds.; VCH Publishers INC: New York, 1990; Vol. 1, pp 45-82.

40. Zerner, M. C. In *Reviews in Computational Chemistry*; Lipkowitz, K. B., Boyd, D. B. Eds.; VCH Publishers INC: New York, 1991; Vol. 2, pp 313-366.

41. Wiberg, K. B. *J. Am. Chem. Soc.* **1965**, *87*, 1070-1078.

42. Allinger, N. L.; Yuh, Y. H.; Lii, J.-H. *J. Am. Chem. Soc.* **1989,** *111*, 8551-8566.

43. Bowen, J. P.; Allinger, N. L. In *Reviews in Computational Chemistry*; Lipkowitz, K. B., Boyd, D. B. Eds.; VCH Publishers INC: New York, 1991; Vol. 2, pp 81-98.

44. Boyd, D. B.; Lipkowitz, K. B. *J. Chem. Ed.* **1982**, *59*, 269-274.

45. Cornell, W. D.; Cieplak, P.; Bayly, C. I.; Gould, I. R.; Merz, Jr., K. M.; Ferguson, D. M.; Spellmeyer, D. C.; Fox, T.; Caldwell, J. W.; Kollman, P. A. *J. Am. Chem. Soc.* **1995,** *117*, 5169-5197.

46. Brooks, B. R.; Bruccoleri, R. E.; Olafson, B. D.; States, D. J.; Swaminathan, S.; Karplus, M. *J. Comp. Chem.* **1983**, *4*, 187-217.

47. Lii, J.-H.; Allinger, N. L. *J. Am. Chem. Soc.* **1989**, *111*, 8566-8575.

48. Lii, J.-H.; Allinger, N. L. *J. Am. Chem. Soc.* **1989**, *111*, 8576-8582.

49. Pettersson, I.; Liljefors, T. In *Reviews in Computational Chemistry*; Lipkowitz, K. B., Boyd, D. B. Eds.; VCH Publishers INC: New York, 1996; Vol. 9, pp 167-190.

50. Gundertofte, K.; Liljefors, T.; Norrby, P.-O.; Pettersson, I. *J. Comp. Chem.* **1996**, *17*, 429-449.

51. Boyd, D. B.; Coner, R. D. *J. Mol. Struct. (Theochem)* **1996**, *368*, 7-15.

52. Hwang, M. J.; Stockfisch, T. P.; Hagler, A. T. *J. Am. Chem. Soc.* **1994**, *116*, 2515-2525.

53. Allinger, N. L.; Chen, K. S.; Lii, J.-H. *J. Comp. Chem.* **1996**, *17*, 642-668.

54. Nevins, N.; Chen, K. S.; Allinger, N. L. *J. Comp. Chem.* **1996**, *17*, 669-694.

55. Nevins, N.; Allinger, N. L. *J. Comp. Chem.* **1996**, *17*, 730-746.

56. Allinger, N. L.; Chen, K. S.; Katzenellenbogen, J. A.; Wilson, S. R.; Anstead, G. M. *J. Comp. Chem.* **1996**, *17*, 747-755.

57. Nevins, N.; Lii, J.-H.; Allinger, N. L. *J. Comp. Chem.* **1996**, *17*, 695-729.

58. Kollman, P. A. *Acc. Chem. Res.* **1996**, *29*, 461-469.

59. Dowd, M. K.; Reilly, P. J.; French, A. D. *Biopolymers.* **1994**, *34*, 625-638.

60. Barrows, S. E.; Dulles, F. J.; Cramer, C. J.; French, A. D.; Truhlar, D. G. *Carbohydr. Res.* **1995**, *276*, 219-251.

61. French, A. D.; Rowland, R. S.; Allinger, N. L. In *Computer Modelling of Carbohydrate Molecules*; French, A. D., Brady, J. W. Eds.; ACS: Washington, 1990; pp 120-140.

62. Woods, R. J. In *Reviews in Computational Chemistry*; Lipkowitz, K. B., Boyd, D. B. Eds.; VCH Publishers INC: New York, 1996; Vol. 9, pp 129-166.

63. Wolfe, S.; Rauk, A.; Tel, L. M.; Csizmadia, I. G. *J. Chem. Soc. B* **1971**, 136-145.

64. Wolfe, S. *Acc. Chem. Res.* **1972**, *5*, 102-110.

65. Pinto, B. M.; Leung, R. Y. N. In *The Anomeric Effect and Associated Stereoelectronic Effects*; Thatcher, G. R. J. Ed.; ACS: Washington, D.C. 1993; Vol. 539, pp 126-155.

66. Allinger, N. L.; Rahman, M.; Lii, J.-H. *J. Am. Chem. Soc.* **1990,** *112*, 8293-8307.

67. Lii, J.-H.; Allinger, N. L. *J. Phys. Org. Chem.* **1994,** *7*, 591-609.

68. Grindley, T. B.; Cude, A.; Kralovic, J.; Thangarasa, R. In *Levoglucosenone and Levoglucosans, Chemistry and Applications*; Witczak, Z. J. Ed.; ATL Press: Mount Prospect, ILL, 1994; pp 147-164.

69. Senderowitz, H.; Golender, L.; Fuchs, B. *Tetrahedron.* **1994,** *50*, 9707-9728.

70. Tsuzuki, S.; Tanabe, K. *J. Chem. Soc., Perkin Trans. II.* **1991,** 181-185.

71. Zefirov, N. S.; Samoshin, V. V.; Subbotin, O. A.; Baranenkov, V. I.; Wolfe, S. *Tetrahedron* **1978**, *34*, 2953-2959.

72. Ogawa, Y.; Ohta, M.; Sakakibara, M.; Matsuura, H.; Harada, I.; Shimanouchi, T. *Bull. Chem. Soc. Jpn.* **1977,** *50*, 650-660.

73. Yoshida, H.; Kaneko, I.; Matsuura, H.; Ogawa, Y.; Tasumi, M. *Chem. Phys. Lett.* **1992,** *196*, 601-606.

74. Iwamoto, R. *Spectrochim. Acta.* **1971,** *27*, 2385-2399.

75. Connor, T. M.; McLauchlan, K. A. *J. Phys. Chem.* **1965**, *69*, 1888-1893.

76. Matsuzaki, K.; Ito, H. *J. Polym. Sci. Polym. Chem. Phys. Ed.* **1974**, *12*, 2507-2520.

77. Viti, V.; Indovina, P. L.; Podo, F.; Radics, L.; Némethy, G. *Molec. Phys.* **1974**, *27*, 541-559.

78. Dutkiewicz, M. *J. Mol. Struct.* **1994,** *318*, 171-177.

79. Astrup, E. E. *Acta Chem. Scand.* **1979**, *A33*, 655-664.

80. Abe, A.; Inomata, K. *J. Mol. Struct.* **1991**, *245*, 399-402.

81. Inomata, K.; Abe, A. *J. Phys. Chem.* **1992**, *96*, 7934-7937.

82. Yoshida, H.; Tanaka, T.; Hiroatsu, M. *Chem. Lett.* **1996**, 637-638.

83. Gil, F. P. S. C.; Teixeira-Dias, J. J. C. *J. Mol. Struct. (Theochem)* **1996**, *363*, 311-317.

84. Tsuzuki, S.; Uchimaru, T.; Tanabe, K.; Hirano, T. *J. Phys. Chem.* **1993**, *97*, 1346-1350.

85. Murcko, M. A.; DiPaola, R. A. *J. Am. Chem. Soc.* **1992**, *114*, 10010-10018.

86. Jaffe, R. L.; Smith, G. D.; Yoon, D. Y. *J. Phys. Chem.* **1993**, *97*, 12745-12751.

87. Williams, D. J.; Hall, K. B. *J. Phys. Chem.* **1996**, *100*, 8224-8229.

88. Smith, G. D.; Jaffe, R. L.; Yoon, D. Y. *J. Am. Chem. Soc.* **1995**, *117*, 530-531.

89. Zefirov, N. S.; Samoshin, V. V.; Baranenkov, V. I.; Subbotin, O. A.; Sergeev, N. M. *Zh. Obshch. Khim.* **1977**, *13*, 2232-2233.

90. Kuhlmann, K. F.; Grant, D. M.; Harris, R. K. *J. Chem. Phys.* **1970**, *52*, 3439-3448.

91. *CRC Handbook of Chemistry and Physics*; Weast, R. C. Ed.; CRC Press: Boca Raton, 1985; pp E49-E53.

92. Abraham, R. J.; Banks, H. D.; Eliel, E. L.; Hofer, O.; Kaloustian, M. K. *J. Am. Chem. Soc.* **1972**, *94*, 1913-1918.

93. Abraham, R. J.; Rossetti, Z. L. *J. Chem. Soc., Perkin Trans. I.* **1973**, 582-587.

94. Reichardt, C. *Solvents and Solvent Effects in Organic Chemistry.* VCH: Weinheim, Germany, 1988.

95. Eliel, E. L.; Hofer, O. *J. Am. Chem. Soc.* **1973**, *95*, 8041-8045.

96. Romers, C.; Altona, C.; Buys, H. R.; Havinga, E. *Topics Stereochem.* **1969**, *4*, 39-97.

97. Davis, M.; Hassel, O. *Acta Chem. Scand.* **1963**, *17*, 1181.

98. Pitzer, K. S.; Gwinn, W. D. *J. Chem. Phys.* **1942**, *10*, 428-440.

99. Eliel, E. L.; Enanoza, R. M. *J. Am. Chem. Soc.* **1972**, *94*, 8072-8078.

100. Abe, A.; Tasaki, K. *J. Mol. Struct.* **1986**, *145*, 309-318.

101. Woods, R. J.; Dwek, R. A.; Edge, C. J.; Fraser-Reid, B. *J. Phys. Chem.* **1995**, *99*, 3832-3846.

102. Miyajima, T.; Hirano, T.; Sato, H. *J. Mol. Struct.* **1984**, *125*, 97-107.

103. Haasnoot, C. A. G.; DeLeeuw, F. A. A. M.; Altona, C. *Tetrahedron* **1980**, *36*, 2783-2792.

104. Haigh, C. W. *Ann. Rep. NMR Spectrosc.* **1971**, *4*, 311-362.

105. Hirano, T.; Tsuruta, T. *J. Phys. Chem.* **1967**, *71*, 4184-4189.

106. Huggins, M. L. *J. Am. Chem. Soc.* **1953**, *75*, 4123-4126.

107. a) French, A. D.; Brady, J. W. In *Computer Modelling of Carbohydrate Molecules*; French, A. D., Brady, J. W. Eds.; ACS: Washington, 1990; pp 1-19. b) Dowd, M. K.; Reilly, P. J.; French, A. D. *Biopolymers* **1994**, *34*, 625-638. c) Dowd, M. K.; French, A. D.; Reilly, P. J. *J. Carbohydr. Chem.* **1995**, *14*, 589-600.

108. Bock, K.; Duus, J. Ø. *J. Carbohydr. Chem.* **1994**, *13*, 513-543.

109. Tvaroska, I.; Carver, J. P. *J. Phys. Chem. B* **1997**, *101*, 2992-2999.

110. Singelenberg, F. A. J.; Lutz, E. T. G.; Van der Maas, J. H. *Applied Spectroscopy.* **1986**, *40*, 1093-1098.

111. Singelenberg, F. A. J.; Van der Maas, J. H.; Kroon-Batenburg, L. M. J. *J. Mol. Struct.* **1991**, *245*, 183-194.

112. Singelenberg, F. A. J.; Van der Maas, J. H. *J. Mol. Struct.* **1990**, *240*, 213-223.

113. Buckley, P.; Brochu, M. *Can. J. Chem.* **1972**, *50*, 1149-1156.

114. Krueger, P. J.; Mettee, H. D. *J. Mol. Spectrosc.* **1965**, *18*, 131-140.

115. Gil, F. P. S. C.; Teixeira-Dias, J. J. C. *J. Mol. Struct. (Theochem).* **1995**, *332*, 269-275.

116. Gil, F. P. S. C.; Fausto, R.; da Costa, A. M. A.; Teixeira-Dias, J. J. C. *J. Chem. Soc., Faraday Trans.* **1994**, *90*, 689-695.

117. Kuhn, L. P.; Wires, R. A. *J. Am. Chem. Soc.* **1964,** *86,* 2161-2165.

118. Feeney, J.; Walker, S. M. *J. Chem. Soc. A.* **1966,** 1148-1152.

119. Suryanarayana, I.; Someswar, G. P.; Subrahmanyam, B. *Z. phys. Chemie.* **1990,** *271,* 621-627.

120. Prabhumirashi, L. S.; Jose, C. I. *J. Chem. Soc., Faraday Trans. II.* **1976,** *72,* 1721-1729.

121. Brown, J. W.; Wladkowski, B. D. *J. Am. Chem. Soc.* **1996,** *118,* 1190-1193.

122. Vedejs, E.; Erdman, D. E.; Powell, D. R. *J. Org. Chem.* **1993**, *58*, 2840-2845.

123. Pommier, J. C.; Mendes, E.; Valade, J.; Housty, J. *J. Organomet. Chem.* **1973**, *55*, C19-C23.

124. Vogel, A. I. In *Textbook of Practical Organic Chemistry*; Richard Clay Ltd: Bungay, Suffolk, England, 1956; pp 894-895.

125. Davidson, R. I.; Kropp, P. J. *J. Org. Chem.* **1982,** *47,* 1904-1909.

126. Winstein, S.; Henderson, R. B. *J. Am. Chem. Soc.* **1943**, *65*, 2196-2199.

127. Varki, A. *Glycobiology* **1993**, *3*, 97-130.

128. Wassarman, P. M. *Theriogenology.* **1994,** *41,* 31-44.

129. van Boeckel, C. A. A.; Petitou, G. *Angew. Chem. Int. Ed. Engl.* **1993**, *32*, 1671-1690.

130. Lemieux, R. U. *Chem. Soc. Rev.* **1978**, *7*, 423-452.

131. Williams, D. H. *Natural Product Reports* **1996**, 469-477.

132. Collins, P. M.; Ferrier, R. J. *Monosaccharides: Their Chemistry and Their Roles in Natural Products*; John Wiley & Sons: Chichester, 1995.

133. Kirby, A. J. *The Anomeric Effect and Related Stereoelectronic Effects at Oxygen*; Springer-Verlag: New York, 1983.

134. Stoddart, J. F. *Stereochemistry of Carbohydrates*; Wiley-Interscience: New York, 1971.

135. a) Marchessault, R. H.; Perez, S. *Biopolymers* **1979**, *18*, 2369-2374. b) Kouwijzer, M. L. C. E.; Grootenhuis, P. D. J. *J. Phys. Chem.* **1995**, *99*, 13426-13436.

136. Woodcock, C.; Sarko, A. *Macromolecules* **1980**, *13*, 1183-1187.

137. Sarko, A.; Chen, C.-H.; Hardy, B. J.; Tanaka, F. In *Computer Modeling of Carbohydrate Molecules*; French, A. D., Brady, J. W. Eds.; ACS: Washington, D.C. 1990; Vol. 430, pp 345-360.

138. Lemieux, R. U.; Martin, J. C. *Carbohydr. Res.* **1970**, *13*, 139-161.

139. Lemieux, R. U.; Brewer, J. T. In *Carbohydrates in Solution*; Gould, R. F. Ed.; ACS: Washington D.C. 1971; Vol. 117, pp 121-146.

140. Liu, H.-W.; Nakanishi, K. *J. Am. Chem. Soc.* **1981**, *103*, 5591-5593.

141. Wiesler, W. T.; Vázquez, J. T.; Nakanishi, K. *J. Am. Chem. Soc.* **1987**, *109*, 5586-5592.

142. Morales, E. Q.; Padrón, J. I.; Trujillo, M.; Vázquez, J. T. *J. Org. Chem.* **1995**, *60*, 2537-2548.

143. Nishida, Y.; Hori, H.; Ohrui, H.; Meguro, H. *J. Carbohydr. Chem.* **1988**, *7*, 239-250.

144. De Bruyn, A.; Anteunis, M. *Carbohydr. Res.* **1976**, *47*, 311-314.

145. Hori, H.; Nishida, Y.; Ohrui, H.; Meguro, H. *J. Carbohydr. Chem.* **1990**, *9*, 601-618.

146. de Vries, N. K.; Buck, H. M. *Carbohydr. Res.* **1987**, *165*, 1-16.

147. Ohrui, H.; Nishida, Y.; Watanabe, M.; Hori, H.; Meguro, H. *Tetrahedron Lett.* **1985**, *26*, 3251-3254.

148. Nishida, Y.; Ohrui, H.; Meguro, H. *Tetrahedron Lett.* **1984**, *25*, 1575-1578.

149. Hori, H.; Nishida, Y.; Ohrui, H.; Meguro, H.; Uzawa, J. *Tetrahedron Lett.* **1988**, *29*, 4457-4460.

150. Poppe, L.; van Halbeek, H. *J. Magn. Reson.* **1992**, *96*, 185-190.

151. Breg, J.; Kroon-Batenburg, L. M. J.; Strecker, G.; Montreuil, J.; Vliegenthart, J. F. G. *Eur. J. Biochem.* **1989**, *178*, 727-739.

152. Imai, K.; Osawa, E. *Magn. Reson. Chem.* **1990,** *28,* 668-674.

153. Barfield, M.; Smith, W. B. *J. Am. Chem. Soc.* **1992,** *114,* 1574-1581.

154. Rao, V. S.; Perlin, A. S. *Can. J. Chem.* **1983**, *61*, 2688-2694.

155. Ohrui, H.; Horiki, H.; Kishi, H.; Meguro, H. *Agric. Biol. Chem.* **1983**, *47*, 1101-1106.

156. Ohrui, H.; Nishida, Y.; Meguro, H. *Agric. Biol. Chem.* **1984**, *48*, 1049-1053.

157. Gagnaire, D.; Horton, D.; Taravel, F. R. *Carbohydr. Res.* **1973**, *27*, 363-372.

158. Bock, K.; Refn, S. *Acta Chem. Scand., Ser. B* **1987**, *41*, 469-472.

159. Bock, K.; Pedersen, H. *Acta Chem. Scand., Ser. B* **1988**, *42*, 190-195.

160. Nishida, Y.; Hori, H.; Ohrui, H.; Meguro, H. *Agric. Biol. Chem.* **1988**, *52*, 887-889.

161. Nishida, Y.; Hori, H.; Ohrui, H.; Meguro, H.; Uzawa, J. *Tetrahedron Lett.* **1988**, *29*, 4461-4464.

162. Nishida, Y.; Hori, H.; Ohrui, H.; Meguro, H.; Zushi, S.; Uzawa, J.; Ogawa, T. *Agric. Biol. Chem.* **1988**, *52*, 1003-1011.

163. Beeson, C.; Pham, N.; Shipps, Jr., G.; Dix, T. A. *J. Am. Chem. Soc.* **1993,** *115,* 6803-6812.

164. Tvaroska, I.; Taravel, F. R. *Adv. Carbohydr. Chem. Biochem.* **1995,** *51,* 15-61.

165. Tvaroska, I.; Gajgos, J. *Carbohydr. Res.* **1995,** *271,* 151-162.

166. Podlasek, C. A.; Wu, J.; Stripe, W. A.; Bondo, P. B.; Serianni, A. S. *J. Am. Chem. Soc.* **1995,** *117,* 8635-8644.

167. Jiménez-Barbero, J.; Junquera, E.; Martín-Pastor, M.; Sharma, S.; Vicent, C.; Penadés, S. *J. Am. Chem. Soc.* **1995**, *117*, 11198-11204.

168. Abraham, R. J.; Chambers, E. J.; Thomas, W. A. *Carbohydr. Res.* **1992**, *226*, C1-C5.

169. Streefkerk, D. G.; de Bie, M. J. A.; Vliegenthart, J. F. G. *Tetrahedron* **1973**, *29*, 833-844.

170. Streefkerk, D. G.; Stephen, A. M. *Carbohydr. Res.* **1976**, *49*, 13-25.

171. Brisson, J. R.; Carver, J. P. *Biochemistry* **1983**, *22*, 3680-3686.

172. Paulsen, H.; Peters, T.; Sinnwell, V.; Heume, M.; Meyer, B. *Carbohydr. Res.* **1986**, *156*, 87-106.

173. Ohrui, H.; Nishida, Y.; Higuchi, H.; Hori, H.; Meguro, H. *Can. J. Chem.* **1987**, *65*, 1145-1153.

174. de Vries, N. K.; Buck, H. M. *Rec. Trav. Chim. Pays-Bas* **1987**, *106*, 453-460.

175. Angyal, S. J.; Christofides, J. C. *J. Chem. Soc., Perkin Trans. II.* **1996,** 1485-1491.

176. Dionne, P.; St-Jacques, M. *J. Am. Chem. Soc.* **1987**, *109*, 2616-2623.

177. Juaristi, E.; Antúnez, S. *Tetrahedron* **1992**, *48*, 5941-5950.

178. Jansson, K.; Kenne, L.; Kolare, I. *Carbohydr. Res.* **1994**, *257*, 163-174.

179. Hardy, B. J.; Gutierrez, A.; Lesiak, K.; Seidl, E.; Widmalm, G. *J. Phys. Chem.* **1996**, *100*, 9187-9192.

180. Senderowitz, H.; Parish, C.; Still, W. C. *J. Am. Chem. Soc.* **1996,** *118*, 2078-2086.

181. Reiling, S.; Schlenkrich, M.; Brickmann, J. *J. Comp. Chem.* **1996,** *17*, 450-468.

182. Polavarapu, P. L.; Ewig, C. S. *J. Comp. Chem.* **1992**, *13*, 1255-1261.

183. Salzner, U.; Schleyer, P. v. R. *J. Org. Chem.* **1994**, *59*, 2138-2155.

184. Zheng, Y.-J.; Le Grand, S. M.; Merz, Jr., K. M. *J. Comp. Chem.* **1992**, *13*, 772-791.

185. Tvaroska, I.; Imberty, A.; Pérez, S. *Biopolymers* **1990**, *30*, 369-379.

186. Tvaroska, I.; Kozár, T. *Theor. Chim. Acta* **1986**, *70*, 99-114.

187. Cramer, C. J.; Truhlar, D. G. *J. Am. Chem. Soc.* **1993,** *115*, 5745-5753.

188. Brady, J. W. *J. Am. Chem. Soc.* **1986**, *108*, 8153-8160.

189. Brady, J. W. *J. Am. Chem. Soc.* **1989**, *111*, 5155-5165.

190. Kroon-Batenburg, L. M. J.; Kroon, J. *Biopolymers* **1990**, *29*, 1243-1248.

191. Ha, S.; Gao, J.; Tidor, B.; Brady, J. W.; Karplus, M. *J. Am. Chem. Soc.* **1991**, *113*, 1553-1557.

192. van Eijck, B. P.; Hooft, R. W. W.; Kroon, J. *J. Phys. Chem.* **1993**, *97*, 12093-12099.

193. Glennon, T. M.; Zheng, Y.-J.; Le Grand, S. M.; Shutzberg, B. A.; Merz, Jr., K. M. *J. Comp. Chem.* **1994**, *15*, 1019-1040.

194. Cheetham, N. W. H.; Lam, K. *Carbohydr. Res.* **1996**, *282*, 13-23.

195. Kojima, N.; Araki, Y.; Ito, E. *Eur. J. Biochem.* **1985**, *148*, 479-484.

196. Bollenback, G. N. In *Methods in Carbohydrate Chemistry Vol. II*; Whistler, R. L., Wolfrom, M. L. Eds.; Academic Press: New York, 1963; pp 326-327.

197. Brimacombe, J. S.; Jones, B. D.; Stacey, M.; Willard, J. J. *Carbohydr. Res.* **1966**, *2*, 167-169.

198. Reichardt, C. *Angew. Chem. Int. Ed. Engl.* **1965**, *4*, 29-40.

199. Kamlet, M. J.; Abboud, J.-L. M.; Abraham, M. H.; Taft, R. W. *J. Org. Chem.* **1983**, *48*, 2877-2887.

200. Chastrette, M.; Rajzmann, M.; Chanon, M.; Purcell, K. F. *J. Am. Chem. Soc.* **1985**, *107*, 1-11.

201. Abraham, R. J.; Cooper, M. A. *J. Chem. Soc. B.* **1967**, 202-205.

202. Abraham, R. J.; Siverns, T. M. *J. Chem. Soc., Perkin Trans. II.* **1972**, 1587-1594.

203. Rathbone, E. B.; Stephen, A. M.; Pachler, K. G. R. *Carbohydr. Res.* **1971**, *20*, 141-150.

204. Schmidt, R. R.; Gaden, H.; Iatzke, H. *Tetrahedron Lett.* **1990**, *31*, 327-330.

205. Buckingham, A. D.; Schaefer, T.; Schneider, W. G. *J. Chem. Phys.* **1960**, *32*, 1227-1233.

206. Franke, F.; Guthrie, R. D. *Austral. J. Chem.* **1977**, *30*, 639-647.

207. Shekhani, M. S.; Khan, K. M.; Mahmood, K. *Tetrahedron Lett.* **1988**, *29*, 6161-6162.

208. Qin, H. Ph. D. Thesis, Dalhousie University, 1997.

209. Rader, C. P. *J. Am. Chem. Soc.* **1969**, *91*, 3248-3256.

210. Fraser, R. R.; Kaufman, M.; Morand, P.; Govil, G. *Can. J. Chem.* **1969**, *47*, 403-409.

211. King, G.; Lee, F. S.; Warshel, A. *J. Chem. Phys.* **1991**, *95*, 4366-4377.

212. Warshel, A.; Åqvist, J. *Annu. Rev. Biophys. Biophys. Chem* **1991**, *20*, 267-298.

213. Garbisch, Jr., E. W. *J. Chem. Ed.* **1968**, *45*, 311-321.

214. Garbisch, Jr., E. W. *J. Chem. Ed.* **1968**, *45*, 402-416.

215. Garbisch, Jr., E. W. *J. Chem. Ed.* **1968**, *45*, 480-493.

216. Hirst, E. L.; Percival, E. In *Methods in Carbohydrate Chemistry Vol. II*; Whistler, R. L., Wolfrom, M. L. Eds.; Academic Press: New York, 1963; pp 145-150.

217. Whittaker, M. M.; Chuang, Y.-Y.; Whittaker, J. W. *J. Am. Chem. Soc.* **1993**, *115*, 10029-10035.

218. Watzky, M. A.; Waknine, D.; Heeg, M. J.; Endicott, J. F.; Ochrymowycz, L. A. *Inorg. Chem.* **1993**, *32*, 4882-4888.

219. Eichhorn, G. L. *Coord. Chem. Rev.* **1993**, *128*, 167-173.

220. Desper, J. M.; Powell, D. R.; Gellman, S. H. *J. Am. Chem. Soc.* **1990**, *112*, 4321-4324.

221. Lockhart, J. C.; Mousley, D. P.; Hill, M. N. S.; Tomkinson, N. P.; Teixidor, F.; Almajano, M. P.; Escriche, L.; Casabo, J. F.; Sillanpaa, R.; Kivekas, R. *J. Chem. Soc.,Dalton Trans.* **1992**, 2889-2897.

222. de Groot, B.; Loeb, S. J. *Inorg. Chem.* **1990**, *29*, 4084-4090.

223. Gordillo, B.; Juaristi, E.; Martínez, R.; Toscano, R. A.; White, P. S.; Eliel, E. L. *J. Am. Chem. Soc.* **1992**, *114*, 2157-2162.

224. Rizo, J.; Koerber, S. C.; Bienstock, R. J.; Rivier, J.; Hagler, A. T.; Gierasch, L. M. *J. Am. Chem. Soc.* **1992**, *114*, 2852-2859.

225. Sanaullah; Kano, K.; Glass, R. S.; Wilson, G. S. *J. Am. Chem. Soc.* **1993**, *115*, 592-600.

226. Robandt, P. V.; Schroeder, R. R.; Rorabacher, D. B. *Inorg. Chem.* **1993**, *32*, 3957-3963.

227. Ramirez, B. E.; Malmström, B. G.; Winkler, J. R.; Gray, H. B. *Proc. Natl. Acad. Sci. USA* **1995**, *92*, 11949-11951.

228. Colman, P. M.; Freeman, H. C.; Guss, J. M.; Murata, M.; Norris, V. A.; Ramshaw, J. A. M.; Venkatappa, M. P. *Nature* **1978**, *272*, 319-324.

229. Cooper, S. R.; Rawle, S. C. *Struct. Bonding (Berlin).* **1990**, *72*, 1-72.

230. Blake, A. J.; Schröder, M. *Adv. Inorg. Chem.* **1990**, *35*, 1-80.

231. Broan, C. J.; Cox, J. P. L.; Craig, A. S.; Kataky, R.; Parker, D.; Harrison, A.; Randall, A. M.; Ferguson, G. *J. Chem. Soc., Perkin Trans. II* **1991**, 87-99.

232. Goswami, N.; Alberto, R.; Barnes, C. L.; Jurisson, S. *Inorg. Chem.* **1996**, *35*, 7546-7555.

233. Matondo, S. O. C.; Mountford, P.; Watkin, D. J.; Jones, W. B.; Cooper, S. R. *J. Chem. Soc., Chem. Commun.* **1995**, 161-162.

234. Bach, R. D.; Vardhan, H. B. *J. Org. Chem.* **1986**, *51*, 1609-1610.

235. van Nostrum, C. F.; Benneker, F. B. G.; Brussaard, H.; Kooijamn, H.; Veldman, N.; Spek, A. L.; Schoonman, J.; Feiters, M. C.; Nolte, R. J. M. *Inorg. Chem.* **1996**, *35*, 959-969.

236. Guyon, V.; Guy, A.; Foos, J.; Lemaire, M.; Draye, M. *Tetrahedron.* **1995**, *51*, 4065-4074.

237. Murray, S. G.; Hartley, F. R. *Chem. Rev.* **1981**, *81*, 365-414.

238. Wilson, G. S.; Swanson, D. D.; Glass, R. S. *Inorg. Chem.* **1986**, *25*, 3827-3829.

239. Küppers, H. J.; Wieghardt, K.; Nuber, B.; Weiss, J.; Bill, E.; Trautwein, A. X. *Inorg. Chem.* **1987**, *26*, 3762-3769.

240. Blake, A. J.; Gould, R. O.; Holder, A. J.; Hyde, T. I.; Lavery, A. J.; Odulate, M. O.; Schröder, M. *J. Chem. Soc., Chem. Commun.* **1987**, 118-120.

241. Cooper, S. R.; Rawle, S. C.; Yagbasan, R.; Watkin, D. J. *J. Am. Chem. Soc.* **1991**, *113*, 1600-1604.

242. Cooper, S. R. *Acc. Chem. Res.* **1988**, *21*, 141-146.

243. Wieghardt, K.; Küppers, H. J.; Weiss, J. *Inorg. Chem.* **1985**, *24*, 3067-3071.

244. Grant, G. J.; Carpenter, J. P.; Setzer, W. N.; VanDerveer, D. G. *Inorg. Chem.* **1989**, *28*, 4128-4131.

245. Setzer, W. N.; Cacioppo, E. L.; Guo, Q.; Grant, G. J.; Kim, D. D.; Hubbard, J. L.; VanDerveer, D. G. *Inorg. Chem.* **1990**, *29*, 2672-2681.

246. DeSimone, R. E.; Glick, M. D. *J. Am. Chem. Soc.* **1976**, *98*, 762-767.

247. Dale, J. *Acta Chem. Scand.* **1973**, *27*, 1115-1129.

248. Wolf, Jr., R. E.; Hartman, J. R.; Storey, J. M. E.; Foxman, B. M.; Cooper, S. R. *J. Am. Chem. Soc.* **1987**, *109*, 4328-4335.

249. Lucas, C. R.; Liu, S.; Newlands, M. J.; Charland, J. P.; Gabe, E. J. *Can. J. Chem.* **1989**, *67*, 639-647.

250. Lucas, C. R.; Shuang, L.; Newlands, M. J.; Charland, J. P.; Gabe, E. J. *Can. J. Chem.* **1988**, *66*, 1506-1512.

251. Lucas, C. R.; Liu, S.; Newlands, M. J.; Charland, J. P.; Gabe, E. J. *Can. J. Chem.* **1990**, *68*, 644-649.

252. Dalley, N. K.; Larson, S. B.; Smith, J. S.; Matheson, K. L.; Izatt, R. M.; Christensen, J. J. *J. Heterocycl. Chem.* **1981**, *18*, 463-467.

253. Rawle, S. C.; Admans, G. A.; Cooper, S. C. *J. Chem. Soc., Dalton Trans.* **1988**, 93-96.

254. de Groot, B.; Loeb, S. J. *Chem. Commun.* **1990**, 1755-1756.

255. de Groot, B.; Jenkins, H. A.; Loeb, S. J. *Inorg. Chem.* **1992**, *31*, 203-208.

256. Cram, D. J.; Lein, G. M. *J. Am. Chem. Soc.* **1985**, *107*, 3657-3668.

257. Lockhart, J. C.; Tomkinson, N. P. *J. Chem. Soc., Perkin Trans. II.* **1992**, 533-543.

258. Forsyth, G. A.; Lockhart, J. C. *J. Chem. Soc., Dalton Trans.* **1994**, 2243-2249.

259. Lehn, J.-M. *Structure and Bonding* **1973**, *16*, 1-69.

260. Chandrasekhar, S.; McAulay, A. *Inorg. Chem.* **1992**, *31*, 2663-2665.

261. Bennett, M. A.; Canty, A. J.; Felixburger, J. K.; Rendina, L. M.; Sunderland, C.; Willis, A. C. *Inorg. Chem.* **1993**, *32*, 1951-1958.

262. Willey, G. R.; Lakin, M. T.; Alcock, N. W. *J. Chem. Soc., Dalton Trans.* **1992**, 591-596.

263. Bur, D.; Nikles, M.; Sequin, U.; Neuburger, M.; Zehnder, M. *Helv. Chim. Acta* **1993**, *76*, 1863-1875.

264. Setzer, W. N.; Coleman, B. R.; Wilson, G. S.; Glass, R. S. *Tetrahedron.* **1981**, *37*, 2743-2747.

265. Park, Y. S.; Shurvell, H. F. *J. Mol. Struct.* **1995**, *335*, 169-176.

266. Park, Y. S.; Shurvell, H. F. *J. Mol. Struct.* **1996**, *378*, 165-175.

267. Allinger, N. L.; Quinn, M.; Rahman, M.; Chen, K. *J. Phys. Org. Chem.* **1991**, *4*, 647-658.

268. Schmitz, L. R.; Allinger, N. L. *J. Am. Chem. Soc.* **1990**, *112*, 8307-8315.

269. Saunders, M. *J. Am. Chem. Soc.* **1987**, *109*, 3150-3152.

270. Saunders, M.; Houk, K. N.; Wu, Y.-D.; Still, W. C.; Lipton, M.; Chang, G.; Guida, W. C. *J. Am. Chem. Soc.* **1990**, *112*, 1419-1427.

271. Ferguson, D. M.; Glauser, W. A.; Raber, D. J. *J. Comp. Chem.* **1989**, *10*, 903-919.

272. Weinberg, N.; Wolfe, S. *J. Am. Chem. Soc.* **1994**, *116*, 9860-9868.

273. Kolossváry, I.; Guida, W. C. *J. Am. Chem. Soc.* **1996**, *118*, 5011-5019.

274. Ferguson, D. M.; Raber, D. J. *J. Am. Chem. Soc.* **1989**, *111*, 4371-4378.

275. Beech, J.; Cragg, P. J.; Drew, M. G. B. *J. Chem. Soc., Dalton Trans.* **1994**, 719-729.

276. Setzer, W. N.; Guo, Q.; Meehan, Jr., E. J.; Grant, G. J. *Heteroatom Chem.* **1990**, *1*, 425-431.

277. Oyanagi, K.; Kuchitsu, K. *Bull. Chem. Soc. Jpn.* **1978**, *51*, 2243-2248.

278. Durig, J. R.; Compton, D. A. C.; Jalilian, M.-R. *J. Phys. Chem.* **1979,** *83,* 511-515.

279. Sakakibara, M.; Matsuura, H.; Harada, I.; Shimanouchi, T. *Bull. Chem. Soc. Jpn.* **1977,** *50,* 111-115.

280. Nogami, N.; Sugeta, H.; Miyazawa, T. *Bull. Chem. Soc. Jpn.* **1975,** *48,* 3573-3575.

281. Jensen, F. R.; Bushweller, C. H.; Beck, B. H. *J. Am. Chem. Soc.* **1969,** *91,* 344-351.

282. Eliel, E. L.; Kandasamy, D. *J. Org. Chem.* **1976,** *41,* 3899-3904.

283. Hayashi, M.; Shimanouchi, T.; Mizushima, S.-I. *J. Chem. Phys.* **1957**, *26*, 608-612.

284. Scott, D. W.; Finke, H. L.; Gross, M. E.; Williamson, K. D.; Waddington, G.; Huffman, H. M. *J. Am. Chem. Soc.* **1951**, *73*, 261-265.

285. Ohta, M.; Ogawa, Y.; Matsuura, H.; Harada, I.; Shimanouchi, T. *Bull. Chem. Soc. Jpn.* **1977,** *50,* 380-390.

286. Pennington, R. E.; Scott, D. W.; Finke, H. L.; McCullough, J. P.; Messerly, J. F.; Hossenlopp, A.; Waddington, G. *J. Am. Chem. Soc.* **1956**, *78*, 3266-3272.

287. Hargittai, I.; Schultz, G. *J. Chem. Phys.* **1986**, *84*, 5220-5221.

288. Nandi, R. N.; Su, C.-F.; Harmony, M. D. *J. Chem. Phys.* **1984,** *81,* 1051-1053.

289. Hayashi, M.; Shiro, Y.; Osima, T.; Murata, H. *Bull. Chem. Soc. Jpn.* **1966,** *39,* 118-121.

290. Zefirov, N. S.; Gurvich, L. G.; Shashkov, A. S.; Krimer, M. Z.; Vorob'eva, E. A. *Tetrahedron.* **1976,** *32,* 1211-1219.

291. Hayashi, M.; Shiro, Y.; Murata, H. *Bull. Chem. Soc. Jpn.* **1966,** *39,* 112-117.

292. Bultinck, P.; Goeminne, A.; Van de Vondel, D. *J. Mol. Struct. (Theochem).* **1995,** *334,* 101-107.

293. Subbotin, O. A.; Palyulin, V. A.; Kozhushkov, S. I.; Zefirov, N. S. *Zh. Organich. Khim.* **1978**, *14*, 209.

294. Willer, R. L.; Eliel, E. L. *J. Am. Chem. Soc.* **1977,** *99,* 1925-1936.

295. Schultz, G.; Kucsman, A.; Hargittai, I. *Acta Chem. Scand., Ser. A.* **1988,** *42,* 332-337.

296. Marsh, R. E. *Acta Crystallogr.* **1955,** *8,* 91-94.

297. Sokol, L. S. W. L.; Ochrymowycz, L. A.; Rorabacher, D. B. *Inorg. Chem.* **1981,** *20,* 3189-3195.

298. Kitchin, R. W.; Malloy, Jr., T. B.; Cook, R. L. *J. Mol. Struct.* **1975,** *57,* 179-188.

299. Cumper, C. W. N.; Vogel, A. I. *J. Chem. Soc.* **1959,** 3521-3526.

300. Glass, R. S.; Wilson, G. S.; Setzer, W. N. *J. Am. Chem. Soc.* **1980,** *102,* 5068-5069.

301. Durrant, M. C.; Richards, R. L.; Firth, S. *J. Chem. Soc., Perkin Trans. II.* **1993,** 445-450.

302. Novak, I.; Ng, S. C.; Potts, A. W. *Spectrochim. Acta.* **1994,** *50A,* 353-356.

303. Blower, P. J.; Cooper, S. R. *Inorg. Chem.* **1987,** *26,* 2009-2010.

304. Altona, C.; Havinga, E. *Tetrahedron* **1966,** *22,* 2275-2280.

305. Lambert, J. B. *Acc. Chem. Res.* **1971,** *4,* 87-94.

306. Barfield, M.; Smith, W. B. *Magn. Reson. Chem.* **1993,** *31,* 696-697.

307. Fyfe, C. A. In *Solid State NMR for Chemists*; C.F.C. Press: Guelph, 1984; pp 298-472.

308. Barfield, M. *J. Am. Chem. Soc.* **1995,** *117,* 2862-2876.

309. Barfield, M.; Yamamura, S. H. *J. Am. Chem. Soc.* **1990,** *112,* 4747-4758.

310. Clarkson, J. A.; Yagbasan, R.; Blower, P. J.; Cooper, S. R. *J. Chem. Soc., Chem. Commun.* **1989,** 1244-1245.

311. Blake, A. J.; Gould, R. O.; Greig, J. A.; Holder, A. J.; Hyde, T. I.; Schröder, M. *J. Chem. Soc., Chem. Commun.* **1989,** 876-878.

312. Hendrickson, J. B. *J. Am. Chem. Soc.* **1967,** *89,* 7043-7047.

313. Grant, G. J.; Sanders, K. A.; Setzer, W. N.; VanDerveer, D. G. *Inorg. Chem.* **1991,** *30,* 4053-4056.

314. Adams, R. D.; Falloon, S. B.; McBride, K. T. *Organometallics.* **1994,** *13,* 4870-4874.

315. Edwards, A. J.; Johnson, B. F. G.; Khan, F. K.; Lewis, J.; Raithby, P. R. *J. Organomet. Chem.* **1992**, *426*, C44-C48.

316. Dalling, D. K.; Grant, D. M. *J. Am. Chem. Soc.* **1967**, *89*, 6612-6622.

317. Rawle, S. C.; Sewell, T. J.; Cooper, S. R. *Inorg. Chem.* **1987**, *26*, 3769-3775.

318. Adams, R. D.; Falloon, S. B.; McBride, K. T.; Yamamoto, J. H. *Organometallics.* **1995**, *14*, 1739-1747.

319. Yates, P. C.; Richardson, C. M. *J. Mol. Struct. (Theochem).* **1996**, *363*, 17-22.

320. Robinson, G. H.; Sangokoya, S. A. *J. Am. Chem. Soc.* **1988**, *110*, 1494-1497.

321. Sevdic, D.; Curic, M.; Tusek-Bozic, L. *Polyhedron* **1989**, *8*, 505-512.

322. Davis, P. H.; White, L. K.; Belford, R. L. *Inorg. Chem.* **1975**, *14*, 1753-1757.

323. Glick, M. D.; Gavel, D. P.; Diaddario, L. L.; Rorabacher, D. B. *Inorg. Chem.* **1976**, *15*, 1190-1193.

324. DeSimone, R. E.; Glick, M. D. *J. Am. Chem. Soc.* **1975**, *97*, 942-943.

325. Corfield, P. W. R.; Ceccarelli, C.; Glick, M. D.; Moy, I. W.-Y.; Ochrymowycz, L. A.; Rorabacher, D. B. *J. Am. Chem. Soc.* **1985**, *107*, 2399-2404.

326. Blake, A. J.; Pasteur, E. C.; Reid, G.; Schröder, M. *Polyhedron* **1991**, *10*, 1545-1548.

327. Blake, A.; Gould, R. O.; Reid, G.; Schröder, M. *J. Chem. Soc., Chem. Commun.* **1990**, 974-976.

328. Blake, A. J.; Gould, R. O.; Halcrow, M. A.; Schröder, M. *Acta Crystallogr., Sect. B.* **1993**, *49*, 773-779.

329. Setzer, W. N.; Tang, Y.; Grant, G. J.; VanDerveer, D. *Inorg. Chem.* **1991**, *30*, 3652-3656.

330. Pett, V. B.; Diaddario, Jr., L. L.; Dockal, E. R.; Corfield, P. W.; Ceccarelli, C.; Glick, M. D.; Ochrymowycz, L. A.; Rorabacher, D. B. *Inorg. Chem.* **1983**, *22*, 3661-3670.

331. Setzer, W. N.; Afshar, S.; Burns, N. L.; Ferrante, L. A.; Hester, A. M.; Meehan, Jr., E. J.; Grant, G. J.; Isaac, S. M.; Laudeman, C. P.; Lewis, C. M.; VanDerveer, D. G.

Heteroatom Chem. **1990,** *1*, 375-387.

332. Jones, T. E.; Zimmer, L. L.; Diaddario, L. L.; Rorabacher, D. B.; Ochrymowycz, L. A. *J. Am. Chem. Soc.* **1975**, *97*, 7163-7165.

333. Osvath, P.; Sargeson, A. M. *J. Chem. Soc., Chem. Commun.* **1993,** 40-42.

334. Smith, R. J.; Salek, S. N.; Went, M. J.; Blower, P. J.; Barnard, N. J. *J. Chem. Soc., Dalton Trans.* **1994,** 3165-3170.

335. Desper, J. M.; Gellman, S. H. *J. Am. Chem. Soc.* **1990**, *112*, 6732-6734.

336. Desper, J. M.; Gellman, S. H.; Wolf, Jr., R. E.; Cooper, S. R. *J. Am. Chem. Soc.* **1991,** *113*, 8663-8671.

337. Gilson, D. F. R. *J. Chem. Ed.* **1992**, *69*, 23-25.

338. Ubbelohde, A. R. In *Melting and Crystal Structure*; Clarendon Press: Oxford, 1965; pp 89-117.

339. Program modified by T. B. Grindley.

IMAGE EVALUATION TEST TARGET (QA-3)

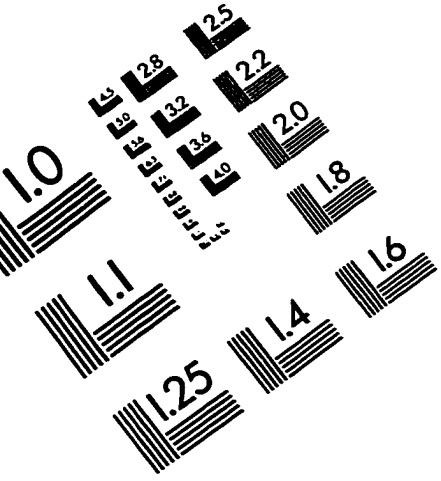

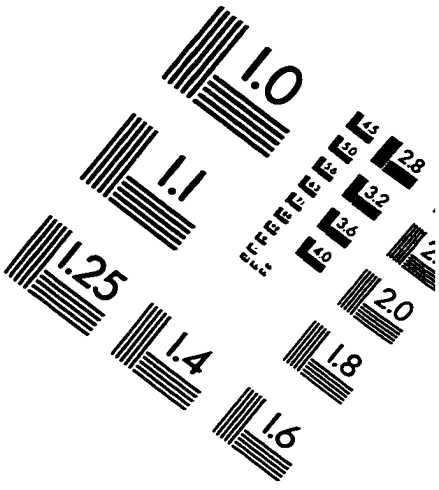

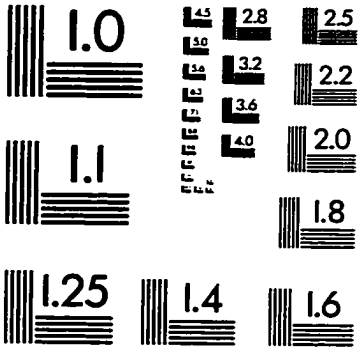

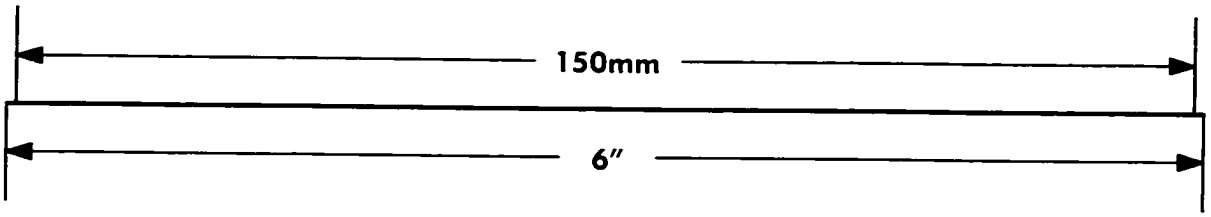

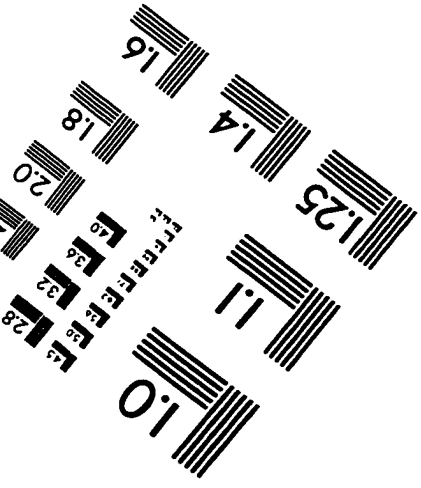

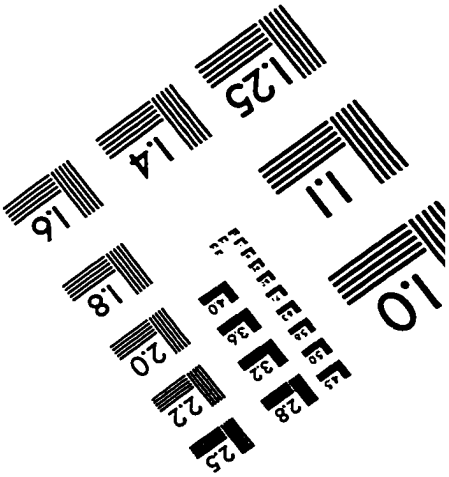

APPLIED IMAGE, Inc
1653 East Main Street
Rochester, NY 14609 USA
Phone: 716/482-0300
Fax: 716/288-5989